ICES Journal of Marine Science

ICES Journal of Marine Science (2016), 73(7), 1825–1830. doi:10.1093/icesjms/fsw079

Introduction to the Themed Section: '*Seascape Ecology*'

Introduction

Observing and managing seascapes: linking synoptic oceanography, ecological processes, and geospatial modelling

Manuel Hidalgo[1]*, David H. Secor[2], and Howard I. Browman[3]

[1]*Instituto Español de Oceanografía, Centro Oceanográfico de les Baleares, Muelle de Poniente s/n, Apdo. 291, 07015 Palma de Mallorca, Spain*
[2]*Chesapeake Biological Laboratory, University of Maryland Center for Environmental Science, PO Box 38, Solomons, MD 20688, USA*
[3]*Institute of Marine Research, Marine Ecosystem Acoustics Group, Austevoll Aquaculture Research Station, 5392 Storebø, Norway*

**Corresponding author: e-mail: jm.hidalgo@ba.ieo.es*

Hidalgo, M., Secor, D. H., and Browman, H. I. Observing and managing seascapes: linking synoptic oceanography, ecological processes, and geospatial modelling. – ICES Journal of Marine Science, 73: 1825–1830.

Received 18 April 2016; accepted 18 April 2016.

The capacity to observe, retrieve, and model the physiographical and hydrographical features of the sea (i.e. seascapes) has surpassed our ability to integrate this information into the assessment and stewardship of marine ecosystems. However, current marine policy that mandates integrated ecosystem assessments demands temporally intensive and spatially extensive predictions of key populations and ecosystem processes and services, particularly those related to habitat use and distribution. In this sense, seascape ecology represents an operational linkage between basic oceanography and applied ecology and management that embraces spatially explicit models of the dynamic distributions of populations, communities and foodwebs through a joint consideration of observational data and ecological processes. For these reasons, the *ICES Journal of Marine Science* solicited contributions to the article theme set, "*Frontiers in seascape ecology*". In this introduction, we present current concepts and developments in seascape ecology, briefly summarize the 10 articles that appear herein, and discuss the most relevant challenges to this nascent discipline. The contributions included in this theme set illustrate the growing relevance of seascape ecology in the multidisciplinary management of marine ecosystems.

Keywords: ecosystem based management, ecosystems oceanography, fisheries oceanography, geospatial modeling, habitat ecology, integrated ecosystem assessments, ocean landscapes, ocean observing systems, operational ocean data products, seascape ecology.

Background and motivation for this article theme set

In the digital era, the capacity to observe, store, retrieve, and synoptically model environmental information has greatly surpassed our ability to integrate these data into the assessment and stewardship of our marine ecosystems. Nowhere is this better demonstrated than in seascapes (i.e. physiographical and hydrographical features of the sea) which, by their nature, are dynamic, diffuse, transient, and without obvious physical boundaries. New technologies allow us to observe key oceanographic variables at multiple scales across ocean basins, or more intensively in coastal and reef habitats. "Operationalizing" these variables through global availability and rapid delivery (telecommunications) permits translation of data into synoptic oceanography—classification and data visualization of water masses structured by constituent physics or energy flow (Kavanaugh *et al.*, 2016). Current marine policy that mandates integrated ecosystem assessments demands temporally intensive and spatially extensive predictions of key populations, and ecosystem processes and services. The nascent field of "seascape ecology" tries to reproduce dynamic oceanography and expand it to include a limited number of controlling ecological processes to make predictions about the complex nature of marine populations and their ecosystems. This discipline moves us away from traditional approaches to define spatial management domains either through stipulation (e.g. unit stock boundary, Secor, 2013) or through spatially implicit modelling (e.g. the Basin Model, MacCall, 1990). In a broad sense, seascape ecology embraces spatially explicit models of dynamic distributions of populations, communities, and foodwebs,

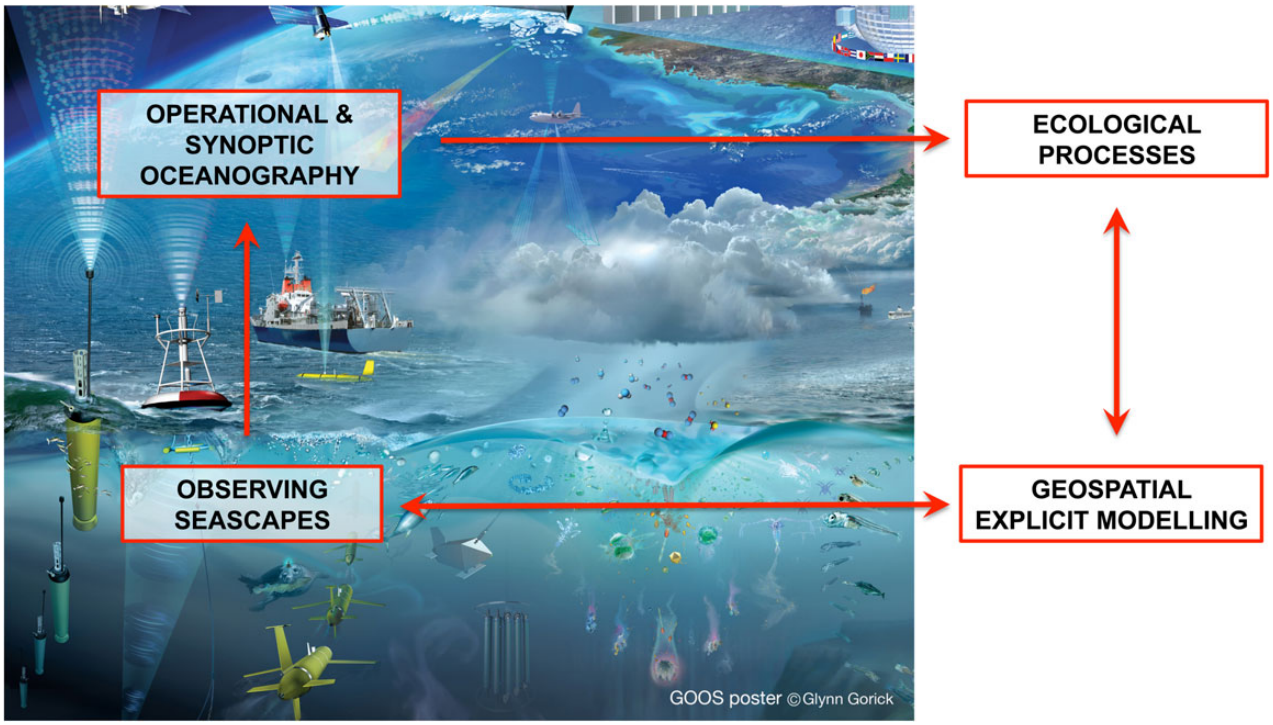

Figure 1. Seascape ecology entails a recursive approach, where observed oceanographic variables are made operational (accessible) and synoptic through wide bandwidth telecommunication. Knowledge of ecological and oceanographic processes is incorporated into spatially explicit models that permit predictions of the dynamic distributions of marine populations and related ecosystem properties (image adapted with the permission of the artist, Glynn Gorick; see also http://unesdoc.unesco.org/images/0018/001878/187825e.pdf).

doing so through joint consideration of observing data and ecological processes (Figure 1). Here, we adopt Manderson's definition: "seascape ecology is a science measuring the effects of the heterogeneity in the properties and processes of the ocean on the interactions of individual organisms, their populations and ecosystems including human socio-economic components" (Manderson, 2016).

Seascape ecology finds its roots in the concepts and analytical methods developed in landscape ecology for terrestrial ecosystems (Wedding *et al.*, 2011). Such a framework readily applies to coastal benthic environments, studies of which have long focused on habitat heterogeneity, patchiness, edge effects, and corridors. From this perspective, seascapes are merely "flooded landscapes" (e.g. seagrass beds, intertidal zones, reefs) with stationary and fixed patch structure and topographies (Pittman *et al.*, 2011). However, pelagic seascapes are fluid in nature; they are non-stationary with high diffusivity, advection, and turbulence (Manderson, 2016). Further, most benthic marine ecosystems may also reflect transience in their physical states that does not allow explicit characterization of spatial features that structure marine populations and communities. Physical variables within seascapes also show a broader range of scale-dependence in their actions than do terrestrial landscapes, requiring data to be collected and integrated across multiple scales (Kavanaugh *et al.*, 2016; Manderson, 2016; Scales *et al.*, 2016a). Therefore, techniques and metrics needed to characterize the pelagic seascape are far more challenging owing to the high frequency and spatial extent over which they must be observed (e.g. Bertrand *et al.*, 2014; Alvarez-Berastegui *et al.*, 2014; Scales *et al.*, 2016a). One of the main applications of seascape ecology, particularly from a dynamic perspective, is the understanding of habitat use and migrations over relevant time-scales—for instance, from hours to days in larvae, or from years to decades in populations. The increasing availability of data from ocean observing systems has the potential to provide near real-time benthic and pelagic habitat modelling of species of importance in a conservation and management context.

A principal goal of seascape ecology is to make efficient use of oceanographic data and ecological process models to predict the distributions and migrations of marine organisms. Such an integrative approach is highly relevant to efforts to assess and manage ecosystems that support major commercial fisheries as they are altered by climate change and other stressors (Link and Browman, 2014). In this sense, seascape ecology can provide a dynamic and adaptive framework over which important oceanographic properties and drivers of change occur. The tools of seascape ecology bear on all ecosystem attributes including habitats, food-webs, ocean connectivity, species demography and spatial structure, anthropogenic impacts, and ecosystems services. For these reasons, and given the broad spectrum of implications and applications of seascape ecology, the *ICES Journal of Marine Science* solicited contributions to the article them set, "Frontiers in seascape ecology: new approaches to investigate dynamic benthic and pelagic habitats".

We sought contributions that would bring into sharper focus advances in seascape ecology that underlie more dynamic and real-time depictions and understanding of seascapes as drivers of ecosystems attributes, particularly on fish habitat use and migration. This included the dynamic influence of seascapes over relevant time-scales; near real-time habitat modelling; improvements in the parameterization of ecological and behavioural processes shaping benthic and pelagic habitat use and migration; and

temporal changes of scale-dependent processes influencing marine habitats. The contributions to this article theme set are strong evidence that seascape ecology is a growing and increasingly relevant discipline, marrying basic oceanography with applied ecology and management.

About the articles in this theme set: aligning observations with ecology

Seascape ecology has relied on developments in "operational oceanography", and on an improved understanding of mechanisms of the interaction between aquatic organisms and their physical environment. Kavanaugh *et al.* (2016) emphasize the basic influence of physical and energetic properties of the ocean, and how multi-scale synoptic measurements permit observation of ocean processes relevant from the microbe to the whale. Physical hierarchies emerge from processes that are structured by turbulence and advection, but also by high rates of energy dissipation and turnover. They illustrate how complex interdependence between energy dissipation, biology, and other physical processes triggers cross-scale interactions that require large amounts of data to reproduce context-dependent ecological outcomes (e.g. species distributions). Manderson (2016) examines basic physical differences between terrestrial and marine realms but concludes that the foundation of seascape ecology lies in the physiological and behavioural adaptations to life in water. This involves weak physiological regulation and strong habitat selection for ocean properties, structures, and dynamics. Although the perspectives of these two essays differ, Kavanaugh *et al.* (2016) and Manderson (2016) both emphasize how underlying component parts, for instance, the influence of a parcel of water on hourly or daily habitat selection, give rise to aggregate processes such as the dynamic distribution of fish populations. However, in practice, seascape ecology often entails an epiphenomenal approach involving statistical analyses of distributional data together with relevant operational oceanographic information and expected ecological responses.

From an applied point of view, Kavanaugh *et al.* (2016) presents a dynamic and hierarchical seascape framework to address the issue of integrating information across multiple spatial scales and international observing networks. This framework attempts to provide both a broad environmental context to model organismal data and a biogeographic perspective to compare ecosystems and to scale observations to global phenomena. At a mesoscale level, Alvarez-Berastegui *et al.* (2016) illustrate how the dynamic spawning habitat of a top predator with a high commercial value, bluefin tuna *Thunnus thynnus*, can be predicted using operational satellite data. This study, which employs sophisticated numerical modelling, opens new opportunities to implement dynamic spatial management of this species and to adjust larval indices to improve estimates of the spawning-stock biomass. Similarly, Alabia *et al.* (2016) develop an ensemble modelling approach that efficiently utilizes three-dimensional oceanographic information to investigate the habitat associations of Neon flying squid (*Ommastrephes bartramii*) in the North Pacific Ocean.

Seascape ecology also attempts to reveal underlying "ecological processes" that are often obscured when the driving mechanisms are dynamic or otherwise not well captured by asynoptic oceanographic information. For instance, ontogenetic, seasonal, and climate-driven changes in distributions are poorly resolved from distribution data alone. Petrik *et al.* (2016) effectively integrate interannual variability of ocean currents at different spawning locations to understand walleye Pollock (*Gadus chalcogrammus*) nursery habitat on the Bering Sea shelf, and how it affects juvenile survival in contrasting cold and warm years. This highlights the importance of combining information on the spatio-temporal distribution of spawners (when, where, and how many) with ocean currents to properly understand the influence of ocean connectivity on observed distribution patterns at nursery areas (e.g. Hidalgo *et al.*, 2012). Spawning areas are highly context-dependent and, in cold systems such as the Bering Sea, are generally well defined by species-specific ranges of temperature. Vestfals *et al.* (2016) demonstrate the contrasting responses to changes in temperature in the habitat use of two flatfish (Greenland halibut, *Reinhardtius hippoglossoides*, and Pacific halibut, *Hippoglossus stenolepis*) at opposite extremes of their distributional ranges in the eastern Bering Sea. Alvarez-Berastegui *et al.* (2016) illustrate methodologically how to combine mean values and gradients (i.e. rate of spatial variation) of hydrographic variables that capture the heterogeneity in seascape properties and processes at short spatial scales (i.e. fronts and mesoscale structures) that strongly influence the spawning habitat of bluefin tuna.

Spatio-temporal overlap in species distributions is often assessed to infer potential competition and depends on forage resources, oceanographic variables, and habitat physiography. The effect of these drivers is spatially variable, altering the strength of species overlap, and this aspect can be relevant to management. Puerta *et al.* (2016) explore patterns of spatial overlap between the octopus (*Eledone cirrhosa*) and the catshark (*Scyliorhinus canicula*), including shared diets and distributional preferences. The study combines seascape characteristics from surface waters (productivity and temperature) and community characteristics at the bottom (prey abundance, total density, and diversity) to differentiate areas of coexistence and those of competitive exclusion. Turner *et al.* (2016) investigate incidental catches of two riverine herring species (*Alosa pseudoharengus* and *Alosa aestivalis*) in the American Atlantic Herring (*Clupea harengus*) and Atlantic Mackerel (*Scomber scombrus*) fisheries, by characterizing bottom seascapes that influence their distributions and overlap with the targeted species.

Seascape genetics refers to how oceanographic variables and ecological processes structure population genotypes. Silva and Gardner (2016) show that environmental variation in the pelagic habitat can be a barrier to gene flow in New Zealand scallop (*Pecten novaezelandiae*) due to ecophysiological constraints associated with the low tolerance of scallops to high concentrations of either freshwater input or suspended sediment. Padrón and Guizien (2016) show, in contrast, the importance of disentangling the relative contribution of local demography (e.g. recruitment failure) and environmental connectivity in shaping seascape genetics of complex benthic metapopulations.

Improvements in "geospatial modelling" have allowed for a closer alignment between seascape observations and ecological processes. This implies a more conscientious consideration of the spatially explicit nature of ecological interactions. The studies included in this article theme set illustrate that one of the main analytical tools to model species distribution, in terms of habitat and seascape characteristics, are non-linear regression techniques (e.g. general additive modelling). These techniques have proven useful to differentiate local from regional effects of seascape characteristics and to incorporate them into a spatially explicit modelling framework (Bartolino *et al.*, 2012; Ciannelli *et al.*, 2012; Alabia *et al.*, 2016; Alvarez-Berastegui *et al.*, 2016; Puerta *et al.*, 2016; Turner

et al., 2016; Vestfals *et al.*, 2016). This statistical approach allows environmental drivers to be captured at spatial scales relevant to the ecological process of interest. This characteristic is of relevance because species distribution models are widely used nowadays to project potential species expansion or contraction under different climate change scenarios (e.g. Pinsky *et al.*, 2013). However, these models do not capture seascape information at the medium and short scales required for more fully dynamic modelling of spatial distributions, e.g. those occurring over weeks or months. An emerging and flexible geospatial technique that accommodates this limitation is ensemble niche modelling (Alabia *et al.*, 2016; Scales *et al.*, 2016b), which can capture the influence of oceanographic processes on species distributions at different spatial scales.

Seascape ecology represents an operational linkage between ocean science and "applied marine conservation and management". This can lead to improvement in the spatial planning of the use of coastal and reef areas (Silva and Gardner, 2016; Padrón and Guizien, 2016), or setting the methodological framework for near real-time prediction of favourable habitat for pelagic species of commercial importance (Alabia *et al.*, 2016; Alvarez-Berastegui *et al.*, 2016; Turner *et al.*, 2016). This may increase the resolution and effectiveness of management measures by including ecological processes in assessment models.

Conclusions and challenges

The refinement of information obtained from ocean processes, combined with an improvement in the accessibility of oceanographic variables, will play an important role in developing dynamic ocean management (Tintoré *et al.*, 2013; Hobday and Hartog, 2014). The studies included in this article theme set demonstrate that data, tools, and analytical frameworks are already at hand to develop near real-time forecasting of key ecological processes, particularly those related to the sustainability of marine ecosystems and economic activities such as fisheries. The field of "fisheries oceanography" has evolved considerably since the pioneering work of Hjort (1914) and his contemporaries. Nowadays, the increasing availability of operational information from ocean observing systems has prompted scientific and management agendas to make best use of such information, including temporally intensive and spatially extensive predictions that are driving a new era of research towards "operational fisheries oceanography" (e.g. Svendsen *et al.*, 2007; Manderson *et al.*, 2011; Alvarez-Berastegui *et al.*, 2016). Still, many challenges remain to effectively assimilate and integrate data and analyses across multiple scales to produce outcomes that provide robust ecological predictions. There is no single natural scale at which ecological phenomena can be studied because organisms and communities respond on a range of spatial, temporal, and hierarchical scales (Levin, 1992). For instance, distribution of demersal finfish, particularly those displaying vertical migrations such as gadoids, can be shaped by a combination of benthic static features and dynamic characteristics of the pelagic realm. In addition, the relative contribution of benthic and pelagic seascapes drivers can also change with ontogeny (e.g. from nursery to spawning areas).

The perspectives on seascape ecology contributed by Kavanaugh *et al.* (2016) and Manderson (2016) align well with the Movement Ecology Paradigm (Nathan, 2008), under which dispersal and movement of individuals can be predicted from first principles; hydrodynamics, energy transfer, and physiology. Although seemingly abstract, the marriage of these subdisciplines can produce effective management outcomes. As a recent example, operational oceanographic variables in the California Current are collected, transmitted, and assimilated, and then filtered through a state-space habitat model for blue whales; the result is "Whale Watch" real-time alerts to mariners on regions prone to ship strikes (Irvine *et al.*, 2014, http://www.umces.edu/cbl/whalewatch). On the other hand, a challenge for both movement and seascape ecology is to better incorporate collective behaviours (e.g. Couzin *et al.*, 2005), which are fundamental to how individuals interact with their environment and can produce strong departures from predicted spatial dynamics (Bakun, 2010; Secor, 2015).

A nascent literature is demonstrating the capacity of seascape ecology to predict the dynamic spatial distributions of higher trophic level organisms (Manderson *et al.*, 2011; Alabia *et al.*, 2016; Alvarez-Berastegui *et al.*, 2016; Breece *et al.*, 2016; Queiroz *et al.*, 2016), although this has not as yet been incorporated into formal stock assessments. Simulation modelling, such as management strategy evaluation, can be conducted in parallel with conventional assessment models to improve the conversation between stock assessment scientists and seascape ecologists (Kerr and Goethel, 2013). However, the real challenge is to implement a transdisciplinary integration in which indicators of the spatio-temporal distribution of a species are explicitly included in analytical assessment schemes (e.g. Cadrin and Secor, 2009; Cooke *et al.*, 2016). This integration into applied research will require the development of novel parameterizations of key ecological and behavioural processes incorporating operational seascape information.

A growing body of research is directed towards long-term forecasting of species and ecosystem responses to climate change (i.e. to 2100, IPCC, 2014; e.g. Cheung *et al.*, 2015; Payne *et al.*, 2016, and references therein). However, it is our responsibility to balance our efforts on these long-term scenarios with accurate shorter term predictions, directly applicable to management aims, which are increasingly feasible through effective integration of operational environmental information (Godø *et al.*, 2014). Research on seascape ecology will continue to evolve towards meeting such needs.

Acknowledgements

MH is grateful to Diego Álvarez-Berastegui for inspiring discussions that enriched his view of seascape ecology. MH is supported by a postdoctoral contract co-funded by the Regional Government of the Balearic Islands and the European Social Fund 2014-2020. HIB's contribution to this initiative was supported by Projects 81529 ("Fine scale interactions in the plankton") and 83741 ("Scientific publishing and editing") from the Institute of Marine Research, Norway.

References

Alabia, I., Saitoh, S-I., Igarashi, H., Ishikawa, Y., Usui, N., Kamachi, M., Awaji, T., *et al.* 2016. Ensemble squid habitat model using three-dimensional ocean data. ICES Journal of Marine Science, 73: 1863–1874.

Alvarez-Berastegui, D., Ciannelli, L., Aparicio-Gonzalez, A., Reglero, P., Hidalgo, M., López-Jurado, J. L., Tintoré, J., *et al.* 2014. Spatial scale, means and gradients of hydrographic variables define pelagic seascapes of bluefin and bullet tuna spawning distribution. PLoS ONE, 9: e109338.

Alvarez-Berastegui, D., Hidalgo, M., Tugores, M. P., Aparicio, A., Ciannelli, L., Reglero, P., Juza, M., *et al.* 2016. Pelagic seascape

ecology for operational fisheries oceanography: modelling and predicting spawning distribution of Atlantic bluefin tuna in Western Mediterranean. ICES Journal of Marine Science, 73: 1851–1862.

Bakun, A. 2010. Linking climate to population variability in marine ecosystems characterized by non-simple dynamics: conceptual templates and schematic constructs. Journal of Marine Systems, 79: 361–373.

Bartolino, V., Ciannelli, L., Spencer, P., Wilderbuer, T. K., and Chan, K. S. 2012. Scale-dependent detection of the effects of harvesting a marine fish population. Marine Ecology Progress Series, 444: 251–261.

Bertrand, A., Grados, D., Colas, F., Bertrand, S., Capet, X., Chaigneau, A., Vargas, G., *et al.* 2014. Broad impacts of fine-scale dynamics on seascape structure from zooplankton to seabirds. Nature Communications, 15: 5239.

Breece, M., Fox, D. A., Dunton, K. J., Frisk, M. G., Jordaan, A., and Oliver, M. J. 2016. Dynamic seascapes predict the marine occurrence of an endangered species: Atlantic Sturgeon *Acipenser oxyrinchus oxyrinchus*. Methods in Ecology and Evolution, doi: 10.1111/2041-210X.12532.

Cadrin, S. X., and Secor, D. H. 2009. Accounting for spatial population structure in stock assessment: past, present, and future. *In* The Future of Fisheries Science in North America, pp. 405–426. Ed. by R. J. Beamish, and B. J. Rothschild. Springer, Dordrecht.

Cheung, W. W. L., Frölicher, T. L., Asch, R. G., Jones, M. C., Pinsky, M. L., Reygondeau, K. B., Rodgers, K. B., *et al.* 2015. Building confidence in projections of the responses of living marine resources to climate change. ICES Journal of Marine Science, 73: 1283–1296.

Ciannelli, L., Bartolino, V., and Chan, K. S. 2012. Non-additive and non-stationary properties in the spatial distribution of a large marine fish population. Proceedings of the Royal Society Series B, 279: 3635–3642.

Cooke, S. J., Martins, E. G., Struthers, D. P., Gutowsky, L. F. G., Power, M., Doka, S. E., Dettmers, J. M., *et al.* 2016. A moving target-incorporating knowledge of the spatial ecology of fish into the assessment and management of freshwater fish populations. Environmental Monitoring and Assessment, doi: 10.1007/s10661-016-5228-0.

Couzin, I. D., Krause, J., Franks, N. R., and Levin, S. A. 2005. Effective leadership and decision making in animal groups on the move. Nature, 433: 513–516.

Godø, O. R., Handegard, N. O., Browman, H. I., Macaulay, G. J., Kaartvedt, S., Giske, J., One, E., *et al.* 2014. Marine ecosystem acoustics (MEA): quantifying processes in the sea at the spatio-temporal scales on which they occur. ICES Journal of Marine Science, 71: 2357–2369.

Hidalgo, M., Gusdal, Y., Dingsør, G. E., Hjermann, D., Ottersen, G., Stige, L. C., Melsom, A., *et al.* 2012. A combination of hydrodynamical and statistical modelling reveals non-stationary climate effects on fish larvae distributions. Proceedings of the Royal Society B: Biological Sciences, 279: 275–283.

Hjort, J. 1914. Fluctuations in the great fisheries of Northern Europe. Conseil Permanent International pour l'Exploration de la Mer, 20: 1–228.

Hobday, A. J., and Hartog, J. R. 2014. Derived ocean features for dynamic ocean management. Oceanography, 27: 134–145.

IPCC. 2014. Climate Change 2014: Impacts, Adaptation, and Vulnerability. Part A: Global and Sectoral Aspects. Contribution of Working Group II to the Fifth Assessment Report of the Intergovernmental Panel on Climate Change. Cambridge University Press, Cambridge, UK and New York, NY, USA. 1132 pp.

Irvine, L. M., Mate, B. R., Winsor, M. H., Palacios, D. M., Bograd, B. J., Costa, D. P., and Bailey, H. 2014. Spatial and temporal occurrence of blue whales off the US West Coast, with implications for management. PLoS ONE, 9: e102959.

Kavanaugh, M. T., Oliver, M. J., Chavez, F. P., Letelier, R. M., Muller-Karger, F. E., and Doney, S. C. 2016. Seascapes as a new vernacular for ocean monitoring, management and conservation. ICES Journal of Marine Science, 73: 1839–1850.

Kerr, L. A., and Goethel, D. R. 2013. Simulation modeling as a tool for synthesis of stock identification and information. *In* Stock Identification Methods: Applications in Fisheries Science, 2nd edn, pp. 501–534. Ed. by S. X. Cadrin, L. A. Kerr, and S. Mariani. Academic Press, London.

Levin, S. M. 1992. The problem of pattern and scale in ecology. Ecology, 73: 1943–1947.

Link, J. S., and Browman, H. I. 2014. Integrating what? Levels of marine ecosystem-based assessment and management. ICES Journal of Marine Science, 71: 1170–1173.

MacCall, A. D. 1990. Dynamic Geography of Marine Fish Populations. Washington Sea Grant, Seattle, WA. 153 pp.

Manderson, J. 2016. An essay exploring differences between seascapes and landscapes using Berhard Riemann's rules for analysis. ICES Journal of Marine Science, 73: 1831–1838.

Manderson, J., Palamara, L., Kohut, J., and Oliver, M. J. 2011. Ocean observatory data are useful for regionalhabitat modeling of species with different vertical habitat preferences. Marine Ecology Progress Series, 438: 1–17.

Nathan, R. 2008. An emerging movement ecology paradigm. Proceedings of the National Academy of Sciences of the United States of America, 105: 19050–19051.

Padrón, M., and Guizien, K. 2016. Modelling the effect of demographic traits and connectivity on the genetic structuration of marine metapopulations of sedentary benthic invertebrates. ICES Journal of Marine Science, 73: 1935–1945.

Payne, M. R., Barange, M., Cheung, W. L., Mackenzie, B. R., Batchelder, H. P., Cormon, X., Eddy, T. D., *et al.* 2016. Uncertainties in projecting climate-change impacts in marine ecosystems. ICES Journal of Marine Science, 73: 1272–1282.

Petrik, C., Duffy-Anderson, J., Castruccio, F., Curchitser, E., Hedstrom, K., Mueter, F., and Danielson, S. 2016. Modelled connectivity between Walleye Pollock (*Gadus chalcogrammus*) spawning and age-0 nursery areas in warm and cold years with implications for juvenile survival. ICES Journal of Marine Science, 73: 1890–1900.

Pinsky, M. L., Worm, B., Fogarty, M. J., Sarmiento, J. L., and Levin, S. A. 2013. Marine taxa track local climate velocities. Science, 141: 1239–1242.

Pittman, S. J., Kneib, R. T., and Simenstad, C. A. 2011. Practicing coastal seascape ecology. Marine Ecology Progress Series, 427: 187–190.

Puerta, P., Hunsicker, M., Hidalgo, M., Reglero, P., Ciannelli, L., Esteban, A., González, M., *et al.* 2016. Community–environment interactions explain octopus-shark spatial overlap. ICES Journal of Marine Science, 73: 1901–1911.

Queiroz, N., Humphries, N. C., Mucientes, G., Hammerschlag, N., Lima, F. P., Scales, K. L., and Miller, P. I., *et al.* 2016. Ocean-wide tracking of pelagic sharks reveals extent of overlap with longline fishing hotspots. Proceedings of the National Academy of Sciences of the United States of America, 113: 1582–1587.

Scales, K. L., Hazen, E. L., Jacox, M. J., Edwards, C. A., Boustany, A. M., Oliver, M. J., and Bograd, S. J. 2016a. Scales of inference: on the sensitivity of habitat models for wide ranging marine predators to the resolution of environmental data. Ecography, doi: 10.1111/ecog.02272.

Scales, K. L., Miller, P. I., Ingram, S. N., Hazen, E. L., Bograd, S. J., and Phillips, R. A. 2016b. Identifying predictable foraging habitats for a wide-ranging marine predator using ensemble ecological niche models. Diversity Distributions, 22: 212–224.

Secor, D. H. 2013. The unit stock concept: bounded fish and fisheries. *In* Stock Identification Methods: Applications in Fisheries Science, 2nd edn, pp. 7–28. Ed. by S. X. Cadrin, L. A. Kerr, and S. Mariani. Academic Press, London.

Secor, D. H. 2015. Migration Ecology of Marine Fishes. Johns Hopkins Press, Baltimore, 292 pp.

Silva, C., and Gardner, J. 2016. Identifying environmental factors that are associated with the genetic structure of the New Zealand scallop: linking seascape genetics and ecophysiological tolerance. ICES Journal of Marine Science, 73: 1925–1934.

Steele, J. H. 1991. Can ecological theory cross the land sea boundary? Journal of Theoretical Biology, 153: 425–436.

Svendsen, E., Skogen, M., Budgell, P., Huse, G., Ådlandsvik, B., Vikebø, F., Stiansen, J. E., *et al.* 2007. An ecosystem modelling approach to predicting cod recruitment. Deep Sea Research II, 54: 2810–2821.

Tintoré, J., Vizoso, G., Casas, B., Heslop, E., Pascual, A., Orfila, A., Ruiz, S., *et al.* 2013. SOCIB: the Balearic Islands Coastal ocean observing and forecasting system, responding to science, technology and society needs. Marine Technology Society Journal, 47: 101–117.

Turner, S., Manderson, J., Richardson, D., Hoey, J., and Hare, J. 2016. Using habitat association models to predict Alewife and Blueback Herring marine distributions and overlap with Atlantic Herring and Atlantic Mackerel: can incidental catches be avoided. ICES Journal of Marine Science, 73: 1912–1924.

Vestfals, C., Ciannelli, L., and Hoff, G. 2016. Changes in habitat utilization of slope-spawning flatfish across a bathymetric gradient. ICES Journal of Marine Science, 73: 1875–1889.

Wedding, L. M., Lepczyk, C. A., Pittman, S. J., Friedlander, A. M., and Jorgensen, S. 2011. Quantifying seascape structure: extending terrestrial spatial pattern metrics to the marine realm. Marine Ecology Progress Series, 427: 219–232.

ICES Journal of Marine Science

ICES Journal of Marine Science (2016), 73(7), 1831–1838. doi:10.1093/icesjms/fsw069

Contribution to the Themed Section: '*Seascape Ecology*'

Food for Thought

Seascapes are not landscapes: an analysis performed using Bernhard Riemann's rules

John Pilling Manderson*

NOAA/North East Fisheries Science Center Cooperative Research Program, 74 Magruder Road, Highlands, NJ 07732, USA

**Corresponding author: e-mail: john.manderson@noaa.gov*

Manderson, J. P. Seascapes are not landscapes: an analysis performed using Bernhard Riemann's rules. – ICES Journal of Marine Science, 73: 1831–1838.

Received 15 July 2015; revised 18 March 2016; accepted 3 April 2016.

Applied seascape ecology rests on paradigms of terrestrial landscape ecology. Patches defined by persistent seabed features are the basic units of analysis. Persistent oceanographic features provide context while dynamic features are usually ignored. Should seascape ecology rest on terrestrial paradigms? I use Reimann's rules of analysis to identify differences between seascapes and landscapes. Reimann's method uses hypotheses about system function to guide the development of models of system components based upon fundamental "laws". The method forced me to avoid using terrestrial analogies in understanding of organism-habitat relationships. The fundamental laws applying to all organisms were the conservative metabolic requirements underlying individual performance and population growth. Physical properties of the environment; specifically those dictating strategies available to organisms meeting metabolic requirements, were the "laws" applying to the external environment. Organisms living in the ocean's liquid meet most metabolic requirements using strong habitat selection for properties of the liquid that are controlled by "fast", often episodic, atmospheric and tidal forces. Seascapes are therefor primarily driven by dynamic hydrography including mixing processes. In contrast, most terrestrial organisms are decoupled by gravity and physiological regulation from an atmospheric fluid that is metabolically more challenging. They show strong habitat selection for many essential metabolic materials concentrated on the land surface where slower biogeochemical processes including soil development drive ecological dynamics. Living in a liquid is different from living in a gas and resource use management in the oceans needs to be tuned to seascapes dynamics that is driven primarily by hydrodynamics and secondarily by seabed processes. Advances in ocean observing and data assimilative circulation models now permit the rapid development of applied seascape ecology. This development is essential now that changes in global climate are being rapidly translated into changes in the dynamics of the ocean hydrosphere that structures and controls ecological dynamics within seascapes.

Keywords: seascape ecology, landscape ecology, marine habitat ecology, analysis and synthesis, thought experiment.

Introduction

The management of natural resource use needs to be accurately tuned to the dynamics of ecosystems producing the resources. Spatial planning is currently considered to be the tool most useful for tactical management of resource use in marine ecosystems (Crowder *et al.*, 2006; Douvere, 2010; Norse, 2010). The approach apportions "common property" marine resources to conservation, fisheries, energy production, and other uses to balance tradeoffs among ecological, social, and economic objectives. Since it emphasizes apportionment in space, spatial planning relies on habitat classification that divides up seascapes based on locations of relatively stationary and steep resource gradients. Usually topographic, geological, and biogenic features associated with the seabed define the primary gradients. Most classification frameworks get seascapes wet by placing seabed patch mosaics within broader scale oceanographic contexts defined by relatively stationary, persistent gradients in water column properties such as temperature, salinity, oxygen, and wave motions. Ocean currents controlling the transport of particles, including pelagic larvae, are sometimes considered (Mumby *et al.*, 2011). However, persistent, relatively stationary features associated with the seabed are usually the furniture on the oceanographic stage and the basic units of analysis and spatial

management. Dynamic water column properties and processes are often viewed as a nuisance and sometimes ignored. The paradigms of terrestrial landscape ecology including the patch-mosaic paradigm currently lie at the foundation of marine habitat classification and applied seascape ecology. Should applied seascape ecology rest on the foundation of terrestrial paradigms? The question is of great practical importance because marine ecosystems are changing rapidly in space and time as a result of global climate change while human demand for marine resources is also increasing. In this essay, I attempt to answer this question by performing a formal analysis of the basic ecological differences between seascapes and landscapes.

Method

Seascape ecology can be defined as a discipline describing the effects of interactions between heterogeneity in ocean properties and processes and individual organisms, their populations and ecosystems including human socio-ecological and economic activities. As whole systems emerging from interactions between organisms and the environment, seascapes invite the application of synthesis as the primary method for developing a coherent, "bottom up" understanding of whole system processes arising from causes at the level of system components. Analysis which applies a "top down" approach, using hypotheses about whole system function to guide the development of conceptual models about the ways interacting components could give rise to system function based upon fundamental "laws", usually plays a supportive role. If we replace the phrase "heterogeneity in ocean properties and processes" with "heterogeneity in terrestrial properties and processes" in the definition of seascape ecology above, the objectives of seascape and landscape ecology are exactly the same. Furthermore, both disciplines rely on synthesis as the primary method of scientific inquiry.

The 19th century German mathematician Bernhard Riemann discussed the foundations and requirements of analysis and synthesis as scientific procedures in his investigation of "The mechanism of the ear" (reviewed by Ritchey, 1991). Analysis and synthesis are complementary and require different degrees of certainty in our knowledge of the whole system and its component parts. Analysis begins with a sufficient hypothesis about what the whole system "does". This function then guides the development of conceptual models about the ways components may allow the system to accomplish its function. Analysis does not require components and their interactions to be understood with certainty; only that our conceptual models of them are consistent with fundamental laws. Analysis is best applied in early investigations of opaque systems whose functions are relatively clear but accomplished through interactions of components we don't know with certainty. Synthesis, on the other hand, uses knowledge of components and their interactions to infer whole system function. As a result, synthesis requires relatively certain knowledge of system components and is a good starting point for the investigation of transparent systems. Performing synthesis on opaque systems can be tricky. When uncertain about the nature of components we often resort to analogy to explain how they may work and interact. Important discoveries have been made by likening components and their interactions to more familiar phenomena. For example, Nicolas Carnot (1824) developed a mechanistic theory of the heat engine by analogy to the flow of water over a waterfall (reviewed in Gentner and Jeziorski, 1993). However, analogies can also fail spectacularly when we force our understanding of a system to match expectations that are inconsistent with the true properties and processes underlying the system.

We are warm blooded, air-breathing creatures living along the interface between land and a transparent atmosphere abundant with gases essential to life. Our ecological intuitions are shaped by experience on terrestrial landscapes and with landscape components we easily observe. Applying synthesis as the primary method for understanding the ecology of terrestrial landscapes makes perfect sense. Landscapes are transparent to us and our terrestrial intuitions usually serve us well when we are forced to rely on analogy to describe interactions of components we do not fully understand. Seascapes, on the other hand, are among the most remote and opaque ecosystems on the earth to us. Our knowledge of marine organisms and their interactions with the environment is highly uncertain. Living in a liquid is different from living in a gas and our terrestrial intuitions can fail us as we draw analogies to describe the ways marine organisms interact with the liquid surrounding them. It is therefore risky to rely on synthesis as the primary method of investigation in the early development of seascape ecology. To avoid traps set by terrestrial intuition and analogies, I apply Riemann's rules of analysis to explore the basic ecological differences between seascapes and landscapes.

An analysis of seascapes and landscapes using Bernhard Riemann's rules

Every analysis begins with a hypothesis describing the function of the whole system. We must therefore decide what seascapes actually do. All ecologists can probably agree that the task of any functioning seascape is to provide resources sufficient to maintain important life history processes of individuals belonging to one or more species. Seascapes and the habitats composing them function only if they support living organisms over some time horizon. We can make our hypothesis about the function of seascapes relevant to the species populations by grounding it in classical ideas about the species niche. Niches are defined by external physical and biological variables and resources, including species interactions producing population growth rates greater or equal to zero (Grinnell, 1917; Elton, 1927; Hutchinson, 1957; Chase and Leibold, 2003; Holt, 2009). Niches are abstract "spaces", defined by abiotic and biotic environmental variables that have no spatial or temporal dimensions. This follows Hutchinson's concept of the basic niche as an abstract "hypervolume" defined by N environmental dimensions (Hutchinson, 1957; Hutchinson, 1978). Habitats, on the other hand, are projections of species niches on the spatial and temporal heterogeneity of the external environment. Habitats are niches manifested in space and time (see also Colwell and Rangel, 2009).

We can use the niche-habitat concept to refine our hypothesis about what seascapes do. Seascapes supply the spatial and temporal diversity of resources required for one or more species to achieve population growth rates greater than or equal to zero. Using the duality of the niche-habitat concept to define the function of ecological systems forces us to identify important external environmental properties and processes structuring and controlling the dynamics of seascapes, landscapes, and their habitats purely based on their effects on organism performance rates underlying population growth. Every functioning landscape also supplies the diversity of specific resources required for one or more terrestrial species to achieve population growth rates greater than or equal to zero. The ecological function of seascapes and landscapes is exactly the same.

The next step in the analysis is to use the system function to guide the development of conceptual models of interacting components

based on fundamental "laws". The components of seascapes are living organisms and the specific external environmental characteristics and resources that regulate, control, and limit performance rates underlying population growth. The fundamental "law" that applies to all living organisms is that cellular metabolism fuels individual performance and population productivity (Fry, 1947; Neill *et al.*, 1994; Brown, 2004; Sousa *et al.*, 2008; Sibly *et al.*, 2012). The core metabolic machinery and processes through which energy is acquired, transformed, and allocated to do biological work are conservative (Hochachka and Somero, 2002). For metabolism to occur: proteins, enzymes, nucleic acids, lipids and lipoprotein cell walls, and the structured water supporting them must be both stable and flexible. The dynamic stability of metabolic machinery and its sustained operation are extremely sensitive to specific conditions in the extracellular environment that are universally required. These specific extracellular conditions are defined by the availability of water, the nature and concentrations of solutes, the availability of molecular oxygen, and for plants, carbon dioxide. Pressure affects the availability of gases essential to specific metabolic pathways and enzyme structure. Temperature also affects the structural integrity of enzymes and regulates metabolic reaction rates. Finally raw materials serving as building blocks for metabolic machinery and as "fuel" for respiration, photosynthesis, and chemosynthesis are required. These materials include light, inorganic nutrients required by photosynthetic plants, chemical compounds for chemosynthesizers, as well as organic "food" for respiration. Our models of living organisms: the way they are structurally, physiologically and behaviorally designed; must be consistent with the law that organisms must meet these specific, universal and conservative requirements of metabolism. Organisms living in the sea and on land must meet exactly the same core metabolic requirements using structural adaptation, physiological regulation and behavioural habitat selection.

The fundamental "law" pertaining to the external environment must be its physical properties. Here, the sea and land are very different, particularly with respect to external environmental properties affecting the intracellular environment and metabolism (Table 1). We can use the specific metabolic requirements to organize a discussion of the physical properties of the environment and the degree to which organisms meet a requirement by habitat selection and, or mechanisms of internal regulation that allow for physiological decoupling from the external environment. Since seascape and landscape systems emerge from interactions between organisms and the environment, the approach should allow us to identify basic differences in the properties and processes structuring and regulating seascape and landscape systems.

The challenge of maintaining water-solute balance in tissues required for cellular metabolism is determined by the strengths of concentration gradients of water and solutes crossing from tissues to the external environment (Denny, 1993; Hochachka and Somero, 2002; Costa *et al.*, 2013; Larsen *et al.*, 2014). Organisms in seawater are exposed to much weaker concentration gradients for both water and osmotically active solutes than are terrestrial organisms surrounded by the atmosphere (Table 1). In the oceans, liquid water is certainly not a limited habitat resource. Furthermore, when compared with the atmosphere, osmotically active elements and compounds are abundant in seawater at concentrations relatively near those required by metabolically active tissues. Concentrations of hydrogen ions in seawater are also relatively close to concentrations necessary for the normal functioning of mitochondria and blood. Since water, salt, and pH content of the external environment is relatively similar to concentrations required within metabolically active tissues, organism in the sea conform to, or rely on relatively weak physiological regulation and habitat selection for volumes of ocean liquid with required properties. In contrast, the atmosphere surrounding terrestrial organisms is largely devoid of biologically accessible water and solutes including hydrogen ions. To maintain concentrations of water, salts, and ions required by metabolically active tissues against strong concentration gradients, terrestrial organisms use strong physiological regulation of tissue water-ion balance to partially decouple internal from external environments. They combine internal regulation with strong habitat selection for patches of water and food containing essential ions concentrated by gravity along the interface between land and the atmosphere.

On the other hand, gases essential to respiration and photosynthesis are much scarcer in the sea than on land. Oxygen dissolved in seawater is about 2.5% of the concentration of the gas in the atmosphere (Denny, 1993; Table 1). Oxygen diffuses ~10 000 times more slowly in seawater than air. In the ocean, most organisms inspire seawater to extract oxygen from solution using specialized structures like gills. Oxygen is an important limiting habitat resource in the sea and most marine organisms seek out volumes of ocean liquid with the oxygen concentrations necessary for specific levels of metabolic performance (Prince *et al.*, 2010; Trueblood and Seibel, 2012; Brady and Targett, 2013). Carbon dioxide concentrations are not low in the ocean, but diffusion of the gas is just as slow in seawater as it is for oxygen (Table 1). Carbohydrate synthesis would be limited by the slow diffusion of carbon dioxide for many photosynthetic marine plants if it were not for their small body sizes, high surface area to volume ratios and the ability to use bicarbonate as an alternative carbon source (Denny, 1993). The solubility and exchange of gases between tissues and the external environment are also affected by pressure. At sea level pressure is about 1.013 bar and increases 1.013 bar with each 10 m increase in water depth in the ocean. Decreases in pressure with each 10 m increase in altitude in the atmosphere occur nearly 1000 times more slowly (0.0012 bar 10 M^{-1}). In the atmosphere, concentrations of oxygen and carbon dioxide and their diffusivities and partial pressures are usually high enough that essential gases are not limited habitat resources except in subterranean and high altitude landscapes (Denny, 1993; Hochachka and Somero, 2002). Oxygen is, in fact, superabundant in most of the atmosphere and many terrestrial organisms have evolved metabolic pathways to cope with the oxygen toxicity (Hochachka and Somero, 2002).

Temperature sets the pace of metabolism and the thermal properties of seawater in the ocean and air in the atmosphere are also profoundly different (Denny, 1993; Kingsolver, 2009; Table 1). The heat capacity of the ocean is four times higher than the atmosphere while the rate of heat transfer by conduction is 23 times faster in seawater than air. The exchange of heat between objects with temperatures different from the surrounding fluid by free convection and forced convection occurs ~100 times, and 200 times faster in the sea than on land. High heat capacity and transfer rates combined with the huge volume of seawater in the ocean limits ranges and rates of change of temperature in the marine environment (Steele, 1991; Mamayev, 1996). Most organisms living in the ocean do not need strong internal mechanisms of thermoregulation to maintain body temperatures in the range required by metabolism. This is fortuitous because rates of convective heat transfer are so high in the sea that physiological thermoregulation is too costly for most water "breathing" organisms (Pauly, 2010). With oxygen in such short

Table 1. Physical properties of seawater surrounding organisms in seascapes and air surrounding organisms on landscapes, their ratios and effects on metabolic requirements and energetics.

Physical property (units)	Seawater (@20 °C and 3.5%)	Air (@20 °C)	Ratio seawater:air	Effect on metabolism and energetics	Additional comments
Density (kg m^{-3})	1024.76	1.205	850.4232	Relative effects of drag and gravity on particle transport, movement, and buoyancy	Tissue densities: fat = 930, muscle = 1065, bone = 2500, shell = 2700
Dynamic viscosity (N s^{-1} m^{-2})	1.09×10^{-3}	1.82×10^{-5}	59.9560	Relative effects of drag and gravity on particle transport, movement, and buoyancy	
Pressure (bar)	11.0651	1.00125	11.0513	Gas partial pressures. Availability of O_2 for respiration and CO_2 for photosynthesis	Values are for 100 m below and 100 m above sea level
Water content (% by weight)	~100	2	50	Osmotic balance. Scaffold for metabolic machinery	Tissues: 65–90%
Concentration of solutes (% by weight)	3.5	1×10^{-4}	3.5×10^{4}	Osmotic balance	Tissues: 2.8–3.2%
Hydrogen ions in solution ($^{-}$log[mol H^{+} l^{-1}])	7.8–8.4	0		Proper functioning of mitochondria and blood	Mitochondria: 7.5 Blood: 7.34–7.45 Dry air has no PH
Oxygen concentration (mol m^{-3})	0.231	8.714	0.0265	Terminal acceptor in electron transport chain in aerobic respiration	
Oxygen diffusion coefficient (m^{-2} s^{-1})	2.1×10^{-9}	2.03×10^{-5}	1.03×10^{-4}	Terminal acceptor in electron transport chain in aerobic respiration	
Carbon dioxide concentration (mol m^{-3})	9.7×10^{-3}	1.38×10^{-2}	0.7055	Inorganic carbon source for sugar synthesis by plants	
Carbon dioxide diffusion coefficient (m^{-2} s^{-1})	1.77×10^{-9}	1.60×10^{-5}	1.11×10^{-4}	Inorganic carbon source for sugar synthesis by plants	Many marine plants can use bicarbonate
Temperature range (°C)	−2 −32	−88 −58		Enzyme structure. Biochemical reaction rates	
Specific heat capacity (J kg^{-1} K^{-1})	4.18×10^{9}	1.01×10^{3}	4.157	Enzyme structure. Biochemical reaction rates	
Thermal diffusivity (m^{-2} s^{-1})	1.43×10^{7}	2.15×10^{5}	6.65×10^{-3}	Enzyme structure. Biochemical reaction rates	
Thermal expansivity (K^{-1})	2.20×10^{4}	2.15×10^{5}	6.65×10^{-3}	Enzyme structure. Biochemical reaction rates	
Thermal conductivity (W m^{-1} K^{-1})	0.6011	0.0261	23.0307	Enzyme structure. Biochemical reaction rates	
Free convection of heat			~100	Enzyme structure. Biochemical reaction rates	
Forced convection of heat			~200	Enzyme structure. Biochemical reaction rates	At equal Reynolds numbers
Light attenuation coefficient (m^{-1} for wavelength (λ) = 700 nm])	3	3.00×10^{-5}	1.00×10^{5}	Physical energy transformed into biochemical energy by plants. Sensory: Prey detection and predator avoidance	
Speed of sound (m s^{-1})	1521.5	343.4	4.4307	Sensory: Prey detection and predator avoidance	
Acoustic resistance (kg m^{-2} s^{-1})	1.56×10^{6}	4.14×10^{-2}	3767	Sensory: Prey detection and predator avoidance	
Acoustic attenuation (dB km^{-1} [1000 Hz])	0.01	1	0.01	Sensory: Prey detection and predator avoidance	
Electrical resistivity (Ω m^{-1})	2.00×10^{3}	4.00×10^{13}	5.00×10^{11}	Sensory: Prey detection and predator avoidance	

Compiled from Denny (1993), Vogel (1996), and Hochachka and Somero (2002).

supply, generating necessary internal heat in the sea requires complex structural and physiological adaptations that are metabolically expensive. The cost of maintaining body temperature a degree warmer than the surrounding environment by respiration is ~3400 times higher for an organism living in the ocean than for an organism living on land surrounded by the atmosphere (Denny, 1993). Temperature is tyrannical to organisms in the sea and most are "cold blooded" ectotherms whose metabolic rates are strongly

regulated by the temperature of the liquid surrounding them. Mobile marine organisms govern metabolic rates by selecting volumes of liquid at preferred temperatures that are often unique for specific life history stages and events (Magnuson *et al.*, 1979; Magnuson and Destasio, 1997).

In contrast, the heat capacity and heat transfer rates in the atmosphere are low. Temperature ranges and rates of change on land can therefore be extreme and exceed values required for normal, active metabolism on a seasonal or even an hourly basis (Denny, 1993; Hochachka and Somero, 2002). Many terrestrial organisms have combined strong physiological and behavioural regulation to manufacture biochemicals protecting metabolic machinery when conditions become damaging and to regulate internal body temperatures independently of atmospheric temperatures. Even "cold blooded" terrestrial organisms guard against the damaging effects of high and low temperatures and control whole body temperatures by synthesizing macromolecules, generating metabolic heat, by wetting and evaporative cooling, or basking in the sun light or shade available near the land's surface (Angilletta, 2009). Temperature is an important habitat resource for terrestrial organisms too. However, thermal properties of the atmosphere demand a much greater degree of physiological and behavioural decoupling of body temperatures from ambient environmental temperatures. Slow heat transfer rates and the abundance of oxygen in the atmosphere make physiological decoupling from environmental temperatures energetically "cheap" for terrestrial organisms. Species geographic ranges appear shifting in response to rapid changes in environmental temperatures with climate change an order of magnitude more slowly on land than in the sea (Chueng *et al.*, 2009; Sorte *et al.*, 2010). Differences in species range shift speeds in terrestrial and marine ecosystems that are related to environmental temperature should reflect differences in constraints and opportunities for thermoregulation available to organisms immersed in the atmosphere's gases or the liquid of the ocean.

The density and viscosity of water in the ocean and air in the atmosphere ultimately control the availability of the building blocks of metabolism, the generation of metabolic fuel, and the strategies organisms must use to search for and acquire them. The ocean liquid is ~850 times more dense than the gases in the atmosphere and much closer to densities of most living tissues (Table 1; Denny, 1993; Vogel, 1996). The dynamic viscosity of seawater; its resistance to stretching and shearing, is also ~60 times greater than the viscosity of air. The dominant forces controlling movements of particles, including living organisms, and dynamics of foodwebs are different in seascapes and on landscapes because of the differences in densities and viscosities of seawater and air.

In the sea, drag is the primary force controlling movements of materials and organisms because seawater densities and viscosities are so high. Gravity exerts secondary control over movement. A particle the size and density of a phytoplankton sinks 1020 times more slowly in seawater (@20C and 3.5% salt concentration) than a pollen grain, the same size and density, does in air (@ 20C; Vogel, 1996). Drag thins the oceans "soup", dispersing slowly sinking materials required for metabolism that are easily carried downstream. Because most living tissues have densities close to densities of seawater, marine organisms without shells or tests are nearly neutrally buoyant. Most of the three-dimensional structure of the ocean hydrosphere is therefore accessible at little cost to organisms that can adjust buoyancy by changing the specific gravity of their tissues slightly. These organisms then combine morphology and behaviour to manage and sometimes exploit the forces of drag in the moving ocean liquid. Even sessile organisms strongly associated with the seabed have body forms structured to efficiently manage and sometimes exploit the forces of drag with, for example, appendages that sift particles from turbulent flows of the ocean's viscous "soup" (Vogel, 1996; Fish and Lauder, 2006).

Sunlight required for photosynthesis enters the sea surface but is attenuated ~100 000 times faster in seawater than in the nearly transparent atmosphere (Table 1). Organic particles are remineralized back into inorganic nutrients by bacteria as they sink slowly away from well-lit surface waters where mostly mobile, tiny, and short-lived marine plants can use them to synthesize carbohydrates. Vertical mixing and horizontal current flows caused by wind, differences in the salinity and temperature and thus density of the liquid, or tides are required to resupply nutrients to sunlit waters where plants can use them for photosynthesis. Nutrients and other organic compounds essential to metabolism are brought to the surface by divergent upwelling flows or from terrestrial sources upstream. They are carried downstream and concentrated along horizontal or vertical fronts where currents converge to "thicken" the soup (Bakun, 1996). Under these circumstances, ocean habitats are not "places", but diffuse networks of horizontal and vertical flows that converge on nodes concentrating resources derived from sometimes remote upstream sources (Tew Kai *et al.*, 2009; Prants *et al.*, 2014; Prants, 2015). Foodwebs assemble along downstream transport pathways as the building blocks move toward convergent nodes. They assemble over time scales determined by the duration of the forces of wind, density and tide creating networked divergent, transport and convergent flows combined with the generation times and search capabilities of the organisms occupying different trophic levels (Olson, 2002). These diffuse networks are ephemeral oases built upon heterogeneities in the mixing of the ocean liquid because drag is the primary force controlling movement in the sea and episodic atmospheric and planetary tidal forcing control mixing. These are not just open and coastal ocean phenomena associated with large eddies, shelf break canyons, offshore banks, and coastlines (e.g. McGillicuddy *et al.*, 1999; Glenn *et al.*, 2004; Hu *et al.*, 2008; Allen and Hickey 2010). They also occur as structures like turbidity maxima that are essential engines of ecosystem productivity in coastal estuaries (Martino and Houde, 2010).

On terrestrial landscapes processes regulating the generation and availability of the materials and fuels for metabolism are very different because the density and viscosity of air are low enough that gravity is the primary force controlling movements. Terrestrial ecosystems are fuelled by relatively large, long-lived, stationary photosynthetic plants living along the interface between land and the transparent atmosphere where sunlight is abundant. Bacteria remineralize sources of nutrients deposited by gravity along with water in soils in proximity to the roots of plants and available light. The building blocks of terrestrial foodwebs are transported over short distances and brief periods of time except when groundwater flows intervene. On land, most crucial habitat resources are localized and diffuse slowly along the interface between land and the atmosphere. Slow geophysical and biogeochemical processes associated with soil development set the pace of terrestrial foodwebs that have slower, more persistent spatial dynamics than foodwebs in the sea that are regulated by much faster, often episodic hydrodynamic processes (Steele, 1985, 1989).

Summary and implications

Based on analysis performed using Bernhard Riemann's rules, seascapes are fundamentally different from landscapes because organisms living in the ocean's liquid and surrounded by the atmosphere's gases must meet the same core requirements of metabolism using very different mechanisms of internal regulation and habitat selection for external environmental properties. Seascapes and landscapes both provide resources supporting the viability of at least one population of organisms. This ecological function, grounded in the duality of niche and habitat, requires than we identify environmental properties and processes structuring seascapes and landscapes purely based on effects on organism vital rates underlying population growth and inextricable linked to metabolism. In the analysis, the system function guided the development of models of the components of seascapes and landscapes, organisms and the external environment, in a manner consistent with fundamental laws. The universal requirements of metabolism were the laws that applied to organisms. The "laws" applying to the environment were its physical properties that are very different for seascapes and landscapes. Organisms living in the ocean's liquid face a shortage of oxygen required for respiration, energetic constraints on thermoregulation, but relatively weak demand for internal regulation of body temperatures and tissue ion-water balance. Most marine organisms combine strong habitat selection for volumes of ocean liquid with preferred oxygen partial pressures, temperatures, and salt concentrations. Furthermore, since seawater is dense and viscous and drag is the dominant force controlling movements, many marine organisms have access to the three spatial dimensions of the ocean hydrosphere in which the availability of essential metabolic building blocks and fuels are controlled by hydrodynamics. Seascapes are therefore primarily structured by hydrographic properties and hydrodynamics that control their ecological dynamics. The seabed and associated structures provide organisms with important refuges from predation, refuges from or access to high velocity current flows, as well as particle trapping surfaces that are relatively impermeable compared with discontinuities in density and current flow in the water column. Nevertheless, seascapes and the habitats composing them are primarily structured and regulated by properties and processes of the ocean liquid.

In contrast, geography and biogeochemical processes associated with soil development along the interface between land and the atmosphere lie at the foundation of landscape ecology (Troll, 1950). Most terrestrial organisms are partially decoupled by gravity and strong physiological regulation from the dynamics of a thermally variable atmosphere largely devoid of water and salts but abundant with essential gases. Since gravity is the dominant force controlling movement, the atmosphere is inaccessible to most terrestrial organisms that show strong habitat selection for water, food, and other materials concentrated along the land surface. Biogeophysical properties and processes occurring along the interface between land and the atmosphere are the primary features structuring landscapes and driving ecological dynamics. Interactions between organisms with the external environment are different enough in the sea and on land that seascape ecology should not rest on the paradigms of terrestrial landscape ecology. Seascape ecology needs to rest on paradigms consistent with the importance of properties and dynamics of the ocean fluid in driving dynamics if it is to be effectively applied for resource use management in the sea.

Usually, new paradigms emerge from observations made with new tools, not vice versa. New tools are allowing us, right now, to move beyond terrestrial paradigms and to integrate hydrography and hydrodynamics along with functionally important seabed features into a seascape ecology useful for adaptive management in the sea (Allen *et al.*, 2015). These tools are the data and models integrated into the regional Ocean Observing Systems currently being established around the world (Liu *et al.*, 2015). Ocean Observing Systems integrate measurements of ocean properties made by satellites in space, radar on the earth's surface, and robots underwater. The observations are assimilated into numerical ocean models that describe with greater accuracy, precision and transparency, the hydrography and hydrodynamics driving seascape dynamics at scales relevant to the population ecology and marine resource management (Carr *et al.*, 2010; Manderson *et al.*, 2011; Breece *et al.*, 2016). Regional data and models describing the dynamics of the ocean liquid can be integrated with descriptions of ecologically important seabed features into hydrodynamic information systems (HIS) used in applied seascape ecology in the same manner geographic information systems (GIS) are used in applied landscape ecology. HIS are already being used in innovative approaches that could be applied to tune adaptive management strategies to the dynamics of seascapes producing marine resources (Game *et al.*, 2009; Hobday and Hartog, 2014; Hobday and Pecl, 2014; Breece *et al.* 2016; Dunn *et al.* 2016).

Acknowledgements

I thank John Quinlan, Chris Roebuck, Jeff Pessutti, and Josh Kohut whose deep curiosity and intelligent insights into the ocean and the ways organism might live it have been inspiring and have shaped ideas I explored in this essay. I thank David Secor, a coeditor of this issue, for encouraging me to write the essay and pushing it into better shape. Finally, I thank John Lee and my wife Joyce Ferris for helping to make the essay more clear and intelligible.

References

Allen, A. L., Brown, C. W., Lewitus, A. J., and Sandifer, P. A. 2015. The roles of emerging technology and modeling techniques in operational ecological forecasting at NOAA. Marine Technology Society Journal, 49: 193–203.

Allen, S. E., and Hickey, B. M. 2010. Dynamics of advection-driven upwelling over a shelf break submarine canyon. Journal of Geophysical Research: Oceans, 115: C08018.

Angilletta, M. J. 2009. Thermal Adaptation: A Theoretical and Empirical Synthesis. Oxford University Press, Oxford. 285 pp.

Bakun, A. 1996. Patterns in the Ocean: Ocean Processes and Marine Population Dynamics. University of California Sea Grant, San Diego, CA, USA, in cooperation with Centro de Investigaciones Biológicas de Noroeste, La Paz, Baja California Sur, Mexico. 323 pp.

Brady, D. C., and Targett, T. E. 2013. Movement of juvenile weakfish *Cynoscion regalis* and spot *Leiostomus xanthurus* in relation to diel-cycling hypoxia in an estuarine tidal tributary. Marine Ecology Progress Series, 491: 199–219.

Breece, M. W., Fox, D. A., Dunton, K. J., Frisk, M. G., Jordaan, A., and Oliver, M. J. 2016. Dynamic seascapes predict the marine occurrence of an endangered species: Atlantic Sturgeon Acipenser oxyrinchus oxyrinchus. Methods in Ecology and Evolution, 7: doi 10.1111/2041-210X.12532.

Brown, J. H. 2004. Toward a metabolic theory of ecology. Ecology, 85: 1771–1789.

Carnot, S. 1824. Réflexions sur la puissance motrice du feu et sur les machines propres à développer cette puissance. Bachelier, Paris. 38 pp.

Carr, M. H., Woodson, C. B., Cheriton, O. M., Malone, D., McManus, M. A., and Raimondi, P. T. 2010. Knowledge through partnerships: integrating marine protected area monitoring and ocean observing systems. Frontiers in Ecology and the Environment, 9: 342–350.

Chase, J. M., and Leibold, M. A. 2003. Ecological niches: linking classical and contemporary approaches. University of Chicago Press, Chicago. 221 pp.

Chueng, W. W. L., Lam, V. W. Y., Sarmiento, J. L., Kearney, K., Watson, R., and Pauly, D. 2009. Projecting global marine biodiversity impacts under climate change scenarios. Fish and Fisheries, 10: 2–14.

Colwell, R. K., and Rangel, T. F. 2009. Hutchinson's duality: the once and future niche. Proceedings of the National Academy of Sciences of the United States of America, 106: 19651–19658.

Costa, D. P., Houser, D. S., and Crocker, D. E. 2013. Fundamentals of Water Relations and Thermoregulation in Animals. *In* eLS. John Wiley & Sons, Chichester.

Crowder, L. B., Osherenko, G., Young, O. R., Airamé, S., Norse, E. A., Baron, E. A., Day, J. C., *et al.* 2006. Resolving mismatches in U.S. Ocean Governance. Science, 313: 617.

Denny, M. W. 1993. Air and Water: The Biology and Physics of Life's Media. Princeton University Press, Princeton, NJ. 341 pp.

Douvere, F. 2010. The importance of marine spatial planning in advancing ecosystem-based sea use management. Marine Policy, 32: 762–771.

Dunn, D. C., Maxwell, S. M., Boustany, A. M., and Halpin, P. N. 2016. Dynamic ocean management increases the efficiency and efficacy of fisheries management. Proceedings of the National Academy of Sciences of the United States of America, 113: 668–673.

Elton, C. 1927. Animal Ecology. The University of Chicago Press, Chicago. 209 pp.

Fish, F. E., and Lauder, G. V. 2006. Passive and Active Flow Control by Swimming Fishes and Mammals. Annual Review of Fluid Mechanics, 8: 193–224.

Fry, F. E. J. 1947. Effects of the environment on animal activity. University of Toronto Studies Biology Series, 55: 1–62.

Game, E. T., Grantham, H. S., Hobday, A. J., Pressey, R. L., Lombard, A. T., Beckley, L. E., Gjerde, K., *et al.* 2009. Pelagic protected areas: the missing dimension in ocean conservation. Trends in Ecology and Evolution, 24: 360–369.

Gentner, D., and Jeziorski, M. 1993. The shift from metaphor to analogy in western science. *In* Metaphor and Thought, pp. 447–480. Ed. by A. Ortony. Cambridge University Press, Cambridge, UK. 696 pp.

Glenn, S., Arnone, R., Bergmann, T., Bissett, W. P., Crowley, M., Cullen, J., Gryzmski, J., *et al.* 2004. Biogeochemical impact of summertime coastal upwelling on the New Jersey Shelf. Journal of Geophysical Research, 109: C12S02.

Grinnell, J. 1917. The niche-relationships of the California Thrasher. The Auk, 34: 427–433.

Hobday, A. J., and Hartog, J. R. 2014. Derived ocean features for dynamic ocean management. Oceanography, 27: 134–145.

Hobday, A. J., and Pecl, G. T. 2014. Identification of global marine hotspots: sentinels for change and vanguards for adaptation action. Reviews in Fish Biology and Fisheries, 24: 415–425.

Hochachka, P. W., and Somero, G. N. 2002. Biochemical Adaptation: Mechanism and Process in Physiological Evolution. Oxford University Press, Oxford. 480 pp.

Holt, R. D. 2009. Bringing the Hutchinsonian niche into the 21st century: Ecological and evolutionary perspectives. Proceedings of the National Academy of Sciences of the United States of America, 106: 19659–19665.

Hu, S. D., Townsend, W., Chen, C., Cowles, G., Beardsley, R. C., Ji, R., and Houghton, R. W. 2008. Tidal pumping and nutrient fluxes on Georges Bank: A process-oriented modeling study. Journal of Marine Systems, 74: 528–544.

Hutchinson, G. E. 1957. Concluding remarks. Cold Spring Harbor Symposia on Quantitative Biology, 22: 415–442.

Hutchinson, G. E. 1978. An Introduction to Population Biology. Yale University Press, New Haven. 260 pp.

Kingsolver, J. G. 2009. The well-temperatured biologist. The American Naturalist, 174: 755–768.

Larsen, E. H., Deaton, L. E., Onken, H., O'Donnell, M., Grosell, M., Dantzler, W. H., and Weihrauch, D. 2014. Osmoregulation and excretion. Comprehensive Physiology, 4: 405–573.

Liu, Y., Kerkering, H., and Weisberg, R. H. 2015. Coastal Ocean Observing Systems. Academic Press, London. 490 pp.

Magnuson, J. J., Crowder, L. B., and Medvick, P. A. 1979. Temperature as an ecological resource. American Zoologist, 19: 331–343.

Magnuson, J. J., and Destasio, B. T. 1997. Thermal niche of fishes and global warming. *In* Global Warming: Implications for Freshwater and Marine Fish, pp. 377–408. Ed. by C. M. Wood, and D. G. McDonald. Cambridge University Press, Cambridge. 425 pp.

Mamayev, O. I. 1996. On space-time scales of oceanic and atmospheric processes. Oceanology, 36: 731–734.

Manderson, J., Palamara, L., Kohut, J., and Oliver, M. J. 2011. Ocean observatory data is useful for regional habitat modeling of species with different vertical habitat preferences. Marine Ecology Progress Series, 438: 1–17.

Martino, E. J., and Houde, E. D. 2010. Recruitment of striped bass in Chesapeake Bay: spatial and temporal environmental variability and availability of zooplankton prey. Marine Ecology Progress Series, 409: 213–228.

McGillicuddy, D. J., Johnson, R., Siegel, D. A., Michaels, A. F., Bates, N. R., and Knap, A. H. 1999. Mesoscale variations of biogeochemical properties in the Sargasso Sea. Journal of Geophysical Research: Oceans, 104: 13381–13394.

Mumby, P. J., Elliott, I. A., Eakin, C. M., Skirving, W., Paris, C. B., Edwards, H. J., Enríquez, S., *et al.* 2011. Reserve design for uncertain responses of coral reefs to climate change. Ecology Letters, 14: 132–140.

Neill, W. H., Miller, J. M., Van Der Veer, H. W., and Winemiller, K. O. 1994. Ecophysiology of marine fish recruitment: a conceptual framework for understanding interannual variability. Netherlands Journal of Sea Research, 32: 135–152.

Norse, E. A. 2010. Ecosystem-based spatial planning and management of marine fisheries: why and How? Bulletin of Marine Science, 86: 179–195.

Olson, D. B. 2002. Biophysical dynamics of ocean fronts. In The Sea, 12, pp. 187–218. Ed. by A. R. Robinson, J.J. McCarthy, and B.J. Rothchild. Harvard University Press, Cambridge, MA.

Pauly, D. 2010. Gasping fish and panting squids: oxygen, temperature and the growth of water-breathing animals. *In* Excellence in Ecology: Book 22. Ed by O. Kinne. International Ecology Institute, ldendorf/Luhe, Germany. 216 pp.

Prants, S. V. 2015. Chaotic Lagrangian transport and mixing in the ocean. arXiv:1502.01419 [physics.ao-ph].

Prants, S. V., Budyansky, M. V., and Uleysky, M. Y. 2014. Identifying Lagrangian fronts with favourable fishery conditions. Deep Sea Research Part I: Oceanographic Research Papers, 90: 27–35.

Prince, E. D., Luo, J., Phillip Goodyear, C., Hoolihan, J. P., Snodgrass, D., Orbesen, E. S., Serafy, J. E., *et al.* 2010. Ocean scale hypoxia-based habitat compression of Atlantic istiophorid billfishes. Fisheries Oceanography, 19: 448–462.

Ritchey, T. 1991. Analysis and synthesis: on scientific method – based on a study by Bernhard Riemann. Systems Research, 8: 21–41.

Sibly, R. M., Brown, J. H., and Kedric-Browth, A. 2012. Metabolic Theory: A Scaling Approach. Wiley-Blackwell, West Sussex. 361 pp.

Sorte, C. J. B., Williams, S. L., and Carlton, J. T. 2010. Marine range shifts and species introductions: comparative spread rates and community impacts. Global Ecology and Biogeography, 19: 303–316.

Sousa, T., Domingos, T., and Kooijman, S. A. L. M. 2008. From empirical patterns to theory: a formal metabolic theory of life. Philosophical Transactions of the Royal Society of London, Series B: Biological Sciences, 363: 2453–2464.

Steele, J. H. 1985. A comparison of terrestrial and marine ecological systems. Nature, 313: 355–358.

Steele, J. H. 1989. The ocean "landscape". Landscape Ecology, 3/4: 185–192.

Steele, J. H. 1991. Marine ecosystem dynamics: comparison of scales. Ecological Research, 6: 175–183.

Tew Kai, E., Rossi, V., Sudre, J., Weimerskirch, H., Lopez, C., Hernandez-Garcia, E., Marsac, F., *et al.* 2009. Top marine predators track Lagrangian coherent structures. Proceedings of the National Academy of Sciences of the United States of America, 106: 8245–8250.

Troll, C. 1950. The geographic landscape and its investigation. Stadium Generale, 3: 163–181.

Trueblood, L. A., and Seibel, B. A. 2012. Critical depth in the jumbo squid, *Dosidicus gigas* (Ommastrephidae), living in oxygen minimum zones I. Oxygen consumption rates and critical oxygen partial pressures. Deep Sea Research, 95: 218–224.

Vogel, S. 1996. Life in Moving Fluids: The Physical Biology of Flow, 2nd edn. Princeton University Press, Princeton. 488 pp.

Handling editor: David Secor

ICES Journal of Marine Science

ICES Journal of Marine Science (2016), 73(7), 1839–1850. doi:10.1093/icesjms/fsw086

Contribution to the Themed Section: '*Seascape Ecology*'

Quo Vadimus

Seascapes as a new vernacular for pelagic ocean monitoring, management and conservation

Maria T. Kavanaugh[1]*‡, Matthew J. Oliver[2‡], Francisco P. Chavez[3], Ricardo M. Letelier[4], Frank E. Muller-Karger[5], and Scott C. Doney[1]

[1]*Marine Chemistry and Geochemistry, Woods Hole Oceanographic Institution, Woods Hole, MA 02540, USA*
[2]*School of Marine Science and Policy, University of Delaware, Lewes, DE 19958, USA*
[3]*Monterey Bay Aquarium Research Institute. Moss Landing, CA 95039, USA*
[4]*College of Earth, Ocean, and Atmospheric Sciences, Oregon State University, Corvallis, OR 97331, USA*
[5]*College of Marine Science, University of South Florida, St. Petersburg, FL 33701, USA*

**Corresponding author: tel: +1 508 289 3552; fax: +1 508 289 2193; e-mail: mkavanaugh@whoi.edu.*
‡These authors contributed equally to this manuscript.

Kavanaugh, M. T., Oliver, M. J., Chavez, F. P., Letelier, R. M., Muller-Karger, F. E., and Doney, S. C. 2016. Seascapes as a new vernacular for pelagic ocean monitoring, management and conservation. – ICES Journal of Marine Science, 73: 1839–1850.

Received 17 September 2015; revised 25 April 2016; accepted 28 April 2016.

For terrestrial and marine benthic ecologists, landscape ecology provides a framework to address issues of complexity, patchiness, and scale—providing theory and context for ecosystem based management in a changing climate. Marine pelagic ecosystems are likewise changing in response to warming, changing chemistry, and resource exploitation. However, unlike spatial landscapes that migrate slowly with time, pelagic seascapes are embedded in a turbulent, advective ocean. Adaptations from landscape ecology to marine pelagic ecosystem management must consider the nature and scale of biophysical interactions associated with organisms ranging from microbes to whales, a hierarchical organization shaped by physical processes, and our limited capacity to observe and monitor these phenomena across global oceans. High frequency, multiscale, and synoptic characterization of the 4-D variability of seascapes are now available through improved classification methods, a maturing array of satellite remote sensing products, advances in autonomous sampling of multiple levels of biological complexity, and emergence of observational networks. Merging of oceanographic and ecological paradigms will be necessary to observe, manage, and conserve species embedded in a dynamic seascape mosaic, where the boundaries, extent, and location of features change with time.

Keywords: biodiversity, conservation, landscape, ocean observations, pelagic, phytoplankton, seascape.

Beyond the yellow pine woods there lies a world of rocks of wildest architecture . . . towers and spires, pinnacles and slender domed columns, are crowded together, and feathered with sharp-pointed Engelmann spruces, making curiously mixed forests,–half trees, half rocks. Level gardens . . . in the midst . . . offer charming surprises, and so do the many small lakes with lilies on their meadowy borders . . . together forming landscapes delightfully novel, and made still wilder by many interesting animals,–elk, deer, beavers, wolves squirrels, and birds. – John Muir, Our National Parks

Introduction

John Muir was one of the most persuasive naturalists and conservationists of the 19th and 20th centuries. Muir's capacity to weave

his observations into the language of grand emergent landscapes led to a transformation in the consciousness about conservation in United States. The idea of conserving whole landscapes, pieces of land on length scales of 10s to 1000s of kilometres, continues to be a driving force for environmental legislation (Mace, 2014). On terra firma, the landscape concept and development of landscape ecology science have informed our understanding of the controls on biodiversity, system responses to climate change or land-use strategies, and the application of ecosystem management practices (Turner *et al.*, 2003; Turner, 2005). Likewise, understanding and planning for marine pelagic ecosystem change will require a comprehensive and multi-scale seascape framework (Game *et al.*, 2009; Lewison *et al.*, 2015) that draws upon the domains of landscape ecology and oceanography.

Marine ecosystems face multiple stressors associated with global change, including warming, reduced oxygen, reduced pH, and reduced productivity (Gruber, 2011; Doney *et al.*, 2012). Projecting future change is problematic because individual pressures may have different and or overlapping spatial footprints (Bopp *et al.*, 2013; Boyd *et al.*, 2015) or affect ecosystems differently at local and global scales. Climate-related drivers can also interact with over- or selective harvesting, eutrophication, and land-use change (Perry *et al.*, 2010; Hidalgo *et al.*, 2012; Saunders *et al.*, 2015) leading to context dependency. Furthermore, geographic shifts are evident in species ranges (Pereira *et al.*, 2010; Sorte *et al.*, 2010), extents of whole ecosystems (Polovina *et al.*, 2008; Irwin and Oliver, 2009), and boundaries or dispersal corridors via shifting current regimes (Treml *et al.*, 2008; Ling *et al.*, 2009). Thus scale, context-dependency, and shifting geographies make it difficult for managers and policy makers to adapt to, plan for, or mitigate the multiple stressors on pelagic ecosystems (Crowder *et al.*, 2006; Muller-Karger *et al.*, 2014).

Since Muir's time, problems of environmental complexity, patchiness, and scale have become areas of intensive research for terrestrial and marine ecologists (Paine and Levin, 1981; Steele, 1991; Levin, 1992; Schneider, 2001). Terrestrial and marine benthic ecology draw from landscape ecology theory to address these issues, which also include spatial context sampling bias, and edge effects (Turner, 2005). Landscapes are conceptual models of systems shaped by the local geomorphology, environmental conditions, and biological processes (Wiens, 1976; Turner *et al.*, 2001; Turner, 2005). Landscapes are typically analysed as mosaics of habitats or patches in a region (Forman, 1995; Turner *et al.*, 2001). Landscape models describe the varying composition and shapes of different adjacent habitats (Forman and Godron, 1981), as well as the composite dynamics of individual patches and their interactions at adjacent hierarchical levels (Wu and Loucks, 1995; Moorcroft *et al.*, 2001).

The marine environment can also be viewed as a mosaic of distinct seascapes, with unique combinations of biological, chemical, geological, and physical processes that define habitats which change over time (Steele, 1991; Karl and Letelier, 2009; Kavanaugh *et al.*, 2014*a*). Intertidal zones, coral reefs, seamounts, and seagrass beds can be treated as flooded, marine versions of landscapes that structure mobile populations (Paine and Levin, 1981; Wedding *et al.*, 2011). Traditional definitions of seascape ecology have focused on the study of how relatively static habitat structure influences the ecological processes and the spatial patterns of marine species (Pittman *et al.*, 2011). However, pelagic seascapes are fuelled by planktonic processes, where the size and behaviour of organisms contribute to patch scales that are coherent with dynamic physical oceanographic structures. Pelagic seascapes are shaped by hydrology and turbulence that varies in space, time, and depth. Thus to adapt tenets of landscape ecology to the pelagic realm, we must create a framework that allows for dynamic geographic shifts in planktonic habitat that influence the spatiotemporal patterns of ecological interactions and species distributions. In the next sections, we review the key differences between landscapes and seascapes and historical understanding of seascape structure in the pelagic realm. We then discuss the transfer of the landscape paradigm to modern oceanography through the maturation of synoptic time series from satellites and models, robust methods for classifying seascape patches in space and time, and emergence of autonomous observing systems and networks. Finally, we provide recommendations that facilitate the application of dynamic seascape ecology to marine resource management.

Pelagic seascapes are fuelled by microbes

Mostly invisible to the naked eye, photosynthetic phytoplankton are responsible for approximately half of the global primary production (Field *et al.*, 1998; Behrenfeld *et al.*, 2001), and form the biogeochemical and ecological foundation of pelagic ecosystems. Phytoplankton, bacterioplankton, and many zooplankton have rapid response times to physical perturbation or blooms, often with generation times-scales as short as a day. Observations of lower trophic level dynamics, the primary biophysical interactions of the seascape, require technologies that can measure quick changes in small life forms that are spread out over large areas, in often harsh and remote environments.

The cumulative distribution of variability, from subseasonal to interannual, and across different landscapes and seascapes, is in part, a function of the interaction between physical perturbations and of the life history of primary producers that supply and structure the rest of the ecosystem. This partitioning of variability, and thus the potential upon which natural selection to act, is much different from land to sea (Steele, 1985; Caswell and Cohen, 1995). For example, there are areas of the ocean and on continental masses where annual primary production levels are similar (Figure 1a), but the response time of marine primary producers is much more rapid than dominant terrestrial primary producers (Figure 1b) shifting the distribution of variance to higher frequencies. These are the time scales at which secondary consumers must respond, and the scales at which observers of these phenomena must sample to characterize, and predict these processes. Ultimately, these are also scales over which human activities should be managed in order to affect an outcome on a changing ecosystem services.

Seascapes in motion: advection vs. behaviour

Dispersal and diffusion create and maintain physical and ecological patchiness in terrestrial and aquatic systems (Okubo and Levin, 2001; Turner *et al.*, 2001). However, pelagic organisms inhabit a turbulent, moving fluid where advection interacts with organism size, swimming speed (Beamish, 1978; Blackburn and Fenchel, 1999; Hansen *et al.*, 1997) and behaviour (Keister *et al.*, 2011; Kiørboe and Jiang, 2013) to affect dispersal and migration scales and strategies. Particularly, at intermediate sizes and trophic levels, vertical migration, predator avoidance, and foraging or reproductive behaviour can affect aggregation (Folt and Burns, 1999), and our capacity to predict distributions from more easily observed or modelled physical phenomena.

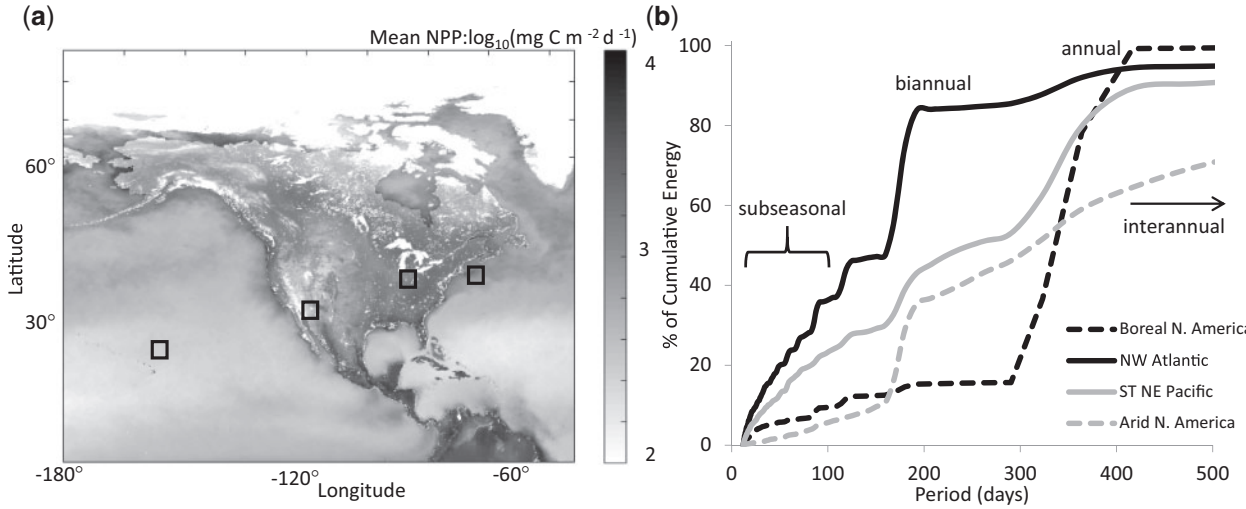

Figure 1. Temporal variability of comparable landscapes and seascapes. (a) Mean Net Primary Production on land and sea derived from Zhao *et al.* (2005), and Behrenfeld and Falkowski (1997). (b) Cumulative variability of primary producer standing stock derived from spectral analysis of time series within landscapes and seascapes (black boxes). Time series were spatially binned 8-d averages of Leaf Area Index in landscapes and Chl *a* in seascapes from the Terra and Aqua MODIS sensors.

The Reynolds number (*Re*) is a dimensionless number that relates the density (ρ), viscosity (μ) and velocity (U) of a body relative to the fluid to the length scale (L) of an object:

$$\mathrm{Re} = \frac{\rho U L}{\mu}$$

where $\rho = \mathrm{kg\ m^{-3}}$, $\mu = \mathrm{kg\ m^{-1}\ s^{-1}}$, $U = \mathrm{m\ s^{-1}}$, $L = \mathrm{m}$.

The length scales of organisms moving through the marine environment span over seven orders of magnitude (Figure 2). At $Re < \sim 100$, an organism's movement through the fluid is limited by the viscosity of the fluid. The dispersal of neutrally buoyant, microscopic phytoplankton, therefore, is driven by advection, although some phytoplankton can escape physicochemical regimes by swimming vertically or adjusting buoyancy (Villareal *et al.*, 1999; Mitchell *et al.*, 2008).

Zooplankton and krill occupy a intermediate range of *Re;* variation in ocean currents, life history stage, and behaviour determine the relative importance of advection compared to movement, growth, and death to the patch scale. Copepods and small euphausiids on average have swimming speeds that are slow relative to horizontal velocities, but fast relative to vertical velocities allowing them to utilize the depth gradients to their advantage (Keister *et al.*, 2011; Lindsey and Batchelder, 2011), but also smearing the apparent patch scale. Copepods swim slowly while foraging, but burst to a speed equivalent to 500 body-lengths per second to avoid being eaten (Kiørboe and Jiang, 2013). Larger zooplankton and fish aggregate in swarms or schools to avoid predation by their larger and faster predators (Parrish and Edelstein-Keshet, 1999). Within swarm heterogeneity is affected by foraging and reproductive behaviours (Folt and Burns, 1999), but also may be a response to smaller predators (Kaltenberg and Benoit-Bird, 2013). Thus, this intermediate control can influence trophic interactions, population connectivity, and very local to mesoscale patchiness of the system.

Large organisms can overcome physical water movement, through complex body structures, physiological adaptations, and behaviour (Nathan *et al.*, 2008). However, the location of large

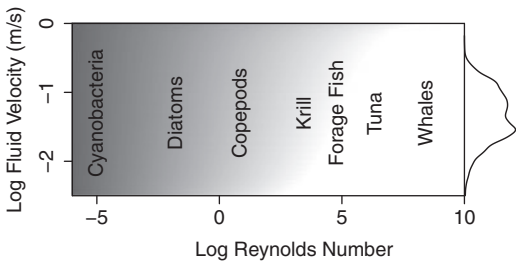

Figure 2. Reynolds number of potential seascape constituents and their environmental fluid velocities. Both axes are $\log_{10}$ transformed. Reynolds number for marine organisms is shown only for adults and is primarily determined by size. Shading indicates the relative importance of advection relative to organism migration patterns, with darker grey showing greater importance. The normalized distribution of upper ocean (100 m) horizontal current speeds across the global ocean is shown in the right margin from the NOAA OSCAR product.

organisms is also related to advective and physicochemical components of seascapes, because of life history, physiological, or food web linkages. For example, the *Re* for an adult tuna is $\sim 10^6$, whereas juvenile tuna are planktonic with $Re < 100$, creating advective control of early life history patch scales that are similar to lower trophic levels. Large-scale seasonal migrations are often strongly related to temperature and productivity, both of which also have strong seasonal signals. Larger predators often aggregate at ocean frontal boundaries, where physical processes such as upwelling enhance local planktonic productivity and biomass (Polovina *et al.*, 2001; Woodson and Litvin, 2015). Indeed, spatial heterogeneity of the prey field may structure predators even with vastly different foraging strategies (Santora *et al.*, 2012; Benoit-Bird *et al.*, 2013). Thus, despite differences across size classes, trophic status, and behavioural complexity, there are coherent scales of "apparent" diffusivity (Okubo and Levin, 2001), where biological organization may align with physical organization, but due to multiple mechanistic processes.

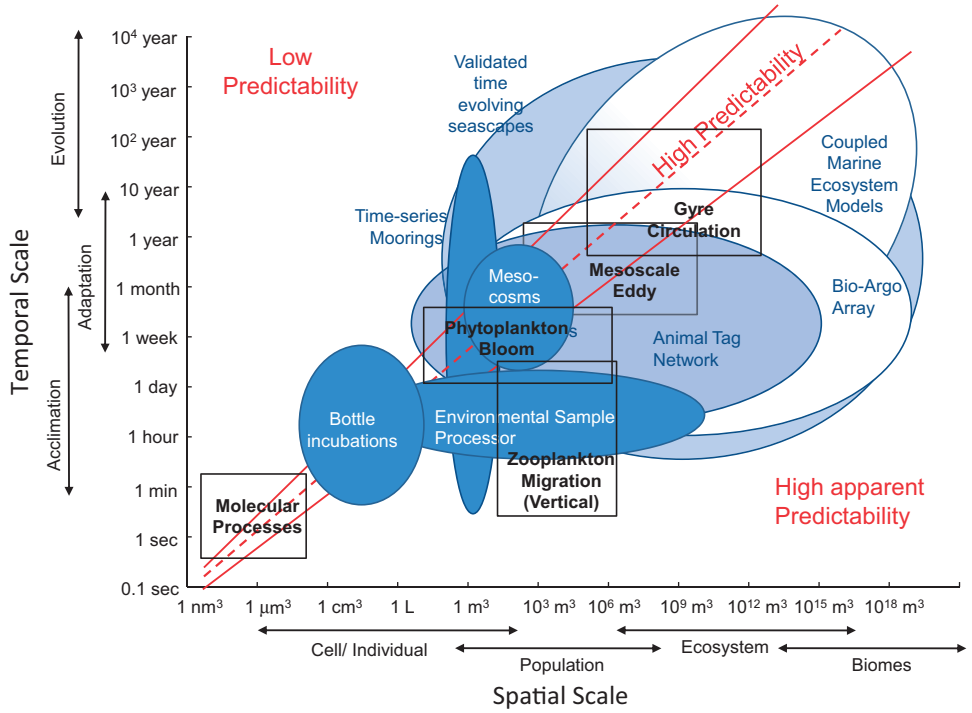

Figure 3. Stommel diagram showing time and space scales for typical biophysical phenomenon (squares) and our current observational capacity (ovals) (after Marquet *et al.*, 1993; Dickey, 2003). Shading denotes level of ecological complexity that the measurements provide with explicit community structure provided by the darkest shading. See text for further detail.

Seascapes organization and dynamic bio-physical hierarchies

Hierarchy theory has provided a means to scale between local mechanistic observations and regional and global models (Wu and Loucks, 1995; Wu, 1999). One focus of hierarchies within landscape ecology has been on spatial scales (Kotlier and Wiens, 1990; Wu and Hobbs, 2002; but see Gillson, 2009); e.g. episodic erosion by rivers and streams results in hierarchical or fractal scaling of a tributary system (Burrough, 1981). Other hierarchies are defined in terms of food chain dynamics and directions of cascades; the role of evolution in population dynamics, of populations in communities, and communities in ecosystems; and the role of "functional" diversity in organizing an otherwise chaotic biosphere (Levins, 1969; O'Neill *et al.*, 1986, 1992; Lidecker, 2008; Devictor *et al.*, 2010).

Physical hierarchies, driven by atmospheric ocean interactions and ocean circulation features, have led historical studies of seascapes. Stommel (1963) recognized that physical ocean structures followed a power law cascade as energy dissipated from gyre circulation to small-scale turbulence (Kolmogorov, 1941; Okubo, 1971). Biological oceanographers and fisheries ecologists modified Stommel's space–time diagram to depict dominant patch scales observed for phytoplankton, zooplankton, and fish (Haury *et al.*, 1978; Steele, 1978). Concurrently, oceanographers and limnologists recognized that the fractal nature of the physical phenomenon could be used to predict biological scales (Denman *et al.*, 1977; Fasham, 1978; Gower *et al.*, 1980). Experimental and modelling evidence have also demonstrated that phytoplankton aggregate at centimetre to metre scales (Mitchell *et al.*, 2008). Thus the biophysical structure of seascapes span the scales of intermittent turbulent eddies to fronts or boundaries associated with vertical mixing, mesoscale circulation, and gyres.

The complex interdependency between energy dissipation, other physical processes, and biology is evident within the Stommel diagram (Figure 3). Many phenomena align along an axis in time–space dimensions with what would be predicted with either energy dissipation or apparent scale-dependent eddy diffusivity (Okubo, 1971). For example, the horizontal spatial scale of mesoscale eddies is set by the Rossby radius of deformation, where planetary rotational effects on ocean flow become important, with characteristic times-scales. Mesoscale (~10–100 km; days to weeks) and submesoscale (~1–10 km; hours to days) physical dynamics act to influence biological growth/loss and stir large-scale bio-geophysical property gradients, down to smaller scales (Mackas *et al.*, 1985).

The space–time hierarchy determines the capacity of different methods of observations to observe phenomena of interest (Figure 3). How observations translate to predictive ability is also a matter of continuity and persistence. For example, sampling at fine spatial scales gives little predictive capacity for large scale and long-term processes unless such fine-scale sampling is conducted over long periods. Conversely, sampling shorter term processes infrequently or over larger scales misses key features and characteristics of the processes being observed. This results in poor predictive skill and masks underlying mechanisms (from Wiens, 1989). However, a hierarchical seascape framework presents an effective means to translate local measurements to broader spatio-temporal scales, scales relevant for modelling the effects of global change and enabling whole-ecosystem management in the dynamic ocean (Kavanaugh *et al.*, 2014*a*).

While larger scale circulation patterns can drive linear covariation in biophysical properties (Figure 4a), physiological or

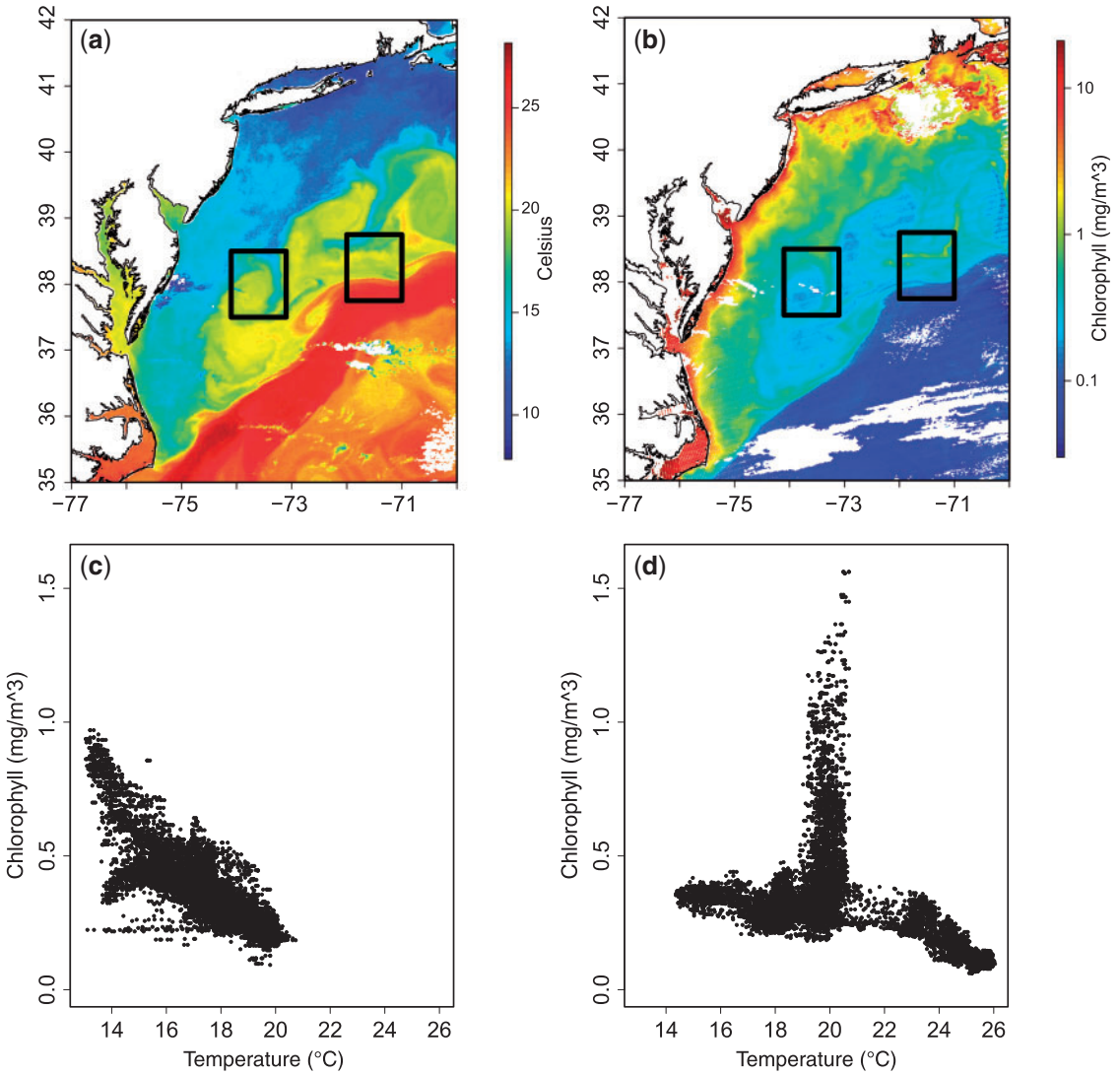

Figure 4. The 23 May 2015 sea surface temperature (a), chlorophyll (b), and the relationship between these two scape predictors in the western box (c) and the eastern box (d). In the western box, temperature and Chl *a* covary, suggesting that biological patterns are driven by regional physics with mixing occurring across a gradient from biomass-rich, cold coastal waters to biomass-poor open ocean conditions. A linear interaction would sufficiently characterize the seascape. In the eastern box, Chl *a* responds in a non-linear fashion to ocean physics with a local peak in Chl *a* values and Chl *a* variance occurring near 19–20 °C associated with the surface expression of the Gulf Stream front. A time-dependent reaction term, e.g. phytoplankton growth or buoyancy response, is necessary to characterize the seascape.

trophic processes may decouple biological and physical scales (Abbott and Letelier, 1998; Lovejoy *et al.*, 2001), particularly at scales < 1 km. Thus, locally, the relationship between physical forcing and biological response may be non-linear (Figure 4b). Indeed, non-linearities are common in biogeochemical (Gruber, 2011; Hales *et al.*, 2012), biophysical (Hsieh *et al.*, 2005), physiological (Jassby and Platt, 1976) and trophic (Litzow and Ciannelli, 2007; Brander, 2010) interactions. Therefore, the heuristic for seascape classification needs to consider a dynamic, hierarchical, and potentially non-linear multivariate topology.

Seascape classification

A major challenge in seascape ecology is the appropriate delineation of hierarchical categories, particularly, in regions where boundaries are diffuse and gradients are shallow (Hinchey *et al.*, 2008). While some argue that the patch mosaic paradigm may obscure underlying pattern–process relationship (Cushman *et al.*, 2010), we assert that the objective partitioning into emergent categories may actually illuminate mechanistic relationships, by disentangling driver responses of different, but adjacent systems (Hales *et al.*, 2012; Kavanaugh *et al.*, 2014b). Furthermore, with maturation of classification methods, synoptic time series, and *in situ* observing systems, oceanography can now employ a piecewise continuous approach (Platt and Sathyendranath, 1999, 2008), where both the mosaic (discrete patches) and continuous nature of the fluid environment within patches are recognized.

Pelagic classification approaches have different names, e.g. biomes, biophysical provinces, seascapes; all represent the practice of identifying water masses with particular biogeochemical features organized in a spatially coherent mosaic. Classification schemes became spatially explicit with the extensive data

provided by satellite-derived measurements (Platt and Sathyendranth, 1999; Longhurst *et al.*, 1995; Longhurst, 1998; Hooker *et al.*, 2000) and biogeochemical models (Sarmiento *et al.*, 2004; Dutkiewicz *et al.*, 2012). These divisions were based primarily on the spatial covariation of annual or multi-year climatological means.

However, climatologies do not adequately characterize dynamic ocean ecosystems (Hardman-Mountford *et al.*, 2008), thus there have been efforts to classify seascapes on seasonal, interannual, and multiple spatial scales. Seasonal dynamics for coastal regions have been inferred with dynamic but discontinuous boundaries (Saraceno *et al.*, 2006; Devred *et al.*, 2007) or by explicitly including seasonal and spatial forcing in their assessments (Hales *et al.*, 2012). Others have applied *post hoc* classifications based on distributions of variables within subjective Longhurst province boundaries on seasonal and annual scales (Fay and McKinley, 2013; Reygondeau *et al.*, 2013). Objective and dynamic seascapes have been classified using satellite remote sensing data on basin (Kavanaugh *et al.*, 2014*a*) and global (Oliver and Irwin, 2008; Irwin and Oliver, 2009) scales by simultaneously clustering pixels in space and time. Each of these methods assumes that seascapes have unique multivariate distributions, that there are natural discontinuities or gradients that delimit seascapes, and that the boundaries change with time. Thus, modern seascape classification merges lower trophic level ecology, geography, and ocean dynamics using observations that are updated regularly and that provide a historical context for reference against which to measure change.

Classification efforts involve a multivariate covariance analysis and will benefit by the use of flexible parametric and non-parametric approaches that explicitly recognize that many processes and interactions in the ocean are non-linear. For example, fuzzy sets and copula (Fauvel *et al.*, 2006; Voisin *et al.*, 2014) have been used to approximate the underlying spatial structure of synthetic aperture radar (SAR) data. Neural networks or self-organizing maps (SOM; Kohonen, 2001) have been used in oceanography to classify coastal biophysical regions (Richardson *et al.*, 2003; Saraceno *et al.*, 2006), to define regions of mechanistic coherence in predictive models (Hales *et al.*, 2012), and to find drivers of net primary productivity (Lachkar and Gruber, 2012). In an extension of the hierarchical patch mosaic paradigm (Wu and Loucks, 1995), Kavanaugh *et al.* (2014*a*) combined a probabilistic SOM with a hierarchical agglomerative clustering algorithm to allow for non-linear interactions and hierarchical organization of seascapes.

Steps toward a seascape framework for conservation or management

The effects of global change and declining ecosystem health are evident in many regional marine systems (Halpern *et al.*, 2014). Seascape ecology can guide conservation, policy, and management strategies. Where and when possible, existing tools and paradigms can be modified to expedite this process and facilitate a cautious, yet deliberate transfer of ecological concepts from landscape ecology to the pelagic realm. Seascape ecology now has the tools to both characterize the spatial heterogeneity in a dynamic fluid environment, while there is also better technology to sample the rich diversity of life within seascapes. Below, we list five specific considerations to focus seascape ecology research in the near-term future.

Develop and test ecological theories

The main principles of landscape ecology (Risser, 1987; Forman, 1995), can be adapted to the sea (Steele, 1989, 1991). These include concepts about the development and dynamics of spatial heterogeneity, interactions and exchanges across heterogeneous landscapes (e.g. how disturbance or invasion is communicated between adjacent patches), influences of spatial heterogeneity on biotic and abiotic processes, and the management of spatial heterogeneity (e.g. forest cuts). Given the influence of advection on both patch-scale and organization, however, the heterogeneity of focus should not be just spatial, but spatiotemporal.

We have focused primarily on challenges associated with adapting the patch mosaic paradigm. Incorporating complementary paradigms, e.g. the gradient paradigm (Cushman *et al.*, 2010) will strengthen our understanding of the drivers of spatiotemporal patterns. This process needs to include a comparison of the efficiency of classification methods, evaluating the assumptions of underlying structure (e.g. hierarchical or diffuse systems), and validating seascape metrics at higher trophic levels (Oliver *et al.*, 2013; Breece *et al.*, 2016). Classification approaches also be complemented by edge or frontal detection techniques (Belkin *et al.*, 2009), and subsequent analysis of the interaction between persistence of features and community structure (Hidalgo *et al.*, 2015). If the underlying topology is maintained, patch boundaries should be demarcated by the discontinuities that result from strong gradients. Multi-scale gradient analysis (Alvarez-Berastegui *et al.*, 2014) can be compared to occupancy metrics within seascape categories (Breece *et al.*, 2016) to determine if habitat preferences can be predicted from the mean seascape state or gradual or abrupt gradients in the underlying hydrographical variables.

Studies should also assess the connectivity between seascape patches and the interactions between adjacent patches across multiple trophic levels and size classes (e.g. between open-ocean and coastal seascapes, or communication between gyres, transition zones). Convergent zones or open ocean fronts delimiting seascapes are ecotones (Ribalet *et al.*, 2010; Woodson and Litvin, 2015), and oceanographers can borrow from landscape theory on boundaries (Cadenasso *et al.*, 2003) to predict or generalize patterns of endemism, exchange, production, and connectivity. Network analysis and graph theoretic approaches may facilitate a lingua franca for conservation ecologists across marine and terrestrial realms (Saunders *et al.*, 2015).

Increase spatial, temporal, and spectral scales

The growing body of satellite based observations can provide multivariate and synoptic characterization of seascape structure. The polar-orbiting SeaWiFS, MODIS-Aqua, and VIIRS ocean colour sensors, have provided an extended time series of global, near daily, ocean colour observations since 1997, providing synoptic information to quantify lower trophic level dynamics at scales from 1 km to global. LIDAR (Young *et al.*, 2013) and polarimetry (Tonizzo *et al.*, 2011) may assist with quantifying ocean particle composition, in addition to facilitating atmospheric correction for ocean colour. Incorporating geostationary and hyperspectral ocean colour data into seascape classification or validation will increase temporal resolution and improve characterization of habitats and assemblages that are affected by tidal scale mixing, diurnal migration, and benthic vegetation (Davis *et al.*, 2007). For example, the multi-spectral radiometers on the

European Sentinel satellites can provide observations of a range of ocean and coastal parameters, at scales ranging from 10 m resolution data on a 5 -d repeat cycle to 1 km resolution every few days. NASA's Pre-Aerosol, Clouds, ocean Ecosystems mission will provide high resolution ocean colour data, possibly with polarimetry to help understand ocean ecosystem and cloud dynamics. Observations from these satellites will be beneficial for mapping benthic and pelagic habitat quality, improve the capacity to detect phytoplankton community structure, and food quality for higher trophic levels. Integrating long wavelength sensors (e.g. radar and microwave) will allow for assessment of spatiotemporal habitat shifts associated with variation in winds (Rykaczewski and Checkley, 2008; Asch, 2015), sea surface topology (including currents and eddies: Cotté *et al.*, 2007; Gaube *et al.*, 2013), temperature, and sea ice (Kavanaugh *et al.*, 2015).

Merge observations with regional and global marine ecosystem models

Coupled regional and global models are tools that help integrate observations to advance understanding of the causes for a particular state of ocean ecosystems (Denman *et al.*, 2010). Model results can fill the gaps, particularly, in the vertical, to understand 3-D patterns of seascapes variables, nutrient dynamics, salinity and mixed layer depth. Once spatial patterns are validated, models can also be used to provide predictions of habitat shifts (Cheung *et al.*, 2010; Hazen *et al.*, 2013).

Integrate organismal level observations

Ship-based and autonomous platforms continue to advance our understanding of the distributions and interactions of pelagic organisms across many trophic and organizational levels. At higher trophic levels, ship-mounted sensors using active acoustic now enable 3-D acoustic imaging of aggregations of fish and large zooplankton (Korneliussen *et al.*, 2009), providing insight into pelagic ecosystem structure (Benoit-Bird and McManus, 2012) and multi-scale patchiness (Kaltenberg and Benoit-Bird, 2013). Several optical imaging sensors, with computer-based image analysis, exist and continue to be developed (Sieracki *et al.*, 2010). Animals are increasingly used as platforms for sensors by use of tags (archival and pop-up satellite), biologging (e.g. instruments attached temporarily to marine mammals) (Boehme *et al.*, 2010; Block *et al.*, 2011), and acoustic listening networks, in which animals with implanted sensors are detected at listening nodes (O'Dor *et al.*, 2009). The ability of autonomous underwater vehicles (AUVs) to track and detect telemetered animals is also becoming a significant tool for understanding seascapes (Grothues *et al.*, 2008; Clark *et al.*, 2013). AUVs provide greater environmental coverage than node-based detection, extend the depth capacity and spatial resolution of acoustic identification (Moline *et al.*, 2016), and facilitate evaluation of dynamic habitat preference of foraging pelagic species (Oliver *et al.*, 2013; Haulsee *et al.*, 2015; Breece *et al.*, 2016).

At lower trophic levels, pigments and microscopy remain critical to distinguishing different components of the phytoplankton and microbial assemblage. Multi- and hyperspectral optics can extend measurements of absorption and scattering spatially, and link in-water qualities to that measured by satellites. Imaging flow cytometry (Sosik and Olson, 2007; Sosik *et al.*, 2014) automates cell counts and discriminates among different types of individual phytoplankton and microzooplankton cells. Using a suite of probes and chemical sensing arrays, the Environmental Sample Processor can detect specific microorganisms and proteins (Scholin *et al.*, 2009) and can archive of samples for microscopy and more detailed molecular analysis (Preston *et al.*, 2009). These are but a few of the technologies being developed that can provide organismal level information to identify and validate dynamic seascapes.

Complement existing management tools and embed seascape ecology and classifications into existing networks

Open-ocean environmental policies are beginning to embrace the concept of dynamic boundaries and subsequent management strategies (Game *et al.*, 2009), although coastal ocean policies are embedded in primarily static, place-based or population-based frameworks. Adaptive management is needed (Agardy *et al.*, 2011), because a static framework simplifies or ignores the dynamic nature of the boundaries of the systems it is trying to manage. From a conservation policy perspective, understanding the spatio-temporal dynamics of seascapes can help local and regional governments plan for, respond and adapt to these changes as well as build partnerships to mitigate jurisdiction mismatches (Crowder *et al.*, 2006). While dynamic seascape ecology serves to characterize basic spatiotemporal patterns of pelagic community structure and function, it can also inform biogeographic assessments for spatially explicit (Caldow *et al.*, 2015) or dynamic ocean management (Lewison *et al.*, 2015; Maxwell *et al.*, 2015). For example, Breece *et al.* (2016) determined that satellite-derived dynamic seascapes were highly predictive of the Endangered Species Act (ESA) listed Atlantic sturgeon (*Acipenser oxyrinchus*), during their spring migration. This study merged of AUV and satellite observations, metrics of occupancy by sturgeon and indices of seascape persistence. Because the ESA listing of Atlantic sturgeon potentially impacts major sink-gillnet fisheries, alternative energy development, and shipping practices in the Mid-Atlantic, these dynamic seascapes are likely to be used to help manage the human impact on this species.

How pelagic seascape ecology is incorporated into observational or management operational strategies may depend on specific conservation goals (Figure 5). Once the periodicity and extent of the processes of interest are defined, relevant technologies can be used to extend the observational capacity to higher frequencies, and horizontal and vertical resolution. For example, satellite-derived dynamic seascape classifications are an integral part of the Marine Biodiversity Observing Network (MBON; Duffy *et al.*, 2013; Muller-Karger *et al.*, 2014). A goal of the MBON is to better understand the effects of climate and coastal ocean dynamics on spatiotemporal dynamics of marine species distributions in order to inform state and federal management. In concert with ship, buoy, and AUV measurements, seascapes categories are being used as an objective extent to plan sampling, conduct rarefaction studies, inter-compare spatial and temporal patterns across trophic levels, test hypotheses of fisheries habitat affinities (Santora *et al.*, 2012), quantify seascape habitat diversity (Whitaker, 1977; Turner, 2005), and examine temporal shifts in habitat quality and availability within existing jurisdictional units.

A seascape observational/analysis framework needs to integrate with national and international observing networks (Figure 5). These include but are not limited to the Global Ocean Observing

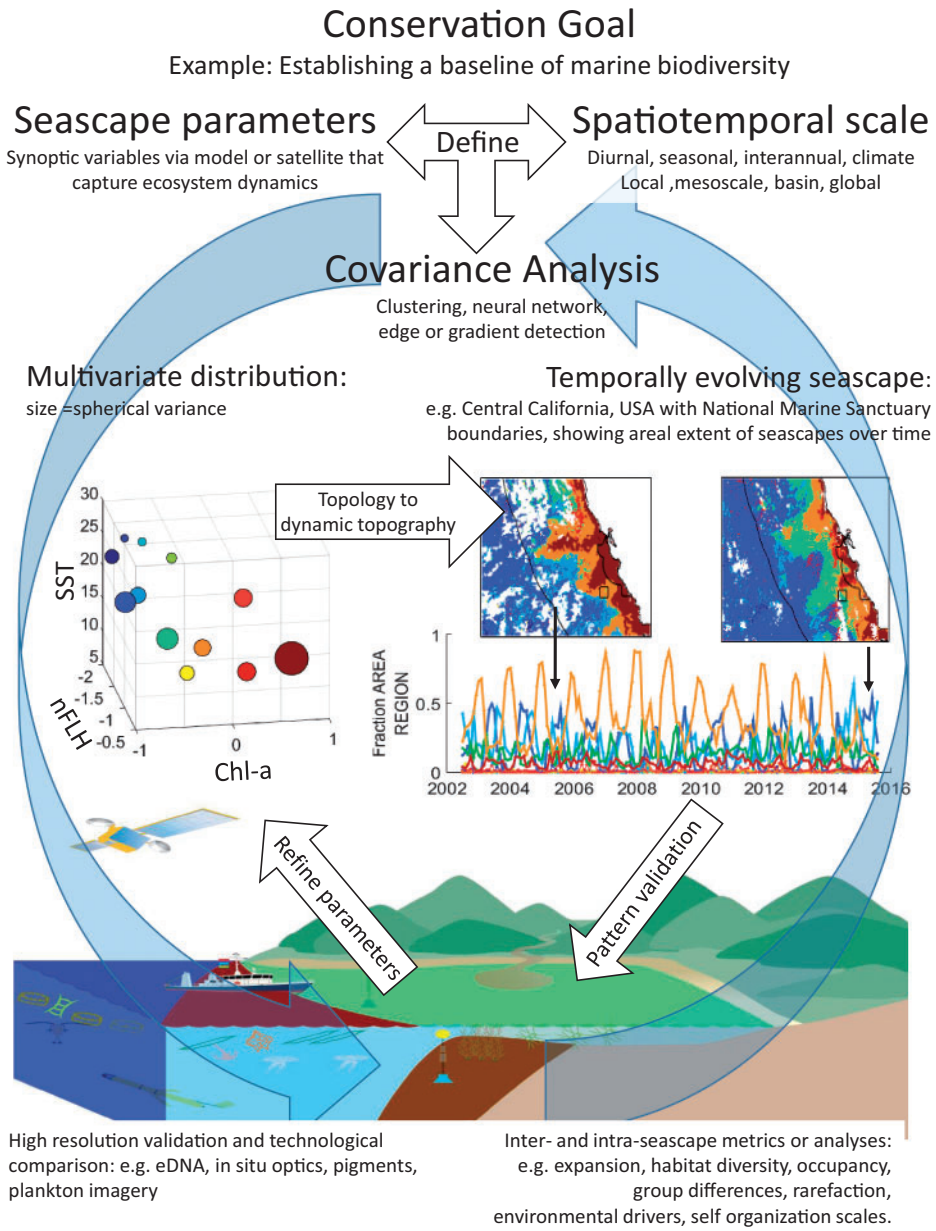

Figure 5. Seascapes as an observational and management tool. Blue arrows denote the interplay between mechanistic hypotheses testing and analyses of emergent patterns. The conservation goal, spatiotemporal scale, and parameters of interest may determine whether synoptic time series of satellite remote sensing (2-D), assimilated marine ecosystem models (3-D) or both are used to define seascapes. Higher resolution *in situ* data can provide vertical data, but also higher resolution organismal information than that provided by remote sensing reflectances or model functional types. Finally, in addition to informing conservation (e.g. rarefaction, patch and boundary analyses), management (trends and oscillations of major habitats) inter- and intra-seascape analyses can inform basic scientific inquiry such as dominant environmental drivers, and scales of biological self-organization (e.g. through partial-mantel tests).

System, the Animal Telemetry Network, Ocean Tracking Network, Ocean Observatories Initiative, Long-Term Ecological Research, ocean time series programs, in addition to the recent MBON. These observatories will provide the organismal data and environmental context necessary for a whole ecosystem understanding of coastal and oceanic systems (Oliver *et al.*, 2013). Conversely, the dynamic and hierarchical seascape framework will provide the biogeographic context to intercompare ecosystems (Murawski *et al.*, 2010) and scale observations to global phenomena.

Conclusion

Ocean ecologists have sought to characterize the hierarchical patch structure of the marine seascapes for over four decades. Adapting landscape ecology concepts to the dynamic open ocean had been hampered by lack of observational capacity and theoretical framework that can address a system fuelled by planktonic processes, moving and expanding patches, and multiple, yet interrelated scales of biophysical interactions. We now have the observational suite necessary and the opportunity to build operational seascape observing systems that integrate multiple

platforms, consider multiple levels of ecological complexity, and accounts for geophysical dynamics of pelagic ecosystems. By combining satellite remote sensing, marine ecosystem models, ship-based measurement and advanced autonomous measurements, we now can evaluate distributions, processes and spatio-temporal patterns of organisms and populations that reflect large variations from plankton to megafauna in mobility, life span, range, and behaviour. A hierarchical seascape observational framework will facilitate transfer and modification of landscape theory to the dynamic and advective marine realm, allow for scaling of mechanistic experiments and observations to patterns of global change, and contribute to real time monitoring and adaptive management of marine ecosystems.

Acknowledgements

This work was supported by NASA grant NNX14AP62A "National Marine Sanctuaries as Sentinel Sites for a Demonstration Marine Biodiversity Observation Network (MBON)" funded under the National Ocean Partnership Program (NOPP RFP NOAA-NOS-IOOS-2014-2003803 in partnership between NOAA, BOEM, and NASA), the NOAA Integrated Ocean Observing System (IOOS) Program Office, and the LenFest Ocean Program. We are grateful for the thoughtful comments of anonymous reviewers and the editors of this special issue, who improved the scope and communication of scientific concepts.

References

Abbott, M. R., and Letelier, R. M. 1998. Decorrelation scales of chlorophyll as observed from bio-optical drifters in the California current. Deep Sea Research Part II: Topical Studies in Oceanography, 45: 1639–1667.

Agardy, T., Di Sciara, G.N., Christie, P. 2011. Mind the gap: addressing the shortcomings of marine protected areas through large scale marine spatial planning. Marine Policy, 35: 226–232.

Alvarez-Berastegui, D., Ciannelli, L., Aparicio-Gonzalez, A., Reglero, P., Hidalgo, M., López-Jurado, J. L., Tintoré, J., *et al.* 2014. Spatial scale, means and gradients of hydrographic variables define pelagic seascapes of bluefin and bullet tuna spawning distribution. PloS one, 9: e109338.

Asch, R. G. 2015. Climate change and decadal shifts in the phenology of larval fishes in the California current ecosystem. Proceedings of the National Academy of Sciences, 112: E4065–E4074.

Beamish, F. W. 1978. Swimming capacity. *In* Locomotion, Ed. by W. S. Hoar and D. J. Randall. Academic Press, Cambridge, MA, USA.

Behrenfeld, M. J., and Falkowski, P. G. 1997. Photosynthetic rates derived from satellite-based chlorophyll concentration. Limnology and Oceanography, 42: 1–20.

Behrenfeld, M. J., Randerson, J. T., McClain, C. R., Feldman, G. C., Los, S. O., Tucker, C. J., Falkowski, P. G. *et al.* 2001. Biospheric primary production during an ENSO transition. Science, 291: 2594–2597.

Belkin, I. M., Cornillon, P. C., and Sherman, K. 2009. Fronts in large marine ecosystems. Progress in Oceanography, 81: 223–236.

Benoit-Bird, K. J., Battaile, B. C., Heppell, S. A., Hoover, B., Irons, D., Jones, N., Kuletz, K. J., *et al.* 2013. Prey patch patterns predict habitat use by top marine predators with diverse foraging strategies. PLoS One, 8: e53348.

Benoit-Bird, K. J., and McManus, M. A. 2012. Bottom-up regulation of a pelagic community through spatial aggregations. Biology Letters, 8: 813–816.

Blackburn, N., and Fenchel, T. 1999. Micro-scale nutrient patches, and implications. Marine Ecology Progress Series, 189: 1–7.

Block, B. A., Jonsen, I. D., Jorgensen, S. J., and Winship, A. J. 2011. Tracking apex marine predator movements in a dynamic ocean. Nature, 475: 86–90.

Boehme, L., Kovacs, K., Lydersen, C., Nøst, O. A., Biuw, M., Charrassin, J. B., Roquet, F. *et al.* 2010. Biologging in the global ocean observing system. *In* Proceedings of OceanObs'09: Sustained Ocean Observations and Information for Society, Vol. 2.

Bopp, L., Resplandy, L., Orr, J. C., Doney, S. C., Dunne, J. P., Gehlen, M., Halloran, P., *et al.* 2013. Multiple stressors of ocean ecosystems in the 21st century: Projections with CMIP5 models. Biogeosciences, 10: 6225–6245.

Boyd, P. W., Lennartz, S. T., Glover, D. M., and Doney, S. C. 2015. Biological ramifications of climate-change-mediated oceanic multi-stressors. Nature Climate Change, 5: 71–79.

Brander, K. 2010. Impacts of climate change on fisheries. Journal of Marine Systems, 79: 389–402.

Breece, M. W., Fox, D. A., Funton, K. J., Frisk, M. G., Jordaan, A., and Oliver, M. J. 2016. Predicting the marine occurrence of an endangered species through satellite derived seascapes. Methods in Ecology and Evolution, 7: 725–733.

Burrough, P. A. 1981. Fractal dimensions of landscape and other environmental data. Nature, 294: 240–242.

Cadenasso, M. L., Pickett, S. T., Weathers, K. C., and Jones, C. G. 2003. A framework for a theory of ecological boundaries. BioScience, 53: 750–758.

Caldow, C., Monaco, M. E., Pittman, S. J., Kendall, M. S., Goedeke, T. L., Menza, C., Kinlan, B. P., *et al.* 2015. Biogeographic assessments: a framework for information synthesis in marine spatial planning. Marine Policy, 51: 423–432.

Caswell, H., and Cohen, J. E. 1995. Red, white and blue: environmental variance spectra and coexistence in metapopulations. Journal of Theoretical Biology, 176: 301–316.

Cheung, W. W., Lam, V. W., Sarmiento, J. L., Kearney, K., Watson, R. E. G., Zeller, D., and Pauly, D. 2010. Large-scale redistribution of maximum fisheries catch potential in the global ocean under climate change. Global Change Biology, 16: 24–35.

Clark, C. M., Forney, C., Manii, E., Shinzaki, D., Gage, C., Farris, M., Lowe, C. G., *et al.* 2013. Tracking and following a tagged leopard shark with an autonomous underwater vehicle. Journal of Field Robotics, 30: 309–322.

Cotté, C., Park, Y. H., Guinet, C., and Bost, C. A. 2007. Movements of foraging king penguins through marine mesoscale eddies. Proceedings of the Royal Society of London B: Biological Sciences, 274: 2385–2391.

Crowder, L. B., Osherenko, G., Young, O. R., Airamé, S., Norse, E. A., Baron, N., Day, J. C., *et al.* 2006. Resolving mismatches in US ocean governance. Science, 313: 617–618.

Cushman, S. A., Gutzweiler, K., Evans, J. S., McGarigal, K. 2010. The gradient paradigm: a conceptual and analytical framework for landscape ecology. *In* Spatial Complexity, Informatics, and Wildlife Conservation. Ed. by S. A. Cushman and F Huettmann. Springer, Japan, pp. 83–108.

Davis, C. O., Kavanaugh, M., Letelier, R., Bissett, W. P., Kohler, D. 2007 September. Spatial and spectral resolution considerations for imaging coastal waters. *In* Optical Engineering+ Applications, Ed. by R. Frouin, International Society for Optics and Photonics, pp. 1–12. DOI: 10.1117/12.734288.

Denman, K., Malone, T., Sathyendranath, S., Sieracki, M., and Vanden Burghe, E. 2010. Observing planktonic ecosystems: needs, capabilities, and a strategy for the next decade, *In* Proceedings of OceanObs'09: Sustained Ocean Observations and Information for Society, Vol. 1, Venice, Italy, 21–25 September 2009. Ed. by J., Hall, D. E., Harrison, and D, Stammer., ESA Publication WPP-306.

Denman, K., Okubo, A., and Platt, T. 1977. The chlorophyll fluctuation spectrum in the sea 1, 2. Limnology and Oceanography, 22: 1033–1038.

Devictor, V., Mouillot, D., Meynard, C., Jiguet, F., Thuiller, W., and Mouquet, N. 2010. Spatial mismatch and congruence between taxonomic, phylogenetic and functional diversity: the need for integrative conservation strategies in a changing world. Ecology Letters, 13: 1030–1040.

Devred, E., Sathyendranath, S., and Platt, T. 2007. Delineation of ecological provinces using ocean colour radiometry. Marine Ecology-Progress Series, 346: 1–13.

Dickey, T. D. 2003. Emerging ocean observations for interdisciplinary data assimilation systems. Journal of Marine Systems, 40: 5–48.

Doney, S. C., Ruckelshaus, M., Duffy, J. E., Barry, J. P., Chan, F., English, C. A., Galindo, H. M., *et al.* 2012. Climate change impacts on marine ecosystems. Annual Reviews of Marine Science, 4: 11–37.

Duffy, J. E., Amaral-Zettler, L. A., Fautin, D. G., Paulay, G., Rynearson, T. A., Sosik, H. M., and Stachowicz, J. J. 2013. Envisioning a marine biodiversity observation network. BioScience, 63: 350–361.

Dutkiewicz, S., Ward, B. A., Monteiro, F., and Follows, M. J. 2012. Interconnection between nitrogen fixers and iron in the Pacific Ocean: theory and numerical model. Global Biogeochemical Cycles, 26: GB1012.

Fasham, M. J. R. 1978. The statistical and mathematical analysis of plankton patchiness. Oceanography and Marine Biology: An Annual Review, 16: 43–79.

Fauvel, M., Chanussot, J., and Benediktsson, J. A. 2006. Decision fusion for the classification of urban remote sensing images. IEEE Transactions on Geoscience and Remote Sensing, 44: 2828–2838.

Fay, A. R., McKinley, G. A. 2014. Global open-ocean biomes: mean and temporal variability. Earth System Science Data, 6: 273–284.

Field, C. B., Behrenfeld, M. J., Randerson, J T., and Falkowski, P. J. 1998. Primary production of the biosphere: integrating terrestrial and oceanic components. Science, 28: 237–240.

Folt, C. L., and Burns, C. W. 1999. Biological drivers of zooplankton patchiness. Trends in Ecology & Evolution, 14: 300–305.

Forman, R. T. T. 1995. Some general principles of landscape and regional ecology. Landscape Ecology, 10: 133–142.

Forman, R. T. T., and Godron, M. 1981. Patches and structural components for a landscape ecology. Bioscience, 31: 733–740.

Game, E. T., Grantham, H. S., Hobday, A. J., Pressey, R. L., Lombard, A. T., Beckley, L. E., Gjerde, K., Bustamante, R., Possingham, H. P., and Richardson, A. J. 2009. Pelagic protected areas: the missing dimension in ocean conservation. Trends in Ecology & Evolution, 24: 360–369.

Gaube, P., Chelton, D. B., Strutton, P. G., and Behrenfeld, M. J. 2013. Satellite observations of chlorophyll, phytoplankton biomass, and Ekman pumping in nonlinear mesoscale eddies. Journal of Geophysical Research: Oceans, 118: 6349–6370.

Gillson, L. 2009. Landscapes in time and space. Landscape Ecology, 24: 149–155.

Gower, J. F. R., Denman, K. L., and Holyer, R. J. 1980. Phytoplankton patchiness indicates the fluctuation spectrum of oceanic mesoscale structure. Nature, 288: 157–159.

Grothues, T. M., Dobarro, J., Ladd, J., Higgs, A., Niezgoda, G., and Miller, D. 2008. Use of a multi-sensored AUV to telemeter tagged Atlantic sturgeon and map their spawning habitat in the Hudson River, USA. *In* Autonomous Underwater Vehicles, 2008. AUV 2008. IEEE/OES (pp. 1–7). IEEE.

Gruber, N. 2011. Warming up, turning sour, losing breath: ocean biogeochemistry under global change. Philosophical Transactions of the Royal Society of London A: Mathematical, Physical and Engineering Sciences, 369: 1980–1996.

Hales, B., Strutton, P., Saraceno, M., Letelier, R., Takahashi, T., Feely, R., Sabine, C., *et al.* 2012. Satellite-based prediction of pCO2 in coastal waters. Progress in Oceanography, 103: 1–15.

Halpern, B., Longo, C., Scarborough, C., Hardy, D., Best, B. D., Doney, S. C., Katona, S. K., *et al.* 2014. Assessing the health of the U.S. West Coast with a regional-scale application of the Ocean Health Index. PLoS One, 9: e98995.

Hansen, B. W., Bjørnsen, P. K. and Hansen, B. W. 1997. Zooplankton grazing and growth: Scaling within the 2-2,000-~ III body size range. Limnology and Oceanography, 42: 687–704.

Hardman-Mountford, N. J., Hirata, T., Richardson, K., and Aiken, J. 2008. An objective methodology for the classification of ecological pattern into biomes and provinces for the pelagic ocean. Remote Sensing of the Environment, 112: 3341–3352.

Haulsee, D. E., Breece, M. W., Miller, D. C., Wetherbee, B. M., Fox, D. A., and Oliver, M. J. 2015. Habitat selection of a coastal shark species estimated from an autonomous underwater vehicle. The Marine Ecology Progress Series, 528: 277–288.

Haury, L. R., McGowan, J. A., and Wiebe, P. H. 1978. Patterns and Processes in the Time-Space Scales of Plankton Distributions. Springer, USA, pp. 277–327.

Hazen, E. L., Jorgensen, S., Rykaczewski, R. R., Bograd, S. J., Foley, D. G., Jonsen, I. D . . .., and Block, B. A. 2013. Predicted habitat shifts of Pacific top predators in a changing climate. Nature Climate Change, 3: 234–238.

Hidalgo, M., Reglero, P., Álvarez-Berastegui, D., Torres, A. P., Álvarez, I., Rodríguez, J. M., Carbonell, A., *et al.* 2015. Hidden persistence of salinity and productivity gradients shaping pelagic diversity in highly dynamic marine ecosystems. Marine Environmental Research, 104: 47–50.

Hidalgo, M., Rouyer, T., Bartolino, V., Cerviño, S., Ciannelli, L., Massutí, E., Jadaud, A., *et al.* 2012. Context-dependent interplays between truncated demographies and climate variation shape the population growth rate of a harvested species. Ecography, 35: 637–649.

Hinchey, E. K., Nicholson, M. C., Zajac, R. N., and Irlandi, E. A. 2008. Preface: marine and coastal applications in landscape ecology. Landscape Ecology, 23: 1–5.

Hooker, S. B., Rees, N. W., and Aiken, J. 2000. An objective methodology for identifying oceanic provinces. Progress in Oceanography, 45: 313–338.

Hsieh, C. H., Glaser, S. M., Lucas, A. J., and Sugihara, G. 2005. Distinguishing random environmental fluctuations from ecological catastrophes for the North Pacific Ocean. Nature, 435: 336–340.

Irwin, A. J., and Oliver, M. J. 2009. Are ocean deserts getting larger? Geophysical Research Letters, 36: L18609

Jassby, A. D., and Platt, T. 1976. Mathematical formulation of relationship between photosynthesis and light for phytoplankton. Limnology and Oceanography, 21: 540–547.

Kaltenberg, A. M., and Benoit-Bird, K. J. 2013. Intra-patch clustering in mysid swarms revealed through multifrequency acoustics. ICES Journal of Marine Science, 70: 883–891.

Karl, D. M., and Letelier, R. M. 2009. Seascape microbial ecology: habitat structure, biodiversity and ecosystem function. *In* Guide to Ecology. Ed. by S. A. Levin. Princeton University Press, Princeton, New Jersey, pp. 488–500.

Kavanaugh, M. T., Abdala, F. N., Ducklow, H., Glover, D., Fraser, W., Martinson, D., Stammerjohn, S., *et al.* 2015. Effect of continental shelf canyons on phytoplankton biomass and community composition along the western Antarctic Peninsula. Marine Ecology Progress Series, 524: 11–26.

Kavanaugh, M. T., Hales, B., Saraceno, M., Spitz, Y. H., White, A. E., and Letelier, R. M. 2014a. Hierarchical and dynamic seascapes: a quantitative framework for scaling pelagic biogeochemistry and ecology. Progress in Oceanography, 120: 291–304.

Kavanaugh, M. T., Emerson, S. R., Hales, B., Lockwood, D. M., Quay, P. D., Letelier, R. M. 2014b. Physicochemical and biological controls on primary and net community production across northeast Pacific seascapes. Limnology and Oceanography, 59: 2013–2027.

Keister, J. E., Di Lorenzo, E., Morgan, C. A., Combes, V., and Peterson, W. T. 2011. Zooplankton species composition is linked to ocean transport in the Northern California Current. Global Change Biology, 17: 2498–2511.

Kiørboe, T., and Jiang, H. 2013. To eat and not be eaten: optimal foraging behaviour in suspension feeding copepods. Journal of the Royal Society Interface, 10: 1–8.

Kohonen, T. 2001. Self Organizing Maps. Springer series in Information Sciences, vol 30. Springer, Berlin.

Kolmogorov, A. N. 1941. The local structure of turbulence in incompressible viscous fluid for very large Reynolds' numbers. (In Russian). Doklady Akademiia Nauk SSSR, 30: 301–305.

Korneliussen, R. J., Heggelund, Y., Eliassen, I. K., Øye, O. K., Knutsen, T., and Dalen, J. 2009. Combining multibeam-sonar and multifrequency-echosounder data: examples of the analysis and imaging of large euphausiid schools. ICES Journal of Marine Science, 66: 991–997.

Kotlier, N. B., and Wiens, J. A. 1990. Multiple scales of patchiness and patch structure—a hierarchical framework for the study of heterogeneity. Oikos, 59: 253–260.

Lachkar, Z., and Gruber, N. 2012. A comparative study of biological production in eastern boundary upwelling systems using an artificial neural network. Biogeosciences, 9: 293–308.

Levin, S. A. 1992. The problem of pattern and scale in ecology. Ecology, 73: 1943–1967.

Levins, R. 1969. Some demographic and genetic consequences of environmental heterogeneity for biological control. Bulletin of the Entomological Society of America, 15: 237–240.

Lewison, R. A. J., Hobday, S., Maxwell, E., Hazen, J. R., Hartog, D. C., Dunn, D., Briscoe, S., *et al.* 2015. Identifying the critical ingredients of dynamic approaches to ocean resource management. BioScience, 65: 486–498.

Lindsey, B. J. and Batchelder, H. P. 2011. Cross-shelf distribution of Euphausia pacifica in the Oregon coastal upwelling zone: field evaluation of a differential transport hypothesis. Journal of Plankton Research, 33: 1666–1678.

Ling, S. D., Johnson, C. R., Ridgway, K., Hobday, A. J., and Haddon, M. 2009. Climate-driven range extension of a sea urchin: inferring future trends by analysis of recent population dynamics. Global Change Biology, 15: 719–731.

Litzow, M. A., and Ciannelli, L. 2007. Oscillating trophic control induces community reorganization in a marine ecosystem. Ecology Letters, 10: 1124–1134.

Longhurst, A. R. 1998. Ecological Geography of the Sea. Academic Press, San Diego.

Longhurst, A., Sathyendranath, S., Platt, T. and Caverhill, C. 1995. An estimate of global primary production in the ocean from satellite radiometer data. Journal of Plankton Research, 17: 1245–1271.

Lovejoy, S., Currie, W. J. S., Tessier, Y., Claereboudt, M. R., Bourget, E., Roff, J. C., and Schertzer, D. 2001. Universal multifractals and ocean patchiness: phytoplankton, physical fields and coastal heterogeneity. Journal of Plankton Research, 23: 117–141.

Mace, G. M. 2014. Ecology: whose conservation? Science, 345: 1558–1560.

Mackas, D. L., Denman, K. L., and Abbott, M. R. 1985. Plankton patchiness: biology in the physical vernaculer. Bulletin of Marine Sciences, 37: 652–674.

Marquet, P. A., Fortin, M. J., Pineda, J., Wallin, D. O., Clark, J., Wu, Y., Bollens, S., *et al.* 1993. Ecological and Evolutionary Consequences of Patchiness: A Marine-Terrestrial Perspective. Springer, Berlin Heidelberg, pp. 277–304.

Maxwell, S. M., Hazen, E. L., Lewison, R. L., Dunn, D. C., Bailey, H., Bograd, S. J . . .., and Crowder, L. B. 2015. Dynamic ocean management: defining and conceptualizing real-time management of the ocean. Marine Policy, 58: 42–50.

Mitchell, J. G., Yamazaki, H., Seuront, L., Wolk, F., and Li, H. 2008. Phytoplankton patch patterns: seascape anatomy in a turbulent ocean. Journal of Marine Systems, 69: 247.

Moorcroft, P. R., Hurtt, G. C., and Pacala, S. W. 2001. A method for scaling vegetation dynamics: the ecosystem demography model (ED). Ecological Monographs, 71: 557–586.

Muller-Karger, F. E., Kavanaugh, M. T., Montes, E., Balch, W. M., Breitbart, M., Chavez, F. P., Doney, S. C., *et al.* 2014. A framework for a marine biodiversity observing network within changing continental shelf seascapes. Oceanography, 27: 18–23.

Murawski, S. A., Steele, J. H., Taylor, P., Fogarty, M. J., Sissenwine, M. P., Ford, M., and Suchman, C. 2010. Why compare marine ecosystems? ICES Journal of Marine Science, 67: 1–9.

Nathan, R., Getz, W. M., Revilla, E., Holyoak, M., Kadmon, R., Saltz, D., and Smouse, P. E. 2008. A movement ecology paradigm for unifying organismal movement research. Proceedings of the National Academy of Sciences, 105: 19052–19059.

O'Dor, R., Dagorn, L., Holland, K., Jonsen, I., Payne, J., Sauer, W., Semmens, J., *et al.* 2009. The ocean tracking network. *In* Proceedings of OceanObs' 09: Sustained Ocean Observations and Information for Society Conference, Vol. 1.

Okubo, A. 1971. Oceanic diffusion diagrams. Deep-Sea Research, 18: 789–802.

Okubo, A., and Levin, S. A. 2001. Diffusion and Ecological Problems: Modern Perspectives. Springer Verlag, New York.

Oliver, M. J., Breece, M. W., Fox, D. A., Haulsee, D. E., Kohut, J. T., Manderson, J., and Savoy, T. 2013. Shrinking the haystack: using an AUV in an integrated ocean observatory to map Atlantic sturgeon in the coastal ocean. Fisheries, 38: 210–216.

Oliver, M. J., and Irwin, A. J. 2008. Objective global ocean biogeographic provinces. Geophysical Research Letters, 35: L15601.

O'Neill, R. V., DeAngelis D. L., Waide J. B., and Allen, T. F. H. 1986. A Hierarchical Concept of Ecosystems. Princeton University Press, Princeton, New Jersey.

O'Neill, R. V., Gardner, R. H., and Turner, M. G. 1992. A hierarchical neutral model for landscape analysis. Landscape Ecology, 7: 55–61.

Paine, R. T., and Levin, S. A. 1981. Intertidal landscapes: disturbance and the dynamics of pattern. Ecological Monographs, 51: 145–178.

Parrish, J. K., and Edelstein-Keshet, L. 1999. Complexity, pattern, and evolutionary trade-offs in animal aggregation. Science, 284: 99–101.

Pereira, H. M., Leadley, P. W., Proença, V., Alkemade, R., Scharlemann, J. P., Fernandez-Manjarrés, J. F., Araújo, M. B., *et al.* 2010. Scenarios for global biodiversity in the 21st century. Science, 330: 1496–1501.

Perry, R. I., Cury, P., Brander, K., Jennings, S., Möllmann, C., and Planque, B. 2010. Sensitivity of marine systems to climate and fishing: concepts, issues and management responses. Journal of Marine Systems, 79: 427–435.

Pittman, S. J., Kneib, R. T., and Simenstad, C. A. 2011. Practicing coastal seascape ecology. Marine Ecology Progress Series, 427: 187–190.

Platt, T., and Sathyendranath, S. 1999. Spatial structure of pelagic ecosystem processes in the global ocean. Ecosystems, 2: 384–394.

Platt, T., and Sathyendranath, S. 2008. Ecological indicators for the pelagic zone of the ocean from remote sensing. Remote Sensing of the Environment, 112: 3426–3343.

Polovina, J. J., Howell, E., Kobayashi, D. R., and Seki, M. P. 2001. The transition zone chlorophyll front, a dynamic global feature defining migration and forage habitat for marine resources. Progress in Oceanography, 49: 469–483.

Polovina, J. J., Howell, E. A., and Abecassis, M. 2008. Ocean's least productive waters are expanding. Geophysical Research Letters, 35: L03618

Preston, C. M., Marin, III, R. , Jensen, S. D., Feldman, J., Birch, J. M., Massion, E. I., DeLong, E. F., *et al.* 2009. Near real-time autonomous detection of marine bacterioplankton on a coastal mooring in Monterey Bay, California, using rRNA-targeted DNA probes. Environmental Microbiology, 11: 1168–1180.

Reygondeau, G., Longhurst, A., Martinez, E., Beaugrand, G., Antoine, D., and Maury, O. 2013. Dynamic biogeochemical provinces in the global ocean. Global Biogeochemical Cycles, 27: 1046–1058.

Ribalet, F., Marchetti, A., Hubbard, K. A., Brown, K., Durkin, C. A., Morales, R., Robert, M., *et al.* 2010. Unveiling a phytoplankton hotspot at a narrow boundary between coastal and offshore waters. Proceedings of the National Academy of Sciences, 107: 16571–16576.

Richardson, A., Risien, C., and Shillington, F. 2003. Using self-organizing maps to identify patterns in satellite imagery. Progress in Oceanography, 59: 223–239.

Risser, P. G. 1987. Landscape Ecology: State of the Art. Landscape Heterogeneity and Disturbance. Springer, New York, pp. 3–14.

Rykaczewski, R. R., and Checkley, D. M. 2008. Influence of ocean winds on the pelagic ecosystem in upwelling regions. Proceedings of the National Academy of Sciences, 105: 1965–1970.

Santora, J. A., Field, J. C., Schroeder, I. D., Sakuma, K. M., Wells, B. K., and Sydeman, W. J. 2012. Spatial ecology of krill, micronekton and top predators in the central California current: implications for defining ecologically important areas. Progress in Oceanography, 106: 154–174.

Saraceno, M., Provost, C., and Lebbah, M. 2006. Biophysical regions identification using an artificial neuronal network: a case study in the South Western Atlantic. Advances in Space Research, 37: 793–805.

Sarmiento, J. L., Slater, R., Barber, R., Bopp, L., Doney, S. C., Hirst, A. C., Kleypas, J., *et al.* 2004. Response of ocean ecosystems to climate warming. Global Biogeochemical Cycles, 18: GB3003.

Saunders, M. I., Brown, C. J., Foley, M. M., Febria, C. M., Albright, R., Mehling, M. G., Kavanaugh, M. T., *et al.* 2015. Human impacts on connectivity in marine and freshwater ecosystems assessed using graph theory: a review. Marine and Freshwater Research, 67: 277–290.

Schneider, D. C. 2001. The rise of the concept of scale in ecology. BioScience, 51: 545–553.

Scholin, C., Doucette, G., Jensen, S., Roman, B., Pargett, D., Marin, III, R. , Preston, C., *et al.* 2009. Remote detection of marine microbes, small invertebrates, harmful algae, and biotoxins using the Environmental Sample Processor (ESP). Oceanography, 22: 158–167.

Sieracki, M. E., Benfield, M., Hanson, A., Davis, C., Pilskaln, C. H., Checkley, D., Sosik, H. M., *et al.* 2010. Optical plankton imaging and analysis systems for ocean observation. Proceedings of Ocean Obs, 9: 21–25.

Sorte, C. J., Williams, S. L., and Carlton, J. T. 2010. Marine range shifts and species introductions: comparative spread rates and community impacts. Global Ecology and Biogeography, 19: 303–316.

Sosik, H. M., and Olson, R. J. 2007. Automated taxonomic classification of phytoplankton sampled with imaging-inflow cytometry. Limnology and Oceanography Methods, 5: 204–216.

Sosik, H. M., Sathyendranath, S., Uitz, J., Bouman, H. and Nair, A. 2014. In situ methods of measuring phytoplankton functional types. *In* Phytoplankton functional types from space, Reports of the International Ocean-55 Colour Coordinating Group, No. 15. IOCCG, Ed. by S. Sathyendranath and V. Stuart. International Ocean-Colour Coordinating Group, IOCCG, Dartmouth, Canada.

Steele, J. H. 1978. Some comments on plankton patches, 1–20. *In* Spatial pattern in plankton communities, NATO Conference Series, Series IV: Marine Sciences, Vol. 3. Ed. J. H. Steele. ISBN 0-306-40057-X.

Steele, J. H. 1985. A comparison of terrestrial and marine ecological systems. Nature, 313: 355–358.

Steele, J. H. 1989. The ocean 'landscape'. Landscape Ecology, 3: 185–192.

Steele, J. H. 1991. Can ecological theory cross the land-sea boundary? Journal of Theoretical Biology, 153: 425–436.

Stommel, H. 1963. Varieties of oceanographic experience. Science, 139: 572–576.

Tonizzo, A., Gilerson, A., Harmel, T., Ibrahim, A., Chowdhary, J., Gross, B., Moshary, F., *et al.* 2011. Estimating particle composition and size distribution from polarized water-leaving radiance. Applied Optics, 50: 5047–5058.

Treml, E. A., Halpin, P. N., Urban, D. L., and Pratson, L. F. 2008. Modeling population connectivity by ocean currents, a graph-theoretic approach for marine conservation. Landscape Ecology, 23: 19–36.

Turner, M. G. 2005. Landscape ecology: what is the state of the science? Annual Review of Ecology Evolution and Systematics, 36: 319–344.

Turner, M. G., Gardner, R. H., and O'Neill, R. V. 2001. Landscape Ecology in Theory and Practice. Springer-Verlag, New York

Turner, W., Spector, S., Gardiner, N., Fladeland, M., Sterling, E., and Steininger, M. 2003. Remote sensing for biodiversity science and conservation. Trends in Ecology & Evolution, 18: 306–314.

Villareal, T. A., *et al.* 1999. Upward transport of oceanic nitrate by migrating diatom mats. Nature, 397: 423.

Voisin, A., Krylov, V., Moser, G., Serpico, S. B., and Zerubia, J. 2014. Supervised classification of multisensor and multiresolution remote sensing images with a hierarchical copula-based approach. IEEE Transactions on Geoscience and Remote Sensing, 52: 3346–3358.

Wedding, L. M., Lepczyk, C. A., Pittman, S. J., Friedlander, A. M., and Jorgensen, S. 2011. Quantifying seascape structure: extending terrestrial spatial pattern metrics to the marine realm. Marine Ecology Progress Series, 427: 219–232.

Whitaker, R. 1977. The evolution of species diversity in land communities. Evolutionary Biology, 10: 1–67.

Wiens, J. A. 1976. Population responses to patchy environments. Annual Review of Ecology and Systematics, 7: 81–120.

Wiens, J. A. 1989. Spatial scaling in ecology. Functional Ecology, 3: 385–397.

Woodson, C. B., and Litvin, S. Y. 2015. Ocean fronts drive marine fishery production and biogeochemical cycling. Proceedings of the National Academy of Sciences, 112: 1710–1715.

Wu, J. 1999. Hierarchy and scaling: extrapolating information along a scaling ladder. Canadian Journal of Remote Sensing, 25: 367–380.

Wu, J., and Hobbs, R. 2002. Key issues and research priorities in landscape ecology: an idiosyncratic synthesis. Landscape Ecology, 17: 355–365.

Wu, J., and Loucks, O. L. 1995. From balance of nature to hierarchical patch dynamics: a paradigm shift in ecology. Quarterly Review of Biology, 70: 439–466.

Young, S. A., Vaughan, M. A., Kuehn, R. E., and Winker, D. M. 2013. The retrieval of profiles of particulate extinction from Cloud-Aerosol Lidar and Infrared Pathfinder Satellite Observations (CALIPSO) data: uncertainty and error sensitivity analyses. Journal of Atmospheric and Oceanic Technology, 30: 395–428.

Zhao, M., Heinsch, F. A., Nemani, R. R., and Running, S. W. 2005. Improvements of the MODIS terrestrial gross and net primary production global data set. Remote Sensing of Environment, 95: 164–176.

Handling editor: Manuel Hidalgo

ICES Journal of Marine Science

ICES Journal of Marine Science (2016), 73(7), 1851–1862. doi:10.1093/icesjms/fsw041

Contribution to the Themed Section: '*Seascape Ecology*'

Original Article

Pelagic seascape ecology for operational fisheries oceanography: modelling and predicting spawning distribution of Atlantic bluefin tuna in Western Mediterranean

Diego Alvarez-Berastegui[1]*, Manuel Hidalgo[2], María Pilar Tugores[2], Patricia Reglero[2], Alberto Aparicio-González[2], Lorenzo Ciannelli[3], Mélanie Juza[1], Baptiste Mourre[1], Ananda Pascual[4], José Luís López-Jurado[2], Alberto García[5], José María Rodríguez[6], Joaquín Tintoré[1,4], and Francisco Alemany[2]

[1]*Balearic Islands Coastal Observing and Forecasting System (SOCIB), Parc Bit, Naorte, Bloc A 2°p. pta. 3, Palma de Mallorca, Balearic Islands, Spain*
[2]*Instituto Español de Oceanografía, Centro Oceanográfico de Baleares (COB-IEO), Palma de Mallorca, Balearic Islands, Spain*
[3]*College of Earth, Ocean and Atmospheric Sciences (CEOAS), Oregon State University, Corvallis, OR, USA*
[4]*Instituto Mediterráneo de Estudios Avanzados (IMEDEA), Esporles, Balearic Islands, Spain*
[5]*Instituto Español de Oceanografía, Centro Oceanográfico de Málaga, Fuengirola, Andalucía, Spain*
[6]*Instituto Español de Oceanografía, Centro Oceanográfico de Gijón, Gijón, Spain*

**Corresponding author. tel: +34 971 43 99 98; fax: +34 971 43 99 79; e-mail: dalvarez@socib.es*

Alvarez-Berastegui, D., Hidalgo, M., Tugores, M. P., Reglero, P., Aparicio-González, A., Ciannelli, L., Juza, M., Mourre, B., Pascual, A. López-Jurado, J. L., García, A., Rodríguez, J. M., Tintoré, J., and Alemany, F. Pelagic seascape ecology for operational fisheries oceanography: modelling and predicting spawning distribution of Atlantic bluefin tuna in Western Mediterranean. – ICES Journal of Marine Science, 73: 1851–1862.

Received 19 June 2015; revised 23 February 2016; accepted 28 February 2016.

The ecology of highly migratory marine species is tightly linked to dynamic oceanographic processes occurring in the pelagic environment. Developing and applying techniques to characterize the spatio-temporal variability of these processes using operational oceanographic data is a challenge for management and conservation. Here we evaluate the possibility of modelling and predicting spawning habitats of Atlantic bluefin tuna in the Western Mediterranean, using pelagic seascape metrics specifically designed to capture the dynamic processes affecting the spawning ecology this species. The different seascape metrics applied were processed from operational oceanographic data products providing information about the temporal and spatial variability of sea surface temperature, kinetic energy and chlorophyll *a*. Spawning locations were identified using larval abundances sampled in the Balearic Sea, one of the main reproductive areas for this species in the Mediterranean Sea. Results confirm the high dependence of bluefin tuna spawning ecology on mesoscale oceanographic processes while providing spawning habitat maps as a tool for bluefin tuna assessment and management, based on operational oceanographic data. Finally, we discuss the coming challenges that operational fisheries oceanography and pelagic seascape ecology face to become fully implemented as predictive tools.

Keywords: Balearic sea, ecosystem, ecosystem-based fisheries management, essential fish habitat, habitat forecast, Mediterranean, seascape metrics.

Introduction

Essential habitats of pelagic species are strongly linked to dynamic oceanographic processes such as fronts and eddies which vary in space and time (Shillinger *et al.*, 2008; Reglero *et al.*, 2014; Scales *et al.*, 2014). To define these habitats, it is necessary to design environmental descriptors specific to the dynamic component of the oceanographic scenario in areas where the species occur or where relevant processes such as feeding or spawning take place. For example, various studies have used gradients of hydrographic variables to identify the presence of frontal processes (Worm

et al., 2005; Druon 2010; Louzao *et al.*, 2011; Mannocci *et al.*, 2013). Recently, Alvarez-Berastegui *et al.* (2014) proposed to define the pelagic seascapes as the combination of means and gradients of particular hydrographic variable, evaluating how the spatial scale of observation affects our capability to capture important hydrodynamic processes influencing the spawning ecology of tuna species. These examples reveal the important role that pelagic seascape ecology plays to understand how the environment affects pelagic species ecology, providing new ways to characterize the spatio-temporal dynamics of pelagic environments.

Operational oceanography is a key tool for advancing towards species habitat modelling with applications to management (Manderson *et al.*, 2011; Hobday and Hartog, 2014). Modern ocean observing systems combining *in situ* observations, satellite and modelling data are able to provide realistic characterizations of physical oceanographic processes (Rayner, 2010; Pascual *et al.*, 2013; Tintoré *et al.*, 2013a). In this sense, seascape metrics are of special interest when working with remote sensing and hydrodynamic models that offer continuous data at broad extent in space and time. Spatial and temporal resolution provided by these data sources occurs at adequate scales to describe the dynamics of fluid properties at which the marine top predators interact with their habitat. Environmental scenarios obtained from operational data sources can provide baseline information to produce long-term and near real time forecasting of pelagic essential habitats of paramount interest in fisheries management (Hobday and Hartmann, 2006) and conservation (Game *et al.*, 2009).

The monitoring of bluefin tuna spawning habitats provides a good opportunity to study how the application of operational oceanography and seascape metrics can be relevant to improve current assessment and management of pelagic species. Bluefin tuna is an iconic top predator with a relevant role in pelagic ecosystems (Mather *et al.*, 1995; Fromentin and Powers, 2005) and supports important fisheries in the Mediterranean and along the North East and West Atlantic coasts (Fromentin, 2009). Mounting evidence shows that the spawning ecology and habitat of this species are strongly linked to mesoscale oceanographic processes (Alemany *et al.*, 2010; Reglero *et al.*, 2012; Muhling *et al.*, 2013; Alvarez-Berastegui *et al.*, 2014), and therefore, operational oceanography provides a new potential tool to characterize and track these habitats. Spawning habitat models inferred from *in situ* data have improved the standardization of spawning biomass estimates of bluefin tuna based on larval abundance indices (Ingram *et al.*, 2013). Thus, characterizing and monitoring spawning habitats from operational oceanography products would provide near real-time information for larval sampling design and for larval abundance indices calculation. Besides, this type of information would facilitate the application of new management approaches based on spatial restrictions that could reduce bluefin tuna bycatch in the Mediterranean, such as those measures recently adopted in the Gulf of Mexico (US-DOC/NOAA/NMFS, 2014). Moreover, dynamic habitat mapping could be used to manage pelagic marine protected areas within an adaptive framework, where spatial limits of closure areas may change (Hobday *et al.*, 2010).

In this study, we applied a pelagic seascape approach based exclusively on operational oceanographic information to model the spawning habitats of Atlantic bluefin tuna in the Western Mediterranean Sea. Abundances of early larval stages of bluefin tuna, collected in proximity to a principal spawning region in the Balearic Sea, were used as a proxy for spawning locations (Mather *et al.*, 1995; García *et al.*, 2005a). Seascape metrics, used as input in the modelling process, were selected and included based on known dependencies of the bluefin tuna spawning ecology with local mesoscale oceanography from previous studies. The results will allow the prediction of the spatial location of bluefin tuna spawning areas and provide insights about the spawning ecology of this species.

We develop a specific cross-validation approach to assess the predictive capability of the habitat models. We also propose specific techniques to address possible biases in the predictions derived from displacements of the oceanographic features identified from hydrodynamic models or remote sensing. This work aims to develop and provide operational fisheries oceanography products that directly apply to current assessment and conservation of Atlantic bluefin tuna and other pelagic marine species of interest.

Methods

In situ data acquisition

Atlantic bluefin tuna larvae were collected during five systematic oceanographic campaigns carried out in June–July of 2001–2005. A regular grid of 10 × 10 nautical miles was sampled each year covering the area between 37.85°–40.35° N and 0.77°–4.91° E, (280 × 362 km) (Figure 1). At each sampling location, bluefin tuna larvae were collected with a bongo net of 60 cm mouth diameter, stepped obliquely to a depth of 70 m, or from 5 m above the bottom at coastal stations, to the surface maintaining the vessel speed at two knots. Fishing tows covered ∼600 m. An average of 162 stations was sampled yearly around the Balearic archipelago, additional information about field campaigns is provided in Supplementary Table S1. The volume of water filtered was measured with flowmeters located at the centre of the net. Plankton samples were preserved with 4% formalin buffered with borax. Tuna larvae were identified to the species level and measured in standard length.

Abundances of bluefin tuna larvae belonging to the yolk sac and preflexion stages (<4.5 mm) were used as proxy of spawning locations as in previous research (Reglero *et al.*, 2012; Alvarez-Berastegui *et al.*, 2014). The mean and maximum age of larvae ≤4.5 mm are 6 and 11 days old, respectively, calculated considering bluefin tuna larval growth rates (de la Gándara *et al.*, 2013) and hatching times (Gordoa and Carreras, 2014). At a mean age of 6 days, drift distances from the actual spawning location are <25 km (∼1.4 times the sampling station distance), and for the maximum age, the drift distances are ∼46 km (∼2.6 times the sampling station distances). These values have been calculated following methods in Reglero *et al.* (2013).

Identification of operational oceanographic data sources

Potential explanatory variables providing information on the location of bluefin tuna spawning habitats were identified from previous studies analysing the relations between species ecology and local mesoscale oceanography in the western Mediterranean. These studies found that sea surface temperature (SST), sea surface salinity (SSS), and surface current velocities are key hydrographic variables associated to the oceanographic processes affecting the location of the bluefin tuna spawning areas (Alemany *et al.*, 2010; Reglero *et al.*, 2012). In addition, bluefin tuna spawning mostly occur in areas with low chlorophyll *a* (CHLa) (Muhling *et al.*, 2011, 2013; Koched *et al.*, 2013; Llopiz and Hobday 2015). Therefore, we selected operational oceanography data sources related to temperature, salinity, chlorophyll *a*, and currents, to compute pelagic seascape metrics on oceanographic processes affecting species

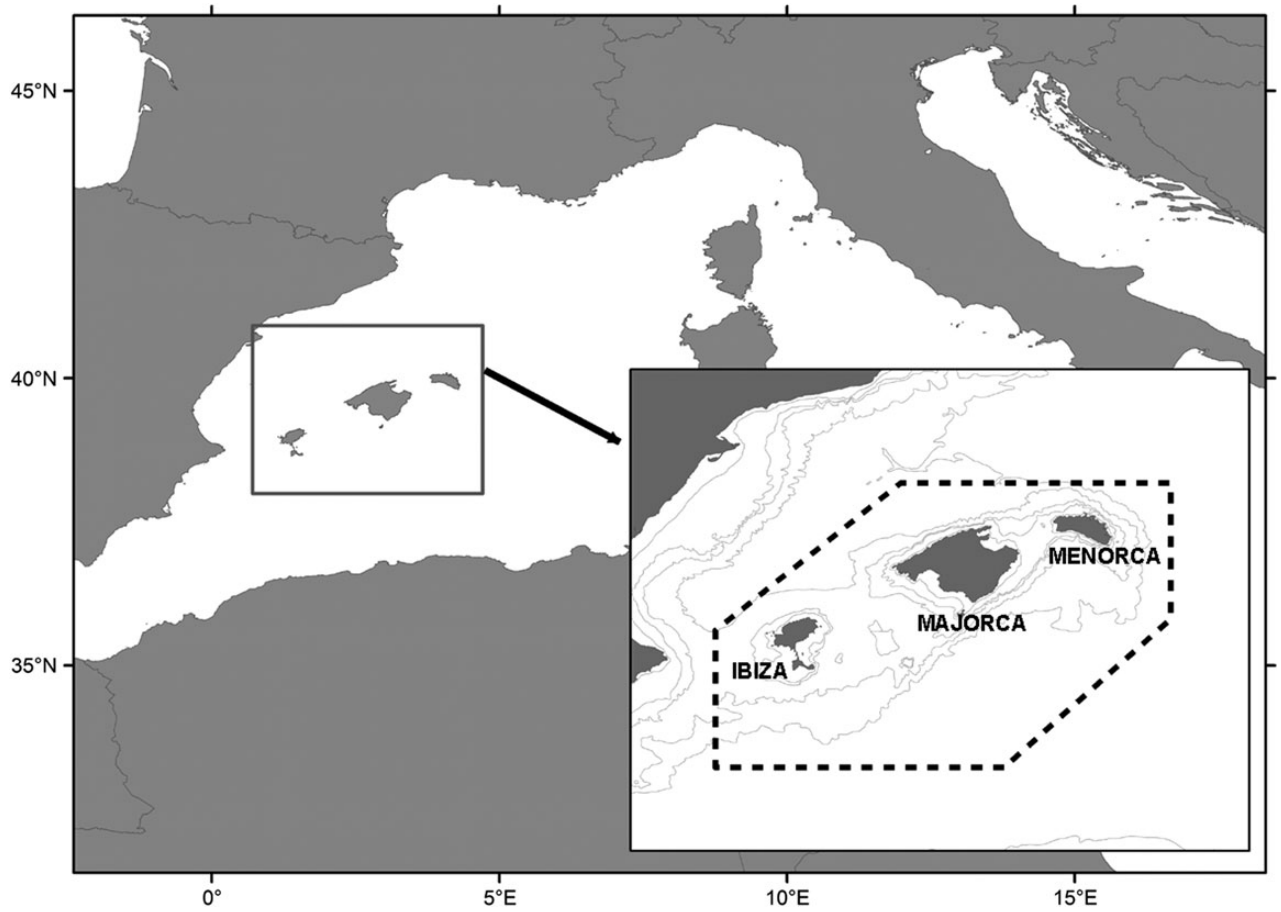

Figure 1. Geographic location of the Balearic Sea and delimitation of the sampling area (dashed line).

Table 1. Seascape metrics (environmental variables) processed from operational data sources.

Variable group	Variable name	Variable acronym	Spatial resolution (degree/km)	Temporal resolution (days)
SST-related variables	Spatial averaged SST	SSTa	0.5/55	1
	Temporal increment of the spatial averaged SST during the previous 15 days	iSSTa	0.5/55	15
KE-related variables	Kinetic energy	KE	0.125/12.5	1
	Kinetic energy frontal index	KEfi	0.5/55	1
CHLa-related variables	Spatial averaged sea surface chlorophyll_*a*	CHLa	0.5/55	7
	Chlorophyll *a* frontal index	CHLafiCHLafi	0.5/55	7

ecology. Acronyms and additional information about selected datasets are provided in Supplementary Table S2. To ensure the development of an operational scheme, data sources were selected only if (i) historical and near real-time data were fully accessible online; (ii) the spatial resolution (grain) of the dataset was similar or better than the *in situ* data; (iii) the temporal resolution was at least 7 days, in relation to the temporal persistence of mesoscale structure in the area (Bouffard *et al.*, 2014); and (iv) if there was published information about the product quality.

Processing of pelagic seascape metrics

Six seascape metrics were selected (Table 1). All metrics were estimated at the sea surface layers, where spawning occurs (Aranda *et al.*, 2013) and larvae are found (Torres *et al.*, 2011). Metrics, based on SST data, sea surface high, and chlorophyll *a*, were designed to provide adequate proxies of oceanographic processes that are known to influence the ecology of bluefin tuna.

SST is a significant variable determining the timing of bluefin tuna spawning in the Mediterranean (Alemany *et al.*, 2010; García *et al.*, 2005b) as well as in other spawning areas (Muhling *et al.*, 2010; Koched *et al.*, 2013; Reglero *et al.*, 2014). Spawning begins at ~19–20°C and the embryo developmental time decreases with increasing temperature (Gordoa and Carreras, 2014). For yellowfin tuna, spawning activity usually begins following a steadily increase in the SST (Margulies *et al.*, 2007), and probably in bluefin tuna as well (Heinisch *et al.*, 2008). Therefore, two SST seascape metrics were computed: (i) the spatial averaged SST (SSTa, Table 1) providing information about the mean sea surface water temperature within an

area of 0.5 × 0.5° around the sampling location and, (ii) the temporal increment of the spatial averaged SST during the previous 15 days (iSSTa, Table 1). The SST from the Mediterranean Forecasting System hydrodynamic model dataset (dataset MFS-SST; Tonani *et al.*, 2014) was selected rather than satellite data (dataset MODIS-SST) for the computation of these metrics. MFS-SST presents the advantage of being cloud-free when compared to MODIS-SST. Moreover, MFS-SST assimilates satellite SST data providing very realistic estimates of the SST over the Western Mediterranean Sea (Juza *et al.*, 2015).

The spawning ecology of bluefin tuna is also linked to mesoscale activity associated to the main fronts during the spawning season (Alemany *et al.*, 2010). Kinetic energy (KE, Table 1) derived from satellite altimetry data (Pascual *et al.*, 2007) was selected as proxy for sea surface currents (dataset AVISO-SSA). A Mediterranean specific mean dynamic topography was used for the calculation of the absolute sea surface height from the satellite observed anomalies (Rio *et al.*, 2014). A KE frontal index seascape (KEfi, Table 1) was calculated as the rate of change (computed as the slope) of the KE at sampling locations using a spatial window of 0.6 × 0.6°. This window filters dynamic processes occurring at smaller spatial scales improving the identification of bluefin tuna spawning areas (Alvarez-Berastegui *et al.*, 2014).

Daily images of chlorophyll *a* data from multisatellite images processed with a Mediterranean specific ocean colour algorithm (Volpe *et al.*, 2007) (dataset RS-CHL) were used to compute weekly means (mean value along the previous 7 days). This approach reduces the percentage of pixels with no data due to clouds (12% of data). The spatial averaged sea surface chlorophyll *a* seascape (CHLa, Table 1) was calculated as the averaged value of the weekly mean in an area of 0.5° around each sampling station. Chlorophyll *a* weekly means were also used to compute the CHLa frontal index at 0.5° as a proxy of the location of well-established chlorophyll *a* fronts (CHLafi, Table 1) in the same manner as KE estimates. Note that SSS from the dataset MFS-SSS (Supplementary Table S2) was excluded for analyses because recent research demonstrated that this parameter was not properly represented by the model in the study area (Juza *et al.*, 2015). Example seascape depictions from the operational data sources for a particular date are shown in Figure 2.

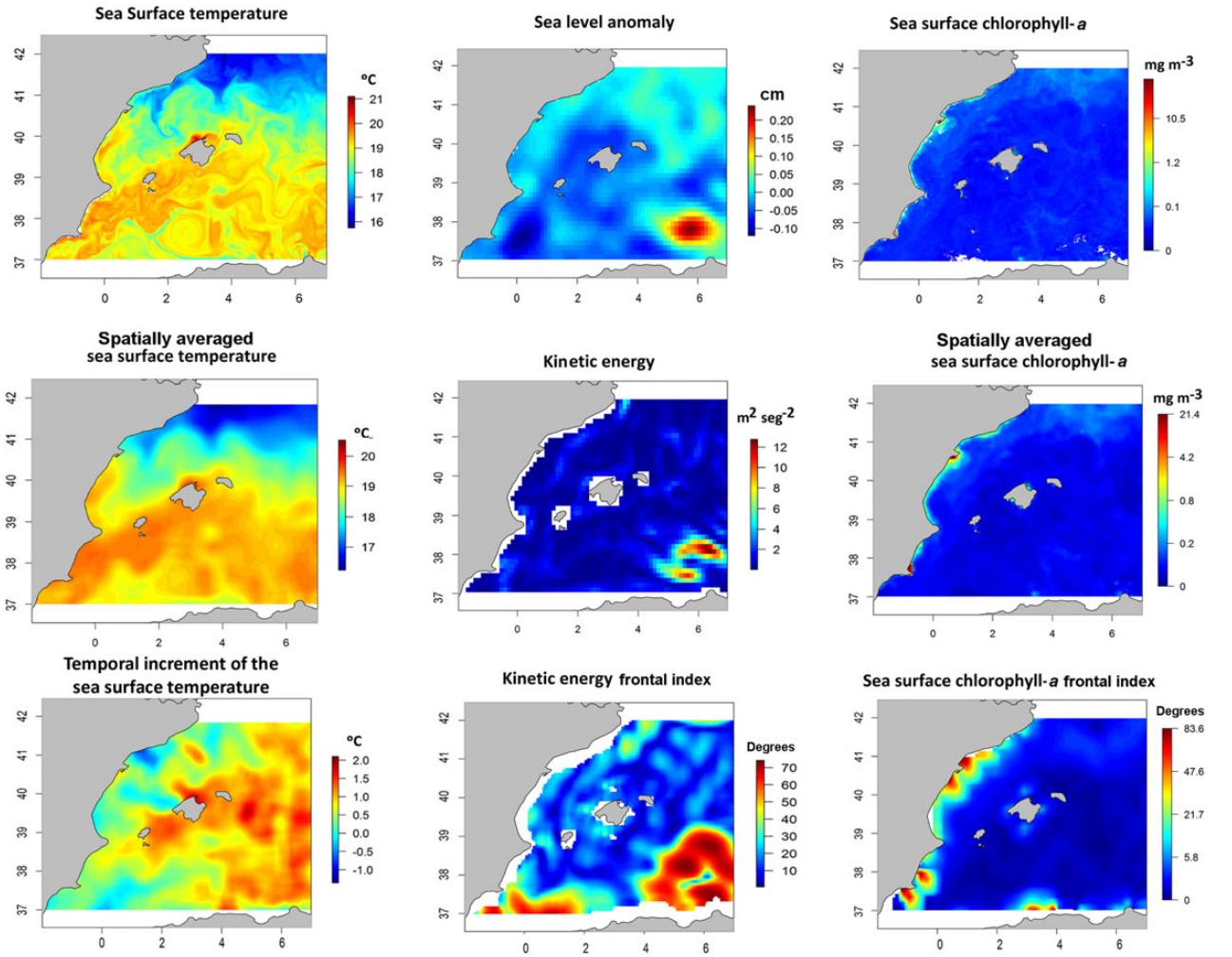

Figure 2. Examples of operational data products and seascape metrics for a specific date (2014/05/29) of original products (top row), spatially averaged seascapes (middle row), and heterogeneity seascapes (bottom row). SST from hydrodynamic model (SST), derived zonal SSTa and its temporal increment in 15 days (iSSTa) (left column). Sea surface anomaly, derived kinetic energy (KE) and kinetic energy frontal index (KEfi) (middle column). Sea surface chlorophyll *a*, derived, spatially averaged CHLa and the CHLafi (right column). This figure is available in black and white in print and in colour at *ICES Journal of Marine Science* online.

Modelling larval abundances

The relationship between environmental variables and abundance (counts) of larvae below 4.5 mm collected along the 5 years was modelled with nonparametric regression (generalized additive models, GAMs; Wood, 2006). We used a negative binomial distribution and a log-link function to account for overdispersion on the larval abundances. To standardize the number of larvae to the fishing effort, the volume of water filtered in each bongo fishing (vol) was included in the GAMs as an offset after natural log transformation (Maunder and Punt, 2004). All GAMs included a bivariate smoother combining latitude (lat) and longitude (long) in the formulation, the year factor accounting for the interannual effect in the abundances and the hour of the day, standardized from 0 to 1 and accounting for effects of solar elevation in the catchability. Collinearity among explanatory variables was tested with pair correlations among explanatory variables always <0.5. Four different model configurations were compared:

(i) no environmental variables (equation 1), referred as *reference model*

$$LA = \text{offset}(\log(\text{vol})) + \text{factor}(\text{year}) + sm_1(\text{long}, \text{lat}) + sm_2(\text{hour}); \quad (1)$$

where LA = larval abundances <4.5 mm; sm = smoothing functions;

(ii) all environmental variables included as additive factors (see Table 1 for abbreviations).

$$LA = \text{offset}(\log(\text{vol})) + \text{factor}(\text{year}) + sm_1(\text{long}, \text{lat}) + sm_2(\text{hour}) + sm_3(SSTa) + sm_4(iSSTa) + sm_5(KE) + sm_6(KEfi) + sm_7(CHLa) + sm_8(CHLafi) \quad (2)$$

(iii) all variables from the same group (see variable groups in Table 1) were included as interactive (see equation 4).

$$LA = \text{offset}(\log(\text{vol})) + \text{factor}(\text{year}) + sm_1(\text{long}, \text{lat}) + sm_2(\text{hour}) + sm_3(SSTa, iSSTa) + sm_4(KE, KEfi) + sm_5(CHLa, CHLafi) \quad (3)$$

(iv) combination of models (ii) and (iii) (one or two groups included as interactive while other groups are included as additive, six different possible combinations).

Including interaction terms combining means and gradients of one particular hydrographic variable improves the capability of seascape metrics for providing information about the location of spawning areas (Alvarez-Berastegui *et al.*, 2014). For all possible combinations (nine in total, see Table 2), a backward selection process was applied to remove variables with no significant effect ($p > 0.05$). To restrict potential over-fitting in the models, the number of knots for each environmental variable was limited up to three for univariate additive terms, and up to nine for interactive terms.

Exploration of the model performance after non-significant variable removal was based on the maximization of the explained deviances and minimization of the Akaike Criterion Index (AIC; Akaike, 1981). The AIC parameter is a trade-off between the model goodness of fit and the model complexity. AIC values from different models were compared by calculation of the delta AIC (ΔAIC), which is the difference between model AIC and minimum AIC found among all models. A value of ΔAIC equal to 2.5 was selected as threshold for no relevant model differences (Hilbe, 2011). Below this threshold, models were considered to be of equal quality and selected as potential candidates for prediction of spawning habitat.

Definition and calculation of the Spawning Habitat Quality

The position of mesoscale oceanographic features, such as fronts, deduced from remote sensing images or hydrodynamic modelling techniques can be a biased representation of the *in situ* observed positions (Ziegeler *et al.*, 2012; Bouffard *et al.*, 2014; Bricheno *et al.*, 2014). In these cases, the spatial distribution of the GAM-modelled larval abundances will be displaced from the real distribution. Therefore, the correlation coefficients between the observed and modelled larval abundance may be biased low, even if the models were able to identify the areas with high larval abundances at coarse spatial resolution. To overcome this limitation, the larval abundance maps, from both observed and modelled data, were spatially smoothed using a moving window average filter at the spatial scale that optimized the correlation coefficients and the spatial resolution of the output maps. The optimal spatial scale for the moving window average filter was assessed with scalogram plots showing the correlation (Spearman coefficient) of the observed and GAM-modelled larval abundances, smoothed at nine spatial scales. Each scale was a multiple of one-half of the spatial resolution of the *in situ* sampling grid (from 7 to 75 km of radius area). Increasing the spatial scale of the moving window used in the spatial average process will increase correlations coefficients, but it can obscure the identification of small spatial patterns. The scale on which the correlation curve in the scalogram becomes asymptotic provides information about the mean spatial distances between observed and modelled larval abundances.

Table 2. Processed models, environmental variables included, and performance indicators.

Model ID	Model characteristics	Model formulation ($n = 805$)	Deviance explained (%)	AIC	ΔAIC
M1	No environmental variables included	(long, lat) + (hour) + year	40.7	1047.71	51.4
Madd	All environmental variables as additive	iSSTa + KEfi + CHLa	52.4	995.60	0
Mint	Environmental variables as interactive	(SSTa,iSSTa) + (KE,KEfi) + (CHLa,CHLafi)	52.6	998.88	3.2
Comb 1	Chla variables as additive, SST and KE as interactive	(SSTa,iSSTa) + (KE,KEfi) + CHLa	52.6	997.59	1.9
Comb 2	KE variables as additive, SST and CHLA as interactive	(SSTa,iSSTa) + KEfi + (CHLa,CHLafi)	52.7	997.04	1.4
Comb 3	SST variables as additive, KE and CHLA as interactive	iSSTa + (KE,KEfi) + (CHLa,CHLafi)	52.6	998.32	2.7
Comb 4	SST and KE variables as additive, CHLA as interactive	iSSTa + KEfi + (CHLa,CHLafi)	52.6	996.39	0.8
Comb 5	SST and Chla variables as additive, KE as interactive	iSSTa + (KE,KEfi) + CHLa	52.5	997.52	1.9
Comb 6	SST variables as interactive, KE and CHLA as additive	(SSTa,iSSTa) + KEfi + CHLa	52.7	995.73	0.1

The spawning habitat quality (hereafter SHQ) was defined as the larval abundance at each sampling location resulting from the moving window average filter at the selected spatial scale. Maps of SHQ are computed to assess the spatial distribution of spawning areas. We computed SHQ maps from larval abundances observed *in situ* and from larval abundances obtained from the GAMs that showed highest deviances and lower AICs in the previous selection process. All computations were coded in R software (R Development Core Team, 2008). A methodological graphical scheme showing the SHQ calculation is provided as Supplementary Figure S1.

Evaluating the predictions of "SHQ" through an interannual cross-validation approach

Maps of SHQ from larval abundances obtained from GAMs fitted with all the 5 years available (hereafter "fitted SHQ") were compared with maps of the SHQ from observed larval abundances (hereafter "observed SHQ") using Spearman correlations. Both fitted and observed SHQ maps were computed at the same spatial resolution depicted from the scalograms. These correlations provided information of the model performance on yearly basis. We processed the correlations for the various models selected during the AIC and deviance analyses. We also applied this processing to the reference model (model with no environmental variables) to assess the relevance of including environmental information.

To assess the predictive capability of the different GAMs, we performed an interannual cross-validation by splitting the data into a validation and training datasets. The former was composed of the 1-year data extracted from the 5 years available. The training dataset was composed of the four remaining years. Selected GAMs were adjusted with the training dataset obtaining a new model in each interaction. Spawning habitat quality was computed from larval abundances obtained with these models (thereafter "predicted SHQ") and compared with observed SHQ values. This process runs for each year available and, therefore, five predictions were estimated. This analysis was applied to each of the models previously selected during the AIC and deviance analyses. In each run, the smoothers were recalculated to assess the robustness of the environmental effects on the SHQ among years.

Results

Performance of the different processed models

General additive models showed higher explained deviances and lower AICs when environmental variables were included in the model design (Table 2). The model including only additive variables (M.add in Table 2) showed the lowest AIC. During the variable selection process, this model retained iSSTa, KEfi, and CHLa, while SSTa, KE, and CHLafi were not significant. These results demonstrated the high relevance of seascapes related to the spatio-temporal variability of SST and KE. However, AIC of M.add did not differ from some of the other processed models, therefore models with a ΔAIC <2.5 (models Madd, comb 1, comb 2, comb 4, comb 5, comb 6 in Table 2) were selected as potential model candidates for calculation of the SHQ. Scalograms were computed for each of these selected models to depict the spatial scale on which the SHQ should be processed.

Scalogram processing and spatial scale selection for definition of the SHQ

The correlations between observed and fitted SHQ (adjusted from models including the 5 years available) show similar trends among the six models selected. That is, correlations increased with increasing spatial scales (Figure 3). After examination of the processed scalograms, we selected 31.5 km as the best radius distance for the spatial smoothing and subsequently used this distance to predict SHQ. At this spatial scale, all models presented a correlation coefficient >0.5. Beyond this threshold, the slope of the correlograms decreased for all years except 2003 and the curve became asymptotic for 2004 and 2005 (Figure 3).

Best operational model selection

The correlations between observed and fitted SHQ varied among years but they showed similar values among selected models with correlation values >0.5 (Table 3). For all models, the year 2005 presented the best correlation (0.8) and 2003 the worst (0.55).

Results from the evaluation of the prediction capabilities through the cross-validation approach showed that correlation coefficients between observed and predicted SHQ from all selected models performed significantly better than the M1 model (model with no environmental variables, Table 4). This result demonstrated the relevance of the proposed seascapes for predicting spawning habitats. Although all selected models showed similar correlation coefficients, the model containing interactive terms for SST and KE related variables and additive for CHLa showed the best predictive capabilities with correlation values >0.5 for 4 out of 5 years predicted (model combined-1 in Table 4). Therefore, the model "combined 1" was selected for computing the prediction maps of the SHQ.

Relation between SHQ and environmental information

The latitude-longitude map displays the mean spatial distribution of larvae along the 5 years with the lowest values found in the Southeast study area (Figure 4a). The main spawning habitats were located Southwest Ibiza Island and West of the archipelago. The bivariate plot of the interactive effects of SSTa-iSSTa indicates a positive effect of both variables on laval abundances (Figure 4b). For the response of the KE-KEfi interaction, the bivariate plot indicates a positive effect of KEfi and a low effect of KE (Figure 4c). The partial effect for the diurnal variation shows changes in catchability along the day, with maximum values at midnight and noon (Figure 4d). The effect associated to CHLa presents a negative trend, indicating higher probability of finding spawning events in areas of low CHLa values (Figure 4e).

Responses obtained from the five models processed during the cross-validation process (1 per year) showed that the patterns associated to the latitude-longitude, hour, and CHLa are consistent throughout the years (Supplementary Figure S2). The effect of the interaction term SSTa-iSSTa was also consistent, with a small variation in year 2002. The low effect of the KE variable in the interaction term KE-KEfi may change when one particular year is removed from the training dataset (see Supplementary Figure S2 year 2001), showing that the interaction terms play a relevant role in explained deviances for years with particular conditions. This explains why the model with lower AIC (only additive variables) did not provide the best predictive capability.

Comparison of "observed", "fitted" and "predicted" SHQ

The SHQ computed from observed data (observed SHQ) shows a patchy pattern (Figure 5). In general, spawning areas were mainly located at the East and Southwest of the archipelago (Figure 5a, from 2001 to 2005). The most intense spawning habitats for each year, excluding 2003, occurred in the East. The 2005 survey shows the patchiest distributions, with spawning habitats distributed

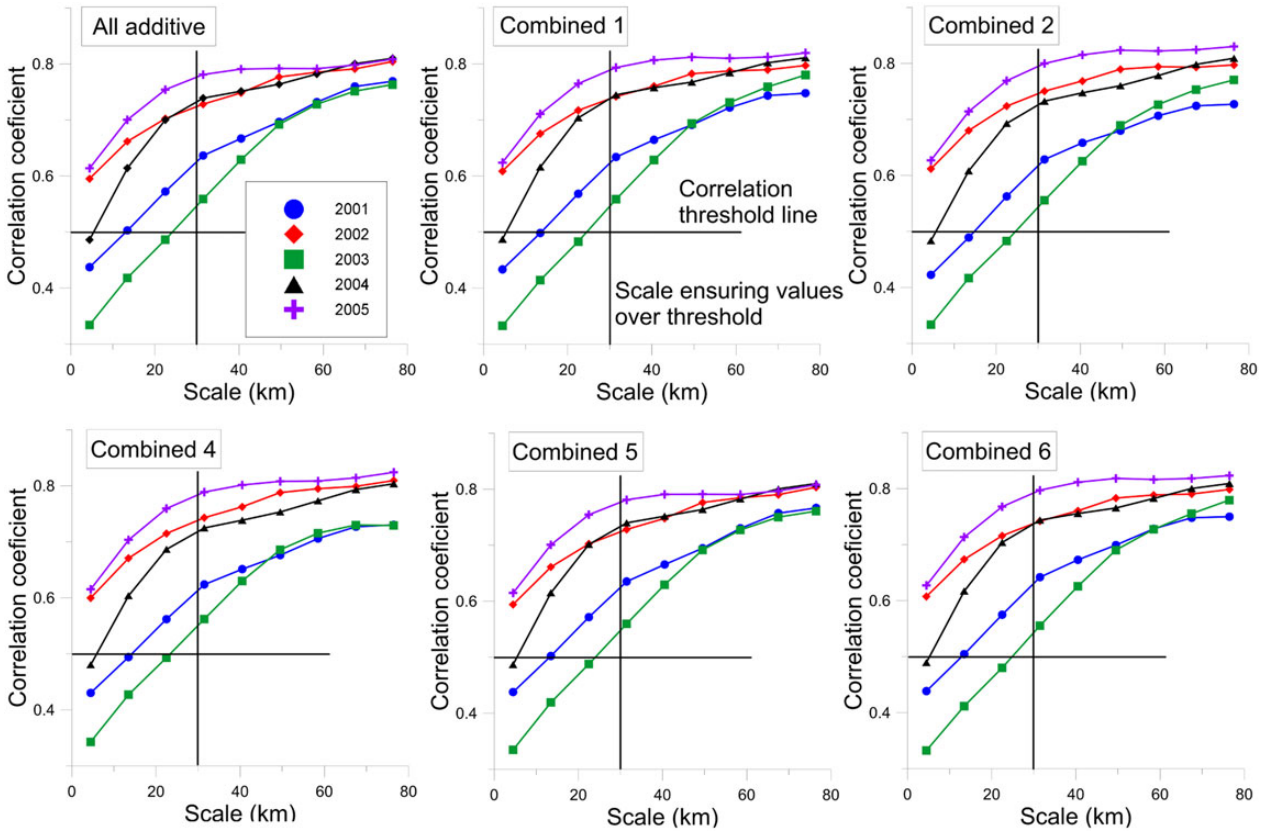

Figure 3. Scalograms computed for each selected model and year. See Table 2 for model name and structure definition. Horizontal lines indicating correlation equal to 0.5. Vertical lines indicating selected spatial scale. This figure is available in black and white in print and in colour at *ICES Journal of Marine Science* online.

Table 3. Spearman correlation of observed and fitted SHQ.

Year	M1	All additive	Comb.1	Comb.2	Comb.4	Comb.5	Comb.6
2001	0.62	0.64	0.63	0.63	0.62	0.63	0.64
2002	0.57	0.73	0.74	0.75	0.74	0.73	0.74
2003	0.50	0.56	0.56	0.56	0.56	0.55	0.55
2004	0.51	0.74	0.75	0.73	0.72	0.74	0.74
2005	0.51	0.78	0.79	0.80	0.79	0.78	0.79

For model specification details, see Table 2.

Table 4. Spearman correlation of observed and predicted SHQ.

Year	M1	All additive	Comb.1	Comb.2	Comb.4	Comb.5	Comb.6
2001	0.42	0.47	0.51	0.44	0.43	0.47	0.48
2002	0.25	0.62	0.62	0.63	0.63	0.62	0.63
2003	0.18	0.28	0.26	0.26	0.26	0.27	0.27
2004	0.40	0.70	0.69	0.69	0.68	0.69	0.70
2005	0.28	0.67	0.73	0.74	0.67	0.66	0.73

For model specification details, see Table 2.

along the southern area of the archipelago and no spawning habitats at the north (Figure 5a for the year 2005). The spatial distributions of fitted and predicted SHQ are similar, and they both identified the patchy distribution and the persistence of the spawning in the western part of the archipelago represented by the observed data (Figure 5b and 5c years 2001–2005). Predictions obtained from the cross-validations located high values of SHQ within a distance range of 60 km from observed maxima for all years except 2005 (Figure 5c of 2005). For 2005, maximum values of SHQ were predicted at the South of Ibiza Island, which was an important spawning area for that year, but the maximum values of the observed SHQ occurred to the Southeast. Graphical outputs and correlation coefficients provided evidence that GAMs fitted from operational data sources allow predicting the spatial patterns of spawning areas (Tables 3 and 4).

Discussion

Pelagic seascapes derived from operational oceanographic data sources can provide new insights on the environmental cues driving the spatial distribution of bluefin tuna spawning areas. Modelling and predicting the spatial distribution of spawning areas was possible by applying pelagic seascape descriptors that provided information on the spatio-temporal variability of sea surface temperature, geostrophic velocities, and chlorophyll *a*. Thus, our results provide new avenues of applied research, particularly in the emerging field of operational fisheries oceanography in which near real-time operational products from integrated ocean observing systems will serve as tools for the 21st century fisheries management (Berx *et al.*, 2011; Manderson *et al.*, 2011; Hobday *et al.*, 2014).

Previous studies have already shown that mesoscale oceanography affects spawning of bluefin tuna around the Balearic Sea (Alemany *et al.*, 2010; Reglero *et al.*, 2012; Muhling *et al.*, 2013). We found

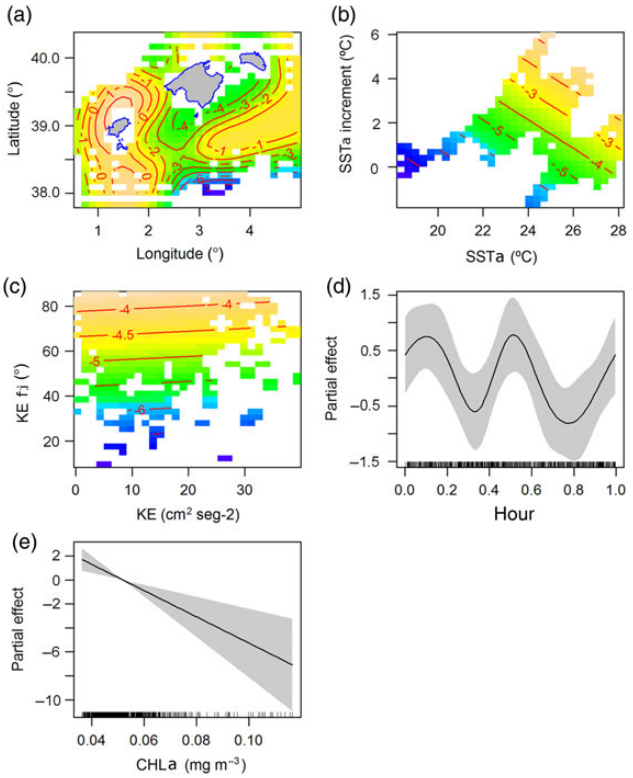

Figure 4. Partial effects of environmental variables on larval abundances for the selected general additive model. (a)–(c) showing the effect of the interaction between variables (isolines indicate partial effect on larval abundances. Light colours indicate higher abundances, dark colours indicate lower abundances). (d) The partial effect of hour of the day, standardized from 0 to 1. (e) The partial effect of chlorophyll *a*. This figure is available in black and white in print and in colour at *ICES Journal of Marine Science* online.

that the temporal evolution of Sea surface temperature and the spatial variability of kinetic energy were more relevant to identify patterns in larval distribution than just the absolute values. These findings confirm previous studies showing that the combination of means and gradients of an oceanographic variable improves our capability to investigate species–environment relationships (Alvarez-Berastegui *et al.*, 2014). The present study thus highlights the importance of using proper pelagic seascape metrics, which convey information about the dynamic behaviour of the oceanographic processes. Sea surface temperature during the beginning of the spawning season may trigger the development of adult gonads since the gonadosomatic index increases as the mature individuals reach the Balearic Sea (Medina *et al.*, 2002). High means of Sea surface temperature may be also a requisite for embryo and larval growth and survival. These two processes, gonadosomatic development and larval survival, may have driven evolutionary constrains for the location of spawning areas (Ciannelli *et al.*, 2015). The combination of the mean and increment of Sea surface temperature measured from operational data sources provides a good proxy for capturing complementary ecological and physiological processes affecting habitat preference of bluefin tuna.

Our results show that the location of hot-spots of larval abundances (yolk sac and preflexion stages) used as a proxy for spawning habitats depends on the interaction of kinetic energy and its spatial variability used as proxy of frontal processes. The main frontal area is formed when recent Atlantic waters enter in the Mediterranean through the strait of Gibraltar and reach the Balearic Sea, mixing with saltier resident waters (Balbín *et al.*, 2014) where spawning occurs (Alemany *et al.*, 2010; Reglero *et al.*, 2012). The highest larval abundances are associated with low–medium kinetic energy values near the front what may indicate the retention role of the front rather than a spawning area. Recent studies analysing the spatial distribution of embryo, identified from genetic analysis, found a relationship between embryo abundances and the location of the main salinity front (P. Reglero, pers. comm.). This result, along with the relative short drifts trajectories found for yolk sac and preflexion larval stages support the hypothesis that spawning is associated to mesoscale activity in the area.

The location of spawning areas has been also associated with salinity, which in turn are associated with frontal areas. Salinity is one of the most relevant environmental variable explaining the spatial distribution of bluefin tuna larvae in the Balearic Sea (Alemany *et al.*, 2010; Reglero *et al.*, 2012), the gulf of Tunisia (Koched *et al.*, 2013), and the Gulf of Mexico (Muhling *et al.*, 2010, 2013). Whether bluefin tuna adults detect salinity gradients or whether they detect other processes associated to the front is not resolved. Improving hydrodynamic models to reach required quality of SSS projections will give the possibility of developing new relevant environmental descriptors for the spawning habitat forecast and to disentangle different causes associated to the dependence of the spawning ecology with the mesoscale activity. This is an important challenge for operational oceanography in the Mediterranean Sea (Juza *et al.*, 2015).

The fact that chlorophyll *a* plays an important role in our models may be also associated to the lack of environmental variables providing information about the different water masses, such as salinity. Within the study area and for some of the studied years, lower values of chlorophyll *a* were associated to the fresher water masses (Balbín *et al.*, 2012). Thus, chlorophyll *a* could be acting as a proxy of water masses. Whether the effect of chlorophyll *a* on the spawning locations is direct or indirect associated to water masses needs further investigation.

Model selection and validation

One of the most relevant results from this study emerges from the cross-validation approach developed. Responses of the spawning habitat (measured by the SHQ), to the different variables could be strongly driven by particular years (i.e. year-specific oceanographic scenarios). By employing the cross-validation approach, we tested whether the response variables were stable among different years, which is of paramount importance to provide projections of potential spatial distributions with appropriate certainty. All variables were consistent among the five test years, but small differences allowed identifying factors that had more relevance in some years than others.

Our models were able to reproduce the spatial distribution of yolk sac and preflexion stages of bluefin tuna larvae, used as a proxy for spawning locations. However, absolute values of SHQ from observed and modelled data differ. This suggests that including additional variables of biological or oceanographic processes not considered in this study would improve the modelling results. For example, considering the interannual variability of the total abundance of the bluefin spawning stock or approaching the habitat quality definition by standardizing the SHQ among years are aspects to explore in the future.

Applications and further research

Predictive modelling of spawning habitats could serve as an operational tool for designing dynamic spatial management approaches

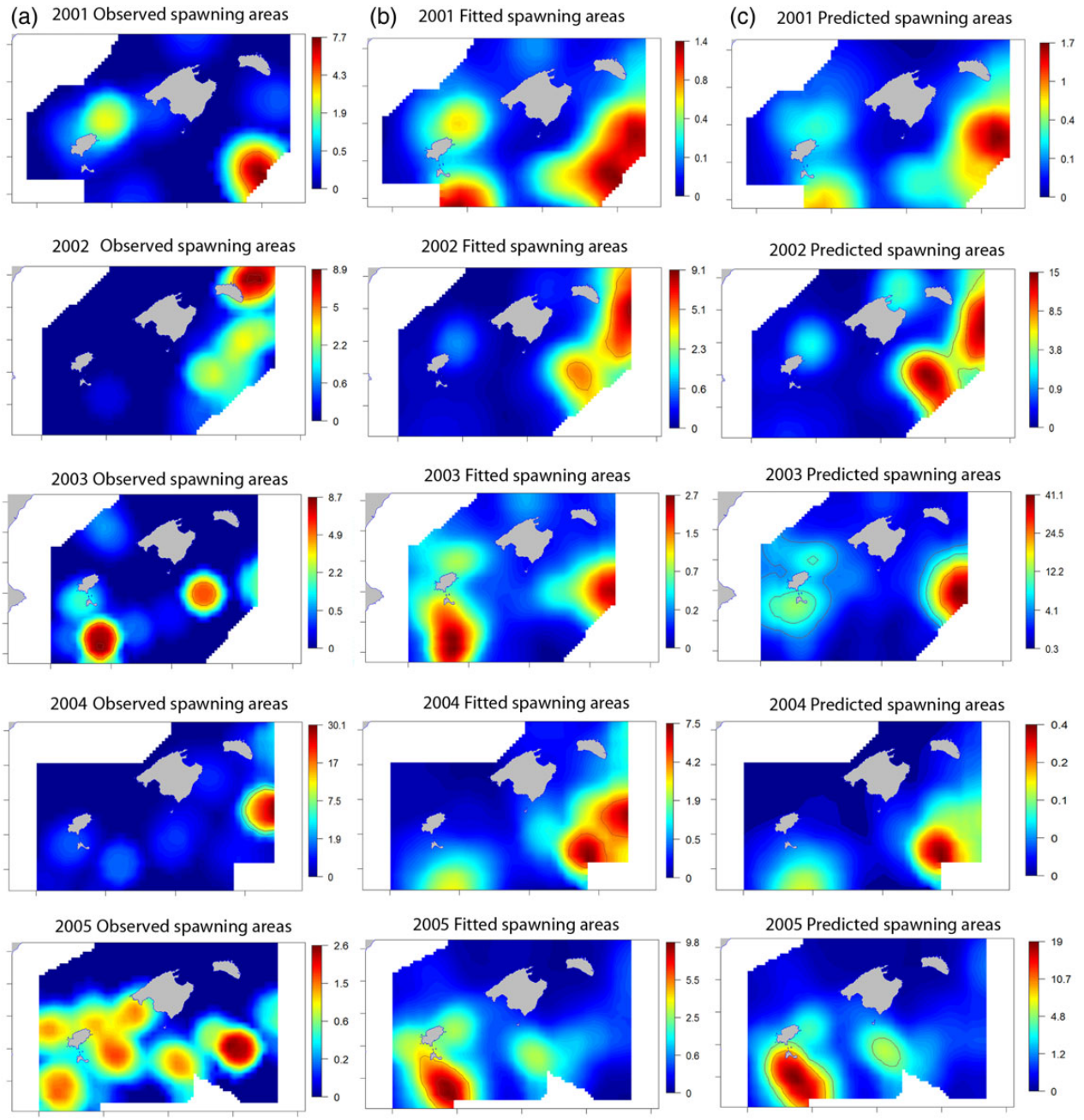

Figure 5. Yearly spatial distribution of real (observed, left), modelled (centre), and cross-predicted (right) SHQ from 2001 to 2005 (from first to fifth row). This figure is available in black and white in print and in colour at *ICES Journal of Marine Science* online.

(Hobday *et al.*, 2010, 2014), and for improving current larvae habitat models used for spawning stock biomass calculations (Ingram *et al.*, 2013). Identification of relevant seascape metrics may also be applicable when predicting pelagic essential habitats under other methodological frameworks applied to larger spatial scales (Druon *et al.*, 2011).

Nevertheless, to advance "pelagic seascape ecology" and "operational fisheries oceanography" some analytical developments are required. Here, we list those we believe most important: (i) the accessibility to long time-series and near real-time predictions of key environmental variables in common data formats, (ii) well-validated environmental data products from remote sensing and hydrodynamic models (long-term simulations and forecasts), (iii) the appropriate knowledge of the oceanographic processes driving species ecology, (iv) the design of appropriated pelagic seascape metrics capturing the dynamic processes affecting the species ecology, and (v) identification of the specific needs in terms assessment and management.

In relation to these challenges, data from remote sensing and hydrodynamic models are available at global, regional, and local scales from multiple operational oceanographic data providers. However, standardization in data formats should occur as well as software libraries for operational oceanographic data handling in open source software packages such "R" (R Development Core Team, 2008), recommendations made also by other researchers in the field (Hobday *et al.*, 2014). Furthermore, software drivers for

old data formats, as some hierarchical data formats, may not be available or easy to handle with new operating systems. In addition, specific calibration and validation of the operational oceanography products in specific areas of interest is a key issue. This needs dedicated efforts at regional and local scales to develop data-assimilative high-resolution hydrodynamic models, which can combine data from multiple sampling platforms (Tintoré *et al.*, 2013b).

Along this study, we have referred to "pelagic seascape ecology" as a particular field within the emerging "seascape ecology". Research in seascape ecology differs when applied to the analysis of benthic habitats or to the pelagic habitats. Analysis of benthic habitats is typically considered as a mixture of categorical habitat patches. In that case, techniques to quantify habitat patterns are mainly the same than those applied in the traditional landscape ecology (Wedding *et al.*, 2011), which provides valuable information for the study of how benthic habitat patterns affects nectobenthic species (Pittman *et al.*, 2011). However, pelagic seascapes are highly dynamic and do not present clear boundaries. Therefore, metrics based on the patch concept are not valid and different techniques and concepts are necessary to investigate species–habitat relationships. Pelagic seascape ecology is strongly linked to satellite remote sensing, hydrodynamic models, and the development of algorithms for identification of specific oceanographic processes such frontal areas (i.e. Hobday and Hartog, 2014), while benthic seascape ecology is arguably linked to categorical benthic habitat and topographic maps (i.e. Bostrom *et al.*, 2011). Both types of seascape ecology can be applied to study ecological processes regarding, for example, how benthic habitat fragmentation affects population distribution (benthic seascape ecological approaches), or how oceanographic processes such as chlorophyll *a* blooms in the area, affects their growth (pelagic seascapes ecological approaches).

Operational fisheries oceanography must provide solutions to actual limitations in fisheries science, therefore the questions addressed in studies of seascape ecology should focus on fisheries assessment and management needs. Here, we focused on the spawning habitat models, with direct applications to current assessment methods, but a diversity of assessment applications are feasible. We recommend deployment of multidisciplinary perspectives that embrace seascape ecology, operational fisheries oceanography and classic assessment approaches.

Conclusions

Previous evidence indicates that the location of bluefin tuna spawning areas around the Balearic Sea depends on dynamic oceanographic conditions that change among years. This association relates to specific ecological requirements of the bluefin tuna adults and larvae, and provides the scientific basis to model the distribution of spawning areas. The present study achieves that objective using exclusively operational oceanography products, such as remote sensing altimetry, chlorophyll *a* and sea surface temperatures from hydrodynamic models. Further processing of these products, as the temporal evolution of the sea surface temperature or the spatial variability of kinetic energy, provided pelagic seascape metrics that better captured the dynamic processes affecting bluefin tuna spawning ecology. These metrics allowed development of a model that predicted the spatial distribution of spawning locations in near real time, which opens a new generation of assessment and management tools. Improving prediction capabilities of the bluefin tuna spawning habitats under a broad variety of oceanographic scenarios can be directly used in assessment and management decision-making. These capabilities will provide robust basis to design pelagic dynamic marine protected areas and to adjust larval indices used in the evaluation of the spawning-stock biomass.

Supplementary data

Supplementary material is available at the *ICESJMS* online version of the manuscript.

Acknowledgements

We first want to thank all the scientists and crew participating in the TUNIBAL cruises on-board the R/V Vizconde de Eza and Cornide de Saavedra. Biological data collection and analysis were financed by the projects TUNIBAL (REN 2003-01176), BALEARES (CTM 2009-07944 MAR) and ATAME (2011-29525-004-02), competitive projects funded by the Spanish Government I + D + I (Research + Development + innovation) National Plan. We acknowledge MyOcean (http://www.myocean.eu) for providing SST data from hydrodynamic models (MFS) and multisensor chlorophyll *a* data. SST data from satellite was provided by NASA (http://oceancolor.gsfc.nasa.gov). The altimeter products were produced by Ssalto/Duacs and distributed by AVISO, with support from CNES (http://www.aviso.altimetry.fr/en/data.html). M.H. was funded by a postdoctoral contract from the regional government of the Balearic Islands, *Dirección General d'Educació, Personal Docent, Universitats i Recerca*, co-funded by the European Social Fund 2014–2020. The research was developed under the framework of the project "PERSEUS" financed by the Seventh Framework Program for Research (FP7) under theme "Oceans Tomorrow", grant Agreement No. 287600 (http://www.perseus-net.eu/site/content.php), and the BLUEFIN TUNA Project, driven by the Balearic Island Observing and Forecasting System (www.socib.es) and the Spanish Institute of Oceanography (www.ieo.es).

References

Akaike, H. 1981. Likelihood of a model and information criteria. Journal of Econometrics, 16: 3–14.

Alemany, F., Quintanilla, L., Velez-Belchi, P., Garcia, A., Cortés, D., Rodriguez, J. M., Fernández de Puelles, M. L., *et al.* 2010. Characterization of the spawning habitat of Atlantic bluefin tuna and related species in the Balearic Sea (western Mediterranean). Progress in Oceanography, 86: 21–38.

Alvarez-Berastegui, D., Ciannelli, L., Aparicio-Gonzalez, A., Reglero, P., Hidalgo, M. J., López-Jurado, L., Tintoré, J., *et al.* 2014. Spatial scale, means and gradients of hydrographic variables define pelagic seascapes of bluefin and bullet tuna spawning distribution. PLoS ONE, 9: e109338.

Aranda, G., Abascal, F. J., Varela, J. L., and Medina, A. 2013. Spawning behaviour and post-spawning migration patterns of Atlantic Bluefin Tuna (Thunnus thynnus) ascertained from satellite archival tags. PLoS ONE, 8: e76445.

Balbín, R., Flexas, M. d. M., López-Jurado, J. L., Peña, M., Amores, A., and Alemany, F. 2012. Vertical velocities and biological consequences at a front detected at the Balearic Sea. Continental Shelf Research, 47: 28–41.

Balbín, R., López-Jurado, J. L., Flexas, M. M., Reglero, P., Vélez-Velchí, P., González-Pola, C., Rodríguez, J. M., *et al.* 2014. Interannual variability of the early summer circulation around the Balearic Islands: driving factors and potential effects on the marine ecosystem. Journal of Marine Systems, 138: 70–81.

Berx, B., Dickey-Collas, M., Skogen, M. D., De Roeck, Y. H., Klein, H., Barciela, R., *et al.* 2011. Does operational oceanography address the needs of fisheries and applied environmental scientists? Oceanography, 24: 166–171.

Bostrom, C., Pittman, S. J., Simenstad, C., and Kneib, R. T. 2011. Seascape ecology of coastal biogenic habitats: advances, gaps, and challenges. Marine Ecology-Progress Series, 427: 191–217.

Bouffard, J., Nencioli, F., Escudier, R., Doglioli, A. M., Petrenko, A. A., Pascual, A., Poulain, P. M., *et al.* 2014. Lagrangian analysis of satellite-derived currents: Application to the North Western Mediterranean coastal dynamics. Advances in Space Research, 53: 788–801.

Bricheno, L. M., Wolf, J. M., and Brown, J. M. 2014. Impacts of high resolution model downscaling in coastal regions. Continental Shelf Research, 87: 7–16.

Ciannelli, L., Bailey, K., and Olsen, E. M. 2015. Evolutionary and ecological constraints of fish spawning habitats. ICES Journal of Marine Science, 72: 285–296.

Dahlin, H., Fleming, N. C., and Petersson, S. E. (Eds). Proceedings of the Sixth International Conference on EuroGOOS 4–6 October 2011, Sopot, Poland, 978-91-974828-9-9, Eurogoos Publication, 2014.

de la Gándara, F., Ortega, A., Blanco, E., Viguri, F. J., and Reglero, P. 2013. La flexión de la notocorda en larvas de atún rojo,Thunnus thynnus (L, 1758) cultivadas a diferentes temperaturas. *In* Sociedad Española de Acuicultura editor. XIV Congreso Nacional de Acuicultura, pp. 181–182. Universidad Laboral de Gijón, Gijón.

Druon, J. N. 2010. Habitat mapping of the Atlantic bluefin tuna derived from satellite data: Its potential as a tool for the sustainable management of pelagic fisheries. Marine Policy, 34: 293–297.

Druon, J. N., Fromentin, J. M., Aulanier, F., and Heikkonen, J. 2011. Potential feeding and spawning habitats of Atlantic bluefin tuna in the Mediterranean Sea. Marine Ecology-Progress Series, 439: 223–240.

Fromentin, J. 2009. Lessons from the past: investigating historical data from bluefin tuna fisheries. Fish and Fisheries, 10: 197–216.

Fromentin, J. M., and Powers, J. E. 2005. Atlantic bluefin tuna: population dynamics, ecology, fisheries and management. Fish and Fisheries, 6: 281–306.

Game, E. T., Grantham, H. S., Hobday, A. J., Pressey, R. L., Lombard, A. T., Beckley, L. E., Gjerde, K., *et al.* 2009. Pelagic protected areas: the missing dimension in ocean conservation. Trends in Ecology and Evolution, 24: 360–369.

García, A., Alemany, F., De la Serna, J. M., Oray, I., Karakulak, S., Rollandi, L., Arigò, A., *et al.* 2005a. Preliminary results of the 2004 bluefin tuna larval surveys off different Mediterranean sites (Balearic Archipelago, Levantine Sea and the Sicilian Channel). Collective Volume of Scientific Papers ICCAT, 58: 1261–1270.

García, A., Alemany, F., Velez-Belchí, P., Jurado, J. L., Cortés, D., De la Serna, J. M., Pola, C. G., *et al.* 2005b. Characterization of the bluefin tuna spawning habitat off the Balearic Archipelago in relation to key hydrographic features and associated environmental conditions. ICCAT Collected Volume of Scientific Papers, 58: 535–549.

Gordoa, A., and Carreras, G. 2014. Determination of temporal spawning patterns and hatching time in response to temperature of atlantic bluefin tuna (Thunnus thynnus) in the Western Mediterranean. PLoS ONE, 9: e90691.

Heinisch, G., Corriero, A., Medina, A., Abascal, F. J., de la Serna, J-M., Vassallo-Agius, R., Ríos, A. B., *et al.* 2008. Spatial-temporal pattern of bluefin tuna (Thunnus thynnus L. 1758) gonad maturation across the Mediterranean Sea. Marine Biology, 154: 623–630.

Hilbe, J. 2011. Negative Binomial Regression. 2nd edn. Cambridge University Press, New York.

Hobday, A. J., and Hartmann, K. 2006. Near real time spatial management based on habitat predictions for a longline bycatch species. Fisheries Management and Ecology, 13: 365–380.

Hobday, A. J., and Hartog, J. R. 2014. Derived ocean features for dynamic ocean management. Oceanography, 27: 134–145.

Hobday, A. J., Hartog, J. R., Timmiss, T., and Fielding, J. 2010. Dynamic spatial zoning to manage southern bluefin tuna (Thunnus maccoyii) capture in a multi-species longline fishery. Fisheries Oceanography, 19: 243–253.

Hobday, A. J., Maxwell, S. M., Forgie, J., and McDonald, J. 2014. Dynamic ocean management: integrating scientific and technological capacity with law, policy, and management. Stanford Environmental Law Journal, 33: 125–165.

Ingram, G. W., Alemany, F., Alvarez-Berastegui, D., and García, A. 2013. Development of indices of larval bluefin tuna (Thunnus thynnus) in the Western Mediterranean Sea. Collective Volume of Scientific Papers, ICCAT, 69: 1057–1076.

Juza, M., Mourre, B., Lellouche, J. M., Tonani, M., and Tintoré, J. 2015. From basin to sub-basin scale assessment and intercomparison of numerical simulations in the Western Mediterranean Sea. Journal of Marine Systems, 149: 36–49.

Koched, W., Hattour, A., Alemany, F., Garcia, A., and Said, K. 2013. Spatial distribution of tuna larvae in the Gulf of Gabes (Eastern Mediterranean) in relation with environmental parameters. Mediterranean Marine Science, 14: 5–14.

Llopiz, J. K., and Hobday, A. J. 2015. A global comparative analysis of the feeding dynamics and environmental conditions of larval tunas, mackerels, and billfishes. Deep Sea Research Part II: Topical Studies in Oceanography, 113: 113–124.

Louzao, M., Pinaud, D., Peron, C., Delord, K., Wiegand, T., and Weimerskirch, H. 2011. Conserving pelagic habitats: seascape modelling of an oceanic top predator. Journal of Applied Ecology, 48: 121–132.

Manderson, J., Palamara, L., Kohut, J., and Oliver, M. J. 2011. Ocean observatory data are useful for regional-habitat modeling of species with different vertical habitat preferences. Marine Ecology Progress Series, 438: 1–17.

Mannocci, L., Laran, S., Monestiez, P., Dorémus, G., Van Canneyt, O., Watremez, P., and Ridoux, V. 2013. Predicting top predator habitats in the Southwest Indian Ocean. Ecography, 37: 261–278.

Margulies, D., Suter, J. M., Hunt, S. L., Olson, R. J., Scholey, V. P., Wexler, J. B., and Nakazawa, A. 2007. Spawning and early development of captive yellowfin tuna (Thunnus albacares). Fish Bulletin, 105: 249–265.

Mather, F. J., Mason, J. M., and Jones, A. C. 1995. Historical document: life history and fisheries of Atlantic bluefin tuna. US Dept. of Commerce, National Oceanic and Atmospheric Administration, National Marine Fisheries Service.

Maunder, M. N., and Punt, A. E. 2004. Standardizing catch and effort data: a review of recent approaches. Fisheries Research, 70: 141–159.

Medina, A., Abascal, F. J., Megina, C., and Garcia, A. 2002. Stereological assessment of the reproductive status of female Atlantic northern bluefin tuna during migration to Mediterranean spawning grounds through the Strait of Gibraltar. Journal of Fish Biology, 60: 203–217.

Muhling, B. A., Lamkin, J. T., and Roffer, M. A. 2010. Predicting the occurrence of Atlantic bluefin tuna (Thunnus thynnus) larvae in the northern Gulf of Mexico: building a classification model from archival data. Fisheries Oceanography, 19: 526–539.

Muhling, B. A., Lee, S. K., Lamkin, J. T., and Liu, Y. 2011. Predicting the effects of climate change on bluefin tuna (Thunnus thynnus) spawning habitat in the Gulf of Mexico. ICES Journal of Marine Science, 68: 1051–1062.

Muhling, B. A., Reglero, P., Ciannelli, L., Alvarez-Berastegui, D., Alemany, F., Lamkin, J. T., and Roffer, M. A. 2013. Comparison between environmental characteristics of larval bluefin tuna Thunnus thynnus habitat in the Gulf of Mexico and western Mediterranean Sea. Marine Ecology Progress Series, 486: 257–276.

Pascual, A., Bouffard, J., Ruiz, S., Buongiorno Nardelli, B., Vidal-Vijande, E., Escudier, R., Sayol, J. M., *et al.* 2013. Recent improvements in mesoscale characterization of the western Mediterranean Sea: synergy between satellite altimetry and other observational approaches. Scientia Marina, 77: 19–36.

Pascual, A., Pujol, M. I., Larnicol, G., Le Traon, P. Y., and l. n. Rio, M. H. 2007. Mesoscale mapping capabilities of multisatellite altimeter missions: first results with real data in the Mediterranean Sea. Journal of Marine Systems, 65: 190–211.

Pittman, S. J., Kneib, R. T., and Simenstad, C. A. 2011. Practicing coastal seascape ecology. Marine Ecology-Progress Series, 427: 187–190.

R Development Core Team. 2008. R: A language and environment for statistical computing. R Foundation for Statistical Computing, Vienna, Austria.

Rayner, R. 2010. The US integrated ocean observing system in a global context. Marine Technology Society Journal, 44: 26–31.

Reglero, P., Balbín, R., Ortega, A., Alvarez-Berastegui, D., Gordoa, A., Torres, A. P., Moltó, V., *et al.* 2013. First attempt to assess the viability of bluefin tuna spawning events in offshore cages located in an a priori favourable larval habitat. Scientia Marina, 77: 585–594.

Reglero, P., Ciannelli, L., Álvarez-Berastegui, D., Balbín, R., López-Jurado, J. L., and Alemany, F. 2012. Geographically and environmentally driven spawning distributions of tuna species in the western Mediterranean Sea. Marine Ecology Progress Series, 463: 273–284.

Reglero, P., Tittensor, D. P., Álvarez-Berastegui, D., Aparicio-González, A., and Worm, B. 2014. Worldwide distributions of tuna larvae: revisiting hypotheses on environmental requirements for spawning habitats. Marine Ecology Progress Series, 501: 207–224.

Rio, M. H., Pascual, A., Poulain, P-M., Menna, M., Barceló-Llull, B., and Tintoré, J. 2014. Computation of a new mean dynamic topography for the Mediterranean Sea from model outputs, altimeter measurements and oceanographic in situ data. Ocean Science, 10: 731–744.

Scales, K. L., Miller, P. I., Hawkes, L. A., Ingram, S. N., Sims, D. W., and Votier, S. C. 2014. On the Front Line: frontal zones as priority at-sea conservation areas for mobile marine vertebrates. Journal of Applied Ecology, 51: 1575–1583.

Shillinger, G. L., Palacios, D. M., Bailey, H., Bograd, S. J., Swithenbank, A. M., Gaspar, P., Wallace, B. P., *et al.* 2008. Persistent leatherback turtle migrations present opportunities for conservation. PLoS Biology, 6: e171.

Tintoré, J., Casas, B., Heslop, E., Vizoso, G., Pascual, A., Orfila, A., Ruiz, S., *et al.* 2013a. The impact of new multi-platform observing systems in science, technology development and response to society needs; from small to large scales. *In* Computer Aided Systems Theory-EUROCAST 2013, pp. 341–348. Springer, Berlin, Heidelberg.

Tintoré, J., Vizoso, G., Casas, B., Heslop, E., Pascual, A., Orfila, A., Ruiz, S., *et al.* 2013b. SOCIB: The Balearic Islands Coastal ocean observing and forecasting system, responding to science, technology and society needs. Marine Technology Society Journal, 47: 101–117.

Torres, A. P., Reglero, P., Balbin, R., Urtizberea, A., and Alemany, F. 2011. Coexistence of larvae of tuna species and other fish in the surface mixed layer in the NW Mediterranean. Journal of Plankton Research, 33: 1793–1812.

US-DOC/NOAA/NMFS. Final Amendment 7 to the 2006 Consolidated Highly Migratory Species Fishery Management Plan. 2014. Highly Migratory Species Management Division-Office of Sustainable Fisherie-National Marine Fisheries Service.

Volpe, G., Santoleri, R., Vellucci, V., d'Alcalá, M. R., Marullo, S., and d'Ortenzio, F. 2007. The colour of the Mediterranean Sea: Global versus regional bio-optical algorithms evaluation and implication for satellite chlorophyll estimates. Remote Sensing of Environment, 107: 625–638.

Wedding, L. M., Lepczyk, C. A., Pittman, S. J., Friedlander, A. M., and Jorgensen, S. 2011. Quantifying seascape structure: extending terrestrial spatial pattern metrics to the marine realm. Marine Ecology-Progress Series, 427: 219–232.

Wood, S. N. 2006. Generalized additive models: an introduction with R., 66 edition. Chapman & Hall, CRC, Boca Raton, Forida.

Worm, B., Sandow, M., Oschlies, A., Lotze, H. K., and Myers, R. A. 2005. Global patterns of predator diversity in the open oceans. Science, 309: 1365–1369.

Ziegeler, S. B., Dykes, J. D., and Shriver, J. F. 2012. Spatial error metrics for oceanographic model verification. Journal of Atmospheric and Oceanic Technology, 29: 260–266.

Handling editor: David Secor

ICES Journal of Marine Science

ICES Journal of Marine Science (2016), 73(7), 1863–1874. doi:10.1093/icesjms/fsw075

Contribution to the Themed Section: '*Seascape Ecology*'

Original Article

Ensemble squid habitat model using three-dimensional ocean data

Irene D. Alabia[1]*, Sei-Ichi Saitoh[1,2], Hiromichi Igarashi[3], Yoichi Ishikawa[3], Norihisa Usui[4], Masafumi Kamachi[4], Toshiyuki Awaji[5], and Masaki Seito[6]

[1]*Arctic Research Center, Hokkaido University, N21 W11 Kita-Ku, Sapporo 001-0021, Japan*
[2]*Laboratory of Marine Environment and Resource Sensing, Graduate School of Fisheries Sciences, Hokkaido University, 3-1-1 Minato-cho, Hakodate, Hokkaido 041-8611, Japan*
[3]*Data Research Center for Marine-Earth Sciences, Japan Agency for Marine Earth-Science and Technology (JAMSTEC), 3173-25 Showamachi, Kanazawa-ward Yokohama City, Kanagawa 236-0001, Japan*
[4]*Oceanographic Research Department, Meteorological Research Institute, 1-1 Nagamine, Tsukuba 305-0052, Japan*
[5]*Graduate School of Science Division of Earth and Planetary Science, Kyoto University, Sakyo-ward, Kyoto 606-8502, Japan*
[6]*Aomori Prefectural Industrial Technology Research Center, 4-11-6 Dainitonya-machi, Aomori-shi, Aomori 030-0113, Japan*

**Corresponding author: e-mail: irenealabia@arc.hokudai.ac.jp*

Alabia, I. D., Saitoh, S-I., Igarashi, H., Ishikawa, Y., Usui, N., Kamachi, M., Awaji, T., and Seito, M. Ensemble squid habitat model using three-dimensional ocean data. – ICES Journal of Marine Science, 73: 1863–1874.

Received 6 January 2016; revised 7 April 2016; accepted 10 April 2016.

Neon flying squid (*Ommastrephes bartramii*) is a large pelagic squid internationally harvested in the North Pacific. Here, we examined its potential habitat in the central North Pacific using an ensemble modelling approach. Initially, ten statistical models were constructed by combining the squid fishing points, selected vertical layers of the sea temperature and salinity, sea surface height (SSH), and SSH gradient from the multi-variate ocean variational estimation system for the western North Pacific from June to July 1999–2011. The variable selection analyses have captured the importance of vertical temperature and salinity layers at the upper 300 and 440 m, respectively, coinciding with the reported vertical ranges of diel migration for the squid's primary prey species in the North Pacific. The evaluation of the habitat predictions using the independent sets of the presence data from 2012 to 2014 showed significant variability in the predictive accuracy, which is likely reflective of the interannual differences in environmental conditions across the validation periods. Our findings from ensemble habitat model approach using three-dimensional oceanographic data were able to characterize the near- and subsurface habitats of the neon flying squid. Moreover, our results underpinned the possible link between interannual environmental variability and spatio-temporal patterns of potential squid habitats. As such, these further suggest that an ensemble model approach could present a promising tool for operational fishery application and squid resource management.

Keywords: ensemble habitat model, neon flying squid, North Pacific, potential habitat, three-dimensional oceanographic data.

Introduction

The spatial changes in the marine species distributions in response to the changing environment result to perceivable variations in the species availability to fisheries (Cabanellas-Reboredo *et al.*, 2012; Mourato *et al.*, 2014). In marine ecosystem, the changes in environmental conditions affecting fisheries resources are notably dynamic and are known to transpire at different spatial and temporal scales (Dickey, 2003). As such, resolving the potential effects of environmental variability to the species habitat requires oceanographic data of high spatio-temporal resolution that are recently made available through the data assimilation model products (Ishikawa *et al.*, 2009; Nakada *et al.*, 2014). More important, these numerical data sources can also provide information on vertical oceanographic structures, affecting the spatial distributions of species suitable habitat. This information is otherwise unavailable from surface measurements derived from satellite data products.

With the recent progress in the scientific research and computing technology, extensive suite of habitat modelling tools has been available to users and has been since widely explored for diverse applications (Inglis *et al.*, 2006; Dambach and Rödder, 2011; Gregr *et al.*, 2013). The concept of the species distribution models is primarily based on classical ecological niche theory (Chase and Leibold,

2003), postulating that each individual species thrive and can have positive population growth within certain ranges of environmental conditions (Hirzel and Le Lay, 2008). In marine environment, species habitat models have been extensively used to infer species habitat characteristics (Mugo *et al.*, 2010) and map species geographical distributions (Kaschner *et al.*, 2006; Cheung *et al.*, 2007). These tools were also used to detect the potential fishing grounds (Zainuddin *et al.*, 2004; Alabia *et al.*, 2015a) in relation to the relevant set of environmental factors that are deemed influential for shaping the species habitat distributions.

Despite the huge selection of model platforms, existing model comparative studies have revealed that different model approaches exhibited variable levels of statistical and predictive performance, ascribed to inherent variations in model features complexity (Pearce and Ferrier, 2000; Elith *et al.*, 2006; Tsoar *et al.*, 2007; McKinney *et al.*, 2012). As such, the multi-model framework has been quite recently explored to generate robust predictions from combining the strengths of individual model algorithms through an ensemble model forecast approach (Araújo *et al.*, 2005; Araújo and New, 2007; Scales *et al.*, 2016). Ensembles of forecasts are produced by making multiple simulations across more than one set of initial conditions, model classes, parameters, and boundary conditions (Araújo and New, 2007). The combination of the forecasts yielded a lower mean error than any of constituent single forecasts when the latter set consisted of independent information (Bates and Granger, 1969). The recent yet limited applications of ensemble model approach to marine habitat mapping concluded its advantage for integrating the habitat predictions from several model algorithms, with reduced bias and higher predictive confidence (Oppel *et al.*, 2012; Scales *et al.*, 2016).

In this paper, we introduced a novel attempt to examine the potential habitats of a key pelagic species in central North Pacific, using ensemble model approach and three-dimensional oceanographic data. Like most cephalopods, the neon flying squid (*Ommastrephes bartramii*) forms an important ecological component of the North Pacific ecosystem (Bower and Ichii, 2005). It is also highly migratory and pelagic in nature, thus making it one of the best candidate species to explore the species–environment interactions at three-dimensional scale. Insights on these interactions could further augment our understanding of the least explored yet important, squid habitat ecology on the vertical plane. As such, these set our paper apart from the recently conducted habitat modelling studies, at least for our target species. Our earlier habitat modelling efforts on neon flying squid fishery in North Pacific have identified key potential research gaps that we are hoping to address in our present habitat analyses. Our previous studies were limited to the use of the single algorithm model and surface oceanographic factors to infer the potential squid habitat in the study region (Alabia *et al.*, 2015a, b, 2016). Although our prior habitat modelling studies yielded modest squid habitat predictions, we were unable to explore the vast selection of modelling platforms and examine the preferential vertical squid habitat characteristics. Hence, our present paper is designed to challenge these potential information gaps by investigating the spatial and temporal patterns of the squid habitat using the weighted mean ensemble forecasts of the species distribution models and three-dimensional ocean data. Here, the ensemble model forecasts could provide critical ideas to better understand the squid habitat characteristics at a three-dimensional scale and the ensuing changes in spatial habitat patterns in response to variable environmental patterns. These could also have important implications on the development of operational applications for a sustainable fishery exploitation. Thus, the goals of this study are (i) to examine the robust three-dimensional squid habitat characteristics from an ensemble of model forecasts, (ii) to explore the mechanistic linkage between the spatial and temporal variability of potential squid habitats and the changing environmental conditions, and finally (iii) to evaluate the predictive performance of ensemble squid habitat model against a 3-year independent set of squid occurrence data, thereby exploring its potential for future operational fishery and management prospects.

Material and methods

Target species and squid fishery data

Neon flying squid (*O. bartramii*) is a large pelagic squid inhabiting the temperate and subtropical oceans (Roper *et al.*, 1984). The North Pacific *O. bartramii* population has two seasonal spawning cohorts (i.e. winter–spring and autumn spawners), exhibiting a north–south migration to their feeding and spawning grounds, respectively (Murata and Nakamura, 1998). Both squid cohorts are internationally targeted by commercial jigging fisheries thus, making them one of the important and abundant pelagic fishery resources in the North Pacific (Bower and Ichii, 2005). Together with other squid species, *O. bartramii* constitutes for ~5% of the total landings in the region, with the largest instantaneous biomass amounting from 3 to 3.5 million t across the different ocean basins within its geographic range (FAO, 2010). Like most marine species, *O. bartramii* life history stages and habitat distributions were closely linked with the changes in the environmental conditions, through fluctuations in the sea surface temperature, salinity, and other available proxies for oceanographic features and processes (e.g. mesoscale eddies and frontal systems; Ichii *et al.*, 2004, 2011; Chen *et al.*, 2010; Mugo *et al.*, 2014; Alabia *et al.*, 2015a).

While the neon flying squid fishery in the North Pacific begins in June and lasts through December and recently extends through February off the northeastern Pacific coasts of Japan, the most productive period falls within the summer season when ~50% of the annual catch is harvested (FAO, 2010). Hence, our habitat modelling analyses were mainly focused on the summer fishing periods, which also represented the bulk of the available fishery data provided by the Aomori Prefectural Industrial Technology Research Center (APITRC). The data covered the Japanese squid jigging periods from June to July, 1999–2011 across the offshore waters

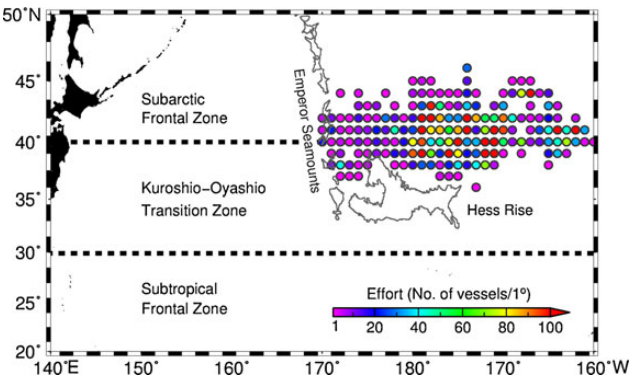

Figure 1. Map of the study area describing the oceanographic and topographic features of the North Pacific. Overlain are the spatial distributions of the squid fishing effort averaged over a 1° pixel from June to July 1999–2011. This figure is available in black and white in print and in colour at *ICES Journal of Marine Science* online.

of the central North Pacific (170°E–160°W; 30–50°N; Figure 1). The squid fishery data recorded the daily geographical coordinates of jigging sites (Longitude, Latitude), date of fishing activity (month, day, and year), and catch-per-unit-effort (cpue; in raw catch ton-per-vessel-per-day). While the available fishery data in the present study contained information on squid abundance, earlier result of comparative modelling studies between effort- and cpue-based habitat models for neon flying squid revealed differences in model performance. The latter models tended to overestimate the optimal extents of the squid habitats and underestimate the monthly variability in spatial habitat distribution (Tian *et al.*, 2009; Yu *et al.*, 2015). Thus, in the light of these previous findings, we utilized the presence-only data for squid habitat mapping and maximized the use of available fishery information during the process of oceanographic variable selection. In the latter analyses, cpue data were used to rank the relative contribution of each vertical layer of the oceanographic factors at the upper 6000 m. All fishing points have positive catches (Supplementary Figure S1) and are thus, valid occurrence data for developing the presence-only models.

Oceanographic data and selection of vertical ocean layers

The oceanographic variables used for the habitat modelling and spatial analyses were obtained from numerical model outputs of the three-dimensional multi-variate ocean variational estimation system for the Western North Pacific (MOVE-WNP), developed and maintained by the Japan's Meteorological Research Institute (MRI) (Usui *et al.*, 2006). Temperature, salinity, and sea surface height (SSH) model outputs were available at daily resolution at source spatial footprint of 10 km for each of the 54 vertical layers of depths between 0.5 and 6000 m and their respective spatial gradients were then computed. To select the most influential temperature and salinity ocean layers to squid relative abundance, generalized additive model (GAM) using the mgcv package version 1.8–2 (Wood, 2006) was adapted using the following equation:

$$\ln(\text{cpue}) = s(\text{SSH}) + s(\nabla\text{SSH}) + s(T_{\text{depth}(n)}) + s(S_{\text{depth}(n)}) + s(\nabla T_{\text{depth}(n)}) + s(\nabla S_{\text{depth}(n)}), \quad (1)$$

where ln(cpue) is the response variable and s the smoothing parameter. The base exploratory model for variable selection used the upper surface values (depth = 0.5 m) of all oceanographic factors, while changing the vertical layers (n) of the SSH, temperature (T), salinity (S), and the respective gradients (∇) one layer at a time, generating a total of 54 models. The final vertical temperature and salinity profiles for squid habitat model development were subsequently selected based on the three highly influential vertical layers, with the lowest Akaike information criterion (AIC; Akaike, 1998). The final set of the oceanographic temperature and salinity layers used for habitat modelling analyses were summarized in Table 1.

The level-3 monthly mapped and merged satellite products of chlorophyll *a* (Chl *a*) (MODIS and VIIRS) at 25 km resolution from June and July, 2012–2014, were also downloaded from the globcolour website of the European Space Agency (ESA) data user element project (www.globcolour.info/). These were mapped and examined to further augment the analyses of the spatial and temporal patterns of squid habitat predictions during the 3-year model validation period (June–July, 2012–2014).

Single-algorithm squid habitat model construction

Following the selection of the final oceanographic variables, ten single-algorithm models with their respective parameterization (Supplementary Table S1), available within BIOMOD2 (Thuiller *et al.*, 2009, 2014), were then developed and evaluated. The BIOMOD2 package is based on presence-availability framework that uses presence-only data to compute for habitat suitability index (HSI), where the values closer to or equal to 1 represent the potential habitat areas. The species distribution models within the package further constitute a suite of statistical algorithms that include the traditional regression-based models and modern machine-learning platforms. The proposed range of these single-algorithm models were all consequently utilized to explore and take advantage of their individual predictive strengths.

Since the pixels with no squid jigging activity cannot be classified as the true absences, a total of 500 background points (pseudo-absence) for each of the daily compiled squid jigging observations were randomly selected from each of the environmental layers. The daily selected values for each layers were then pooled together across the 13-year period and the final pseudo-absences used for the successive single-algorithm model runs were randomly subsampled from the pooled data using a 1:3 presence to pseudo-absence ratio. The random subsampling of the pseudo-absences was done to make the model simulations computationally feasible yet within a moderate sampling prevalence value (0.33). For the ten single-algorithm habitat models, three evaluation runs were developed using the cross-validation method. These resulted to a

Table 1. Summary of environmental dataset, fishery information, and their respective attributes used for the ensemble squid habitat model construction.

	Abbrev	Unit	Temporal resolution	Spatial resolution	Data source
Oceanographic layers					
Sea surface height	SSH	cm	Daily	10 km	MOVE-WNP
Sea surface height gradient	∇SSH	cm m^{-1}	Daily	10 km	MOVE-WNP
Temperature at 0.5 m	T05	°C	Daily	10 km	MOVE-WNP
Temperature at 158 m	T158	°C	Daily	10 km	MOVE-WNP
Temperature at 300 m	T300	°C	Daily	10 km	MOVE-WNP
Salinity at 0.5 m	S05	psu	Daily	10 km	MOVE-WNP
Salinity at 138 m	S138	psu	Daily	10 km	MOVE-WNP
Salinity at 440 m	S440	psu	Daily	10 km	MOVE-WNP
Fishery-dependent data					
Squid fishing locations	SQD	°	Daily	Point data	APITRC[a]

[a]Aomori Prefectural Industrial Technology Research Center.

total of 30 squid habitat model simulations from which, the best performing models were then selected for the ensemble model forecasts. The selection was based on the user-given arbitrary threshold for an evaluation metric within BIOMOD2 (Thuiller *et al.*, 2014). The compiled data for single-algorithm models were randomly apportioned into training (70%) and testing (30%) sets.

Single-algorithm habitat model evaluation

All single models were initially assessed using a suite of prevalence-dependent (i.e. Cohen's κ) and independent metrics (area under the receiver operating characteristics—AUC and true skill statistics—TSS). Cohen's κ or simply referred hereafter as κ, corrects the overall accuracy of predictions by the accuracy expected to occur by chance (Allouche *et al.*, 2006). Its value ranges from -1 to $+1$, where $+1$ indicates a perfect agreement and values of zero or less indicate a performance no better than random (Cohen, 1960). AUC, on the other hand, is a metric independent of prevalence and expressed as a proportion of the total area of the unit square defined by the false-positive and true-positive axes. This index ranging from 0 to 1, where a value of 0.5 further corresponds to models with no discrimination ability and 1 for models with perfect discrimination (Swets, 1988; Pearce and Ferrier, 2000). Moreover, TSS is an evaluation metric that also takes into account sensitivity and specificity and is insensitive to prevalence and closely showed similar pattern to that of AUC (Allouche *et al.*, 2006). TSS further considers both the omission and commission errors and success as a result of the random guessing. Its value ranges from -1 to $+1$ and is interpreted in a similar manner to that of κ (Mercier *et al.*, 2010).

Ensemble model development and validation

Following the performance evaluation of single-algorithm models, a weighted mean ensemble model for the squid habitat was constructed based on the TSS. Since there is no known consensus yet as to the most appropriate evaluation metric for ensemble forecasts (Scales *et al.*, 2016), we used a moderate TSS threshold (≥ 0.65) over the AUC for the model selection. While the AUC has been a widely used model performance metric, its reliability has been heavily criticized (Lobo *et al.*, 2008). The weights for ensemble model were proportional to the computed TSS of best-performing models at each of their cross-validation runs (Thuiller *et al.*, 2014). For the ensemble model validation against an independent squid occurrence data from June to July 2012–2014, AUC evaluation metric was further reinforced by the probability of detection (POD). The POD index simply refers to the "hit rate" of habitat model predictions (www.cawcr.gov.au/projects/verification/#Methods_for_dichotomous_forecasts). Consequent interannual differences in the variances and means of these validation metrics from the 3-year independent sets of squid presences for June and July 2012–2014 were further examined using the Bartlett's test of homogeneity (Bartlett, 1937) and the analysis of variance (ANOVA), respectively. All mapping routines were implemented using the open-source generic mapping tools (GMT) version 4.5.2 (Wessel *et al.*, 2013).

Results

Spatial and vertical squid habitat characteristics

The results of GAM analysis on the effects of vertical temperature and salinity on the squid's relative abundance highlighted the subsurface habitat characteristics of *O. bartramii* (Figure 2a–d). Based on this analysis, the most influential vertical temperature (Figure 2a) and salinity (Figure 2c) layers on top of surface variables (SSH and ∇SSH) were located at depths of 5, 158, and 300 m and 5, 138, and 440 m, respectively. These layers were marked by lowest AIC relative to the upper-surface base models. The density distributions of influential environmental parameters extracted at the squid fishing locations showed differential patterns in the vertical oceanographic structures on the squid preferred habitat with depth (Supplementary Figure S2).

Predictive performance of single-algorithm models

Table 2 shows the predictive performance of the single-algorithm models at each of the three cross-validation runs assessed using AUC, κ, and TSS. Each of the single-algorithm model revealed differences in predictive performance, where seven out of ten model algorithms recorded modest to high performance indices. The single-algorithm models with the highest threshold-independent performance metrics (TSS and AUC) were random forest (RF) and classification tree analysis (CTA), which generally used the combination of regression trees and boosting method. This list is followed by machine-learning platforms such as artificial neural network (ANN), boosted regression trees (BRT), a Maximum entropy (MaxEnt), and the regression-based models [GAM and generalized linear model (GLM)].

The relative variable importance derived from the built-in feature of BIOMOD2 for the ten single-algorithm models, averaged over three cross-validation runs, is shown in Figure 3. The analysis

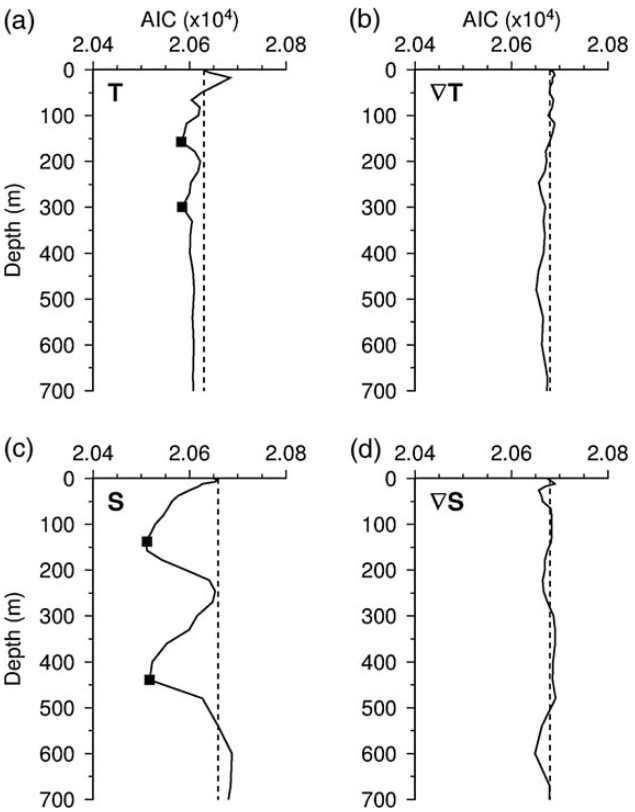

Figure 2. Model-derived variable importance of the vertical (a) temperature, (b) temperature gradient, (c) salinity, and (d) salinity gradient to squid cpue, assessed based on AIC at the upper 700 m. The filled squares are the temperature and salinity layers with the lowest AIC.

Table 2. Summary of model performance metrics (AUC; κ; TSS) computed for single-model algorithm with three cross-validation runs.

	Metrics								
	AUC			Kappa			TSS		
Models	Run1	Run2	Run3	Run1	Run2	Run3	Run1	Run2	Run3
GLM	0.877	0.878	0.879	0.523	0.531	0.537	0.629	**0.651**	0.643
GAM	0.900	0.901	0.899	0.575	0.567	0.570	**0.661**	**0.675**	**0.673**
GBM	0.907	0.912	0.910	0.566	0.585	0.570	**0.669**	**0.679**	**0.686**
CTA	0.908	0.907	0.900	0.619	0.622	0.606	**0.722**	**0.727**	**0.719**
ANN	0.892	0.903	0.908	0.557	0.574	0.579	**0.685**	**0.703**	**0.701**
SRE	0.756	0.758	0.771	0.427	0.429	0.450	0.513	0.515	0.542
FDA	0.880	0.887	0.882	0.528	0.541	0.522	0.627	0.645	0.636
MARS	0.885	0.889	0.884	0.525	0.539	0.527	0.634	0.649	0.637
RF	0.975	0.980	0.979	0.819	0.833	0.828	**0.832**	**0.846**	**0.846**
MaxEnt	0.900	0.906	0.904	0.565	0.578	0.567	**0.657**	**0.676**	**0.675**

Models with TSS $\geq$ 0.65 (bold values) were used to generate the ensemble predictions.

revealed differences in relative contributions of oceanographic predictors across the ten single-algorithm models, with the consistent highest contributions from T05 with values ranging from 0.46 (RF) to 0.88 (multiple adaptive regression splines; MARS). S05 is ranked as the second most important predictor in eight out of ten models, with the contribution values from 0.13 (MaxEnt) to 0.38 (flexible discriminant analysis; FDA). Succeeding ranks of variable importance were as follows: SSH (5 out of 10 models), S138, and T300 (4 out of 10 models). Moreover, Figure 4a–f shows the monthly averaged habitat predictions of the top-performing single-algorithm models during the summer validation periods from 2012 to 2014. The inter-model spatial patterns of potential squid habitats across the 3-year period exhibited pronounced differences. The squid habitat predictions from the RF model (Figure 4a and b) were narrower in the spatial extents with lower HSI magnitudes relative to CTA (Figure 4c and d) and ANN (Figure 4e and f). These apparent differences in the prediction patterns resulted to spatial mismatches between the squid habitat prediction and the actual occurrence. Interestingly, despite the spatial differences between the single-algorithm model predictions, a consistent areal reduction in the potential squid habitats during the summer of 2012 emerged.

Ensemble model habitat predictions and predictive performance

Figure 5a–c shows the spatial maps of the monthly averaged potential squid habitats from the weighted mean ensemble model from June to July, 2012–2014. The areal reduction in potential squid habitat in summer 2012, as earlier observed from single-algorithm model habitat maps, were also captured in the ensemble model habitat predictions. Moreover, potential squid habitat in June (Figure 5a–c, left panels) was distributed over a larger area (36°–43°N) relative to July (Figure 5a–c, right panels). In June, patches of high potential squid habitat (HSI $\geq$ 0.6) were distributed off the southern waters of the central North Pacific. In July, however, the potential squid habitat shifted northward, accompanied with the consistent areal reduction across years. The spatial correspondence between the habitat predictions and actual squid presence data for June was also better than those in July. The monthly averaged statistical model performance from the daily prediction (Table 3) also showed significant differences in the mean and variance (ANOVA, $p < 0.001$ and Bartlett's test, $p < 0.01$).

Spatial and temporal oceanographic patterns during the model validation period

The spatial and temporal distributions of oceanographic factors during the 3-year validation period affect the potential squid habitat patterns across the space and time. Figure 6 shows the scatterplots of temperature–salinity at 0.5 m, scaled to potential density ($\rho\theta$) (Figure 6a and b) and Chl *a* (Figure 6c and d) for June and July, 2012–2014. Both intra-seasonal and interannual environmental signals featured an expansion and contraction of the temperature–salinity limits across seasonal and annual time frames. The thermohaline changes consequently led to alterations in water density and Chl *a* concentration. In June, the putative squid feeding areas were characterized by waters with higher density (Figure 6a) relative to July (Figure 6b). The high-density waters were accompanied by an elevated Chl *a* (Figure 6c), whereas the less dense waters were associated with lower Chl *a* concentration (Figure 6d).

Moreover, strong interannual variability in distributions of the oceanographic variables also emerged during the 3-year period. In June and July 2012 (Figure 6a–d, left panels), the study area revealed a significant expansion of the less dense waters with low Chl *a* (7–8% increase in frequency of pixels with $\rho\theta < 25 \text{kg/m}^3$), as opposed to the summers of 2013 (Figure 6a–d, middle panels) and 2014 (Figure 6a–d, right panels). Despite the wide spatio-temporal variation in the environmental patterns, actual squid occurrences in summer were found sitting on or proximal to the waters with moderate to high potential density and Chl *a* concentration.

Discussion

Our present paper proposed a modern means to infer the potential habitat, based on the vertical oceanographic preferences, of an economically and ecologically important fishery resource in the central North Pacific. Here, we used an ensemble modelling approach to generate the robust habitat predictions for the neon flying squid, featuring the use of state-of-the-art species habitat algorithms and three-dimensional oceanographic data from a high-resolution numerical model. Such approach has allowed us to explore the vertical squid habitat characteristics and potential linkage between the environmental conditions and potential squid habitat. In doing so, we were able to quantitatively evaluate the potential of ensemble

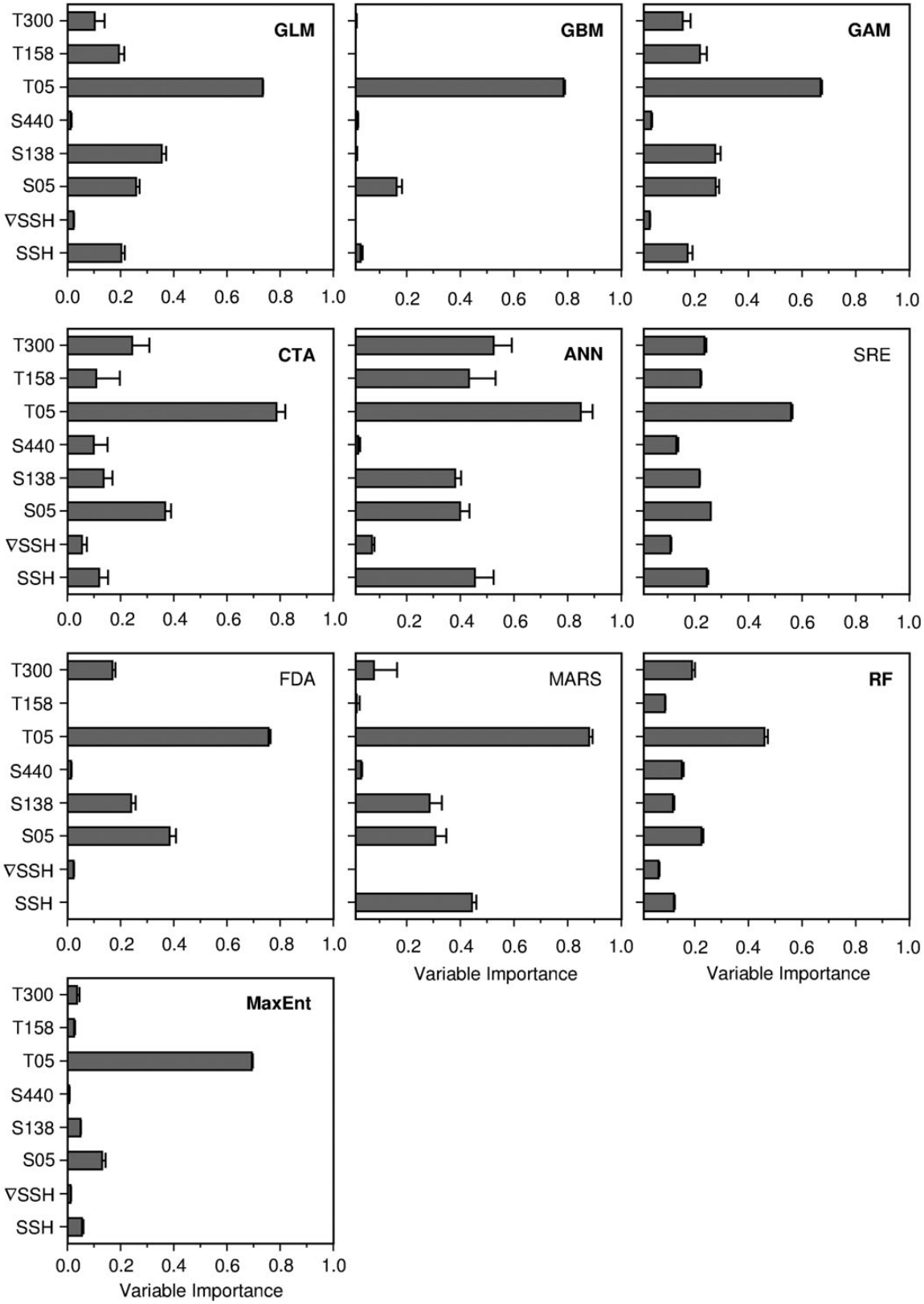

Figure 3. Relative environmental variable importance derived from the single-algorithm models, with the error bars corresponding to ± 1 s.d. computed for each variable. The single-algorithm models used for the ensemble forecast are highlighted in bold.

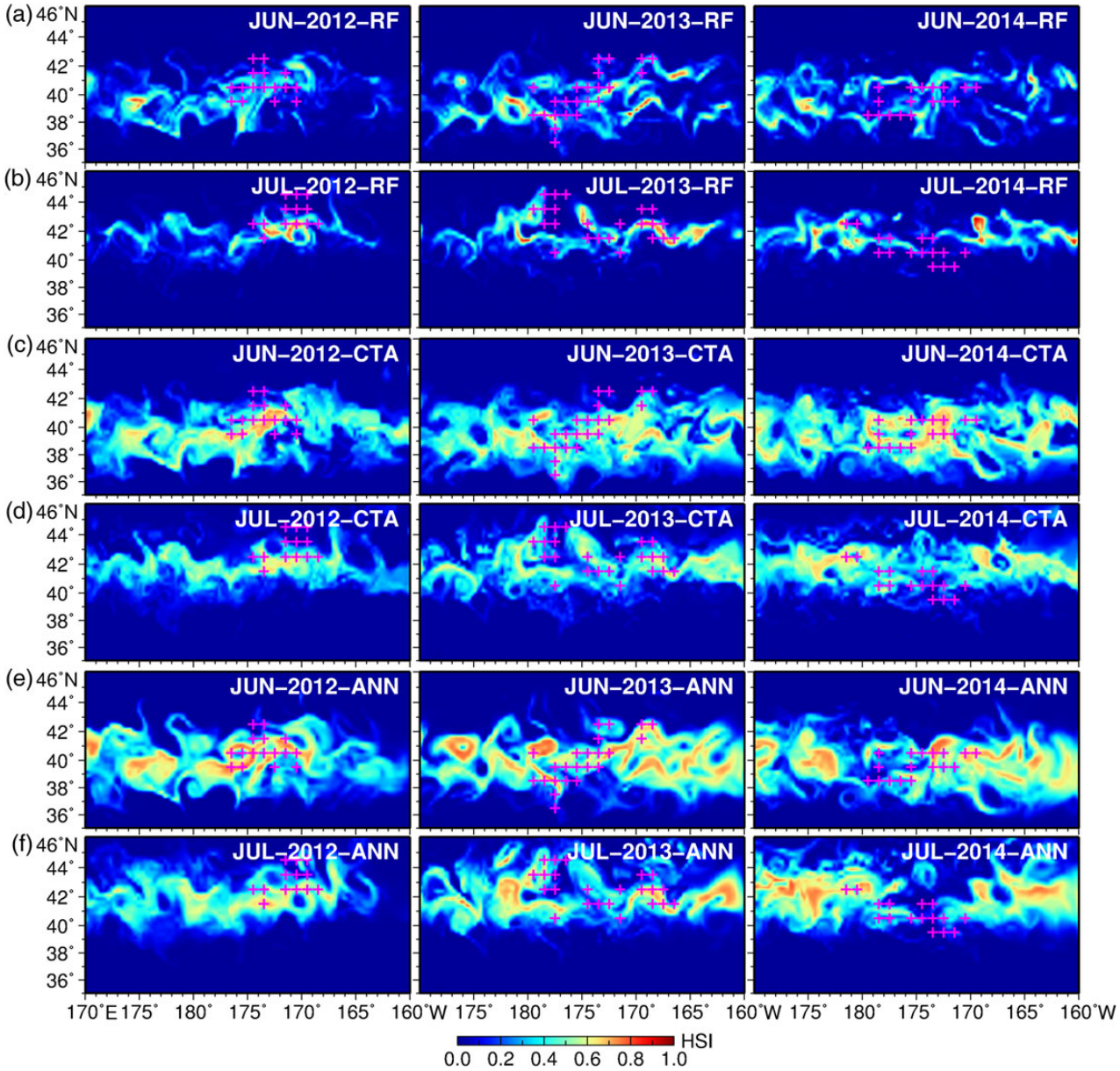

Figure 4. Maps of squid habitat predictions from the top three single-algorithm models with TSS $\geq$ 0.65 for June and July, 2012 – 2014, expressed in terms of the squid habitat suitability index (HSI). The overlain crosses are the monthly compiled squid occurrences at 1° resolution for the respective years. This figure is available in black and white in print and in colour at *ICES Journal of Marine Science* online.

habitat models for operational fishery and squid resource management applications.

The relative squid abundance over the 13-year period revealed different responses to vertical temperature–salinity patterns (Figure 2a and c). This underpinned the importance of the vertical thermohaline features in the spatial distributions of the pelagic squid in the open ocean. Moreover, the high variable contribution of certain vertical temperature–salinity layers to squid abundance reflects the hydrographic conditions, potentially favourable for the prey aggregation. Opportunistic ommastrephid such as jumbo squid have shown strong diel migrations, as they actively search for a depth that is rich in prey and subsequently exploit that zone for foraging (Gilly *et al.*, 2006; Stewart *et al.*, 2014). Another study on the feeding habits of the neon flying squid reported that its diel migration was in tight synchrony with the day (between 300 and 600 m) and night (upper 100 m) movement patterns of its primary forage species (Watanabe *et al.*, 2004). In the same manner, presence-only squid habitat models in this study also captured the highest relative variable contribution of temperature and salinity at 0.5 m (Figure 3). These results suggest that temperature–salinity profiles at the near- and subsurface layers regulate the abundance and occurrence of the squid in the region and can thereby, collectively provide a set of robust squid habitat indicators in the central North Pacific.

While the single-algorithm models showed a quite consistent oceanographic parameter ranking (Figure 3), inter-model statistical performance (Table 2) and spatial habitat predictions (Figure 4a–f) were different. These reflected the inherent inter-model uncertainty,

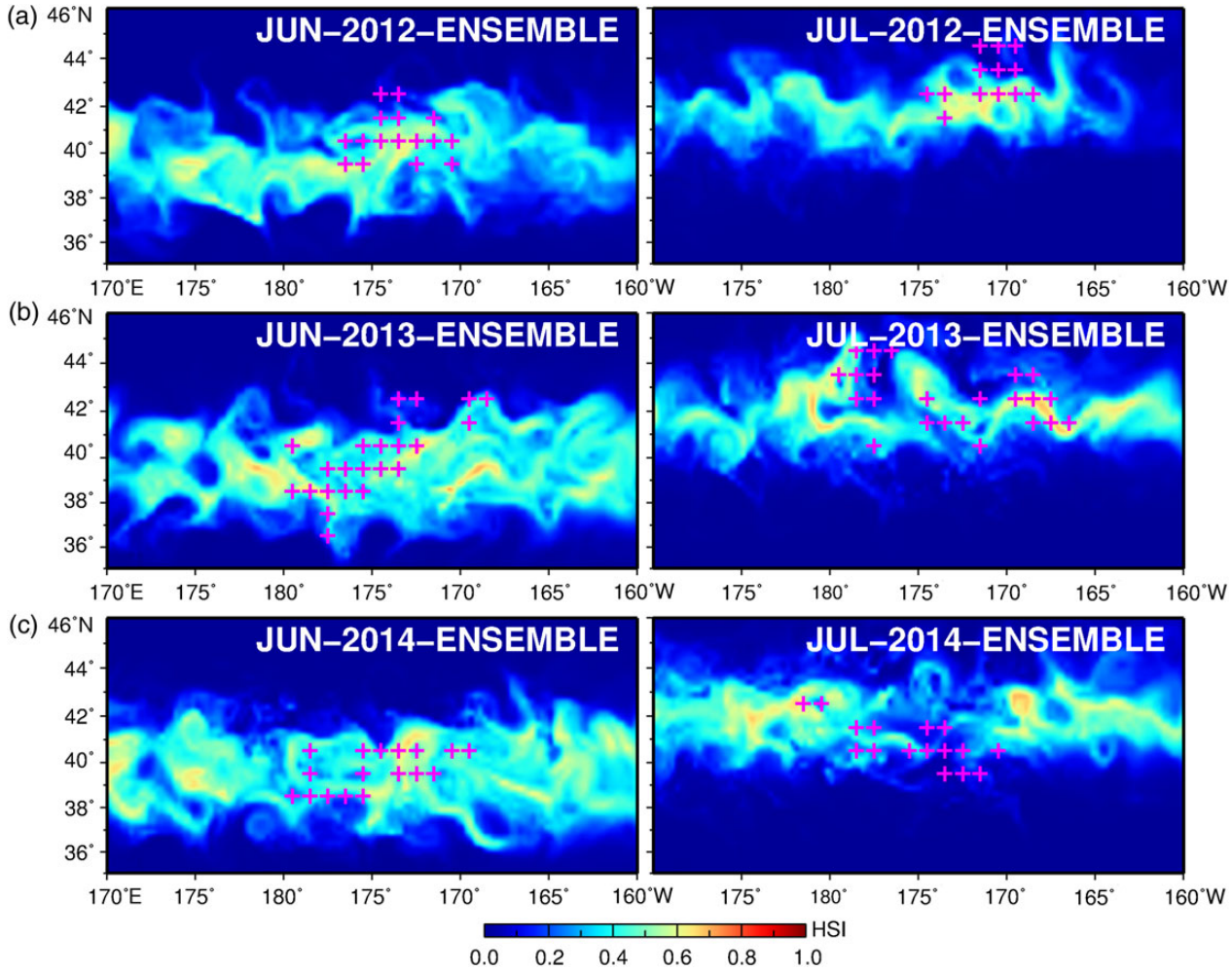

Figure 5. Maps of squid habitat predictions from the weighted ensemble mean model for June and July, 2012 – 2014, expressed in terms of the squid habitat suitability index (HSI). The overlain crosses are the monthly compiled squid occurrences at 1° resolution for the respective years. This figure is available in black and white in print and in colour at *ICES Journal of Marine Science* online.

Table 3. Monthly averaged model performance metrics computed from the daily squid habitat predictions from June to July, 2012 – 2014.

	Metrics			
	AUC ± 1 s.d.		POD ± 1 s.d.	
Year/ month	June	July	June	July
2012	0.784 ± 0.115	0.642 ± 0.294	0.860 ± 0.247	0.516 ± 0.447
2013	0.833 ± 0.067	0.825 ± 0.073	0.997 ± 0.015	0.931 ± 0.138
2014	0.910 ± 0.073	0.836 ± 0.070	1.000 ± 0.000	0.963 ± 0.074

The variances and means for AUC and POD across validation years were significantly different (Bartlett's test, $p < 0.01$ and ANOVA, $p < 0.001$).

suggesting that predictive strength substantially varies across the statistical algorithms (Elith *et al.*, 2006). Moreover, combination of squid habitat forecasts using the weighted mean of seven out of ten best performing models yielded better spatial correspondence between potential squid habitat and actual presence (Figure 5a–c), relative to top-performing single-algorithm predictions (Figure 4a). This reinforces the findings of earlier studies concluding that an ensemble model approach is preferable over single-algorithm platforms for predicting marine habitat affinities (Oppel *et al.*, 2012; Pérez-Jorge *et al.*, 2015; Scales *et al.*, 2016). As such, the ensemble model approach could be an important tool for operational fishery application (e.g. mapping of potential fishing grounds) and resource management (e.g. identification of the predictable foraging habitats that could encompass critical zones for pelagic species).

With the robust squid habitat predictions from the ensemble model, the influence of the oceanographic changes to the spatio-temporal habitat patterns could then be better elucidated. Coupled this with the established potential of cephalopods as near real-time biological beacons of drastic environmental variations (Rodhouse, 2001; Pierce *et al.*, 2008), our study accentuated the potential ecological mechanism that regulates the changes in squid habitat patterns. Indeed, the summer potential squid habitats derived from weighted ensemble model revealed a notable interannual trend in spatial habitat patterns across the validation period (Figure 5a–c). These spatial habitat differences further resulted to substantial drop in model's predictive accuracy in 2012 as opposed to the summers of 2013 and 2014 (Table 3). These could be indicative of the differences in the model transferability through time, in response to interannual changes in the

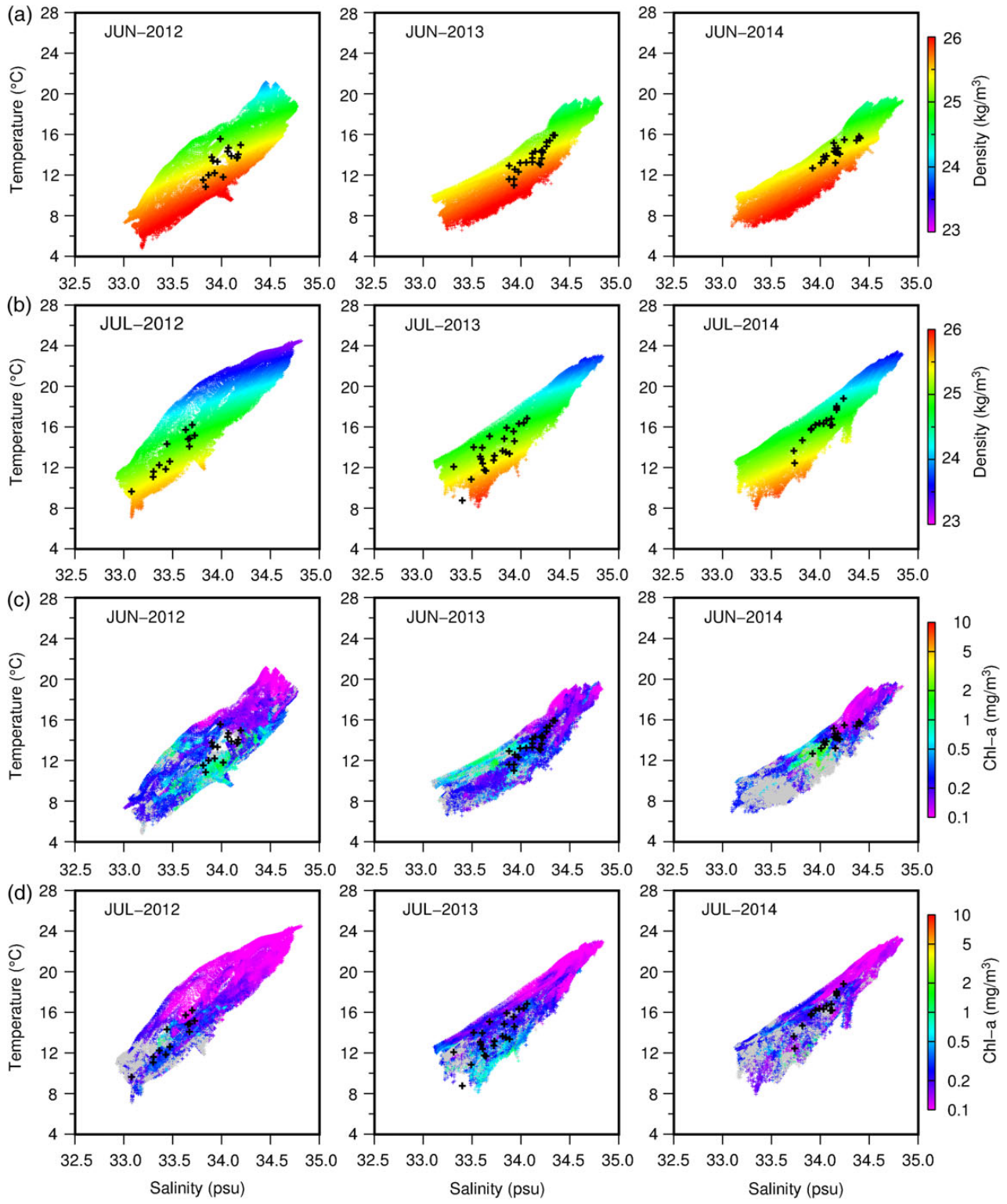

Figure 6. Temperature – salinity scatterplots scaled with the (a and b) potential density ($\rho\theta$) and (c and d) Chl *a* across 170°E – 160°W and 35° – 46°N from June to July, 2012 – 2014. Overlain are the temperature – salinity values (crosses), extracted at each of the squid occurrence points at 1° resolution. This figure is available in black and white in print and in colour at *ICES Journal of Marine Science* online.

environmental conditions. As such, this posed as a potential limitation to the model's capability to capture the actual squid habitats and resulted to the observed spatial prediction mismatches.

Earlier studies have shown that the extrapolative capabilities of the habitat models in space and time were influenced by region-specific habitat preferences (Torres *et al.*, 2015) and local multi-scale

periodicity of oceanographic variations (Jenouvrier *et al.*, 2005), respectively. In our study, interannual environmental changes were shown in the properties of temperature, salinity, and density of water masses (Figure 6a and b). The stratified conditions (warm and salty) in summer 2012 were likely to create an unfavourable foraging environment for the squid, as evident from the interannual Chl *a* distribution patterns (Figure 6c and d). In the ocean, Chl *a* is generally regarded as a proxy for food availability, where the high concentration translates to favourable feeding opportunities (Polovina *et al.*, 2004; Ichii *et al.*, 2011; Alabia *et al.*, 2015b). Chl *a* concentration is further affected by transport and availability of nutrients in the euphotic zone which is, in turn, positively controlled by the vertical mixing (Polovina *et al.*, 1995). Here, the spatial expansion of the low Chl *a* waters coincided with the anomalous stratified condition, with the highest observed spatial anomaly in July 2012. This period is also coincident with the extensive reduction in predicted squid habitat from the ensemble model and substantial drop in AUC and POD (Table 3). Hence, this presents a potential ecological scenario that could account for the interannual variability in squid habitat patterns derived from ensemble weighted mean model predictions. It further reinforces the earlier conclusions that temperature and salinity are strong predictors of the squid habitat in the study area (Alabia *et al.*, 2015a) and that the squid are potential ecological indicators of rapid environmental changes (Ichii *et al.*, 2011).

Summary and conclusion

The ensemble model of potential squid habitat in central North Pacific using three-dimensional oceanographic factors provided relevant information on squid's vertical habitat characteristics. This highlights the importance of near- and subsurface temperature and salinity profiles to the preferred squid habitat. Moreover, single-algorithm models exhibited significant differences in statistical performance, indicating the variable levels of predictive strength among models. The combination of the best-performing single-algorithm models into an ensemble generated robust squid habitat predictions. Thus, allowing us to better elucidate the effects of the environmental changes to the spatio-temporal squid habitat patterns. The interannual environmental signals were marked by pronounced changes in thermohaline properties, leading to density and Chl *a* anomalies on the squid's putative feeding grounds. Hence, our approach of using the ensemble model, three-dimensional oceanographic factors and fishery information, offered a promising potential for operational fishery and management applications.

Supplementary data

Supplementary material is available at the *ICESJMS* online version of the manuscript.

Acknowledgements

This work was supported by the Research on Climate Change Adaptation (RECCA) Project of the Grant-in-Aid from Japan's Ministry of Education, Culture, Sports, Science and Technology (MEXT). The authors also acknowledge Aomori Prefectural Industrial Technology Research Center (APITRC) for providing the squid fishery dataset and Japan Meteorological Agency for providing the numerical model data used for squid habitat analyses. We are also very grateful to the three anonymous reviewers for their constructive comments that significantly improved the manuscript.

References

Akaike, H. 1998. A new look at the statistical model identification. *In* Selected Papers of Hirotugu Akaike, pp. 215–222. Ed. by E. Parzen, K. Tanabe, and G. Kitagawa. Springer, New York.

Alabia, I. D., Saitoh, S-I., Igarashi, H., Ishikawa, Y., Usui, N., Kamachi, M., Awaji, T., *et al.* 2016. Future projected impacts of ocean warming to potential squid habitat in western and central North Pacific. ICES Journal of Marine Science, 73: 1343–1356.

Alabia, I. D., Saitoh, S-I., Mugo, R., Igarashi, H., Ishikawa, Y., Usui, N., Kamachi, M., *et al.* 2015a. Seasonal potential fishing ground prediction of neon flying squid (*Ommastrephes bartramii*) in the western and central North Pacific. Fisheries Oceanography, 24: 190–203.

Alabia, I. D., Saitoh, S-I., Mugo, R., Igarashi, H., Ishikawa, Y., Usui, N., Kamachi, M., *et al.* 2015b. Identifying pelagic habitat hotspots of neon flying squid in the temperate waters of the central North Pacific. PLoS ONE, 10: e0142885.

Allouche, O., Tsoar, A., and Kadmon, R. 2006. Assessing the accuracy of species distribution models: prevalence, kappa and the true skill statistic (TSS). Journal of Applied Ecology, 43: 1223–1232.

Araújo, M. B., and New, M. 2007. Ensemble forecasting of species distributions. Trends in Ecology and Evolution, 22: 42–47.

Araújo, M. B., Whittaker, R. J., Ladle, R. J., and Erhard, M. 2005. Reducing uncertainty in projections of extinction risk from climate change. Global Ecology and Biogeography, 14: 529–538.

Bartlett, M. S. 1937. Properties of sufficiency and statistical tests. Proceedings of the Royal Society of London A: Mathematical, Physical and Engineering Sciences, 160: 268–282.

Bates, J. M., and Granger, C. W. J. 1969. The combination of forecasts. OR, 20: 451–468.

Bower, J. R., and Ichii, T. 2005. The red flying squid (*Ommastrephes bartramii*): a review of recent research and the fishery in Japan. Fisheries Research, 76: 39–55.

Cabanellas-Reboredo, M., Alós, J., Palmer, M., and Morales-Nin, B. 2012. Environmental effects on recreational squid jigging fishery catches. ICES Journal of Marine Science, 69: 1823–1830.

Chase, J. M., and Leibold, M. A. 2003. Ecological Niches: Linking Classical and Contemporary Approaches. University of Chicago Press, USA.

Chen, X., Tian, S., Chen, Y., and Liu, B. 2010. A modeling approach to identify optimal habitat and suitable fishing grounds for neon flying squid (*Ommastrephes bartramii*) in the Northwest Pacific Ocean. Fishery Bulletin, 108: 14.

Cheung, W. W. L., Watson, R., Morato, T., Pitcher, T. J., and Pauly, D. 2007. Intrinsic vulnerability in the global fish catch. Marine Ecology Progress Series, 333: 1–12.

Cohen, J. 1960. A coefficient of agreement for nominal scales. Educational and Psychological Measurement, 20: 37–46.

Dambach, J., and Rödder, D. 2011. Applications and future challenges in marine species distribution modeling. Aquatic Conservation: Marine and Freshwater Ecosystems, 21: 92–100.

Dickey, T. D. 2003. Emerging ocean observations for interdisciplinary data assimilation systems. Journal of Marine Systems, 40–41: 5–48.

Elith, J., Graham, C. H., Anderson, R. P., Dudík, M., Ferrier, S., Guisan, A., Hijmans, R. J., *et al.* 2006. Novel methods improve prediction of species' distributions from occurrence data. Ecography, 29: 129–151.

FAO. 2010. Myopsid and oegopsid squids. *In* Cephalopods of the World. An Annotated and Illustrated Catalogue of Cephalopod Species Known to Date, pp. 1–605. Ed. by P. Jereb, and C. F. E. Roper. Rome.

Gilly, W. F., Markaida, U., Baxter, C. H., Block, B. A., Boustany, A., Zeidberg, L., Reisenbichler, K., *et al.* 2006. Vertical and horizontal migrations by the jumbo squid *Dosidicus gigas* revealed by electronic tagging. Marine Ecology Progress Series, 324: 1–17.

Gregr, E. J., Baumgartner, M. F., Laidre, K. L., and Palacios, D. M. 2013. Marine mammal habitat models come of age: the emergence of ecological and management relevance. Endangered Species Research, 22: 205–212.

Hirzel, A. H., and Le Lay, G. 2008. Habitat suitability modelling and niche theory. Journal of Applied Ecology, 45: 1372–1381.

Ichii, T., Mahapatra, K., Sakai, M., Inagake, D., and Okada, Y. 2004. Differing body size between the autumn and the winter–spring cohorts of neon flying squid (*Ommastrephes bartramii*) related to the oceanographic regime in the North Pacific: a hypothesis. Fisheries Oceanography, 13: 295–309.

Ichii, T., Mahapatra, K., Sakai, M., Wakabayashi, T., Okamura, H., Igarashi, H., Inagake, D., *et al.* 2011. Changes in abundance of the neon flying squid *Ommastrephes bartramii* in relation to climate change in the central North Pacific Ocean. Marine Ecology Progress Series, 441: 151–164.

Inglis, G. J., Hurren, H., Oldman, J., and Haskew, R. 2006. Using habitat suitability index and particle dispersion models for early detection of marine invaders. Ecological Applications, 16: 1377–1390.

Ishikawa, Y., Awaji, T., Toyoda, T., In, T., Nishina, K., Nakayama, T., Shima, S., *et al.* 2009. High-resolution synthetic monitoring by a 4-dimensional variational data assimilation system in the northwestern North Pacific. Journal of Marine Systems, 78: 237–248.

Jenouvrier, S., Weimerskirch, H., Barbraud, C., Park, Y-H., and Cazelles, B. 2005. Evidence of a shift in the cyclicity of Antarctic seabird dynamics linked to climate. Proceedings of the Royal Society B: Biological Sciences, 272: 887–895.

Kaschner, K., Watson, R., Trites, A. W., and Pauly, D. 2006. Mapping world-wide distributions of marine mammal species using a relative environmental suitability (RES) model. Marine Ecology Progress Series, 316: 285–310.

Lobo, J. M., Jiménez-Valverde, A., and Real, R. 2008. AUC: a misleading measure of the performance of predictive distribution models. Global Ecology and Biogeography, 17: 145–151.

McKinney, J., Hoffmayer, E., Wu, W., Fulford, R., and Hendon, J. 2012. Feeding habitat of the whale shark *Rhincodon typus* in the northern Gulf of Mexico determined using species distribution modelling. Marine Ecology Progress Series, 458: 199–211.

Mercier, L., Darnaude, A. M., Bruguier, O., Vasconcelos, R. P., Cabral, H. N., Costa, M. J., Lara, M., *et al.* 2010. Selecting statistical models and variable combinations for optimal classification using otolith microchemistry. Ecological Applications, 21: 1352–1364.

Mourato, B. L., Hazin, F., Bigelow, K., Musyl, M., Carvalho, F., and Hazin, H. 2014. Spatio-temporal trends of sailfish, *Istiophorus platypterus* catch rates in relation to spawning ground and environmental factors in the equatorial and southwestern Atlantic Ocean. Fisheries Oceanography, 23: 32–44.

Mugo, R., Saitoh, S-I., Nihira, A., and Kuroyama, T. 2010. Habitat characteristics of skipjack tuna (*Katsuwonus pelamis*) in the western North Pacific: a remote sensing perspective. Fisheries Oceanography, 19: 382–396.

Mugo, R. M., Saitoh, S-I., Takahashi, F., Nihira, A., and Kuroyama, T. 2014. Evaluating the role of fronts in habitat overlaps between cold and warm water species in the western North Pacific: a proof of concept. Deep Sea Research II: Topical Studies in Oceanography, 107: 29–39.

Murata, M., and Nakamura, Y. 1998. Seasonal migration and diel migration of the neon flying squid, *Ommastrephes bartramii*, in the North Pacific. *In* International Symposium on Large Pelagic Squids, pp. 13–30. Ed. by T. Okutani. Japan Marine Fishery Resources Research Center, Tokyo.

Nakada, S., Hirose, N., Senjyu, T., Fukudome, K-I., Tsuji, T., and Okei, N. 2014. Operational ocean prediction experiments for smart coastal fishing. Progress in Oceanography, 121: 125–140.

Oppel, S., Meirinho, A., Ramírez, I., Gardner, B., O'Connell, A. F., Miller, P. I., and Louzao, M. 2012. Comparison of five modelling techniques to predict the spatial distribution and abundance of seabirds. Biological Conservation, 156: 94–104.

Pearce, J., and Ferrier, S. 2000. Evaluating the predictive performance of habitat models developed using logistic regression. Ecological Modelling, 133: 225–245.

Pérez-Jorge, S., Pereira, T., Corne, C., Wijtten, Z., Omar, M., Katello, J., Kinyua, M., *et al.* 2015. Can static habitat protection encompass critical areas for highly mobile marine top predators? Insights from coastal East Africa. PLoS ONE, 10: e0133265.

Pierce, G. J., Valavanis, V., Guerra, A., Jereb, P., Orsi-Relini, L., Bellido, J., Katara, I., *et al.* 2008. A review of cephalopod–environment interactions in European Seas. Hydrobiologia, 612: 49–70.

Polovina, J. J., Balazs, G. H., Howell, E. A., Parker, D. M., Seki, M. P., and Dutton, P. H. 2004. Forage and migration habitat of loggerhead (*Caretta caretta*) and olive ridley (*Lepidochelys olivacea*) sea turtles in the central North Pacific Ocean. Fisheries Oceanography, 13: 36–51.

Polovina, J. J., Mitchum, G. T., and Evans, G. T. 1995. Decadal and basin-scale variation in mixed layer depth and the impact on biological production in the Central and North Pacific, 1960–88. Deep Sea Research I: Oceanographic Research Papers, 42: 1701–1716.

Rodhouse, P. G. 2001. Managing and forecasting squid fisheries in variable environments. Fisheries Research, 54: 3–8.

Roper, C. F. E., Sweeney, M., and Nauen, C. 1984. Cephalopods of the world. An annotated and illustrated catalogue of species of interest to fisheries. FAO Fisheries Synopsis 125, Rome, 3: 1–277.

Scales, K. L., Miller, P. I., Ingram, S. N., Hazen, E. L., Bograd, S. J., and Phillips, R. A. 2016. Identifying predictable foraging habitats for a wide-ranging marine predator using ensemble ecological niche models. Diversity Distributions, 22: 212–224.

Stewart, J. S., Hazen, E. L., Bograd, S. J., Byrnes, J. E. K., Foley, D. G., Gilly, W. F., Robison, B. H., *et al.* 2014. Combined climate- and prey-mediated range expansion of Humboldt squid (*Dosidicus gigas*), a large marine predator in the California Current System. Global Change Biology, 20: 1832–1843.

Swets, J. A. 1988. Measuring the accuracy of diagnostic systems. Science, 240: 1285–1293.

Thuiller, W., Georges, D., and Robin, E. 2014. biomod2: Ensemble platform for species distribution modeling.

Thuiller, W., Lafourcade, B., Engler, R., and Araújo, M. B. 2009. BIOMOD—a platform for ensemble forecasting of species distributions. Ecography, 32: 369–373.

Tian, S., Chen, X., Chen, Y., Xu, L., and Dai, X. 2009. Evaluating habitat suitability indices derived from CPUE and fishing effort data for *Ommastrephes bartramii* in the northwestern Pacific Ocean. Fisheries Research, 95: 181–188.

Torres, L. G., Sutton, P. J. H., Thompson, D. R., Delord, K., Weimerskirch, H., Sagar, P. M., Sommer, E., *et al.* 2015. Poor transferability of species distribution models for a pelagic predator, the grey petrel, indicates contrasting habitat preferences across ocean basins. PLoS ONE, 10: e0120014.

Tsoar, A., Allouche, O., Steinitz, O., Rotem, D., and Kadmon, R. 2007. A comparative evaluation of presence-only methods for modelling species distribution. Diversity and Distributions, 13: 397–405.

Usui, N., Ishizaki, S., Fujii, Y., Tsujino, H., Yasuda, T., and Kamachi, M. 2006. Meteorological Research Institute multivariate ocean variational estimation (MOVE) system: some early results. Advances in Space Research, 37: 806–822.

Watanabe, H., Kubodera, T., Ichii, T., and Kawahara, S. 2004. Feeding habits of neon flying squid *Ommastrephes bartramii* in the transitional region of the central North Pacific. Marine Ecology Progress Series, 266: 173–184.

Wessel, P., Smith, W. H. F., Scharroo, R., Luis, J., and Wobbe, F. 2013. Generic mapping tools: improved version released. Eos, Transactions American Geophysical Union, 94: 409–410.

Wood, S. N. 2006. Generalized Additive Models: an Introduction with R. Chapman and Hall/CRC, Boca Raton, FL.

Yu, W., Chen, X., Yi, Q., Chen, Y., and Zhang, Y. 2015. Variability of suitable habitat of western winter–spring cohort for neon flying squid in the northwest Pacific under anomalous environments. PLoS ONE, 10: e0122997.

Zainuddin, M., Saitoh, S-I., and Saitoh, K. 2004. Detection of potential fishing ground for albacore tuna using synoptic measurements of ocean color and thermal remote sensing in the northwestern North Pacific. Geophysical Research Letters, 31: L20311.

Handling editor: Manuel Hidalgo

ICES Journal of Marine Science

ICES Journal of Marine Science (2016), 73(7), 1875–1889. doi:10.1093/icesjms/fsw112

Contribution to the Themed Section: '*Seascape Ecology*'

Changes in habitat utilization of slope-spawning flatfish across a bathymetric gradient

Cathleen D. Vestfals,[1,‡,*] Lorenzo Ciannelli[1] and Gerald R. Hoff[2]

[1]*College of Earth, Ocean, and Atmospheric Sciences, Oregon State University, 104 CEOAS Administration Building, Corvallis, OR 97331, USA*
[2]*NOAA, National Marine Fisheries Service, Alaska Fisheries Science Center, Resource Assessment and Conservation Engineering Division, 7600 Sand Point Way NE, Seattle, WA 98115, USA*

**Corresponding author: tel: +1 5418670240; fax: +1 5418670136; e-mail:* cdvestfals@alaska.edu.
[‡]Present address: School of Fisheries and Ocean Sciences, University of Alaska Fairbanks, Hatfield Marine Science Center, 2030 SE Marine Science Drive, Newport, Oregon, 97365, USA

Vestfals, C. D., Ciannelli, L. and Hoff, G. R. Changes in habitat utilization of slope-spawning flatfish across a bathymetric gradient. – ICES Journal of Marine Science, 73: 1875–1889.

Received 7 August 2015; revised 8 May 2016; accepted 16 May 2016.

Understanding how fish distributions may change in response to environmental variability is important for effective management of fish populations, as predicted climate change will likely alter their habitat use and population dynamics. This research focused on two commercially- and ecologically-important flatfish species in the eastern Bering Sea (EBS), Greenland halibut (*Reinhardtius hippoglossoides*) and Pacific halibut (*Hippoglossus stenolepis*), which may be especially sensitive to climate-induced shifts in habitat due to strong seasonally and ontogenetically variable distributions. We analysed data from fishery-dependent and fishery-independent sources to determine how environmental variability influenced habitat use, thus gaining a uniquely comprehensive range of seasonal and geographic coverage of each species' distribution. Greenland and Pacific halibut exhibited strong and contrasting responses to changes in temperature on the shelf, with catches decreasing and increasing, respectively, beyond 1 °C. The effect of temperature was not as prominent along the slope, suggesting that slope habitats may provide some insulation from shelf-associated environmental variability, particularly for Greenland halibut. With warming, Greenland halibut exhibited more of a bathymetric shift in distribution, while the shift was more latitudinal for Pacific halibut. Our results suggest that habitat partitioning may, in part, explain differences in Greenland and Pacific halibut distributions. This research adds to our understanding of how the distributions of two fish species at opposite extremes of their ranges in the EBS – Greenland halibut at the southernmost edge and Pacific halibut at the northernmost edge – may shift in relation to a changing ocean environment.

Keywords: Bering Sea, climate change, habitat, GAM, Greenland halibut, Pacific halibut.

Introduction

There has been a renewed interest in the role that environmental variables play in structuring habitat use of marine fishes, as fisheries scientists and managers must accurately estimate and manage fish populations amidst a changing climate. Temperature and depth are two important abiotic habitat features that have been shown to influence fish distributions (Mueter and Norcross, 1999). Other factors include salinity, sediment type, currents, tides, light, oxygen, and pH (McConnaughey and Smith, 2000; Munday *et al.*, 2009; Youcef *et al.*, 2013; Sadorus *et al.*, 2014), some of which can vary dramatically across seasons, particularly at northern latitudes (Able and Fodrie, 2014). Biotic factors, such as aquatic vegetation, refuge space, and prey availability are also known to influence habitat use (Gibson, 1994; Stoner and Titgen, 2003; Ryer *et al.*, 2004).

Habitat use in marine fishes can change in response to changing environmental conditions, but it may also change seasonally and throughout a species' life cycle (Gibson, 1997). In particular, deep-water (>400 m) slope-spawning flatfish species utilise both shelf and slope habitats during different stages of their life cycles (e.g. juvenile nursery grounds on the shelf and adult spawning grounds on the slope; Abookire and Bailey, 2007; Loher and

Seitz, 2008; Sohn *et al.*, 2010; Duffy-Anderson *et al.*, 2013) and over different seasons (e.g. summer feeding grounds on the shelf vs. winter spawning grounds on the slope; Loher, 2011). Thus, for fisheries managers to effectively manage mobile fish species in a dynamic marine environment, it is prudent to understand how environmental factors shape the use of different habitats over different stages of their life cycle.

Climate change can impact the distribution and abundance of fish through reducing or expanding available habitat, often through temperature-mediated changes in latitude or depth (Perry *et al.*, 2005; Rose, 2005; van der Veer *et al.*, 2011). For example, two-thirds of North Sea fishes have shifted their mean latitude or depth in response to warming, with fish at the northern extent of their range expanding northward, and fish at the southern extent of their range retracting northwards (Perry *et al.*, 2005). Similar studies of North Sea groundfish have found that most species have deepened over the last 25 years, with cold-water species deepening the fastest and warm-water species shallowing over time (Dulvy *et al.*, 2008, Van Hal *et al.*, 2016). Climate-induced changes in ocean circulation patterns can also influence the life cycle closure by altering connectivity between spawning grounds and nursery areas (Sinclair, 1988; Rijnsdorp *et al.*, 2009; Petitgas *et al.*, 2013). Lastly, climate change can affect the timing of spawning migrations, which can influence the arrival of adults on the spawning grounds (Sims *et al.*, 2004), or the timing of spawning itself (Teal *et al.*, 2008; Fincham *et al.*, 2013).

The eastern Bering Sea (EBS) is extremely productive and supports several important commercial fisheries, however, it has experienced extreme variability in its physical and biological conditions in recent years (Stabeno *et al.*, 2012). These changes have impacted the distribution and abundance of marine organisms, such as seabirds, marine mammals, and fishes. For example, 2001 to 2004 were some of the warmest years on record (Stabeno *et al.*, 2012), and the northern Bering Sea underwent a major ecosystem shift from arctic to subarctic species in response to decreased sea ice, and increased air and ocean temperatures (Grebmeier *et al.*, 2006). Several other studies have shown northward distributional shifts in demersal fish and invertebrate species in association with warming (Mueter and Litzow, 2008; Spencer, 2008; Kotwicki and Lauth, 2013). These shifts have been attributed mostly to changes in the extent of winter sea ice and the resulting summer cold pool (bottom water $< 2\,^{\circ}C$), which is known to structure species assemblages on the EBS shelf (Mueter and Litzow, 2008; Kotwicki and Lauth, 2013), though density-dependent processes, such as changes in abundance, can also play a role (Spencer, 2008; Bartolino *et al.*, 2011; Kotwicki and Lauth, 2013). As a subarctic sea, the EBS is predicted to respond to variations in climate (IPCC, 2007) and future warming may lead to reduced ice cover and earlier ice melt, causing changes in the cold pool size and extent, and potentially changes in the species assemblages that inhabit the EBS shelf ecosystem.

Distributional studies to date have focused on changes occurring on the EBS shelf, but our knowledge about the processes affecting habitat associations and distribution shifts of species that also inhabit the slope is limited. This research focused on two commercially-important slope-spawning flatfish species, Greenland halibut (*Reinhardtius hippoglossoides*) and Pacific halibut (*Hippoglossus stenolepis*), which co-occur in the EBS and have similar life history strategies. For both species, spawning locations, nursery areas, and adult grounds are spatially separated, which requires active migration of adults to spawning grounds and transport of eggs and larvae to juvenile nursery grounds for life cycle closure (Migration Triangle Hypothesis; Harden-Jones, 1968). In the EBS, both species migrate offshore in fall to winter spawning grounds located along the continental slope, mainly from Bering to Pribilof Canyon (Bulatov, 1983; St-Pierre, 1984; Sohn *et al.*, 2010), but as far north as Cape Navarin for Greenland halibut (Musienko, 1970) and Middle Canyon for Pacific halibut (Seitz *et al.*, 2011). Spawning occurs in batches deep in the water column (>400 m) from November through March, after which eggs and larvae must be transported horizontally across the Bering Slope and vertically from depth to shallow nursery areas on the shelf to successfully recruit to the juvenile phase (IPHC, 1987; Alton *et al.*, 1988; Duffy-Anderson *et al.*, 2013). Juveniles actively move into deeper water as they age (IPHC, 1987; Sohn *et al.*, 2010), eventually making contranatant migrations to spawning locations when reproductively mature to close their life cycle (Alton *et al.*, 1988; Loher and Seitz, 2008; Sohn *et al.*, 2010).

The aim of this research was to identify the habitat associations of Greenland and Pacific halibut adults, characterise changes in their distributions on a seasonal basis, and determine how these may change in relation to contrasting environmental conditions. These species may be especially sensitive to climate change because of their strong connectivity requirements. We specifically focused on age-4+ fish due to their importance in the flatfish life cycle through ontogenetic migration and subsequent spawning behaviour.

Comprehensive analyzes of seasonal latitudinal and depth-related changes are complex, given the diverse data involved in surveying species in widely contrasting habitats, and because of the limited seasonal coverage that typically characterise fishery-independent surveys. Our study is unique because it integrates four independent data sources across different habitat types and time spans, which allows us to examine seasonal and interannual changes in habitat use across the EBS slope and shelf. We hypothesize that similar environmental forcing will elicit different responses in the two species. Greenland halibut, a stenothermic species at the southernmost extent of its range, is expected to contract its habitat in response to increases in temperature, while Pacific halibut, a eurythermic species with a more southern distribution, will expand its habitat.

By studying these two species—one at the southernmost edge of its range and the other at the northernmost edge of its range—we can gain insight into the factors that influence spatial dynamics of species at opposite extremes of their distributions, as these extremes represent the community assemblages that inhabit the Bering Sea shelf ecosystem. The results of our study also help us to understand how slope-spawning flatfish distributions may influence recruitment dynamics via changes of adult spawning habitats in relation to a changing ocean environment.

Material and methods

Data sources

Summer distributions from AFSC groundfish survey data

Greenland and Pacific halibut data were collected during the Alaska Fisheries Science Center's (AFSC) EBS continental shelf (1982–2013) and upper continental slope bottom trawl surveys. The AFSC shelf survey has been conducted annually since 1982 and provides extensive geographic coverage over the shelf, as well as detailed information on adult and subadult distributions of groundfish and invertebrates during summer months. The standardised survey is based on a stratified systematic design,

consisting of a regular fixed grid with a sampling station at the centre of each 37.04 km^2 grid square. Depths between 20 and 200 m are sampled over a period of 8–10 weeks from late May to early August (Stauffer, 2004). High-density "corner stations" are sampled to improve abundance estimates of local blue king crab (*Paralithodes platypus*) in areas surrounding St. Matthew and the Pribilof Islands. In 2010, the standard sampling grid was expanded to include an additional 145 stations on the northern EBS shelf; however, our analysis was restricted to stations that have been sampled throughout most of the time series (Figure 1) and excluded stations in the northernmost part of the survey area.

Concurrently with the shelf surveys, bottom trawl surveys were conducted along the EBS upper continental slope (EBSS) in 2002, 2004, 2008, 2010 and 2012. The EBSS survey area is divided into six geographic subareas (Figure 1) to assist in the distribution of trawl effort in relation to the estimated habitat area. Subareas are based on distinct bathymetric types and underwater features (broad low slope areas, canyon areas, and steep slope inter-canyon faces), and are stratified by depth every 200 m from 200 to 1,200 m, resulting in five depth strata for each subarea. Sampling density is based on substratum area and survey stations are selected using a stratified random sampling design, though sampling densities have varied due to the inability to successfully complete tows in some deep strata due to untrawlable bottom (Hoff, 2013).

Tows for both surveys were 30 minutes in duration and the date, time, latitude, longitude, gear depth, bottom temperature and surface temperature were recorded for each tow. Catches were sorted, weighed and enumerated for all species of fishes and invertebrates. Catch per unit effort (CPUE) was calculated by dividing the number of individuals caught for each species by the estimated area swept of the trawl and is expressed in number of fish per square kilometer. Further information on trawl survey protocols can be found at http://www.afsc.noaa.gov/RACE/gear support/tmspo65.pdf. We focused on changes in the distribution

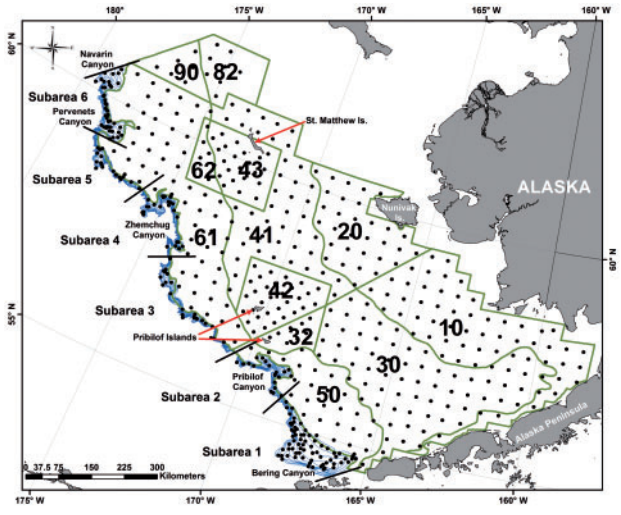

Figure 1. The AFSC's shelf (green: 1982-2013) and slope (blue: 2002, 2004, 2008, 2010 and 2012) survey areas used in the analysis. Slope survey points represent 2012 stations, while shelf survey points are stations that have been consistently sampled each year. Numbers within the shelf survey grid refer to survey strata. Bristol Bay is located in the southeastern portion of survey strata 10 and 30. For interpretation of the references to colour in this figure legend, the reader is referred to the online version of this article.

and abundance of age 4+ Greenland halibut ($\geq$ 340 mm in length) and Pacific halibut ($\geq$ 360 mm in length). Sizes were derived from the age- and sex-specific mean length-at-age estimates in the 2013 Greenland halibut stock assessment (Barbeaux *et al.*, 2013), and also from mean size-at-age information from Pacific halibut specimens collected between 2006 and 2009 during the EBS trawl survey (provided by the IPHC). Shelf and slope survey data were analysed separately to avoid confounding factors in catchability.

Seasonal distributions from AFSC groundfish observer data

Commercial catch data have been collected by observers aboard foreign vessels fishing in U.S. waters since the 1970s, however, it wasn't until the fishing fleet was domesticated and the AFSC's North Pacific Groundfish Observer Program was created that sampling effort and its spatial coverage became more consistent. Therefore, we used commercial catch data from 1991 to 2011 to analyse flatfish distributions and focused on data collected aboard catcher-processor vessels, as the majority of hauls were made by this vessel type. It should be noted that Pacific halibut is considered a prohibited species and is discarded as bycatch in the fisheries represented in the observer data set. The targeted longline fishery for Pacific halibut in U.S. waters is currently unobserved. In the case of Greenland halibut, a portion of the observer data set represented the targeted longline fleet, however, the species is considered bycatch in the remaining fisheries.

For each commercial haul sampled, observers recorded the latitude, longitude, bottom depth and/or fishing depth, and the total catch (numbers and weight) of each species, extrapolated from a subsample. We explicitly assumed that CPUE of Greenland and Pacific halibut was an indicator of their actual abundance. To avoid issues related to the uneven distribution of effort that occurs when using commercial fisheries data to examine changes in species' distributions, the catch was standardized by assigning it to a 400 square kilometer grid. Catch locations and associated length information were imported into ArcGIS (ESRI, 2014), and the underlying grid information was extracted to each haul. Because most spawning occurs along the continental slope from Bering Canyon northwards, and to compare results with the shelf and slope surveys, catch information from outside of the Bering Sea, south of 54°N, and along the Aleutian Island chain (NMFS regulatory areas 541–543) and over the Aleutian Basin (areas 530 and 550), was excluded.

To eliminate differences in gear efficiency, we analysed bottom trawl and longline data separately. For bottom trawl gear, CPUE was calculated as the total number of individuals caught per hour of towing, while longline CPUE was calculated as the total number of individuals caught per standardized skate of gear (n = 100 hooks). Adult CPUE, based on length frequency samples, was calculated for each haul and log-transformed (CPUE +1) to approximate normality and reduce heteroscedasticity. Hauls were aggregated to their corresponding grid cell centre point, and the average catch for each grid cell was calculated for each time period examined. To ensure that fishing information remained confidential, observer data that did not meet the three-vessel minimum per grid cell in each time period were removed from the analysis. Only longline data from 2000 to 2011 were examined, as species information for this gear type was extremely limited prior to 2000. Information on vessel size, net size, or tow speed was not available to compute fishing power correction

factors, therefore, the mean CPUE estimates may be biased, however, by limiting the analysis to larger catcher-processor vessels, these biases should be minimized.

Environmental data

To characterise Greenland and Pacific halibut habitat from the survey datasets, we used statistical models that included several co-located environmental variables, namely bottom depth (BD), bottom temperature (BT), and sea surface temperature (SST). Previous studies have shown that these parameters are important determinants of flatfish distribution in the EBS (Mueter and Litzow, 2008; Spencer, 2008). For the commercial fisheries data analysis, depth refers to either bottom depth for longline gear or fishing depth for trawl gear. Bottom or surface temperature information was not available for the commercial catch data.

An insightful way to examine responses to changing environmental conditions in the EBS has been to classify years into cold, warm, and average, based on characteristics of the water column and sea ice (Stabeno *et al.*, 2012). In this study, a similar classification system was developed, but for warm and cold years only, by combining five indices obtained from the Bering Climate website (http://www.beringclimate.noaa.gov/data/index.php): Ice Cover Index, Ice Retreat Index, surface temperature at Mooring 2 (M2), May SST at M2, and summer bottom temperature from the shelf survey. Years with scores ≤ 2.5 were classified as warm and those > 2.5 were classified as cold (Table 1).

Data analysis

Generalised Additive Models (GAM) were used to study the seasonality and the effects of environmental variability on habitat use of age-4+ Greenland and Pacific halibut in the EBS. The models were separately applied to each of the four different groups of CPUE data: (1) shelf groundfish survey; (2) slope groundfish survey; (3) commercial trawl; and (4) commercial longline. The GAM analysis was restricted to non-zero hauls, which was necessary to stabilise the variance and normalise the distribution of the residuals. Removing the zeros is necessary because the surveys were not designed to catch only Greenland and Pacific halibut, and thus cover areas of the EBS where these species are not likely to occur. However, when the GAM models were used to predict changes in catch between threshold periods (warm vs. cold years, spawning vs. non-spawning seasons; see next section), we included survey stations with at least one record of positive catch and grid centre points with three or more

Table 1. Thermal classifications from 1982 – 2013 based on indices obtained from the Bering Climate website (http://www.beringclimate.noaa.gov/).

Year	Ice cover 1 = high, 0 = low	Ice retreat 1 = late, 0.5 = mid, 0 = early	ST at M2 1 = cold, 0 = warm	May SST 1 = cold, 0 = warm	Summer BT 1 = cold, 0 = warm	Score (out of 5)	Cold-Warm Classification
1982	1	1	0	1	1	4	Cold
1983	0	0	0	0	0	0	Warm
1984	1	0	0.5	1	0	2.5	Warm
1985	0	1	0	1	1	3	Cold
1986	0	0.5	0	1	1	2.5	Warm
1987	0	0	0	0	0	0	Warm
1988	1	1	1	1	1	5	Cold
1989	0	1	1	1	0	3	Cold
1990	0	0.5	1	1	1	3.5	Cold
1991	1	0	1	1	0	3	Cold
1992	1	1	1	1	1	5	Cold
1993	0	0	1	0	0	1	Warm
1994	0	0.5	0	1	1	2.5	Warm
1995	1	1	1	1	1	5	Cold
1996	0	0	0	0	0	0	Warm
1997	1	1	1	1	0	4	Cold
1998	1	0	1	1	0	3	Cold
1999	1	1	1	1	1	5	Cold
2000	1	0	1	1	1	4	Cold
2001	0	0	0	1	0	1	Warm
2002	0	0	1	0	0	1	Warm
2003	0	0	0	0	0	0	Warm
2004	0	1	0	0	0	1	Warm
2005	0	0	0	0	0	0	Warm
2006	0	0.5	1	1	1	3.5	Cold
2007	1	1	1	1	1	5	Cold
2008	1	1	1	1	1	5	Cold
2009	1	1	1	1	1	5	Cold
2010	1	1	1	1	1	5	Cold
2011	1	1	1	1	0	4	Cold
2012	1	1	1	1	1	5	Cold
2013	1	1	1	1	1	5	Cold

ST: surface temperature; M2: Mooring 2; SST: sea surface temperature; BT: bottom temperature; Score: ≤ 2.5, Warm; > 2.5, Cold.

commercial hauls in each period examined, even if there were no other occurrences of catch at that location over the remainder of the time series. All statistical analyses were carried out in R using the "mgcv" library (Wood, 2006).

AFSC groundfish survey data

We limited our Greenland halibut analysis to years during which the shelf and slope surveys overlapped (2002, 2004, 2008, 2010 and 2012) to make results comparable. Preliminary analysis of slope survey data revealed that exploratory GAM models poorly explained adult Pacific halibut catch (Adjusted $R^2 = 0.06$); therefore, for this species we focused on the shelf survey data and expanded our analysis to include the full time series (1982 – 2013).

Survey catch was modelled using thin plate regression splines (Wood, 2003), with the degrees of freedom constrained by limiting the number of knots to 6 for one-dimensional smoothers. Fully additive [Equation (1)] and threshold formulations [Equation (2)] with year (warm or cold) as the threshold variable on spatial covariates (latitude and longitude) were developed to examine the influence of bottom depth, bottom temperature, SST, and location on survey CPUE, and determine whether CPUE varied in relation to thermal conditions on the shelf (warm vs. cold years).

The response variable $x_{y,(\rho,\lambda)}$ is the natural logarithm of the standardised Greenland or Pacific halibut survey catch (n km$^{-2}+1$) at a particular location ρ,λ (in longitude and latitude degrees) and year y. The spatially invariant model formulation was as follows:

$$x_{y,(\rho,\lambda)} = a_y + g_1\left(\mathrm{BD}_{y,(\rho,\lambda)}\right) + g_2\left(\mathrm{BT}_{y,(\rho,\lambda)}\right) + g_3\left(\mathrm{SST}_{y,(\rho,\lambda)}\right) + s_1(\rho,\lambda) + \varepsilon_{y,(\rho,\lambda)} \quad (1)$$

where a is the year-specific intercept, gi and s_1 are 1-dimensional (Wood, 2004) and 2-dimensional (Wood, 2003) smoothing functions, respectively, and $\epsilon_{y,(\rho,\lambda)}$ is a normally-distributed error term. The spatially variant model formulation was expressed as follows:

$$x_{y,(\rho,\lambda)} = a_y + g_1\left(\mathrm{BD}_{y,(\rho,\lambda)}\right) + g_2\left(\mathrm{BT}_{y,(\rho,\lambda)}\right) + g_3\left(\mathrm{SST}_{y,(\rho,\lambda)}\right) + I_{1y} * s_1(\rho,\lambda) + I_{2y} * s_2(\rho,\lambda) + \epsilon_{y,(\rho,\lambda)} \quad (2)$$

$$\left\{\begin{array}{rl} \text{where } I_{1y} & = 0 \text{ if } y \text{ is warm} \\ & = 1 \text{ if } y \text{ is cold} \\ I_{2y} & = 1 \text{ if } y \text{ is warm} \\ & = 0 \text{ if } y \text{ is cold} \end{array}\right\}$$

which is similar to the spatially invariant formulation, except that it includes 2-dimensional smoothing functions, $I_{1y}{}^{*}s_i$ and $I_{2y}{}^{*}s_i$, that describe the spatial variation in the location effect in thermally-contrasting years.

The best model was selected by computing the genuine cross validation (CV, Ciannelli *et al.*, 2007), with the lowest score representing the best model. The CV was calculated by excluding a random sample of 10% of the data from the observations, then fitting the various model formulations with the remaining 90% of the data. The fitted model was then used to estimate the 10% out-of-sample data cases, and the mean squared predictive error was recorded. The process was repeated 500 times, with the final CV being the average of all runs.

The resulting GAM models were checked for residual spatial autocorrelation and if detected, the correlation structure producing the lowest Akaike information criterion (AIC) was incorporated into a Generalised Additive Mixed Model (GAMM) that was used to predict the change in catch between warm (2004) and cold (2012) years. Since the slope survey was not on a standardised grid, it was not possible to compare changes in catch at the same station between years. Instead, stations with a positive catch in 2004 were used as 2012 station locations and bottom temperatures were predicted at these "new" 2012 stations from the original 2012 station information (latitude, longitude and associated bottom temperature) using LOESS regression. The GAM(M) was then used to predict changes in catch at each station (i.e. 2004 and "new" 2012) between warm and cold years.

AFSC groundfish observer data

For Greenland halibut, our analysis was limited to data collected between the months of May and August, which represented the majority of available catch data for this species (Figure S1, Supplement 1) and also overlapped with months during which both the slope and shelf surveys occurred, allowing for direct comparisons between the datasets.

Pacific halibut catch data spanned the full year (Figure S1, Supplement 1), which allowed us to examine seasonal differences in catch, in addition to differences between warm and cold years. For our seasonal analysis, we focused on the spawning and non-spawning seasons. To determine the best demarcation between the two, we tested threshold GAMs for spawning seasons ranging from 3 months to 6 months in length during the on-shore/off-shore migratory period (Loher, 2008, Seitz *et al.*, 2011) and around peak spawning activities (Sohn *et al.*, 2016). The model with spawning between January and May had the lowest AIC for both the trawl and longline data sets (Figure S2, Supplement 2), however, we chose to use the second best model, with spawning between January and April, for our threshold analysis. The two models produced similar results, but the January – April model was selected to ensure that our analysis covered the time frame during which most adults are on the spawning grounds or are migrating to their summer feeding grounds after spawning, and that intrusion into the non-spawning period was minimized. The January – April threshold was then incorporated into GAMs to examine changes in catch between the spawning/non-spawning seasons in both warm and cold years.

Fully additive [Equation (3)] and threshold model [Equation (4)] formulations were developed for each species, with either year (warm or cold) or, for Pacific halibut only, season (spawning or non-spawning) as the threshold variable on spatial covariates, and year, average depth, and location as the predictors of catch. The response variable $x_{y,(\rho,\lambda)}$ was the natural logarithm of the gridded average Greenland or Pacific halibut commercial catch (trawl: n hr$^{-1}+1$; longline: n 100 hooks$^{-1}+1$) at a particular

location ρ,λ (in longitude and latitude degrees) and year y. The spatially invariant model formulation was expressed as follows:

$$x_{y,(\rho,\lambda)} = a_y + g_1\left(\mathrm{BD}_{y,(\rho,\lambda)}\right) + s_1(\rho,\lambda) + \varepsilon_{y,(\rho,\lambda)} \quad (3)$$

where terms correspond to those described for the spatially invariant groundfish survey model [Equation (1)]. The spatially variant model formulation was:

$$x_{y,(\rho,\lambda)} = a_y + g_1\left(\mathrm{BD}_{y,(\rho,\lambda)}\right) + I_{1y} * s_1(\rho,\lambda) + I_{2y} * s_2(\rho,\lambda) + I_{3y} * s_3(\rho,\lambda) + I_{4y} * s_4(\rho,\lambda) + \epsilon_{y,(\rho,\lambda)} \quad (4)$$

$$\left\{\begin{array}{rl} \text{where } I_{1y} & = 0 \text{ if } y \text{ is warm} \\ & = 1 \text{ if } y \text{ is col} \\ I_{2y} & = 1 \text{ if } y \text{ is warm} \\ & = 0 \text{ if } y \text{ is cold} \\ I_{3y} & = 0 \text{ if } y \text{ is between January–April(spawning season)} \\ & = 1 \text{ if } y \text{ is between May–December(non} - \text{spawning season)} \\ I_{4y} & = 1 \text{ if } y \text{ is between January–April(spawning season)} \\ & = 0 \text{ if } y \text{ is between May–December(non} - \text{spawning season)} \end{array}\right\}$$

where terms correspond to those described for the spatially variant groundfish survey model [Equation (2)] and $I_{3y}{}^{*}s_i$ and $I_{4y}{}^{*}s_i$ are 2-dimensional smoothing functions that describe the variation in the location effect in spawning vs. non-spawning seasons.

The model with the lowest CV was selected as the best model and residuals were checked for spatial autocorrelation. If found, the correlation structure producing the lowest AIC was incorporated into a GAMM that was used to predict the change in CPUE between warm (2004) and cold (2011) years.

Results

Summer distributions from AFSC groundfish survey data

For the shelf survey, a total of 272 and 7326 hauls were used to model Greenland and Pacific halibut CPUE, respectively, while a total of 659 hauls were used to model Greenland halibut CPUE along the slope. The mean catch depth for Greenland halibut in the shelf and slope surveys was 111.0 m and 573.0 m, respectively (Table 2). The minimum and mean bottom temperatures of tows with Greenland halibut catch were lower on the shelf than on the slope, though the maximum catch temperature was the same for both surveys (4.1 °C), making the temperature range experienced on the shelf much greater than that experienced on the slope (Table 2). Greenland halibut was mostly caught in the northern part of the shelf survey over the middle (50 – 100 m) and outer (100 – 200 m) shelves, whereas in the slope survey they were caught along the entire length of the slope. Mean CPUE was higher in the slope survey than in the shelf survey (Table 2). Pacific halibut were caught at shallower depths than Greenland halibut, with mean catch depths of 78.1 m and 363.7 m in the shelf and slope surveys, respectively (Table 2). On the shelf, Pacific halibut were caught over a greater range of bottom temperatures than Greenland halibut, though along the slope, their temperature ranges were similar (Table 2). Temperature ranges at the surface were similar for both species, though the range was smaller along the slope (Table 2). Pacific halibut mean CPUE was higher in the shelf survey than in the slope survey (Table 2), with the majority of stations occupied over the shelf.

GAM analysis of AFSC summer groundfish survey data

Environmental factors had statistically significant effects on survey CPUE of Greenland and Pacific halibut in the EBS. Based on the calculated CV, the best model for Greenland halibut in the shelf survey was the threshold model with the ratio correlation structure that included year, location, bottom depth, bottom temperature, and SST (Table 3; Figure 2a–c). Bottom temperature had a significant positive effect on CPUE up to approximately 0.9 °C (BT: $F = 8.79$, equivalent (e)df $= 3.60$, $p \ll 0.001$), above which the effect was slightly negative. The effects of depth and SST were not statistically significant; however, the AIC increased when these covariates were removed, suggesting that they should remain in the model. In warm years, Greenland halibut CPUE was predicted to increase over the northern portion of the middle shelf, whereas during cold years, CPUE was predicted to increase over the middle and outer shelves, and extend farther south over the middle shelf (Figure 3a).

For Pacific halibut in the shelf survey, the best model was the threshold model with the ratio correlation structure that included year, location, bottom depth, bottom temperature, and SST (Table 3; Figure 2d–f), with all covariates being significant (BD: $F = 39.57$, edf $= 4.72$, $p \ll 0.001$; BT: $F = 99.14$, edf $= 4.55$, $p \ll 0.001$), SST: $F = 25.65$, edf $= 4.33$, $p \ll 0.001$). Depth had a positive effect on CPUE to about 50 m, followed by a decrease in CPUE to about 160 m, below which depth again had a slight positive effect (Figure 2d). Pacific halibut CPUE increased in relation to increasing bottom temperature, most notably above 2.0 °C to approximately 7.5 °C (Figure 2e). Overall, SST had a negative effect on CPUE at temperatures above 1.0 °C (Figure 2f). In warm years, Pacific halibut CPUE increased around Nunivak Island in the inner shelf and around the Pribilof Islands over the middle shelf. In cold years, the largest increases in CPUE were in the southern portion of the survey, mainly around Bristol Bay (Figure 3b).

The best model for Greenland halibut CPUE in the slope survey was the threshold model without spatial autocorrelation, where year, location, bottom depth, bottom temperature, and SST were found to be statistically significant (Table 3; Figure 2g–i, BD: $F = 9.12$, edf $= 4.40$, $p \ll 0.001$; BT: $F = 2.91$, edf $= 3.79$, $p = 0.02$; SST: $F = 2.45$, edf $= 3.29$, $p = 0.05$). In contrast to the shelf model, bottom depth had a strong positive effect on Greenland halibut CPUE along the slope to approximately 425 m depth, below which the effect was negative (Figure 2g). Bottom temperature had a negative effect on CPUE to 2.9 °C, a positive effect to about 3.6 °C, above which the effect was negative. Overall, CPUE increased during warm years in the southern portion of the survey region between Bering and Pribilof canyons. During cold years, CPUE increased along the slope northward of Zhemchug Canyon, most notably around Pervenets Canyon (Figure 3a). The slope survey had a greater change in CPUE between warm and cold years than the shelf survey: 6.1 log (n $\mathrm{km}^{-2}+1$) and 1.6 log (n $\mathrm{km}^{-2}+1$), respectively.

Seasonal distributions from AFSC groundfish observer data

A total of 213 and 352 grid cells with aggregated CPUE data were used to analyse Greenland halibut distributions from commercial

Table 2. Bottom depth (survey, commercial longline), fishing depth (commercial trawl), bottom temperature, and sea surface temperature ranges and means with standard errors of Greenland and Pacific halibut CPUE in bottom trawl surveys and commercial fisheries in the eastern Bering Sea.

			Bottom		Sea surface		Catch	
	Depth (m)		temperature (°C)		temperature (°C)		(log(CPUE+1))	
Greenland halibut	**Range**	**Mean**	**Range**	**Mean**	**Range**	**Mean**	**Range**	**Mean**
Survey								
Shelf (n = 272)	62 – 173	111.0 ± 1.3	−1.4 – 4.1	1.13 ± 0.07	−1.1 – 11.2	8.02 ± 0.11	2.82 – 7.67	4.40 ± 0.06
Slope (n = 659)	206 – 1200	573.0 ± 8.8	2.0 – 4.1	3.36 ± 0.02	1.6 – 10.9	6.77 ± 0.07	2.99 – 9.68	5.00 ± 0.05
Commercial fishery								
Trawl (n grid = 213)	88.8 – 859.7	377.1 ± 9.6	–	–	–	–	0.05 – 6.65	2.83 ± 0.12
Longline (n grid = 352)	128.7 – 834.5	564.9 ± 6.8	–	–	–	–	0.05 – 3.08	1.52 ± 0.03
Pacific halibut								
Survey								
Shelf (n = 7326)	16 – 198	78.1 ± 0.4	−1.8 – 11.7	2.64 ± 0.02	−1.1 – 11.6	6.09 ± 0.02	2.76 – 8.38	4.31 ± 0.01
Slope (n = 288)	202 – 683	363.7 ± 6.9	2.0 – 4.2	3.47 ± 0.03	1.6 – 10.9	6.26 ± 0.11	3.03 – 7.01	4.03 ± 0.05
Commercial fishery								
Trawl (n grid = 6639)	7.3 – 859.7	97.7 ± 1.0	–	–	–	–	0.09 – 7.25	3.19 ± 0.01
Longline (n grid = 5084)	39.9 – 812.4	128.5 ± 1.2	–	–	–	–	0.001 – 2.58	0.47 ± 0.00

Table 3. Spatially invariant (1, 3, 5, 7, 9, 11 and 14) and spatially variant (2, 4, 6, 8, 10, 12, 13, 15 and 16) models of Greenland and Pacific halibut CPUE, $x_{y,(\rho,\lambda)}$, estimated from shelf and slope survey data and commercial trawl and longline fisheries data in the eastern Bering Sea.

Model	Formulation	CV	Adj. R^2	SA
	Greenland halibut shelf survey			
1	$x_{y,(\rho,\lambda)} = a_y + g_1(\mathrm{BD}_{y,(\rho,\lambda)}) + g_2(\mathrm{BT}_{y,(\rho,\lambda)}) + g_3(\mathrm{SST}_{y,(\rho,\lambda)}) + s_1(\rho,\lambda) + \epsilon_{y,(\rho,\lambda)}$	0.534	–	–
2	$\boldsymbol{x_{y,(\rho,\lambda)} = a_y + g_1(\mathrm{BD}_{y,(\rho,\lambda)}) + g_2(\mathrm{BT}_{y,(\rho,\lambda)}) + g_3(\mathrm{SST}_{y,(\rho,\lambda)}) + I_{1y}{*}s_1(\rho,\lambda) + I_{2y}{*}s_2(\rho,\lambda) + \epsilon_{y,(\rho,\lambda)}}$	**0.531**	**0.52**	**Ratio**
	Greenland halibut slope survey			
3	$x_{y,(\rho,\lambda)} = a_y + g_1(\mathrm{BD}_{y,(\rho,\lambda)}) + g_2(\mathrm{BT}_{y,(\rho,\lambda)}) + g_3(\mathrm{SST}_{y,(\rho,\lambda)}) + s_1(\rho,\lambda) + \epsilon_{y,(\rho,\lambda)}$	0.947	–	–
4	$\boldsymbol{x_{y,(\rho,\lambda)} = a_y + g_1(\mathrm{BD}_{y,(\rho,\lambda)}) + g_2(\mathrm{BT}_{y,(\rho,\lambda)}) + g_3(\mathrm{SST}_{y,(\rho,\lambda)}) + I_{1y}{*}s_1(\rho,\lambda) + I_{2y}{*}s_2(\rho,\lambda) + \epsilon_{y,(\rho,\lambda)}}$	**0.940**	**0.35**	**-**
	Pacific halibut shelf survey			
5	$x_{y,(\rho,\lambda)} = a_y + g_1(\mathrm{BD}_{y,(\rho,\lambda)}) + g_2(\mathrm{BT}_{y,(\rho,\lambda)}) + g_3(\mathrm{SST}_{y,(\rho,\lambda)}) + s_1(\rho,\lambda) + \epsilon_{y,(\rho,\lambda)}$	0.705	–	–
6	$\boldsymbol{x_{y,(\rho,\lambda)} = a_y + g_1(\mathrm{BD}_{y,(\rho,\lambda)}) + g_2(\mathrm{BT}_{y,(\rho,\lambda)}) + g_3(\mathrm{SST}_{y,(\rho,\lambda)}) + I_{1y}{*}s_1(\rho,\lambda) + I_{2y}{*}s_2(\rho,\lambda) + \epsilon_{y,(\rho,\lambda)}}$	**0.691**	**0.36**	**Ratio**
	Greenland halibut commercial trawl			
7	$\boldsymbol{x_{y,(\rho,\lambda)} = a_y + g_1(\mathrm{BD}_{y,(\rho,\lambda)}) + s_1(\rho,\lambda) + \epsilon_{y,(\rho,\lambda)}}$	**1.374**	**0.63**	**Ratio**
8	$x_{y,(\rho,\lambda)} = a_y + g_1(\mathrm{BD}_{y,(\rho,\lambda)}) + I_{1y}{*}s_1(\rho,\lambda) + I_{2y}{*}s_2(\rho,\lambda) + \epsilon_{y,(\rho,\lambda)}$	1.465	–	–
	Greenland halibut commercial longline			
9	$x_{y,(\rho,\lambda)} = a_y + g_1(\mathrm{BD}_{y,(\rho,\lambda)}) + s_1(\rho,\lambda) + \epsilon_{y,(\rho,\lambda)}$	0.171	–	–
10	$\boldsymbol{x_{y,(\rho,\lambda)} = a_y + g_1(\mathrm{BD}_{y,(\rho,\lambda)}) + I_{1y}{*}s_1(\rho,\lambda) + I_{2y}{*}s_2(\rho,\lambda) + \epsilon_{y,(\rho,\lambda)}}$	**0.167**	**0.61**	**Exp.**
	Pacific halibut commercial trawl			
11	$x_{y,(\rho,\lambda)} = a_y + g_1(\mathrm{BD}_{y,(\rho,\lambda)}) + s_1(\rho,\lambda) + \epsilon_{y,(\rho,\lambda)}$	0.864	–	–
12	$x_{y,(\rho,\lambda)} = a_y + g_1(\mathrm{BD}_{y,(\rho,\lambda)}) + I_{1y}{*}s_1(\rho,\lambda) + I_{2y}{*}s_2(\rho,\lambda) + \epsilon_{y,(\rho,\lambda)}$	0.800	–	–
13	$\boldsymbol{x_{y,(\rho,\lambda)} = a_y + g_1(\mathrm{BD}_{y,(\rho,\lambda)}) + I_{1y}{*}s_1(\rho,\lambda) + I_{2y}{*}s_2(\rho,\lambda) + I_{3y}{*}s_3(\rho,\lambda) + I_{4y}{*}s_4(\rho,\lambda) + \epsilon_{y,(\rho,\lambda)}}$	**0.772**	**0.41**	**-**
	Pacific halibut commercial longline			
14	$x_{y,(\rho,\lambda)} = a_y + g_1(\mathrm{BD}_{y,(\rho,\lambda)}) + s_1(\rho,\lambda) + \epsilon_{y,(\rho,\lambda)}$	0.070	–	–
15	$x_{y,(\rho,\lambda)} = a_y + g_1(\mathrm{BD}_{y,(\rho,\lambda)}) + I_{1y}{*}s_1(\rho,\lambda) + I_{2y}{*}s_2(\rho,\lambda) + \epsilon_{y,(\rho,\lambda)}$	0.061	–	–
16	$\boldsymbol{x_{y,(\rho,\lambda)} = a_y + g_1(\mathrm{BD}_{y,(\rho,\lambda)}) + I_{1y}{*}s_1(\rho,\lambda) + I_{2y}{*}s_2(\rho,\lambda) + I_{3y}{*}s_3(\rho,\lambda) + I_{4y}{*}s_4(\rho,\lambda) + \epsilon_{y,(\rho,\lambda)}}$	**0.061**	**0.40**	**-**

Genuine cross validation (CV) scores, adjusted R^2 values, and spatial autocorrelation (SA) structures used in the best model (bolded font) are shown. a: intercept; g and s: 1- and 2-dimensional smoothing functions, respectively. y: year; BD: bottom depth; BT: bottom temperature; SST: sea surface temperature; (ρ,λ): longitude and latitude coordinates; I_{1y} and I_{2y}: spatial variation in location effect in thermally contrasting years; I_{3y} and I_{4y}: spatial variation in location effect in spawning vs. non-spawning seasons; ϵ: error term.

trawl and longline fisheries data, respectively. For the Pacific halibut analysis, a total of 6639 and 5084 grid cells with aggregated trawl and longline CPUE data were used, respectively (Table 2). The average depth of gridded Greenland halibut catch was shallower for fisheries using bottom trawl gear than those using longline gear, with a mean catch depth of 377.1 m and 564.9 m, respectively (Table 2). The average depths of Pacific halibut catch were shallower than those for Greenland halibut, at 97.7 and 128.5 m for trawl and longline gear, respectively (Table 2).

GAM analysis of AFSC seasonal groundfish observer data

Environmental factors had statistically significant effects on the catch of Greenland and Pacific halibut in EBS groundfish trawl and longline fisheries. The best model for bottom trawl-caught

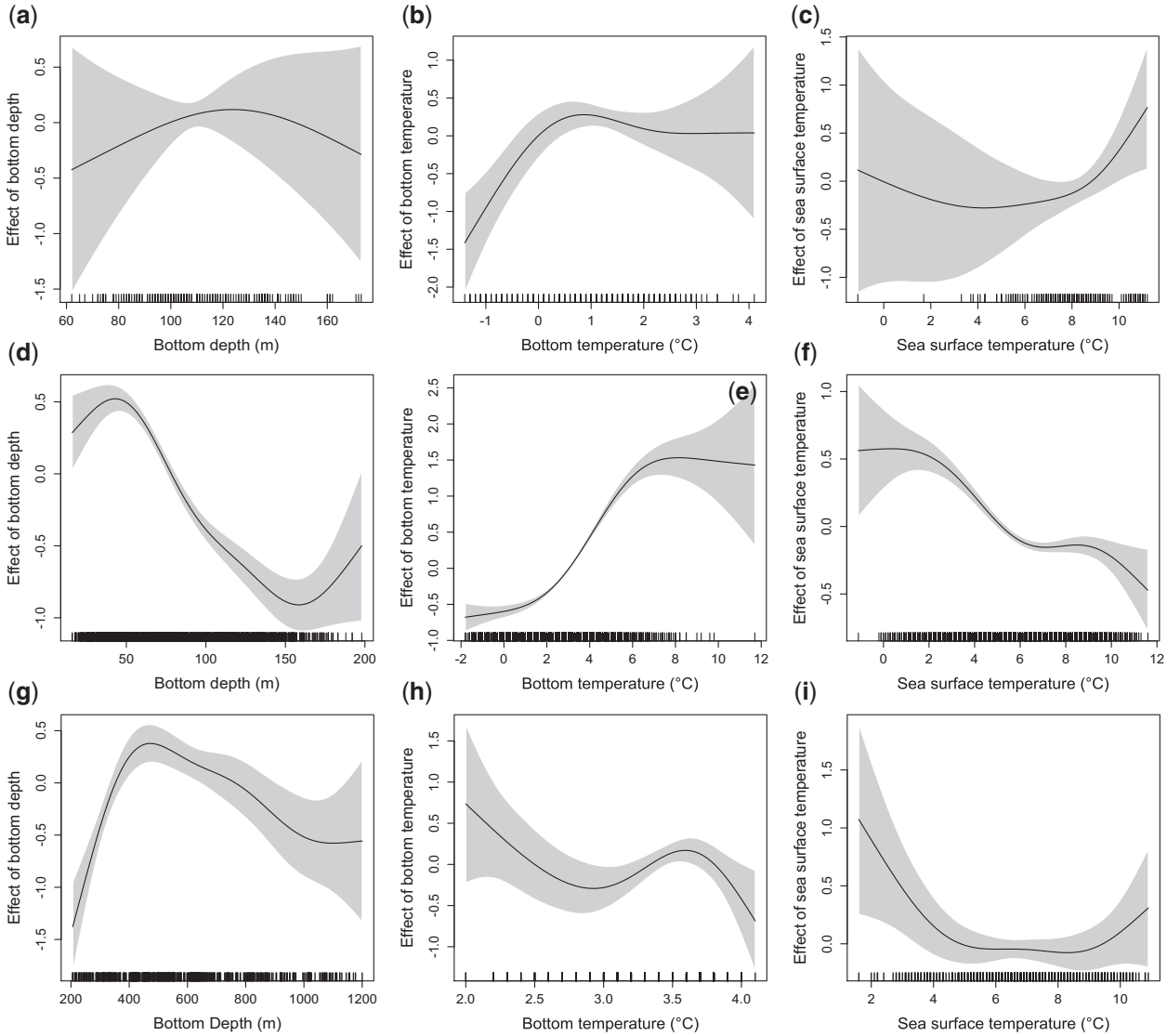

Figure 2. Environmental covariate effects on Greenland halibut (a–c, g–i) and Pacific halibut (d-f) CPUE in the eastern Bering Sea shelf (a-f) and slope (g-i) bottom trawl surveys. Shaded regions indicate the 95% confidence interval for the variables bottom depth (a,d,g), bottom temperature (b,e,h), and sea surface temperature (c,f,i).

Greenland halibut from May – August was the fully additive model with the ratio correlation structure that included year, location, and bottom depth (Table 3). Depth had a significantly positive effect (BD: $F = 19.23$, $edf = 6.12$, $p \ll 0.001$) on trawl CPUE to 450 m depth, after which the effect leveled off (Figure 4a). Model results below this depth should be interpreted with caution due to low sample size at deeper depths. The location effect was greater at more northerly locations than southerly ones, with the highest CPUE over the outer shelf around Pervenets and Navarin canyons (Figure 4b). For longline-caught Greenland halibut, the best model included a threshold effect on distribution in warm vs. cold years and bottom depth, with the exponential correlation structure. Depth had a significantly positive effect on CPUE (BD: $F = 300.58$, $edf = 1.00$, $p \ll 0.001$), with CPUE increasing linearly with increasing depth (Figure 5a). Greenland halibut CPUE increased slope-wide during cold years, with the greatest increases from Zhemchug Canyon northward, whereas no increases in CPUE were found in warm years (Figure 5b).

Pacific halibut CPUE in both the EBS groundfish trawl and longline fisheries was best modelled with a threshold effect on distribution in warm vs. cold years and in spawning January – April) vs. non-spawning (May – December) seasons (Table 3). Depth was highly significant for both trawl ($F = 28.43$, $edf = 7.24$, $p \ll 0.001$) and longline ($F = 95.98$, $edf = 1.00$, $p \ll 0.001$) gear types. Overall, depth had a positive effect on trawl CPUE to about 100 m depth, then a negative effect to about 220 m, below which the effect became more strongly negative until 400 m (Figure S3b, Supplement 3). For the longline gear, depth had a negative effect, with CPUE decreasing linearly with increasing depth (Figure S3b, Supplement 3). Location effects in each thermal and seasonal period were statistically significant for both the trawl and longline groundfish fisheries.

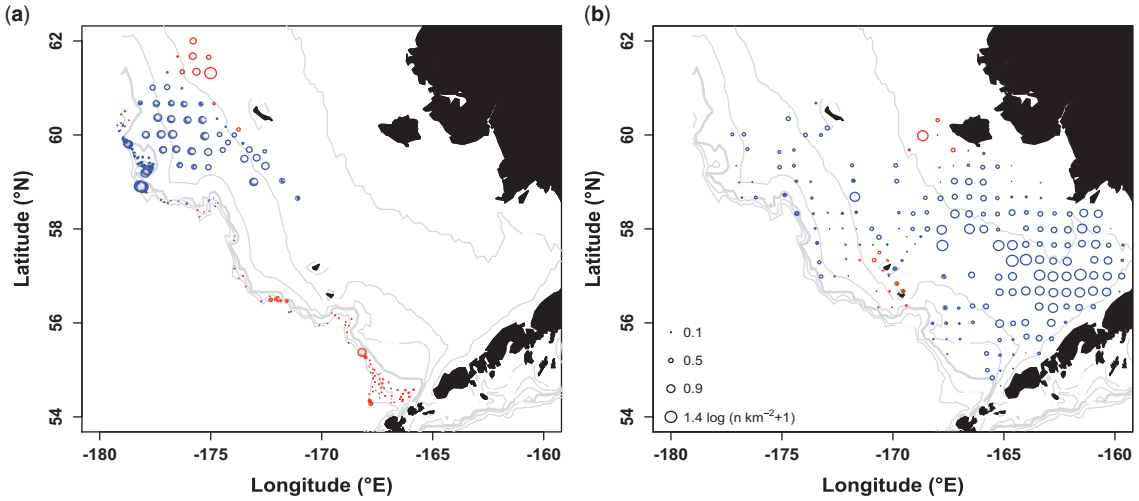

Figure 3. Change in eastern Bering Sea bottom trawl survey CPUE of (a) Greenland halibut and (b) Pacific halibut between warm (2004) and cold (2012) years. Blue (red) circles represent an increase in CPUE during cold (warm) years. Circles for Greenland halibut are scaled to the maximum change in CPUE in the respective slope (6.1 log CPUE + 1) and shelf (1.6 log CPUE + 1) surveys. The grey lines represent the 50, 100, 150, 200 (bolded), 500 and 1,000 m isobaths. For interpretation of the references to colour in this figure legend, the reader is referred to the online version of this article.

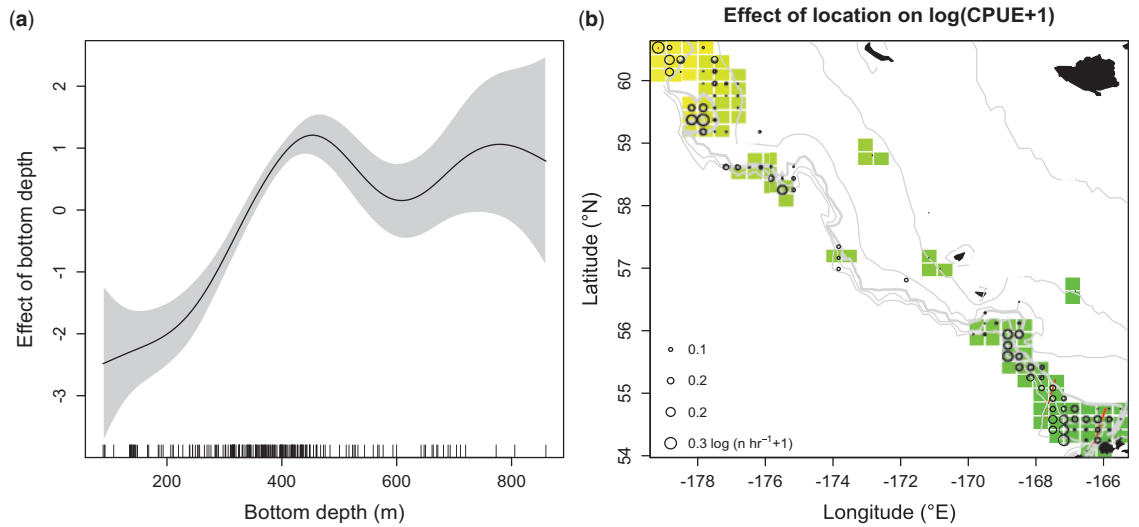

Figure 4. Effects of (a) bottom depth and (b) location on Greenland halibut commercial trawl CPUE from May – August between 1991 and 2011. Colours represent the minimum and maximum modelled spatial effect on Greenland halibut CPUE, with green representing locations with lower CPUE and yellow representing locations with higher CPUE. The grey lines in (b) represent the 50, 100, 150, 200 (bolded), 500 and 1,000 m isobaths. For interpretation of the references to colour in this figure legend, the reader is referred to the online version of this article.

During the spawning season in warm years, Pacific halibut trawl CPUE increased over the southern middle shelf, west of the Pribilof Islands, and along the shelf break north of Zhemchug Canyon (Figure S4a, Supplement 4). In cold years, CPUE increased over the southern portion of the outer shelf, south of Zhemchug Canyon, and in Pervenets Canyon (Figure S4a, Supplement 4). During the non-spawning season in warm years, trawl CPUE increased slightly at northern locations over the middle and outer shelves and in Bristol Bay, whereas in cold years, CPUE increased shelf-wide (Figure S4b, Supplement 4). In cold years, longline CPUE increased over the middle and outer shelves in both the spawning and non-spawning seasons, whereas in warm years, only slight increases in CPUE were seen along the southern portion of the middle and outer shelves (Figure S4c and d, Supplement 4).

Pacific halibut trawl CPUE was mostly concentrated on the middle and outer shelves south of the Pribilof Islands during the spawning season, expanding outwards in warm years (Figure 6a) and a more concentrated pattern in cold years (Figure 6b). During the non-spawning season, CPUE increased farther to the north and east in warm years (Figure 6a) compared to cold years, when CPUE increased along northern portions of the outer shelf and slope and over the central portion of the middle shelf, southeast of the Pribilofs (Figure 6b). Similar patterns were seen for longline CPUE between warm and cold years. However, during the spawning season, the catch was more dispersed over the middle shelf to the south and east in warm years (Figure 6c) compared to cold years, when the catch was more concentrated around Pribilof Canyon (Figure 6d). During the non-spawning

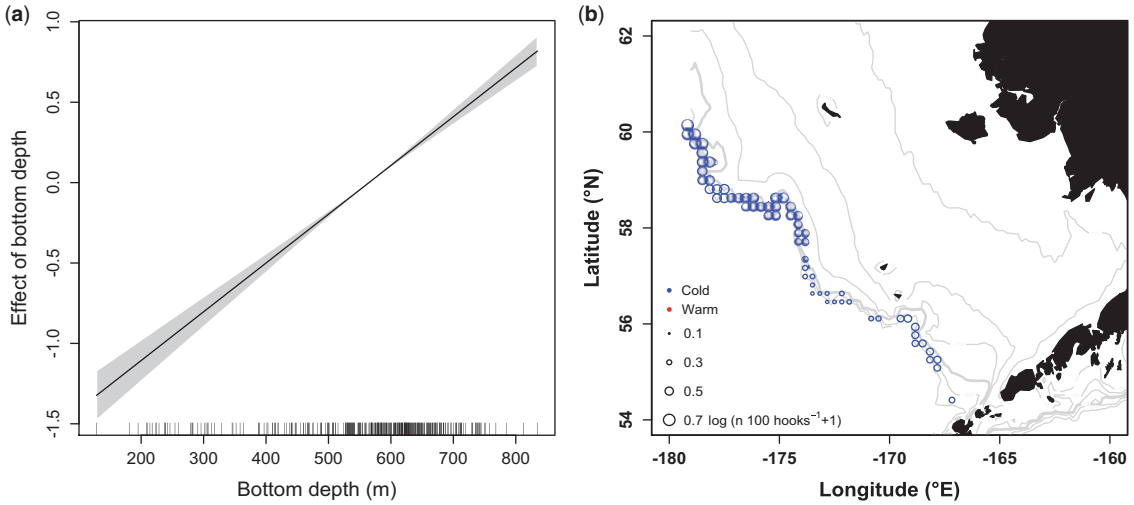

Figure 5. Effect of (a) bottom depth on Greenland halibut commercial longline CPUE from May – August between 2000 and 2011 and (b) change in catch between warm (2004) and cold (2011) years. Blue (red) circles represent an increase in CPUE during cold (warm) years. The grey lines in (b) represent the 50, 100, 150, 200 (bolded), 500 and 1,000 m isobaths. For interpretation of the references to colour in this figure legend, the reader is referred to the online version of this article.

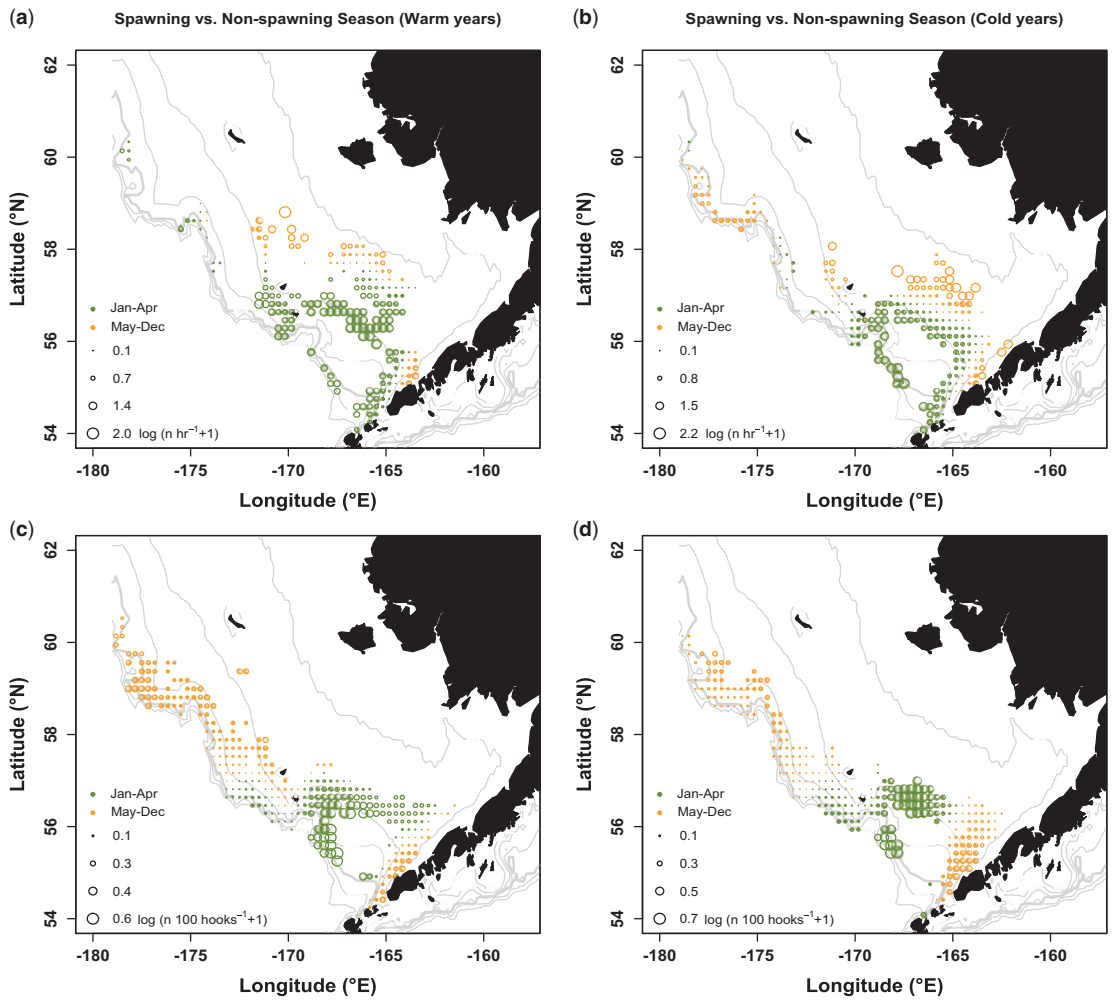

Figure 6. Change in Pacific halibut commercial trawl (a, b) and longline (c, d) CPUE between spawning (January – April) and non-spawning (May – December) seasons in warm (2004: a, c) and cold (2011: b, d) years. Green (orange) circles represent an increase in CPUE during the spawning (non-spawning) season. Circle size is scaled to the maximum change in CPUE for the respective fisheries and seasons. The grey lines represent the 50, 100, 150, 200 (bolded), 500 and 1,000 m isobaths. For interpretation of the references to colour in this figure legend, the reader is referred to the online version of this article.

season, increases in CPUE were greater along the outer shelf and the Pribilof Islands in warm years (Figure 6c), and greater along the southern portion of the middle and outer shelves along the Alaska Peninsula during cold years (Figure 6d).

Discussion

Previous studies have shown that climate change can affect marine species distribution in two ways: through latitudinal and depth shifts. Thus, to understand how species will respond to predicted warming in the EBS, it is important to examine species that occur over a wide range of depths in both slope and shelf habitats. Doing so for species at the opposite extremes of their distribution range will shed light on processes of climate adaptation for species with contrasting thermal tolerances that are at the limits of their ranges. Our analysis, which combined fisheries-independent survey data and fisheries-dependent catch data, examined seasonal habitat use of two slope-spawning flatfish – Pacific halibut at the northernmost extent and Greenland halibut at the southernmost extent of their spatial distributions. We found that species-environment effects influenced their distribution and local abundance, however, these effects did not sufficiently explain the changes in distribution between warm and cold years. Habitat use varied significantly between warm and cold years, with further differences observed between the spawning and non-spawning seasons for Pacific halibut.

Greenland and Pacific halibut had strong and contrasting responses to changes in temperature on the shelf, with catches decreasing and increasing, respectively, beyond 1 °C. The local temperature effect was not as prominent along the slope, suggesting that slope habitats may provide some insulation from shelf-associated environmental variability, particularly for Greenland halibut. The greatest temperature variation observed during the slope survey was 2.2 °C, which occurred in 2002 and 2004, two warm years. In a previous study of EBS flatfish distributions, Greenland halibut occupied lower temperatures than those recorded over the shelf during warm years and higher temperatures during cold years, overall exhibiting less variability than shelf-wide survey temperatures (Spencer, 2008). Polar species, such as Greenland halibut, are stenothermic with a narrow thermal window, which makes them particularly sensitive to changes in temperature. They will likely be marginalized with predicted warming, given their limited ability to move to colder regions (IPCC, 2014).

Our models predict that Greenland halibut will undergo a latitudinal shift northward on the EBS shelf and a bathymetric shift to deeper slope habitats in response to warming, especially along the southern slope. Pacific halibut, on the other hand, are predicted to have a more latitudinal response and will shift northward over the shelf with warming. Our findings align with those from the North Sea, where fishes at the southern extent of their distribution moved northward and into deeper waters in response to warming, while species at their northern extent moved northward, with some species shallowing and some deepening (Perry *et al.*, 2005; Dulvy *et al.*, 2008; Engelhard *et al.*, 2011b; van der Veer *et al.*, 2011). Over the last three decades, there has been a general northward shift in fish populations in the EBS, with global centre of gravity for Greenland and Pacific halibut moving to the northwest by 24 and 54 km, respectively (Kotwicki and Lauth, 2013). Despite this overall northward trend, the global centre of gravity of the Pacific halibut shifted significantly to the southeast when the area of the 1 °C cold pool increased (Kotwicki and Lauth, 2013). Many studies have noted the importance of the cold pool (< 2 °C) in structuring species distributions on the EBS shelf (Grebmeier *et al.*, 2006; Spencer, 2008; Mueter and Litzow, 2008; Hollowed *et al.*, 2012). The contrasting temperature responses of Greenland and Pacific halibut at approximately 1 °C in our study reinforce the findings of Kotwicki and Lauth (2013), who suggested that the 1 °C isotherm is an important threshold for describing temperature preferences of groundfish in the EBS.

Depth did not significantly influence Greenland halibut CPUE on the shelf, yet it was significant along the slope. The temperature response along the slope may be largely tied to bathymetry, rather than a temperature preference. Greenland halibut slope survey CPUE increased between 200 and 425 m, depths which corresponded with the temperature range over which CPUE was found to increase (2.9 – 3.6 °C, Figure S5, Supplement 5). Interestingly, the eastern band of the northwestward-flowing Bering Slope Current impinges upon the slope at depths of 250 – 500 m, creating a sub-surface layer of maximum temperature (Kinder *et al.* 1975; Vestfals *et al.*, 2014) and the species could be responding to the current and its associated properties. Increases in Greenland halibut survey CPUE were seen along the southern portion of slope in warm years, which was composed almost exclusively of adults (Figure S6e, Supplement 6) and suggests that they are seeking an optimal temperature range. Increases in CPUE in the northern part of the slope in cold years may be attributed, in part, to the influx of strong year classes in 2007 – 2009 moving into the region from shelf nursery areas (Barbeaux *et al.*, 2013). Analysis of shelf and slope survey sexed length frequencies showed higher numbers of smaller-sized (< 600 mm) Greenland halibut of both sexes during cold years compared to warm (Figure S6, Supplement 6). Results for Pacific halibut showed no influx of smaller-sized individuals in the shelf survey between warm and cold years (Figure S7, Supplement 7). Sexed length frequencies were not collected regularly by groundfish observers outside of the Greenland halibut longline fishery, therefore, we did not examine changes in size distributions between warm and cold years for the commercial data sets.

While depth had a significant effect on Pacific halibut CPUE for both the survey and commercial datasets, the fact that the species is widely distributed across the EBS shelf suggests that it is not an important driver of their distribution, at least not to the same extent as for Greenland halibut. However, depth is considered a composite habitat factor that integrates temperature, pressure, and sediment composition, and a species' response to depth can be complex, especially if one of the components varies temporally (e.g. temperature; McConnaughey and Smith, 2000). Most investigations into the environmental factors that affect Pacific halibut have focused primarily on temperature, with adults preferring water temperatures ranging from 3 – 8 °C (IPHC, 1987). In the Bering Sea and Gulf of Alaska, tagged adults have been found between 0.2 and 13.6 °C, though the majority of their time is spent in the middle of the range (Loher and Seitz, 2006; Loher and Blood, 2009; Seitz *et al.*, 2007; Seitz *et al.*, 2011). Significant increases in catch between 2.0 and 7.5 °C on the shelf in our study reinforces the conclusion of strong associations with temperatures that have been identified in previous studies, though our slope model poorly explained changes in Pacific halibut CPUE, with only depth and SST being significant (Vestfals, unpublished data). Similarly, Seitz *et al.* (2011) found no trends in ambient water temperature for tagged Pacific halibut along the

slope (> 200 m), likely because they occupied depths that isolated them from seasonal temperature fluctuations.

Changes in temperature can influence spatial distributions, but they can also affect fish behaviour and their vulnerability to capture. For example, temperature increases have been associated with increases in fish swimming speed (Peck *et al.*, 2006). Several EBS flatfish species have shown a strong relationship between bottom temperature and trawl survey catchability (Wilderbuer and Nichol, 2002; Spencer *et al.*, 2004). Yellowfin sole, for example, may be less active when temperatures are low, resulting in lower catchability due to reduced herding effects or increased escapement due to less activity (Wilderbuer *et al.*, 2008). Temperature has been shown to impact Pacific halibut activity and feeding motivation, which can have a large impact on longline catchability and can potentially lead to underestimates of catch in cold years or at depths where temperatures are low (Stoner *et al.*, 2006). While temperature-dependent changes in trawl survey catchability have been incorporated into stock assessment models for yellowfin sole (*Limanda aspera)* in the EBS (Wilderbuer *et al.*, 2008), insufficient data were available to accurately conduct such adjustments for our study.

Other factors not investigated here may affect the distribution of Greenland and Pacific halibut. Sediment grain size has been shown to influence the distribution of flatfish in the EBS (McConnaughey and Smith, 2000; Bartolino *et al.*, 2012), though Greenland halibut had relatively weak sediment associations (McConnaughey and Smith, 2000). We found no meaningful relationships with sediment grain size for either species during our preliminary investigations, so these associations were not pursued further. Dissolved oxygen (DO) may be an important factor, as it can influence the abundance, distribution, and catchability of flatfish (Youcef *et al.*, 2013; Sadorus *et al.*, 2014; Keller *et al.*, 2015). We were unable to explore relationships between CPUE and DO, as this information was not available for either the survey or commercial data sets. Density-dependent factors may also play a role in driving the spatial dynamics of EBS flatfish (Bartolino *et al.*, 2011), however, both Greenland and Pacific halibut are well-below their historic population levels, and density-dependence is likely not a factor outside of their juvenile nursery areas.

Changes in Pacific halibut distribution were greater in the summer than in the winter. Slope-spawning flatfish in the EBS spawn during the winter and early spring and their distribution during this time is expected to remain relatively constant, as spawning locations are fixed by evolutionary constraints (Ciannelli *et al.*, 2015). However, temperature may influence the timing of migration to or from the spawning grounds (Sims *et al.*, 2004; Wilderbuer *et al.*, 2008), as well as the timing of spawning (Teal *et al.*, 2008; Fincham *et al.*, 2013). During the spawning season of warm years, Pacific halibut CPUE increased at shallower locations over the middle shelf compared to cold years, which may indicate earlier migration off the spawning grounds. Similarly, dispersal farther northward and eastward over the shelf in warm years may indicate earlier migrations to summer feeding grounds on the shelf.

Opposite responses to similar environmental forcing suggests that Greenland and Pacific halibut partition their habitat and will likely have contrasting responses to future climate variability. We expect that with increasing warming on the EBS shelf, these two species will further partition their habitats, with Greenland halibut finding colder refuges along the slope and Pacific halibut inhabiting larger portions of the shelf. However, there is a limit to these changes, particularly for Greenland halibut. The post-settlement juvenile portion of the Greenland halibut life cycle may be constrained to specific habitats on the shelf, which will become more restricted with progressive warming. In recent cold years we have, in fact, reported an increase of subadult individuals over the northwest portion of the EBS outer shelf and slope, compared to warm years, where increases were restricted to the northernmost portion of the middle shelf. For species or life history stages that are geographically restricted and cannot remain within their optimal temperature range through latitudinal or bathymetric shifts, the ecological consequences of warming may be more critical (Dulvy *et al.*, 2008; Rijnsdorp *et al.*, 2009).

Commercial fisheries CPUE represents the catch rate of a species by fishermen and therefore reflects the distribution of their fishing effort. Consequently, CPUE can only be used as a relative measure of abundance of Greenland and Pacific halibut, not their actual abundance. Fishing patterns and catches can be greatly influenced by market conditions, regulations, weather, and proximity to port (Maunder *et al.*, 2006). For example, SST, total allowable catch, ice cover, and walleye pollock (*Gadus chalcogrammus*) roe prices influenced a vessel's decision to begin a fishing trip within 5 days of the start of the winter fishing season (Haynie and Pfeiffer, 2013). In the North Pacific groundfish fishery, Pacific halibut is a prohibited species and fishermen actively avoid areas where catch rates are high to avoid fishery closure when the prohibited species cap is reached. Thus, the CPUE information for Pacific halibut likely underestimates their overall abundance and model estimates of their response to warming are likely conservative. Similarly, except for the targeted longline fishery, Greenland halibut is only encountered as bycatch in EBS fisheries and therefore our model likely underestimates their response to warming. It is also important to mention that declines in abundance can be masked by hyperstability (Hilborn and Walters, 1992), which can be affected by the behaviour of fish (through the formation of spawning aggregations) and fishermen (through their ability to repeatedly locate fish aggregations and exploit them)(Erismen *et al.*, 2011 and references therein). Hyperstability is likely not a problem in our commercial data analysis, as neither species are targeted during their spawning seasons and are encountered as bycatch in EBS fisheries, except for the Greenland halibut longline fishery.

Regulation changes should also be considered when using CPUE data to evaluate changes in species distributions. For example, Amendment 80 (Am80) was implemented in 2008 to improve retention and utilization of fishery resources (NPFMC, 2006), and bottom trawl vessels now retain groundfish species with previously high rates of discard. Greenland halibut catch has increased since the emergence of an arrowtooth/Kamchatka flounder (*Astheresthes stomias*/*A. evermanni*) fishery, with the trawl catch now exceeding that of the longline fishery (Barbeaux *et al.*, 2013). Since Am80 was implemented, only cold years have been represented in the available commercial trawl dataset, making it difficult to disentangle the effects of climate vs. Am80 regulations that have resulted in increased Greenland halibut CPUE. However, we found no differences in trawl CPUE in Am80 years relative to the reference year (1991), or between warm and cold years. Despite their drawbacks, commercial fisheries data have been useful in understanding the influence of environmental variability on fish distributions in the EBS, which has led to a greater understanding of fish and fishing behaviours. For example, in

warmer years with a smaller cold pool, Pacific cod were more dispersed over the shelf, leading to more vessel movement over the fishing grounds, lower CPUE, longer trips, and higher fishing costs (Haynie *et al.*, 2014).

Our study is the first to provide a comprehensive analysis of seasonal habitat use of groundfish species across the EBS slope and shelf. Previous studies have used shelf survey data to examine changes in species distributions or species assemblages in the EBS (Grebmeier *et al.*, 2006; Mueter and Litzow, 2008; Kotwicki and Lauth, 2013); however, the seasonal and spatial components were missing. By utilizing both survey and commercial fisheries data sources, our analysis offers an integrated picture of Greenland and Pacific halibut distributions over time and across different habitats. This research provides valuable information to stock assessors and fisheries managers by identifying habitat associations of commercially important flatfish species and predicting how these may change in relation to environmental variability. Understanding how the distribution, abundance, and population dynamics of slope-spawning flatfish may respond to climate change can lead to better estimates of climate impacts on marine populations and more informed management decisions.

Supplementary data

The following supplementary material is available at ICESJMS online.

Acknowledgements

The authors wish to thank the scientists and volunteers that collected the EBS shelf and slope survey data, and the observers that collected the commercial fisheries data for the North Pacific Groundfish Observer Program. We would also like to thank Steven Hare for providing Pacific halibut length-at-age information and Kathryn Sobocinski, Janet Duffy-Anderson, Yvette Spitz, Stanley Gregory, Douglas Draper, and two external reviewers for helpful comments on this manuscript.

Funding

This research was supported by grants from the North Pacific Research Board (Projects 905 and 1205).

References

Able, K. W., and Fodrie, F. J. (2014). Distribution and dynamics of habitat use by juvenile and adult flatfishes. Flatfishes: Biology and Exploitation 242–282.

Abookire, A. A., and Bailey, K. M. (2007). The distribution of life cycle stages of two deep-water pleuronectids, Dover sole (*Microstomus pacificus*) and rex sole (*Glyptocephalus zachirus*), at the northern extent of their range in the Gulf of Alaska. Journal of Sea Research 57, 198–208.

Alton, M. S., Bakkala, R. G., Walters, G. E., and Munro, P. T. 1988. Greenland turbot *Reinhardtius hippoglossoides* of the East Bering Sea and the Aleutian Islands Region. NOAA Technical Report NMFS 71, Seattle, WA: U.S. Department of Commerce, 31 p.

Barbeaux, S. J., Ianelli, J., Nichols, D., and Hoff, J. 2013. Assessment of Greenland Turbot (*Reinhardtius hippoglossoides*) in the Bering Sea and Aleutian Islands. In: Stock Assessment and Fishery Evaluation Document for Groundfish Resources in the Bering Sea /Aleutian Islands Region. Section 5. Anchorage: North Pacific Fishery Management Council.

Bartolino, V., Ciannelli, L., Bacheler, N. M., and Chan, K. S. (2011). Ontogenetic and sex-specific differences in density-dependent habitat selection of a marine fish population. Ecology 92, 189–200.

Bartolino, V., Ciannelli, L., Spencer, P., Wilderbuer, T. K., and Chan, K. S. (2012). Scale-dependent detection of the effects of harvesting a marine fish population. Marine Ecology Progress Series 444, 251–261.

Bulatov, O. A. (1983). Distribution of eggs and larvae of Greenland halibut, *Reinhardtius hippoglossoides* (Pleuronectidae) in the eastern Bering Sea. Journal of Ichthyology 23, 157–159.

Ciannelli, L., Bailey, K. M., Chan, K. S., and Stenseth, N. C. (2007). Phenological and geographical patterns of walleye pollock (*Theragra chalcogramma*) spawning in the western Gulf of Alaska. Canadian Journal of Fisheries and Aquatic Sciences 64, 713–722.

Ciannelli, L., Bailey, K., and Olsen, E. M. (2015). Evolutionary and ecological constraints of fish spawning habitats. ICES Journal of Marine Science: ~~Journal Du Conseil~~ 72, 285–296.

Duffy-Anderson, J. T., Blood, D. M., Cheng, W., Ciannelli, L., Matarese, A. C., Sohn, D., Vance, T. C., and Vestfals, C. (2013). Combining field observations and modeling approaches to examine Greenland halibut (*Reinhardtius hippoglossoides*) early life ecology in the southeastern Bering Sea. Journal of Sea Research 75, 96–109.

Dulvy, N. K., Rogers, S. I., Jennings, S., Stelzenmüller, V., Dye, S. R., and Skjoldal, H. R. (2008). Climate change and deepening of the North Sea fish assemblage: a biotic indicator of warming seas. Journal of Applied Ecology 45, 1029–1039.

Engelhard, G. H., Pinnegar, J. K., Kell, L. T., and Rijnsdorp, A. D. (2011b). Nine decades of North Sea sole and plaice distribution. ICES Journal of Marine Science: ~~Journal Du Conseil 68~~, 1090–1104.

Erisman, B. E., Allen, L. G., Claisse, J. T., Pondella, D. J., Miller, E. F., and Murray, J. H. (2011). The illusion of plenty: hyperstability masks collapses in two recreational fisheries that target fish spawning aggregations. Canadian Journal of Fisheries and Aquatic Sciences 68, 1705–1716.

ESRI. 2014. ArcGIS Desktop: Release 10.2. Redlands, CA: Environmental Systems Research Institute.

Fincham, J. I., Rijnsdorp, A. D., and Engelhard, G. H. (2013). Shifts in the timing of spawning in sole linked to warming sea temperatures. Journal of Sea Research 75, 69–76.

Gibson, R. N. (1994). Impact of habitat quality and quantity on the recruitment of juvenile flatfishes. Netherlands Journal of Sea Research 32, 191–206.

Gibson, R. N. (1997). Behaviour and the distribution of flatfishes. Journal of Sea Research 37, 241–256.

Grebmeier, J. M., Overland, J. E., Moore, S. E., Farley, E. V., Carmack, E. C., Cooper, L. W., Frey, K. E., Helle, J. H., McLaughlin, F. A., and McNutt, S. L. (2006). A major ecosystem shift in the northern Bering Sea. Science 311, 1461–1464.

Harden-Jones, F. R. 1968. Fish Migration. London: Edward Arnold.

Haynie, A. C., and Pfeiffer, L. (2013). Climatic and economic drivers of the Bering Sea walleye pollock (*Theragra chalcogramma*) fishery: implications for the future. Canadian Journal of Fisheries and Aquatic Sciences 70, 841–853.

Haynie, A. C., Pfeiffer, L., and Watson, J. 2014. Spatial Economic Models of Pollock and Cod. NPRB BSIERP Project B72 Final Report, 128 pp.

Hilborn, R., and Walters, C. J. 1992. In: Quantitative Fisheries Stock Assessment: choice, dynamics and uncertainty. Chapman and Hall, New York.

Hoff, G. R. 2013. Results of the 2012 eastern Bering Sea upper continental slope survey of groundfish and invertebrate resources. U.S. Department of Commerce, NOAA Technical Memorandum. NMFS-AFSC-258, 268 p.

Hollowed, A. B., Barbeaux, S. J., Cokelet, E. D., Farley, E., Kotwicki, S., Ressler, P. H., Spital, C., and Wilson, C. D. (2012). Effects of climate variations on pelagic ocean habitats and their role in structuring forage fish distributions in the Bering Sea. Deep Sea Research Part II: Topical Studies in Oceanography 65, 230–250.

IPCC. 2007. Climate Change 2007: The Physical Science Basis. Intergovernmental Panel on Climate Change, Geneva, Switzerland.

IPCC. 2014. Climate Change 2014: Impacts, Adaptation, and Vulnerability. Part A: Global and Sectoral Aspects. Contribution of Working Group II to the Fifth Assessment Report of the Intergovernmental Panel on Climate Change [Field, C. B., Barros, V. R., Dokken, D. J., Mach, K. J., Mastrandrea, M. D., Bilir, T. E., Chatterjee, M., Ebi, K. L., Estrada, Y. O., Genova, R. C., Girma, B., Kissel, E. S., Levy, A. N., MacCracken, S., Mastrandrea, P. R., and White, L. L. (eds.)]. Cambridge University Press, Cambridge, United Kingdom and New York, NY, USA, 1132 pp.

International Pacific Halibut Commission. 1987. The Pacific Halibut: Biology, Fishery & Management. International Pacific Halibut Commission Technical Report 22: 59 p.

Keller, A. A., Ciannelli, L., Wakefield, W. W., Simon, V., Barth, J. A., and Pierce, S. D. (2015). Occurrence of demersal fishes in relation to near-bottom oxygen levels within the California Current large marine ecosystem. Fisheries Oceanography 24, 162–176.

Kinder, T. H., Coachman, L. K., and Galt, J. A. (1975). The Bering Slope Current System. Journal of Physical Oceanography 5, 231–244.

Kotwicki, S., and Lauth, R. R. (2013). Detecting temporal trends and environmentally-driven changes in the spatial distribution of bottom fishes and crabs on the eastern Bering Sea shelf. Deep Sea Research Part II: Topical Studies in Oceanography 94, 231–243.

Loher, T. (2008). Investigating variability in catch rates of halibut (*Hippoglossus stenolepis*) in the Pribilof Islands: is temperature important? Deep-Sea Research II, Topical Studies in Oceanography 55, 1801–1808.

Loher, T. (2011). Analysis of match-mismatch between commercial fishing periods and spawning ecology of Pacific halibut (*Hippoglossus stenolepis*), based on winter surveys and behavioural data from electronic tags. ICES Journal of Marine Science 68, 2240–2251.

Loher, T., and Blood, C. A. (2009). Seasonal dispersion of Pacific halibut (*Hippoglossus stenolepis*) summering off British Columbia and the US Pacific Northwest evaluated via satellite archival tagging. Canadian Journal of Fisheries and Aquatic Sciences 66, 1409–1422.

Loher, T., and Seitz, A. (2006). Seasonal migration and environmental conditions of Pacific halibut *Hippoglossus stenolepis*, elucidated from pop-up archival transmitting (PAT) tags. Marine Ecology Progress Series 317, 259–271.

Loher, T., and Seitz, A. C. (2008). Characterization of active spawning season and depth for eastern Pacific halibut (*Hippoglossus stenolepis*), and evidence of probable skipped spawning. Journal of Northwest Atlantic Fishery Science 41, 23–36.

Maunder, M. N., Sibert, J. R., Fonteneau, A., Hampton, J., Kleiber, P., and Harley, S. J. (2006). Interpreting catch per unit effort data to assess the status of individual stocks and communities. ICES Journal of Marine Science: Journal Du Conseil 63, 1373–1385.

McConnaughey, R. A., and Smith, K. R. (2000). Associations between flatfish abundance and surficial sediments in the eastern Bering Sea. Canadian Journal of Fisheries and Aquatic Sciences 57, 2410–2419.

Mueter, F. J., and Litzow, M. A. (2008). Sea ice retreat alters the biogeography of the Bering Sea continental shelf. Ecological Applications 18, 309–320.

Mueter, F. J., and Norcross, B. L. (1999). Linking community structure of small demersal fishes around Kodiak Island, Alaska, to environmental variables. Marine Ecology Progress Series 190, 37–51.

Munday, P. L., Dixson, D. L., Donelson, J. M., Jones, G. P., Pratchett, M. S., Devitsina, G. V., and Døving, K. B. (2009). Ocean acidification impairs olfactory discrimination and homing ability of a marine fish. Proceedings of the National Academy of Sciences 106, 1848–1852.

Musienko, L. N. 1970. Razmnozheine I razvitie ryb Beringova moray (Reproduction and development of Bering Sea fishes). Tr. Vses. Nauchno-issled. Inst. Morsk. Rybn. Koz. Okeanogr. In: Moiseev, P. A. (Ed.), Soviet Fisheries Investigations in the North Eastern Pacific, Pt. 5, vol. 70, pp. 161–224 (Avail. Natl. Tech. Info. Serv., Springfield, VA as TT74-50127).

North Pacific Fisheries Management Council. 2006. Amendment 80 – Council Motion. http://www.npfmc.org/wp-content/PDFdocuments/catch_shares/AM80/Am80motion_406.pdf

Peck, M. A., Buckley, L. J., and Bengtson, D. A. (2006). Effects of temperature and body size on the swimming speed of larval and juvenile Atlantic cod (*Gadus morhua*): implications for individual-based modelling. Environmental Biology of Fishes 75, 419–429.

Perry, A. L., Low, P. J., Ellis, J. R., and Reynolds, J. D. (2005). Climate change and distribution shifts in marine fishes. Science 308, 1912–1915.

Petitgas, P., Rijnsdorp, A. D., Dickey-Collas, M., Engelhard, G. H., Peck, M. A., Pinnegar, J. K., Drinkwater, K., Huret, and M Nash, R. D. (2013). Impacts of climate change on the complex life cycles of fish. Fisheries Oceanography 22, 121–139.

Rijnsdorp, A. D., Peck, M. A., Engelhard, G. H., Möllmann, C., and Pinnegar, J. K. (2009). Resolving the effect of climate change on fish populations. ICES Journal of Marine Science: Journal Du Conseil 66, 1572–1583.

Rose, G. A. (2005). On distributional responses of North Atlantic fish to climate change. ICES Journal of Marine Science: Journal Du Conseil 62, 1360–1374.

Ryer, C. H., Stoner, A. W., and Titgen, R. H. (2004). Behavioral mechanisms underlying the refuge value of benthic habitat structure for two flatfishes with differing anti-predator strategies. Marine Ecology Progress Series 268, 231–243.

Sadorus, L. L., Mantua, N. J., Essington, T., Hickey, B., and Hare, S. (2014). Distribution patterns of Pacific halibut (*Hippoglossus stenolepis*) in relation to environmental variables along the continental shelf waters of the US West Coast and southern British Columbia. Fisheries Oceanography 23, 225–241.

Seitz, A. C., Loher, T., and Nielsen, J. L. 2007. Seasonal movements and environmental conditions experienced by Pacific halibut in the Bering Sea, examined by pop-up satellite tags. International Pacific Halibut Commission Scientific Report No. 84, 24 pp.

Seitz, A. C., Loher, T., Norcross, B. L., and Nielsen, J. L. (2011). Dispersal and behavior of Pacific halibut *Hippoglossus stenolepis* in the Bering Sea and Aleutian Islands region. Aquatic Biology 12, 225–239.

Sims, D. W., Wearmouth, V. J., Genner, M. J., Southward, A. J., and Hawkins, S. J. (2004). Low-temperature-driven early spawning migration of a temperate marine fish. Journal of Animal Ecology 73, 333–341.

Sinclair, M. 1988. Marine Populations: an Essay on Population Regulation and Speciation. University of Washington Press, Seattle.

Sohn, D., Ciannelli, L., and Duffy-Anderson, J. T. (2010). Distribution and drift pathways of Greenland halibut (*Reinhardtius hippoglossoides*) during early life stages in the eastern Bering Sea and Aleutian Islands. Fisheries Oceanography 19, 339–353.

Sohn, D., Ciannelli, L., and Duffy-Anderson, J. T. In press. Distribution of early life Pacific halibut and comparison with Greenland halibut in the eastern Bering Sea. Journal of Sea Research 107, 31–42

Spencer, P. D. (2008). Density-independent and density-dependent factors affecting temporal changes in spatial distributions of eastern Bering Sea flatfish. Fisheries Oceanography 17, 396–410.

Spencer, P. D., Walters, G. E., and Wilderbuer, T. K. 2004. Flathead sole. In Stock Assessment and Fishery Evaluation Document for Groundfish Resources in the Bering Sea/Aleutian Islands Region

as Projected for 2005, p. 515-616. North Pacific Fishery Management Council, P.O. Box 103136, Anchorage, Alaska 99510.

St-Pierre, G. 1984. Spawning Locations and Season for Pacific Halibut. International Pacific Halibut Commission Scientific Report No. 70, 46 pp.

Stabeno, P. J., Kachel, N. B., Moore, S. E., Napp, J. M., Sigler, M., Yamaguchi, A., and Zerbini, A. N. (2012). Comparison of warm and cold years on the southeastern Bering Sea shelf and some implications for the ecosystem. Deep Sea Research Part II: Topical Studies in Oceanography 65, 31–45.

Stauffer, G. 2004. NOAA protocols for groundfish bottom trawl surveys of the nation's fishery resources. U.S. Department of Commerce, NOAA, Technical Memorandum NMFS-SPO-65. http://www.afsc.noaa.gov/RACE/gearsupport/tmspo65.pdf

Stoner, A. W., Ottmar, M. L., and Hurst, T. P. (2006). Temperature affects activity and feeding motivation in Pacific halibut: implications for bait-dependent fishing. Fisheries Research 81, 202–209.

Stoner, A. W., and Titgen, R. H. (2003). Biological structures and bottom type influence habitat choices made by Alaska flatfishes. Journal of Experimental Marine Biology and Ecology 292, 43–59.

Teal, R., de Leeuw, J. J., van der Veer, H. W., and Rijnsdorp, A. D. (2008). Effects of climate change on growth of 0-group sole and plaice. Marine Ecology Progress Series 358, 219–230.

van der Veer, H. W., Koot, J., Aarts, G., Dekker, R., Diderich, W., Freitas, V., and Witte, J. I. (2011). Long-term trends in juvenile flatfish indicate a dramatic reduction in nursery function of the Balgzand intertidal, Dutch Wadden Sea. Marine Ecology Progress Series 434, 143–154.

Van Hal, R., van Kooten, T., and Rijnsdorp, A. D. (2016). Temperature-induced changes in size dependent distributions of two boreal and three Lusitanian flatfish species: a comparative study. Journal of Sea Research 107, 14–22.

Vestfals, C. D., Ciannelli, L., Duffy-Anderson, J. T., and Ladd, C. (2014). Effects of seasonal and interannual variability of along-shelf and cross-shelf transport on groundfish recruitment in the eastern Bering Sea. Deep-Sea Research Part II: Topical Studies in Oceanography 109, 190–203.

Wilderbuer, T. K., and Nichol, D. 2002. Chapter 3: Yellowfin sole. In Stock Assessment and Fishery Evaluation Document for Groundfish Resources in the Bering Sea/Aleutian Islands Region, p. 522-592. North Pacific Fishery Management Council, P.O. Box 103136, Anchorage, Alaska 99510.

Wilderbuer, T. K., Nichol, D., and Ianelli, J. 2008. Chapter 4: Yellowfin sole. In Stock Assessment and Fishery Evaluation Document for Groundfish Resources in the Bering Sea/Aleutian Islands Region, p. 207-254. North Pacific Fishery Management Council, P.O. Box 103136, Anchorage, Alaska 99510.

Wood, S. N. (2003). Thin plate regression splines. Journal of the Royal Statistical Society B 65, 95–114.

Wood, S. N. (2004). Stable and efficient multiple smoothing parameter estimation for generalized additive models. Journal of the American Statistical Association 99, 637–686.

Wood, S. N. 2006. Generalized additive models: an introduction with R. Chapman and Hall/CRC, Boca Raton, FL.

Youcef, W. A., Lambert, Y., and Audet, C. (2013). Spatial distribution of Greenland halibut *Reinhardtius hippoglossoides* in relation to abundance and hypoxia in the estuary and Gulf of St. Lawrence. Fisheries Oceanography 22, 41–60.

ICES Journal of Marine Science

ICES Journal of Marine Science (2016), 73(7), 1890–1900. doi:10.1093/icesjms/fsw004

Contribution to the Themed Section: '*Seascape Ecology*'

Original Article

Modelled connectivity between Walleye Pollock (*Gadus chalcogrammus*) spawning and age-0 nursery areas in warm and cold years with implications for juvenile survival

Colleen M. Petrik[1†*], Janet T. Duffy-Anderson[2], Frederic Castruccio[3§], Enrique N. Curchitser[3], Seth L. Danielson[4], Katherine Hedstrom[5], and Franz Mueter[1]

[1]*School of Fisheries and Ocean Sciences, University of Alaska Fairbanks, 17101 Point Lena Loop Rd., Juneau, AK 99801, USA*
[2]*Alaska Fisheries Science Center, National Oceanographic and Atmospheric Administration, 7600 Sand Point Way NE, Seattle, WA 98115, USA*
[3]*Department of Environmental Sciences, Rutgers University, 14 College Farm Road, New Brunswick, NJ 08901, USA*
[4]*Institute of Marine Science, University of Alaska Fairbanks, 112 O'Neill Building, PO Box 757220, Fairbanks, AK 99775, USA*
[5]*University of Alaska Fairbanks, Arctic Region Supercomputing Center, 105 West Ridge Research Building, PO Box 756020, Fairbanks, AK 99775, USA*

**Corresponding author: e-mail: cpetrik@princeton.edu*
[‡]*Present address: Atmospheric and Oceanic Sciences, Princeton University, 300 Forrestal Rd., Princeton, NJ 08540, USA.*
[§]*Present address: National Center for Atmospheric Research, Climate and Global Dynamics Division, P.O. Box 3000, Boulder, CO 80307, USA.*

Petrik, C. M., Duffy-Anderson, J. T., Castruccio, F., Curchitser, E. N., Danielson, S. L., Hedstrom, K., and Mueter, F. Modelled connectivity between Walleye Pollock (*Gadus chalcogrammus*) spawning and age-0 nursery areas in warm and cold years with implications for juvenile survival. – ICES Journal of Marine Science, 73: 1890–1900.

Received 8 June 2015; revised 4 January 2016; accepted 9 January 2016.

Adult and early life stage distributions of the commercially important demersal fish Walleye Pollock (*Gadus chalcogrammus*) have varied in relation to the warm and cold environmental conditions on the eastern Bering Sea (EBS) shelf. Previous modelling studies indicate that transport alone does not account for the disparate juvenile distributions in warm and cold years, but that spawning locations are important. Our objective was to determine the potential connectivity of EBS pollock spawning areas with juvenile nursery areas between warm and cold years from an 18-year hindcast (1995–2012). We calculated the connectivity between larval sources and juvenile positions that were produced by a coupled biological-physical individual-based model that simulated transport, growth, and vertical behavior of pollock from the egg until the juvenile stage. Three connectivity patterns were seen in most simulations: along-isobaths to the northwest, self-retention, and transport around the Pribilof Islands. The major differences in connectivity between warm and cold years, more northwards in warm years and more off-shelf in cold years, mimicked wind-driven flow characteristics of those years that were related to winter mean zonal position of the Aleutian Low. Connectivity relationships were more sensitive to spatial alterations in the spawning areas in cold years, while they were more responsive to spawn timing shifts in warm years. The strongest connectivity to advantageous juvenile habitats originated in the well-known spawning areas, but also in a less well-studied region on the Outer Shelf. This northern Outer Shelf region emerged as a very large sink of pollock reaching the juvenile transition from all spawning sources, suggesting more thorough sampling across multiple trophic levels of this potentially important juvenile pollock nursery is needed.

Keywords: Bering Sea, connectivity, fish early life history, pollock.

Introduction

One of the most commercially important semi-demersal fishes in the eastern Bering Sea (EBS) is Walleye Pollock (*Gadus chalcogrammus*), hereafter referred to as "pollock." Over the EBS shelf, pollock spawn consistently at at least two spawning sites, one north of Unimak Island (Figure 1, region 1), and the other near the Pribilof Islands (Figure 1, region 5), beginning near Unimak and spreading towards the Pribilof Islands (Bacheler *et al.*, 2010). Eggs

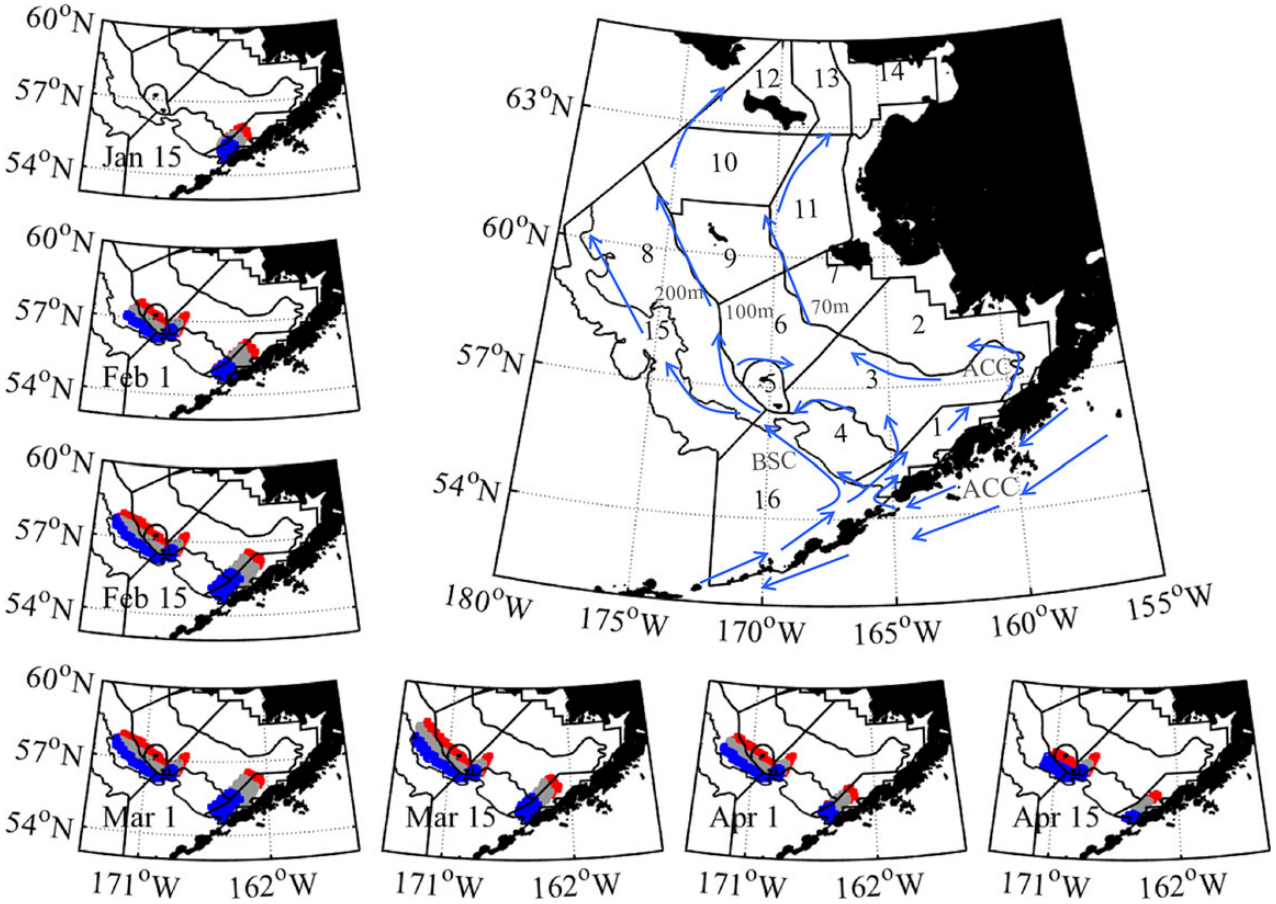

Figure 1. (Large panel) Map of the Eastern Bering Sea with bathymetry (50, 100, and 200-m isobaths) and major currents shown in blue and the BEST-BSIERP regions in black. ACC, Alaska Coastal Current; BSC, Bering Slope Current. 1: AK Peninsula, 2: South Inner Shelf, 3: South Middle Shelf, 4: South Outer Shelf, 5: Pribilofs, 6: Midnorth Middle Shelf, 7: Midnorth Inner Shelf, 8: North Outer Shelf, 9: St Matthews, 10: North Middle Shelf, 11: North Inner Shelf, 12: St Lawrence, 13: South Bering Strait, 14: Norton Sound, 15: Off-shelf North, 16: Off-shelf Southeast. (Small subpanels) Spawning initial locations released on the dates shown. Blue: contracted simulation, grey: base, late, early simulations, red: expanded simulation. Polygons are overlapping and all share the same western and southern boundaries.

are found in the water column from December to August, but the annual peak occurs in either April or May (Bacheler *et al.*, 2010). Eggs are predominantly found within the mixed layer (Smart *et al.*, 2013) and incubation time depends on temperature (Blood, 2002). After hatching, larvae develop through a series of stages known as the yolksac, preflexion, and postflexion (or late), classified by anatomical differences (Matarese *et al.*, 1989). Pollock transition from larvae to pelagic juveniles between 30 and 40 mm (Matarese *et al.*, 1989), become more bottom-oriented with age (Brodeur and Wilson, 1996; Duffy-Anderson *et al.*, 2015), and finally recruit to the fishery at age-3 or age-4 (Ianelli *et al.*, 2012b).

The EBS (Figure 1) is a very productive region, supporting large marine bird and mammal populations and several commercial fisheries. Recently the EBS experienced alternating stanzas of temperatures that were either warmer (2001–2005) or colder (2007–2012) than average (Stabeno *et al.*, 2012). In cold years, winter ice extends farther offshore creating a larger cold pool that could influence the spawning and movements of demersal fishes (Mueter and Litzow, 2008). The water circulation is also influenced by atmospheric and hydrographic conditions, which affect the dispersal of pelagic early life stages. For example, the predominantly northwesterly winds in cold years that extend sea ice and the cold pool also promote off-shelf Ekman transport (Danielson *et al.*, 2011b, 2012; Stabeno *et al.*, 2012). On the other hand, the more southeasterly winds in warm years resulted in northward or weak on-shelf flows over the Middle Shelf (50–100 m bottom depth; Danielson *et al.*, 2012; Stabeno *et al.*, 2012). Moreover, the intensity and timing of setup of the Inner and Middle Fronts, which separate the inner (0–50 m), middle (50–100 m), and outer (100–200 m) shelves, varies with temperature, also potentially affecting the transport of larval fishes on the shelf. Concomitant with the atmospheric and oceanographic differences, the distributions of early life stages diverged in cold and warm years (Smart *et al.*, 2012), likely due to thermally mediated variability in spawning locations of adults (Petrik *et al.*, 2015).

Early life stage transport contributes greatly to population connectivity and persistence. Studies of connectivity between spawning regions and nursery habitats advance our understanding of genetic exchange, processes during the early life period, and recruitment (reviewed in Cowen and Sponaugle, 2009). Alternate transport pathways between spawning grounds and nursery areas can influence early life survival because of spatial differences in growth and mortality (Cowen and Sponaugle, 2009). Survival to recruitment of individuals is further influenced by the distribution of individuals

at the end of the larval period in regard to spatial differences in prey and predators. For example, the overlap between juvenile and cannibalistic adult pollock explains 30–50% of interannual recruitment variability (Mueter *et al.*, 2011). Additionally, match–mismatch between the spatial distribution of juvenile pollock and prey energy density may explain the low and high year classes of 2005 and 2010, respectively (Siddon *et al.*, 2013). Thus, it is important to identify the source regions and oceanographic conditions influencing the cold and warm year patterns of juvenile pollock distribution and survival.

Modelling results suggested that spawning locations and their proximity to different physical oceanographic features drove differences in the distributions of pollock early life stages (Petrik *et al.*, 2015). Following these results, it was our primary objective to determine the potential connectivity between spawning and nursery regions of walleye pollock in the EBS (1995–2012). Our second objective was to resolve how potential connectivity diverged in warm and cold years. This examination provides a projection of the prospective effects of predicted future warming (Wang *et al.*, 2012). To accomplish these objectives we used an individual-based model (IBM) of pollock biology and behavior coupled to a hydrodynamics model of the EBS to simulate transport during the period from spawning to the juvenile transition. Model output was compared with observed distributions of juvenile pollock (1996–2012) to ground-truth model results.

Methods

Study area

The EBS has been divided into regions for reference and comparisons across projects under the Bering Ecosystem Study—Bering Sea Integrated Ecosystem Research Program (BEST-BSIERP). These 16 regions (Figure 1) cover the EBS shelf and slope within the US Exclusive Economic Zone and were delineated by bathymetry, oceanography, animal distributions, ecological domains, and established survey areas (Ortiz *et al.*, 2012). Baker and Hollowed (2014) found that distinct biological communities in the EBS are best delineated by depth, bottom temperature, frontal boundaries, and position north or south of 60°N; these ecoregions are well represented by the BEST-BSIERP regions.

Coupled IBM

A full description of the coupled physical–biological IBM can be found in Petrik *et al.* (2015) and certain details in Supplementary data, Materials Section. To summarize, we used the Regional Ocean Modelling System (ROMS; Shchepetkin and McWilliams, 2009) developed for the Northeast Pacific (NEP6) to represent the hydrodynamics of the EBS. ROMS is a free-surface, hydrostatic primitive equation ocean circulation model. It is a terrain-following, finite volume (Arakawa C-grid) model. The ROMS NEP6 model domain extends over a broader region than the EBS Shelf, from 20°N to 71°N and reaching ~2250 km offshore from the North American west coast. The spatial resolution is a 10 km horizontal grid in a Lambert Conical projection that is rotated relative to lines of constant longitude and has 50 terrain-following depth levels stretched towards the surface boundary in each grid cell. ROMS includes a fully parallel coupled sea-ice model (Budgell, 2005). An older version of ROMS for the Northeast Pacific has been thoroughly validated against observations and had significant skill reproducing aspects of the Bering Sea physical oceanography, such as the horizontal and vertical structure of tidal currents and the frequency of kinetic energy (Curchitser *et al.*, 2010; Danielson *et al.*, 2011a). The NEP6 has further improved upon this model through more comprehensive evaluations with the newly available data collected under the BEST-BSIERP programme, which had much more complete spatial and temporal coverage than earlier datasets. Time of maximum sea-ice cover, south-to-north progression of ice retreat, ice-free years at moorings, and the relationship between ice retreat and spring bloom timing produced by NEP6 are all quantitatively similar to observations (Cheng *et al.*, 2015). The NEP6 coupled ocean-sea-ice model was integrated in hindcast mode for the period from 1994 to 2012 deriving surface forcing from the Modern Era Retrospective-Analysis for Research and Applications (Rienecker *et al.*, 2011), air-sea fluxes computed using bulk formulae (Large and Yeager, 2009), the Dai and Trenberth (2002) method as a surface freshwater flux for the riverine inputs, initial and boundary conditions for this domain from the Simple Ocean Data Assimilation ocean reanalysis (Carton and Giese, 2008) for early years, and boundary conditions from the global Hybrid Coordinate Ocean Model assimilative product (Metzger *et al.*, 2014) for the later ones. Daily averages of velocity, temperature, and mixed layer depth were saved and used as offline inputs to the particle-tracking model.

We utilized the particle-tracking tool TRACMASS to simulate transport of pollock early life stages. TRACMASS computes Lagrangian trajectories from Eulerian velocity fields from general circulation model simulations through an offline coupling. TRACMASS interpolates any general circulation model three-dimensional grid to its own grid and solves the trajectory path through each grid cell with an analytical solution of a differential equation, which depends on the velocities at the grid cell walls (Döös, 1995; Blanke and Raynaud, 1997; de Vries and Döös, 2001). The particle-tracking time step was 1 h and the TRACMASS turbulence subroutine was implemented to incorporate sub-grid scale motion. Physiological and behavioural information was added to TRACMASS to create an IBM of EBS pollock (Petrik *et al.*, 2015). Individuals transitioned from eggs to yolksac larvae, preflexion larvae, and late larvae, ultimately reaching the beginning of the juvenile stage. Stages were defined by length (yolksac: <6 mm SL; preflexion: 6–10 mm SL; late: 10–40 mm SL) that was attained via stage-specific temperature-dependent growth (SM; Petrik *et al.*, 2015). The non-feeding eggs and yolksac larvae were modelled as neutrally buoyant, while the feeding stages, preflexion and late larvae, directed their vertical swimming towards the centre of the mixed layer (SM; Petrik *et al.*, 2015).

Model initialization and simulations

The model simulated spawning by initializing individuals at the egg stage. Spawning locations and times were the same as those used in Petrik *et al.* (2015). The locations concentrated on the major spawning regions identified by Hinckley (1987) and Bacheler *et al.* (2010), with time-specific individual spawning polygons (Figure 1) created from aggregated locations of mature spawning females from observer data (Duffy-Anderson *et al.*, 2015). The Bogoslof Island region, defined by bottom depth >250 m, was disregarded as a spawning ground as this likely represents a distinct population (Ianelli *et al.*, 2012a). Following the literature and the observer data, spawning started in mid-Jan near Unimak Island, then around the Pribilof Islands in February. Spawning expanded to the northwest as the season progressed, peaking in mid-March, then contracting into April. The result was seven different spawning times (15 January, 1 February, 15 February, 1 March, 15 March, 1 April, 15 April) with spawning areas of varying sizes. Eggs were released at these

times at the centre of each ROMS NEP6 grid cell within the spawning polygons. Eggs were distributed uniformly with depth because specific information on spawning depth is lacking and eggs are found at all depths (0–200 m) in the EBS (Duffy-Anderson *et al.*, 2015). Ten eggs were released per 10 m depth increment in each spawning grid cell, except in the "Contracted" simulation (see description below). Because spawning occurred in fewer grid cells compared with the other cases, 15 eggs per 10 m depth were spawned to achieve the total number of particles needed for stable results (SM; Petrik *et al.*, 2015).

Five distinct simulations were run (SM; Petrik *et al.*, 2015) to test the effects of advection, spawning location, and spawn timing on connectivity. In the "Transport Only" case, all years 1995–2012 shared the same initial spawning areas and times and differed only by their physical environments simulated with ROMS NEP6. This was considered the "Base" simulation and was divided into "Base Cold" (1995, 1997, 1999, 2000, and 2006–2012) and "Base Warm" (1996, 2002, 2003, and 2005) years using the temperature anomaly criteria of Smart *et al.* (2012). To simulate hypothesized changes in spawning locations in reference to the cold pool extent, spawning polygons were contracted off-shelf to the southwest in cold years ("Contracted") and expanded on-shelf to the northeast in warm years ("Expanded"). These scenarios were based on a statistical model that estimated adult pollock presence in areas with sea surface temperatures (SSTs) <2.4 and $>3.8^{\circ}$C (Barbeaux, 2012), field observations that demonstrated longitudinal displacements of walleye pollock early life stages over the continental shelf between warm and cold years (Smart *et al.*, 2012), numerical modelling that identified cold pool-dependent spatial shifts in adult spawning distributions as the underlying mechanism of change (Petrik *et al.*, 2015), and walleye pollock roe fishery data that corroborate model results (Duffy-Anderson *et al.*, 2015). Finally, to represent potential shifts in peak spawn timing, spawning times were delayed 40 d in cold years ("Late") and advanced 40 d in warm years ("Early") in concordance with the average difference between cold and warm years in the day of the year of peak egg abundance from generalized additive models estimated from observations (Smart *et al.*, 2012). In each simulation, individuals were followed from spawn until they reached 40 mm, the size at the juvenile transition (Matarese *et al.*, 1989).

Observational data

Net tow surveys

A time series of age-0 pollock juvenile abundances from midsummer collections (1996–2005, 2007) was available from cooperative cruises conducted by the Alaska Fisheries Science Center's (AFSC) Eco-FOCI programme and the Graduate School of Fisheries, Hokkaido University, Japan aboard the T/S *Oshoro Maru* (Busby *et al.*, 2014). Sampling occurred at a grid of stations over the Middle and Outer Shelves, though not all stations were sampled each year. Cumulative over the time series, sampled stations resided within a minimum of two BEST-BSIERP regions (regions 3 and 4) and a maximum of seven BEST-BSIERP regions (1–7). A modified bottom trawl with 5-m^2 mouth opening fitted with a 3×2 mm oval mesh net and a 1-mm mesh codend was towed obliquely through the water column from 200 m depth (or 10 m off-bottom, whichever was shallowest) to the surface. Use of a flowmeter permitted quantitative estimates of catch. Samples were preserved in formalin, taxa were sorted, identified, and enumerated, and pollock catch was expressed as catch 10 m^{-2} sea surface area.

Acoustic surveys

Acoustic backscatter measurements were conducted in conjunction with the Bering Arctic-Subarctic Integrated Survey aboard the NOAA Ship *Oscar Dyson* to determine subsurface age-0 pollock biomass. The surveys spanned 2008 through 2013 and were typically performed mid-August through late September. Measurements were collected with Simrad EK60 echosounders from five split-beam tranducers (18, 38, 70, 120, and 200 kHz) mounted on the bottom of the vessel's retractable centerboard. Data presented herein are the results from 38 kHz-collected data. Verification of midwater and near-bottom acoustic sign was accomplished through targeted trawl sampling conducted opportunistically during daylight hours. Age-0 pollock abundance was estimated by combining echo integration data with species and size-composition information derived from targeted trawl sampling. Post-processing was conducted in accordance with other AFSC surveys (Honkalehto *et al.*, 2011). Comprehensive descriptions of acoustic methodologies are presented in Parker-Stetter *et al.* (2013) and De Robertis *et al.* (2014).

Analyses

Spawning release locations and positions of individuals upon reaching the juvenile transition were both mapped to the BEST-BSIERP regions (Figure 1). Connectivity from spawning region "A" to juvenile region "B" for a given time was defined as the number of individuals released in region "A" that were in region "B" at the time they reached juvenile size divided by the total individuals spawned in "A" at that time. As connectivity is defined as a fraction of the total number of eggs spawned in that region, it is independent of the number of eggs spawned. Connectivity for each spawning region-juvenile region pair was calculated by spawning time, year, and grouped cold or warm years. Connectivity is presented with connectivity matrices, grids with source regions on one axis and sink regions on the other axis that indicate the strength of the connection from source to sink as the value at their intersection. Retention was defined as the special case of connectivity from a region to itself.

Connectivity was analysed in many ways. Connectivity of each pair was classified as strong ($>$75th quartile), moderate (median–75th quartile), or weak ($<$median) to facilitate comparisons. The effect of region size on mean distance travelled from each region and mean distance travelled within a region was determined by a regression analysis (SM). Additionally, cross-shelf transport was evaluated by calculating the longitudinal difference between spawn and juvenile locations and binning results as $>10^{\circ}$W, 5–10°W, $<5^{\circ}$W, $<5^{\circ}$E, 5–10°E, or $>10^{\circ}$E.

Eastward transport was correlated with different climate indices including the mean winter cross-shelf wind velocity, the mean winter alongshelf wind velocity, the May SST anomaly, and the North Pacific Index in winter (NPIw). Correlations with wind velocities were used to test the effect of Ekman transport on eastward movement from spawning regions to juvenile regions. The mean winter cross- and alongshelf wind velocity anomalies represent October–April at the NARR (NARR website) grid point of 60°N, 169.94°W (BEST-BSIERP region 9). Wind velocity anomalies were NE+/SW- for cross-shelf velocities and NW+/SE- for alongshelf velocities (Danielson unpublished data). Seasonal stratification strengthens fronts and inhibits cross-shelf movement (Kachel *et al.*, 2002; Gibson *et al.*, 2013). Its effect on eastward transport was represented by using May SST as a proxy. The May SST index was calculated as mean monthly SST averaged over the area 54.3°N–60.0°N, 161.2°W–172.5°W using the NCEP/NCAR Reanalysis project data (Kalnay *et al.*, 1996). The index values are

deviations from the mean value normalized by the standard deviation for the period 1961–2000 (Kalnay *et al.*, 1996). The North Pacific Index (NPI) is the area-weighted sea level pressure over the region 30°N–65°N, 160°E–140°W that measures the intensity of the Aleutian Low (AL) (Trenberth and Hurrell, 1994). A positive NPI corresponds to a weak AL, while a negative NPI indicates a strong AL, although it does not differentiate between variations in AL zonal displacements. The winter index is the average NPI from November–March and the anomalies were normalized by the mean and standard deviation for 1961–2000 (Trenberth and Hurrell, 1994). The NPI data were provided by the Climate Analysis Section, NCAR, Boulder, USA. The AL is a dominant climate feature of the EBS that represents the distribution and intensity of winter storms. Its position and intensity can influence heat flux, surface winds, advection, mixing, sea-ice production and distribution, and timing of the spring phytoplankton bloom (Vestfals *et al.*, 2013). Correlations with this climate index examined larger scale wind and temperature associations with eastward movement from spawning areas to juvenile areas.

Comparisons between modelled distributions of individuals at the time of reaching the juvenile transition and observations of age-0 pollock were made with the local index of collocation (LIC) as this method of cell-by-cell comparisons has been used to compare distributions of populations (Kotwicki and Lauth, 2013; Petrik *et al.*, 2015) and is similar to the Overlap Coefficient, also used in fisheries studies of distribution overlap (e.g. Hinrichsen *et al.*, 2005). Observations of depth-integrated abundance (# surface area^{-1}) were first binned by BEST-BSIERP region to calculate a mean abundance in each region of each year. Mean depth-integrated abundances (# surface area^{-1}) were then converted into mean total areal abundances (#) by multiplying the areal extent of each region (surface area). Mean numbers of individuals were used to calculate the fraction of individuals observed in each region out of the total number of individuals in all regions observed that year. Since not all 16 BEST-BSIERP regions were sampled by all observations in all years, model-observation comparisons were only made using the regions sampled. Thus, modelled fractions of individuals were calculated as the number of individuals that reached juvenile size in each region sampled by that observational dataset that year out of the total number of individuals that reached juvenile size in all regions sampled by that observational dataset that year. The LIC was then calculated year-by-year for each observational dataset by comparing each specific pair of observed and modelled fractions.

Results

Modelled spawning only occurred in the BEST-BSIERP regions (Figure 1) AK Peninsula (1), South Middle Shelf (3), South Outer Shelf (4), Pribilofs (5), Mid-north Middle Shelf (6), North Outer Shelf (8), and Off-shelf Southeast (16), yet individuals were found in all 16 regions at the time each reached the juvenile transition. Connectivity between spawning and juvenile regions differed by spawn date, year, and simulation. In the following section we describe the major differences by simulation. Results from the Base ("Transport Only") simulation over all spawn times and years (Supplementary Table S1) and by spawning date (Supplementary Figure S1) are provided in the Supplementary Materials.

Connectivity patterns in different simulations

Combining all spawning times and years within each simulation produced different connectivity patterns. Comparing between only the Cold and Warm years of the Base simulation highlighted differences based on temperature regime. In these comparisons, connectivity was classified as strong (>0.058, 75th quartile; thick line Figure 2), moderate (0.009–0.058, median–75th quartile; thin line Figure 2), or weak (<0.009, median; not pictured). Connections from most spawning areas to the northern Middle Shelf regions (6, 9, 10) were stronger in Warm years, while to Off-Shelf North (15) and the Inner Shelf (2,7) were greater in Cold years (Figure 2A and B, D–F). Most connections above the median were to regions north and/or west of spawning regions, with higher off-shelf connectivity in Cold years and greater northward connectivity in Warm years (Figure 2). Retention of juveniles (not visible in Figure 2) decreased in all regions in Cold years, and increased in the South Middle Shelf (3), Pribilofs (5), and North Outer Shelf (8) in Warm years (Figure 3).

When only comparing the cold year simulations (Figure 3, top), the largest differences existed for the Contract simulation because there was no spawning in the Mid-north Middle Shelf (6) (Figure 3, top). Connectivity lessened to southern regions (1, 2, 3, 16) and to St Matthews (9) (Figure 3, top). Heightened connectivity was seen to the Off-shelf North (15) region. Retention was reduced in the North Outer Shelf (8), but increased in the Pribilofs (5) and Off-shelf Southeast (16) (Figure 3 top).

Shifting spawning 40 d later in the Late simulation also produced differences in connectivity from the Cold Base simulation. Connections to mid-north Middle Shelf regions (5, 6) and southern Outer and Off-shelf regions (4, 16) were greater than or equal to those of the Cold simulation (Figure 3, top). Late spawning weakened connectivity to the Inner Shelf (2, 7) and to the northern regions (8–11) (Figure 3, top). Late spawning reduced retention in the South Middle Shelf (3) compared with Base Cold, but increased it for all other regions (Figure 3, top).

Expanding spawning regions differed from Base Warm simulations by increased delivery to the southern Inner and Middle regions (1, 2, 3) (Figure 3, bottom). Expanded spawning lowered connectivity from the Mid-north Middle Shelf (6) to many Middle Shelf regions (3, 4, 5, 6, 9, 10) (Figure 3, bottom). Except for this area, retention was enhanced in all regions when compared with retention in the Warm Base simulation (Figure 3, bottom).

Advancing spawning times by 40 d in the Early simulation created the greatest differences between the warm simulations. Connectivity from the majority of the spawning regions to the Inner Shelf and northern Middle Shelf regions (2, 7, 9, 10, 11, 12) was stronger, as well as to the South Middle Shelf (3) (Figure 3, bottom). Conversely, links from nearly all source regions to the Outer, Off-shelf, and mid-north Middle Shelf regions (4, 5, 6, 8, 15, 16) fell in the Early simulations (Figure 3, bottom).

East–west transport

Connectivity to more on-shelf regions was further exemplified by the fraction of juveniles transported 0°–5°, 5°–10°, or >10° longitude to the east of where they were spawned. The Cold year simulations had greater fractions transported >5°W compared with the Warm simulations, but also greater fractions >5°E (Table 1). When comparing across simulations, roughly 80% or more of all juveniles were found to the west of where they were spawned, with the plurality found a distance of <5°W in all simulations (Table 1). Contracting the spawning grounds off-shelf led to greater westward transport, whereas advancing spawning time by 40 d with the early simulations increased eastward transport more than Expanding the spawning areas on-shelf (Table 1). None of the eastward transport metrics were significantly correlated with

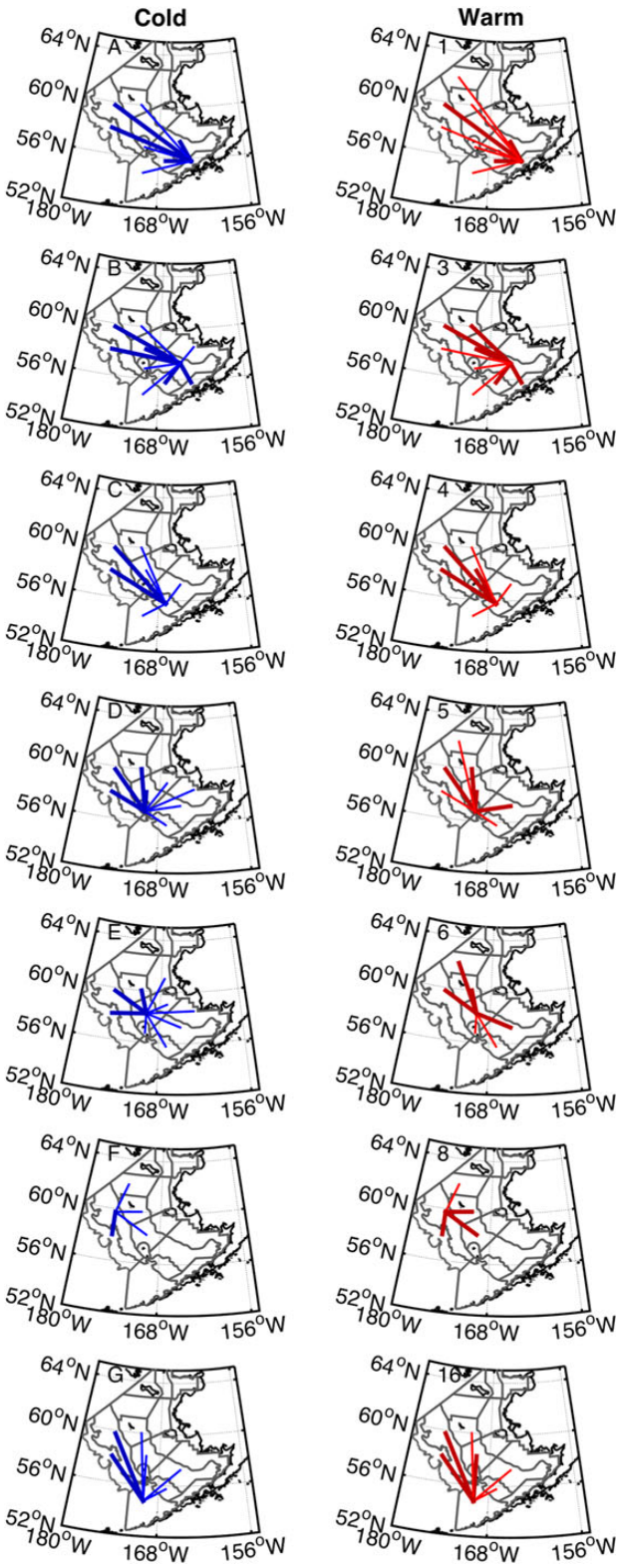

Figure 2. Mean connectivity in the Base simulation from the spawning regions 1: AK Peninsula (A), 3: South Middle Shelf (B), 4: South Outer Shelf (C), 5: Pribilofs (D), 6: Midnorth Middle Shelf (E), 8: North Outer Shelf (F), and 16: Off-shelf Southeast (G) with Cold (blue) and Warm (red) years shown separately. Line thickness indicates the strength of connection; thick: strong connection >0.058 (75th quartile), thin: moderate connection 0.009–0.058 (median–75th quartile). Not pictured: weak connection <0.009 (median).

temperature or wind indices, but dispersal >10°E was significantly positively correlated with the NPIw ($r = 0.55, p = 0.02$). Similar to distance travelled to the east or west, mean total distance travelled by all individuals differed between Cold and Warm years (Supplementary Figure S2A), but not the total distances travelled by individuals retained within each region (Supplementary Figure S2B).

Comparisons with juvenile survey observations

Model agreement with observations from net tow and acoustics surveys were robust, with 76 and 67% mean collocation, respectively (Table 2). The model showed the highest agreement with the net tow observations in all simulations except when spawning was delayed 40 d in the Late simulation, which had a greater LIC with the acoustics surveys (Table 2). Spatial differences between the model and observations are illustrated in the Supplementary data (Figures S3 and S4).

Discussion

The strong connectivity between spawning and juvenile regions exhibited three patterns: (i) along-isobath flow to the northwest, (ii) self-retention within regions, and (iii) persistence near the Pribilof Islands. In all three cases, it was the interaction of regional oceanography and seascape topography that underlied the observed patterns, though the mechanisms of interaction were unique among the three. What these influences share in common is an EBS continental shelf seascape that is relatively unremarkable; the benthic topography is characterized by a broad, flat expanse of muddy bottom with a gradual 200 m depth change over a distance of nearly 500 km. As such, the modest topographic features that mark this homogeneous terrain have the capacity to disproportionately influence oceanographic processes and ensuing connectivity, ultimately generating the three connectivity scenarios outlined above. For (i) observed southeast to northwest linkages, particularly connections to the North Outer Shelf (8), weak (5–10 cm s^{-1}) directional, baroclinic flow along the 100-m and 200-m isobaths emanating from Unimak Pass (Stabeno *et al.*, 2002) was a major contributor to pollock dispersal and early life connectivity. Here, flow along the isobaths that define the outer shelf permitted delivery of propagules to the region, seeding it with late-stage larvae that were retained through development to the age-0 phase. Featureless topography was also a likely contributor to (ii), observed robust connectivity across the middle shelf, though acting through an entirely different mechanism. The AK Peninsula (1), South Middle Shelf (3), and Mid-north Middle Shelf (6) emerged as strong recipients of larvae in these regions due to sluggish, semi-permanent cross-shelf flow (1–2 cm s^{-1}) that facilitated within-region retention over the Middle Shelf. Finally, (iii) the presence of the spatially small but topographically prominent Pribilof Islands (Pribilofs region 5) gave rise to one of the only major eddy features over the shelf, a robust anticyclonic gyre that encircles the islands (Kowalik and Stabeno, 1999). Due to this eddy feature, we anticipated even more connectivity in region 5 than was observed since the Pribilofs are a major spawning ground (Hinckley, 1987; Bacheler *et al.*, 2010) and nursery area for pollock. We suggest that the small size of the delineated region 5 underestimated the radius of anticyclonic transport. As such, region 5 connectivity was in fact realized in adjacent regions (3, 6, 8). Ciannelli *et al.* (2004) have suggested a radius of influence of ~100 nautical mi (185.2 km), which is consistent with the size of the clockwise gyre during summer (Stabeno *et al.*, 1999) and is much larger than the BEST-BSIERP region 5 (<50 nautical mi) used here. Our model results support this conclusion.

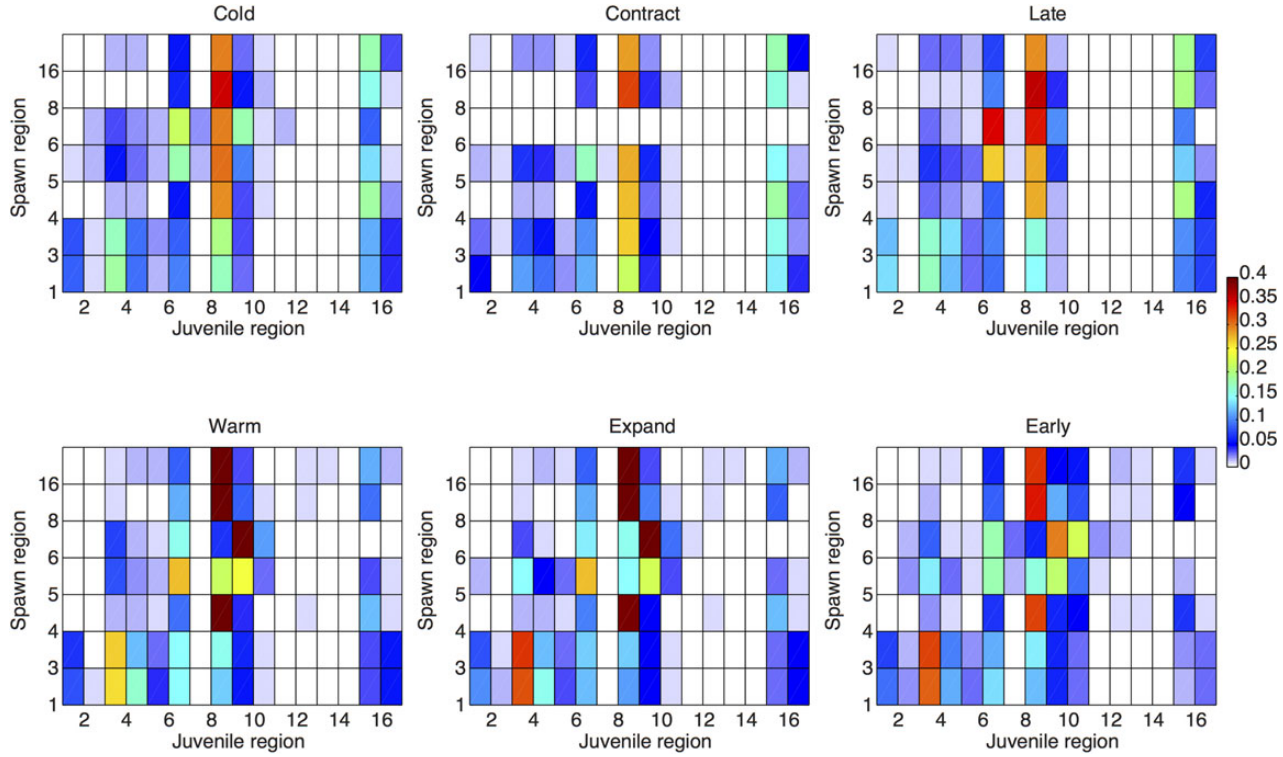

Figure 3. Mean connectivity matrices of the different simulations. The Base simulation is grouped by warm and cold years. Connectivity is presented as the fraction of individuals in a given region when reaching 40 mm length (columns) from a given spawning region (rows).

Table 1. Longitudinal transport of juveniles from spawning location presented as the fraction of the total in each simulation.

	>0°W	>10°W	5–10°W	<5°W	<5°E	5–10°E	>10°E	>0°E
Base all	0.87	0.11	0.34	0.41	0.12	0.007	2.7E−05	0.13
Cold	0.89	0.13	0.35	0.40	0.10	0.007	3.1E−05	0.11
Contract	0.92	0.15	0.38	0.38	0.07	0.005	3.0E−05	0.07
Late	0.85	0.08	0.30	0.47	0.13	0.007	2.1E−06	0.14
Warm	0.86	0.06	0.33	0.47	0.13	0.004	1.6E−05	0.14
Expand	0.82	0.05	0.29	0.48	0.17	0.006	1.4E−05	0.17
Early	0.79	0.06	0.28	0.45	0.19	0.010	5.6E−05	0.20

Temporal variability among seasons and years

Since the EBS seascape is comparatively homogenous, large-scale, cross-shelf transport is principally affected by seasonal variability in baroclinic flow and interannual changes in wind-induced circulation. Seasonally, model output indicated that northward and on-shelf transport was greater when early seasonal spawning times were simulated, while retention was favoured during late seasonal spawning simulations. This is consistent with physical observations that show that both the Bering Slope Current (Ladd, 2014) and Ekman surface currents (Danielson *et al.*, 2011b, 2014; Stabeno *et al.*, 2012) are strongest in winter, decreasing through spring to minima in summer. Likewise, broad-scale seasonal stratification in spring establishes the presence of a coastal front (Kachel *et al.*, 2002) that is present May–September but absent other times of the year. The absence of the front in the early spring substantiates the strong connectivity from region 1 to region 3 during early seasonal spawning times by allowing transport across the 50-m isobath, while its presence in the late spring and early summer supports the higher modelled retention rates observed April–June by preventing cross-shelf transport of individuals.

Interannually, modelled simulations indicated that total eastward transport was greater in warm years compared with cold, an observation that is again corroborated by field observations. Warm year stanzas in the Bering Sea were characterized by westward-displaced ALs, which have been correlated with southeasterly winds, cross-isobath fluxes over the southern Middle Shelf and northward transport (Danielson *et al.*, 2014). We saw manifestations of this pattern in the model results with increased connectivity to the Middle Shelf (regions 1 and 3) and to the north (regions 6 and 9) during warm years (2002–2005). In contrast, cold periods were characterized by an eastward-displaced AL and winds over the EBS shelf that were northwesterly, northerly, and northeasterly, forcing coastal divergence and advection along isobaths to the southwest over the southern Middle Shelf (regions 1 and 3) (Danielson *et al.*, 2014). These characteristics account for the greater modelled westward transport and stronger off-shelf connectivity to the North Outer Shelf (8), Off-shelf North (15), and Off-shelf Southeast (16) in the cold year simulations. Additionally, greater fractions of individuals travelled further distances in cold years compared with warm years, an observation that

Table 2. Local index of collocation values of model-observation comparisons for individual years in the Base simulations and for all years in the alternate simulations.

	Net tows	Acoustics
Base 1995	–	–
Base 1996	0.72	–
Base 1997	0.68	–
Base 1998	0.77	–
Base 1999	0.58	–
Base 2000	0.99	–
Base 2001	0.53	–
Base 2002	0.89	–
Base 2003	0.47	–
Base 2004	0.98	–
Base 2005	0.80	–
Base 2006	–	0.64
Base 2007	0.97	0.43
Base 2008	–	0.74
Base 2009	–	0.44
Base 2010	–	0.91
Base 2011	–	0.89
Base 2012	–	0.61
Base Mean	0.76	0.67
Cold	0.81	0.67
Contract	0.70	0.60
Late	0.65	0.68
Warm	0.72	–
Expand	0.78	–
Early	0.82	–

is backed by observed stronger currents in cold years (Danielson *et al.*, 2011b, 2014; Stabeno *et al.*, 2012).

Comparisons with observations

Modelled and observed juvenile distributions were not identical. Modelled distributions were the locations of individuals at 40 mm; this could be any time between March and the following January, but were typically June–July. Most of the observations were taken later in the year (late July–early October) and field-collected age-0s typically ranged from 40 to 130 mm (Moss *et al.*, 2009), with a mean size of ~70 mm. Differences in spatial distribution between model and observed results could be related to improved locomotor abilities of older, larger fish that permit swimming out of drift model endpoint regions. Moreover, vertical migration increases with age and results in different depth distributions of juveniles.

Further, in contrast to observations, modelled juveniles were found on the Inner Shelf (regions 2, 7, and 11), especially in cold years. The simulations are consistent with the observed extension of a Middle Shelf zooplankton community into the Inner Shelf in cold years, which may be the result of a weaker Inner Front in cold years (Eisner *et al.*, 2014) or one that develops in August rather than June as was observed in 1998 and 1999 (Kachel *et al.*, 2002). Observed transport of zooplankton to the Inner Shelf implies that either behavior or mortality is responsible for the lack of observed juveniles on the Inner Shelf. Analogously, mortality in all regions, which is not represented in the simulations, is yet another factor that could account for differences between modelled and observed juvenile distributions.

Sink regions as critical habitat

In this study, the Pribilof Islands, the southern Middle Shelf, and the Northern Outer Shelf emerge as areas of robust connectivity and particle sinks; we propose that these regions are not only larval sinks but are likely important nursery habitat for age-0 pollock beyond the end of the larval phase. The Pribilof Islands have historically been described as critical production areas for fish, crabs, birds, and mammals. This is likely due to the their proximity to the slope which facilitates nutrient input from the deep basin, the retentive clockwise circulation pattern that promotes mixing and influences primary production (Sullivan *et al.*, 2008), the presence of organized fronts that aggregate zooplankton prey (Brodeur *et al.*, 2000; Schabetsberger *et al.*, 2000; Swartzman *et al.*, 2005), and the presence of microhabitat in the form of ridges, crevices, mounts, and biogenic structures that offer predation refugia across an otherwise barren substratum (Busby *et al.*, 2005). The southern middle shelf, with its strong stratification (Ladd and Stabeno, 2012) and comparatively lower predation risk from voracious arrowtooth flounder (Zador *et al.*, 2011) also has materialized as an important nursery area for pollock, regardless of temperature regime. Finally, more recent studies during the warm and cold periods have begun to shed light on the role of the Outer Shelf (regions 4 and 8) as important habitat, because it contains zooplankton communities of larger sizes and greater lipid content and serves as a beneficial feeding area for age-0 pollock juveniles, especially in cold years (Coyle *et al.*, 2011; Siddon *et al.*, 2013; Eisner *et al.*, 2014). As climate projections forecast increasing temperatures (Wang *et al.*, 2012), we predict that the rather invariant Outer Shelf (4, 8; Siddon *et al.*, 2011; Eisner *et al.*, 2014) will become increasingly important for its high abundances of energy rich prey that are advected onto the shelf from the slope waters (Gibson *et al.*, 2013) and for its greater depths that allow vertical energy conservation and predator avoidance (Hollowed *et al.*, 2012).

Perspectives

The EBS is not isolated from other sources of pollock, but is connected to the Gulf of Alaska by passes through the Aleutian Islands. A similar biophysical IBM of pollock in the Gulf of Alaska has been used to assess connectivity of that stock. Spawning in the Gulf of Alaska resulted in high modelled densities of surviving age-0 pollock juveniles in potential nursery areas of the EBS that were advected through Unimak Pass from source regions in the western Gulf of Alaska (Parada *et al.*, in press). Though this high potential connectivity may represent a substantial loss to the Gulf of Alaska population, it is unclear if transport of Gulf of Alaska pollock subsidizes the EBS stock.

Unlike the EBS and Gulf of Alaska, which are systems that appear to support connectivity across significant distances, studies of Atlantic cod (*Gadus morhua*) connectivity suggest more limited dispersal potential. Working in coastal Canada, Stanley *et al.* (2013) determined that local gyres acted to retain early life stages of Atlantic cod close to spawning areas and Myksvoll *et al.* (2014) determined high retention in fjord areas and intermediate retention in coastal populations for stocks of Atlantic cod, Northeast Arctic cod, and Norwegian Coastal cod. It is likely that these differences in dispersal and connectivity are a function of the underlying landscape ecology that mitigates the oceanographic processes that advect and connect larval and juvenile critical habitat areas. The EBS is characterized by a broad, flat, relatively homogeneous bottom topography, while coastal Canadian and Norwegian coastlines are rugose, heterogeneous, and dissimilar, creating microniches that support local retention and, ultimately, population substocks. Rogers *et al.* (2014) recently explored the influence of habitat landscape on connectivity and recruitment by examining the variability

of Atlantic cod population connectivity across heterogeneous habitats. They found significant habitat effects on both connectivity and recruitment synchrony, with greater connectivity in exposed regions than sheltered. If this observation is scaled up to pollock occurrence in Alaska, it holds promise for better understanding of population structuring within and across the region's Large Marine Ecosystems (Gulf of Alaska, Aleutian Islands, EBS).

Conclusions

The three connectivity patterns of along-isobath flow to the northwest, self-retention, and transport around the Pribilof Islands were seen in most simulations. The major differences in connectivity between warm and cold years, more northwards in warm years and more off-shelf in cold years, mimicked wind-driven flow characteristics of those years (Danielson *et al.*, 2011b; Stabeno *et al.*, 2012) that were related to the winter mean zonal position of the AL (Danielson *et al.*, 2014). Surprisingly, the North Outer Shelf (8) emerged as a very large sink of pollock reaching the juvenile transition from all spawning sources, and we recommend increased sampling across multiple trophic levels since it may be a potentially important juvenile pollock nursery.

Supplementary data

Supplementary material is available at the *ICESJMS* online version of the manuscript.

Acknowledgements

We thank Alexander Andrews, Alexander De Robertis, John Horne, and Sandra Parker-Stetter for providing observational data. This research was funded by NSF award 1108440, is BEST-BSIERP Bering Sea Project publication number 177, NPRB publication number 579, and contribution EcoFOCI-N861 to NOAA's Fisheries-Oceanography Coordinated Investigations. The findings and conclusions in the paper are those of the authors and do not necessarily represent the views of the National Marine Fisheries Service.

References

Bacheler, N. M., Ciannelli, L., Bailey, K., and Duffy-Anderson, J. T. 2010. Spatial and temporal patterns of walleye pollock (*Theragra chalcogramma*) spawning in the eastern Bering Sea inferred from egg and larval distributions. Fisheries Oceanography, 19: 107–120.

Baker, M. R., and Hollowed, A. B. 2014. Delineating ecological regions in marine systems: Integrating physical structure and community composition to inform spatial management in the eastern Bering Sea. Deep-Sea Research, 109: 215–240.

Barbeaux, S. J. 2012. Scientific acoustic data from commercial fishing vessels: eastern Bering Sea walleye pollock (*Theragra chalcogramma*). PhD thesis, University of Washington.

Blanke, B., and Raynaud, S. 1997. Kinematics of the Pacific Equatorial Undercurrent: a Eulerian and Lagrangian approach from GCM results. Journal of Physical Oceanography, 27: 1038–1053.

Blood, D. M. 2002. Low-temperature incubation of walleye pollock (*Theragra chalcogramma*) eggs from the southeast Bering Sea shelf and Shelikof Strait, Gulf of Alaska. Deep-Sea Research II, 49: 6095–6108.

Brodeur, R. D., and Wilson, M. T. 1996. A review of the distribution, ecology and population dynamics of age-0 walleye pollock in the Gulf of Alaska. Fisheries Oceanography, 5: 144–166.

Brodeur, R. D., Wilson, M. T., and Ciannelli, L. 2000. Spatial and temporal variability in feeding and condition of age-0 walleye pollock (*Theragra chalcogramma*) in frontal regions of the Bering Sea. ICES Journal of Marine Science, 57: 256–264.

Budgell, W. 2005. Numerical simulation of ice-ocean variability in the Barents Sea region. Ocean Dynamics, 55: 370–387.

Busby, M., Mier, K., and Brodeur, R. D. 2005. Habitat associations of demersal fishes and crabs in the Pribilof Islands region of the Bering Sea. Fisheries Research, 75: 15–28.

Busby, M. S., Duffy-Anderson, J. T., Mier, K. L., and De Forest, L. G. 2014. Spatial and temporal patterns in summer ichthyoplankton assemblages on the eastern Bering Sea shelf 1996–2007. Fisheries Oceanography, 23: 270–287, doi:10.1111/fog.12062.

Carton, J. A., and Giese, B. S. 2008. A reanalysis of ocean climate using Simple Ocean Data Assimilation (SODA). Monthly Weather Review, 136: 2999–3017.

Cheng, W., Curchitser, E. N., Stock, C., Hermann, A., Cokelet, E., Mordy, C., Stabeno, P., *et al.* 2015. What processes contribute to the spring and fall bloom co-variability on the Eastern Bering Sea shelf? Deep-Sea Research II, doi:10.1016/j.dsr2.2015.07.009.

Ciannelli, L., Robson, B. W., Francis, R. C., Aydin, K., and Brodeur, R. D. 2004. Boundaries of open marine ecosystems: an application to the Pribilof Archipelago, southeast Bering Sea. Ecological Applications, 14: 942–953.

Cowen, R. K., and Sponaugle, S. 2009. Larval dispersal and marine population connectivity. Annual Review of Marine Science, 1: 443–466.

Coyle, K., Eisner, L., Mueter, F., Pinchuk, A., Janout, M., Cieciel, K., Farley, E., *et al.* 2011. Climate change in the southeastern Bering Sea: impacts on pollock stocks and implications for the Oscillating Control Hypothesis. Fisheries Oceanography, 20: 139–156.

Curchitser, E. N., Hedstrom, K., Danielson, S., and Weingartner, T. J. 2010. Modeling the Circulation in the North Aleutian Basin. Department of Interior, OCS Study BOEMRE 2010-028.

Dai, A., and Trenberth, K. E. 2002. Estimates of freshwater discharge from continents: Latitudinal and seasonal variations. Journal of Hydrometeorology, 3: 660–687.

Danielson, S., Curchitser, E., Hedstrom, K., Weingartner, T., and Stabeno, P. 2011a. On ocean and sea ice modes of variability in the Bering Sea. Journal of Geophysical Research, 116: C12034, doi:10.1029/2011JC007389.

Danielson, S., Eisner, L., Weingartner, T., and Aagaard, K. 2011b. Thermal and haline variability over the central Bering Sea shelf: seasonal and interannual perspectives. Continental Shelf Research, 31: 539–554.

Danielson, S., Hedstrom, K., Aagaard, K., Weingartner, T., and Curchitser, E. 2012. Wind-induced reorganization of the Bering shelf circulation. Geophysical Research Letters, 39: L08601–L08606.

Danielson, S. L., Weingartner, T. J., Hedstrom, K. S., Aagaard, K., Woodgate, R., Curchitser, E., and Stabeno, P. J. 2014. Coupled wind-forced controls of the Bering-Chukchi shelf circulation and the Bering Strait throughflow: Ekman transport, continental shelf waves, and variations of the Pacific-Arctic sea surface height gradient. Progress in Oceanography, 125: 40–61.

De Robertis, A., McKelvey, D., Taylor, K., and Honkalehto, T. 2014. Development of acoustic trawl survey methods to estimate the abundance of age-0 walleye pollock in the eastern Bering Sea shelf during the Bering Arctic Subarctic Integrated Survey. U.S. Department of Commerce, NOAA Technical Memorandum, NMFS-AFSC-272. 46 pp.

de Vries, P., and Döös, K. 2001. Calculating Lagrangian trajectories using time-dependent velocity fields. Journal of Atmospheric and Oceanic Technology, 18: 1092–1101.

Döös, K. 1995. Inter-ocean exchange of water masses. Journal of Geophysical Research, 100: 13499–13514.

Duffy-Anderson, J. T., Barbeaux, S., Farley, E., Heintz, R., Horne, J., Parker-Stetter, S., Petrik, C., *et al.* 2015. State of knowledge review and synthesis of the first year of life of walleye pollock (*Gadus chalcogrammus*) in the eastern Bering Sea with comments on implication for recruitment. Deep-Sea Research II, doi:10.1016/j.dsr2.2015.02.001.

Eisner, L., Napp, J., Mier, K., Pinchuk, A., and Andrews, A. 2014. Climate-mediated changes in zooplankton community structure for the eastern Bering Sea. Deep-Sea Research II, doi:10.1016/j.dsr2.2014.03.004.

Gibson, G. A., Coyle, K. O., Hedstrom, K., and Curchitser, E. N. 2013. A modeling study to explore on-shelf transport of oceanic zooplankton in the Eastern Bering Sea. Journal of Marine Systems, 121–122: 47–64.

Hinckley, S. 1987. The reproductive biology of walleye pollock, *Theragra chalcogramma*, in the Bering Sea, with reference to spawning stock structure. Fisheries Bulletin U.S., 85: 481–498.

Hinrichsen, H.-H., Schmidt, J. O., Petereit, C., and Möllmann, C. 2005. Survival probability of Baltic larval cod in relation to spatial overlap patterns with its prey obtained from drift model studies. ICES Journal of Marine Science, 62: 878–885.

Hollowed, A. B., Barbeaux, S. J., Cokelet, E. D., Farley, E., Kotwicki, S., Ressler, P. H., Spital, C., *et al.* 2012. Effects of climate variation on pelagic ocean habitats and their role in structuring forage fish distributions in the Bering Sea. Deep-Sea Research II, 65–70: 230–250.

Honkalehto, T., Ressler, P. H., Towler, R., and Wilson, C. 2011. Using acoustic data to estimate walleye pollock abundance in the eastern Bering Sea. Canadian Journal of Fisheries and Aquatic Sciences, 68: 1231–1242.

Ianelli, J. N., Barbeaux, S. J., McKelvey, D., and Honkalehto, T. 2012a. Assessment of walleye pollock in the Bogoslof Island Region. *In* Stock Assessment and Fishery Evaluation Report for the Groundfish Resources of the Bering Sea/Aleutian Islands Regions, pp. 235–244. North Pacific Fishery Management Council, Anchorage. 1298 pp.

Ianelli, J. N., Honkalehto, T., Barbeaux, S., Kotwicki, S., Aydin, K., and Williamson, N. 2012b. Assessment of the Walleye Pollock stock in the Eastern Bering Sea. *In* Stock Assessment and Fishery Evaluation Report for the Groundfish Resources of the Bering Sea/Aleutian Islands Regions, pp. 51–156. North Pacific Fishery Management Council, Anchorage. 1298 pp.

Kachel, N. B., Hunt, G. L., Jr, Salo, S. A., Schumacher, J. D., Stabeno, P. J., and Whitledge, T. E. 2002. Characteristics and variability of the inner front of the southeastern Bering Sea. Deep-Sea Research II, 49: 5889–5909.

Kalnay, E., Kanamitsu, M., Kistler, R., Collins, W., Deaven, D., Gandin, L., Iredell, M., *et al.* 1996. The NCEP/NCAR 40year reanalysis project. Bulletin of the American Meteorological Society, 77: 437–471.

Kotwicki, S., and Lauth, R. R. 2013. Detecting temporal trends and environmentally-driven changes in the spatial distribution of bottom fishes and crabs on the eastern Bering Sea shelf. Deep-Sea Research II, 94: 231–243.

Kowalik, Z., and Stabeno, P. 1999. Trapped motion around the Pribilof Islands in the Bering Sea. Journal of Geophysical Research, 104: 25,667–25,684. doi:10.1029/1999JC900209.

Ladd, C. 2014. Seasonal and interannual variability of the Bering Slope Current. Deep-Sea Research II, doi:10.1016/j.dsr2.2013.12.005.

Ladd, C., and Stabeno, P. J. 2012. Stratification on the Eastern Bering Sea shelf revisited. Deep Sea Research II, 2: 72–83.

Large, W. G., and Yeager, S. G. 2009. The global climatology of an interannually varying air-sea flux data set. Climate Dynamics, 33: 341–364.

Matarese, A. C., Kendall, A. W., Jr, Blood, D. M., and Vinter, B. M. 1989. Laboratory Guide to Early Life History Stages of Northeast Pacific Fishes. NOAA/National Marine Fisheries Service, NOAA Technical Report NMFS 80. 652 pp.

Metzger, E. J., Smedstad, O. M., Thoppil, P. G., Hurlburt, H. E., Cummings, J. A., Wallcraft, A. J., Zamudio, L., *et al.* 2014. US Navy operational global ocean and Arctic ice prediction systems. Oceanography, 27: 32–43, doi:10.5670/oceanog.2014.66.

Moss, J. H., Farley, E. V., Feldman, A. M., and Ianelli, J. N. 2009. Spatial distribution, energetic status, and food habits of eastern Bering Sea age-0 walleye pollock. Transactions of the American Fisheries Society, 138: 497–505.

Mueter, F. J., Bond, N. A., Ianelli, J. N., and Hollowed, A. B. 2011. Expected declines in recruitment of walleye pollock (*Theragra chalcogramma*) in the eastern Bering Sea under future climate change. ICES Journal of Marine Science, 68: 1284–1296.

Mueter, F. J., and Litzow, M. A. 2008. Sea ice retreat alters the biogeography of the Bering Sea continental shelf. Ecological Applications, 18: 309–320.

Myksvoll, M. S., Jung, K.-M., Albertsen, J., and Sundby, S. 2014. Modelling dispersal of eggs and quantifying connectivity among Norwegian coastal cod populations. ICES Journal of Marine Science, 71: 957–969.

NARR website. http://nomads.ncdc.noaa.gov/dods/NCEP_NARR_DAILY/narr-a_221_uvsfc.subset.info (last accessed 6 May 2015).

Ortiz, I., Wiese, F. K., and Grieg, A. 2012. Marine Regions Boundary Data for the Bering Sea Shelf and Slope. UCAR/NCAR-Earth Observing Laboratory/Computing, Data, and Software Facility. Dataset. doi: 10.5065/D6DF6P6C.

Parada, C., Hinckley, S., Horne, J., Mazur, M., Hermann, A., and Curchitser, E. in press. Modeling connectivity of walleye pollock in the Gulf of Alaska: are there any linkages to Bering Sea and Aleutian Islands? Deep-Sea Research II, doi:10.1016/j.dsr2.2015.12.010.

Parker-Stetter, S. L., Horne, J. K., Farley, E. V., Barbee, D. H., Andrews, A. G., III, Eisner, L. B., and Nomura, J. M. 2013. Summer distributions of forage fish in the eastern Bering Sea. Deep-Sea Research II, doi:10.1016/j.dsr2.2013.04.022.

Petrik, C. M., Duffy-Anderson, J. T., Mueter, F. J., Hedstrom, K., and Curchitser, E. N. 2015. Biophysical transport model suggest climate variability determines distribution of Walleye Pollock early life stages in the eastern Bering Sea through effects on spawning. Progress in Oceanography, 138: 459–474. doi:10.1016/j.pocean.2014.06.004.

Rienecker, M. M., Suarez, M. J., Gelaro, R., Todling, R., Bacmeiseter, J., Liu, E., Bosilovich, M. G., *et al.* 2011. MERRA: NASA's modern-era retrospective analysis for research and applications. Journal of Climate, 24: 3624–3648.

Rogers, L., Olsen, E. M., Knutsen, H., and Stenseth, N. C. 2014. Habitat effects on population connectivity in a coastal seascape. Marine Ecology Progress Series, 511: 153–163.

Schabetsberger, R., Brodeur, R. D., Ciannelli, L., and Napp, J. M. 2000. Diel vertical migration and interaction of zooplankton and juvenile walleye pollock (*Theragra chalcogramma*) at a frontal region near the Pribilof Islands, Bering Sea. ICES Journal of Marine Science, 57: 1283–1295.

Shchepetkin, A. F., and McWilliams, J. C. 2009. Ocean forecasting in terrain-following coordinates: Formulation and skill assessment of the Regional Ocean Modeling System. Journal of Computational Physics, 228: 8985–9000. doi:10.1016/j.jcp.2009.09.002.

Siddon, E. C., Duffy-Anderson, J. T., and Mueter, F. J. 2011. Community-level response of fish larvae to environmental variability in the southeastern Bering Sea. Marine Ecology Progress Series, 426: 225–239.

Siddon, E. C., Kristiansen, T., Mueter, F. J., Holsman, K., Heinz, R. A., and Farley, E. V. 2013. Spatial match-mismatch between juvenile fish and prey explains recruitment variability across contrasting climate conditions in the eastern Bering Sea. PLoS ONE, 8: e84526, doi:10.1371/journal.pone.0084526.

Smart, T. I., Duffy-Anderson, J. T., and Horne, J. K. 2012. Alternating temperature states influence walleye pollock early life stages in the southeastern Bering Sea. Marine Ecology Progress Series, 455: 257–267.

Smart, T. I., Siddon, E. C., and Duffy-Anderson, J. T. 2013. Vertical distributions of the early life stages of walleye pollock (*Theragra chalcogramma*) in the Southeastern Bering Sea. Deep-Sea Research II, 94: 201–210.

Stabeno, P. J., Kachel, N. B., Moore, S. E., Napp, J. M., Sigler, M., Yamaguchi, A., and Zerbini, A. N. 2012. Comparison of warm and

cold years on the southeastern Bering Sea shelf and some implications for the ecosystem. Deep-Sea Research II, 65–70: 31–45.

Stabeno, P. J., Reed, R. K., and Napp, J. M. 2002. Transport through Unimak Pass, Alaska. Deep-Sea Research. II, 49: 5919–5930.

Stabeno, P. J., Schumacher, J. D., Salo, S. A., Hunt, G. L., and Flint, M. 1999. Physical environment around the Pribilof Islands. *In* Dynamics of the Bering Sea, pp. 193–215. Ed. by T. R. Loughlin, and K. Ohtani. Alaska Sea Grant Press AK-SG-99-03, Fairbanks. 838 pp.

Stanley, R. E., de Young, B., Snlegrove, P. V. R., and Gregory, R. R. 2013. Factors regulating early life history dispersal of Atlantic cod (*Gadus morhua*) from coastal Newfoundland. PLoS ONE. doi:10.1371/journal.pone.0075889.

Sullivan, M., Kachel, N., Mordy, C., and Stabeno, P. J. 2008. The Pribilof Islands: Temperature, salinity and nitrate during summer 2004. Deep-Sea Research II, 55: 1729–1737.

Swartzman, G., Winter, A., Coyle, K., Brodeur, R., Buckley, T., Ciannelli, L., Hunt, G., *et al.* 2005. Relationship of age-0 pollock abundance and distribution around the Pribilof Islands, to other shelf regions of the eastern Bering Sea. Fisheries Research, 74: 273–287.

Trenberth, K. E., and Hurrell, J. W. 1994. Decadal atmosphere-ocean variations in the Pacific. Climate Dynamics, 9: 303–319.

Vestfals, C., Ciannelli, L., Duffy-Anderson, J. T., and Ladd, C. 2013. Effects of seasonal and interannual variability in along-shelf and cross-shelf transport on groundfish recruitment in the eastern Bering Sea. Deep-Sea Research II, doi:10.1016/j.dsr2.2013.09.026.

Wang, M., Overland, J. E., and Stabeno, P. J. 2012. Future climate of the Bering and Chukchi Seas projected by global climate models. Deep-Sea Research II, 65–70: 46–57.

Zador, S., Aydin, K., and Cope, J. 2011. Fine-scale analysis of arrowtooth flounder *Atherestes stomias* catch rates reveals spatial trends in abundance. Marine Ecology Progress Series, 438: 229–239.

Handling editor: Manuel Hidalgo

ICES Journal of Marine Science

ICES Journal of Marine Science (2016), 73(7), 1901–1911. doi:10.1093/icesjms/fsw053

Contribution to the Themed Section: '*Seascape Ecology*'

Original Article

Community–environment interactions explain octopus-catshark spatial overlap

Patricia Puerta[1]*, Mary E. Hunsicker[2], Manuel Hidalgo[1], Patricia Reglero[1], Lorenzo Ciannelli[3], Antonio Esteban[4], María González[5], and Antoni Quetglas[1]

[1]*Instituto Español de Oceanografía, Centre Oceanográfico de les Baleares, Muelle de Poniente s/n, Apdo. 291, 07015 Palma de Mallorca, Spain*
[2]*NOAA, Northwest Fisheries Science Center, 2115 SE OSU Drive, Newport, OR 97366, USA*
[3]*College of Earth, Ocean, and Atmospheric Sciences, Oregon State University, 104 CEOAS Administration Building, Corvallis, OR 97331, USA*
[4]*Instituto Español de Oceanografía, Centro Oceanográfico de Murcia, Magallanes 2, Apdo. 22, 30740 San Pedro del Pinatar (Murcia), Spain*
[5]*Instituto Español de Oceanografía, Centro Oceanográfico de Málaga, Puerto Pesquero s/n, Apdo. 285, 29640 Fuengirola (Málaga), Spain*

**Corresponding author: tel: +34 971 133 720; fax: +34 971 404 945; e-mail: patrix.puerta@gmail.com*

Puerta, P., Hunsicker, M. E., Hidalgo, M., Reglero, P., Ciannelli, L., Esteban, A., González, M., and Quetglas, A. Community–environment interactions explain octopus-catshark spatial overlap. – ICES Journal of Marine Science, 73: 1901–1911.

Received 1 July 2015; revised 10 March 2016; accepted 12 March 2016.

The octopus *Eledone cirrhosa* and the catshark *Scyliorhinus canicula* present the same feeding habits and distributional preferences in the Mediterranean Sea. We explore patterns of spatial overlap between these species to address coexistence and infer possible competition from spatial patterns in the western Mediterranean Sea. A spatially explicit modelling approach revealed that spatial overlap mainly responded to the distribution of shared resources, where coexistence is allowed by different ecological processes. Catshark (k-strategy) was highly abundant and widely distributed. However, the fluctuating population dynamics of octopus (r-strategy) explained the variations in spatial patterns of overlap. Spatial structuring across the study area was observed both in population distributions and in species interactions (coexistence or exclusion). Areas with high resources in terms of specific prey items (Catalan Sea) or alternative supplies, such as niche opportunities and ecosystem functions defined by community diversity (Balearic Islands), favoured species coexistence. Sea surface temperature showed opposite effects on overlap in northern and southern regions of the study area, which were not related to differences in species sensitivity. We suggest a surface trophic link, where different phytoplankton communities at each region might have opposite responses to temperature. This triggers contrasting mechanisms of food transfer to deeper benthic communities that subsequently facilitates species overlap. Characterizing how benthic and pelagic seascape properties shape species interactions across space and time is pivotal to properly address community spatial dynamics and move towards ecosystem-based management for sustainable fisheries and conservation planning.

Keywords: benthic-pelagic coupling, coexistence, competition, Eledone cirrhosa, Mediterranean, Scyliorhinus canicula, spatial distribution, species interactions.

Introduction

Species and populations are typically non-randomly allocated in the nature. How they are distributed is a cornerstone in our knowledge of marine ecosystems, not only for addressing ecological and biogeographic questions but also for management and conservation, forecasting and assessment of global change impacts (Dambach and Rödder, 2011; Albouy *et al.*, 2014). Often, species distribution research has focused on the relationships between abundance and environmental conditions. Other factors such as resource availability, community complexity, or interactions among species are more usually than not ignored, despite their importance in dictating spatial patterns of species across different seascapes (Ciannelli *et al.*, 2008; Kordas *et al.*, 2011; Johnson *et al.*, 2013). Multispecies and ecosystem models are an exception because they take into account and quantify interspecific and trophic relationships. However, spatial patterns of foodwebs and ecosystem functioning

are usually excluded due to difficulties in the parameterization and the lack of spatial information on all ecosystems compartments (Kempf *et al.*, 2013 and references therein).

The aforementioned limitations of species distribution modelling are manifest in cephalopod research. Recent studies addressed the keystone role of cephalopods in foodwebs (Coll *et al.*, 2008, 2013; André *et al.*, 2010; Gasalla *et al.*, 2010), but usually trophic interactions are described based on stomach contents and prey–predator relationships without spatial context (e.g. Staudinger *et al.*, 2013; Rodhouse *et al.*, 2014 and references therein). There is particularly a dearth of information on competition between cephalopods and other taxonomic groups (but see for instance Butler and Lear, 2009; Link and Auster, 2013). Trophic interactions are crucial in shaping the population dynamics and distributions of cephalopods (Rodhouse *et al.*, 2014; Stewart *et al.*, 2014; Puerta *et al.*, 2015). However, the high dependence of cephalopods on environmental fluctuations (Pierce *et al.*, 2008; Rodhouse *et al.*, 2014) may mask the effect of species interactions in distributional patterns.

In this study, we explore the patterns in spatial overlap between an octopus, *Eledone cirrhosa*, and one of its putative competitors, the catshark *Scyliorhinus canicula*, in the western Mediterranean Sea. Both species are common in the Mediterranean and especially abundant in the western basin (Belcari *et al.*, 2002; Ellis *et al.*, 2009). They are found mainly on the lower continental shelf and the upper slope between 50 and 400 m depth and across all types of substrates (Boyle and Rodhouse, 2005; Gouraguine *et al.*, 2011; Pennino *et al.*, 2013; Puerta *et al.*, 2015). Additionally, the two species exhibit size segregation in depth distributions, with juveniles inhabiting shallower waters, between 100 and 200 m depth (Belcari *et al.*, 2002; Gouraguine *et al.*, 2011; Puerta *et al.*, 2014a). The octopus and the catshark are bottom dwelling and most active at night (Cobb *et al.*, 1995; Sims *et al.*, 2001). They are opportunistic feeders with similar diets (Boyle *et al.*, 1986; Valls *et al.*, 2011; Martinho *et al.*, 2012; Puerta *et al.*, 2015), mainly predating on decapod crustaceans, usually crabs.

Similarities in the distribution and feeding habits between octopus and catshark can suggest a potential competition for resources. However, while inferring imprints of competition from spatial patterns is challenging, studies indicate that competition effects can be discernible from local to regional (few hundred km) geographical ranges (Gotelli *et al.*, 2010; Araújo and Rozenfeld, 2014). Additionally, habitat and/or feeding overlap do not necessarily imply competition, except for instance when resources are in short supply (Hofer *et al.*, 2004; Link and Auster, 2013). Overlap and competition among species also vary with the environmental and community context (Hofer *et al.*, 2004; Orrock and Watling, 2010; Boström-Einarsson *et al.*, 2014; Cormon *et al.*, 2014) due to the spatial variation of population density, resource availability, fishing impact, or species sensitivity to changing habitat conditions.

In this paper, the patterns in spatial overlap between octopus and catshark are assessed in relation to environmental, trophic, and community indicators, along with density-dependent effects. Here we combine three issues of species interactions and spatial distributions, which have been poorly investigated in empirical systems. We examine the interaction (i) between two species of different taxonomic groups, (ii) at the population level (Link and Auster, 2013 and references therein), and (iii) including biotic factors that can dictate their interactions (e.g. species diversity; Johnson *et al.*, 2013) at broad spatio-temporal scales. For this purpose and attempting to infer possible interspecific competition from spatial patterns, a spatially explicit model is used to assess species coexistence at both local and regional scales in the western Mediterranean. We hypothesize that seascapes with high resources in terms of productivity and diversity will favour the spatial overlap by lessening competitive interactions.

Methods

Biological data

Data on species abundance were collected from the Spanish trawl surveys carried out as part of the Mediterranean International Trawl Survey (MEDITS) project, which has been conducted since 1994. The geographical range of the surveys covers the entire Spanish western Mediterranean Sea, including the Balearic Islands (Figure 1). The MEDITS surveys are performed annually between May and July during day-time. An experimental trawl gear (GOC 73) is used to ensure high catchability of demersal species (Bertrand *et al.*, 2002). Sampling followed an international standardized protocol (Bertrand *et al.*, 2002), with predefined stations based on bathymetric strata (10–50, 50–100, 100–200, 200–500, and 500–800 m) that were approximately replicated each year. For the present study, we included surveys performed from 2001 to 2012 and stations sampled for at least 5 of the 12 available years. Sampling information (date, time, position, depth, duration, distance trawled, vertical, and wing opening of the net) and species weight and number were recorded.

Using the information of each sampling station, the abundances of *E. cirrhosa* and *S. canicula* were transformed to standardized densities (individuals km^{-2}). Similarly, total prey densities were calculated; a broad group of benthic crustaceans were selected as potential prey items based on previous research (Valls *et al.*, 2011; Puerta *et al.*, 2015). Community indicators such as total species biomass ($g\ km^{-2}$) and the Shannon–Wiener diversity index (H') were also calculated per station. Only macrofaunal species (fish, crustaceans, and cephalopods) were included in the calculations of these two indicators, since other taxonomic groups were neither identified nor recorded consistently over time and space. These taxonomical groups account for ~88% of the survey catches. These community indicators can be also interpreted as a proxy of the fishing effort across the study area, since the main consequences of fishing impact is the degradation of the community by diminishing species diversity and biomass (Worm and Lotze, 2009; Coll *et al.*, 2012). Finally, the densities of octopus and catshark were summed across the entire sampling area in each year to estimate plausible population sizes and investigate density-dependent effects on species overlap.

Environmental data

Sea surface temperature (SST, °C) and chlorophyll *a* concentration (Chl*a*, $mg\ m^{-3}$) were obtained from satellite remote sensing data for each sampling station and year. Using 8-day composites files of 4 km resolution, we extracted Chl*a* and SST values in a 9-km radius around each sampled station and calculated monthly averages back from the date of sampling. This spatio-temporal resolution allows characterizing the local oceanography of the study area and minimizes cloud impact on the measurements. Environmental data were obtained from different sensors to cover the temporal range of collected biological data. SST dataset were supplied by AVHRR (2001–2002) and MODIS (2003–2012) sensors (NASA's Goddard Space Flight Center), while Chl*a* dataset were obtained from Sea WiFS (2001–2002) and MODIS (2003–2012) sensors (NOAA CoastWatch Program). Differences in measurement between sensors are negligible (Walton *et al.*, 1998; Kilpatrick *et al.*,

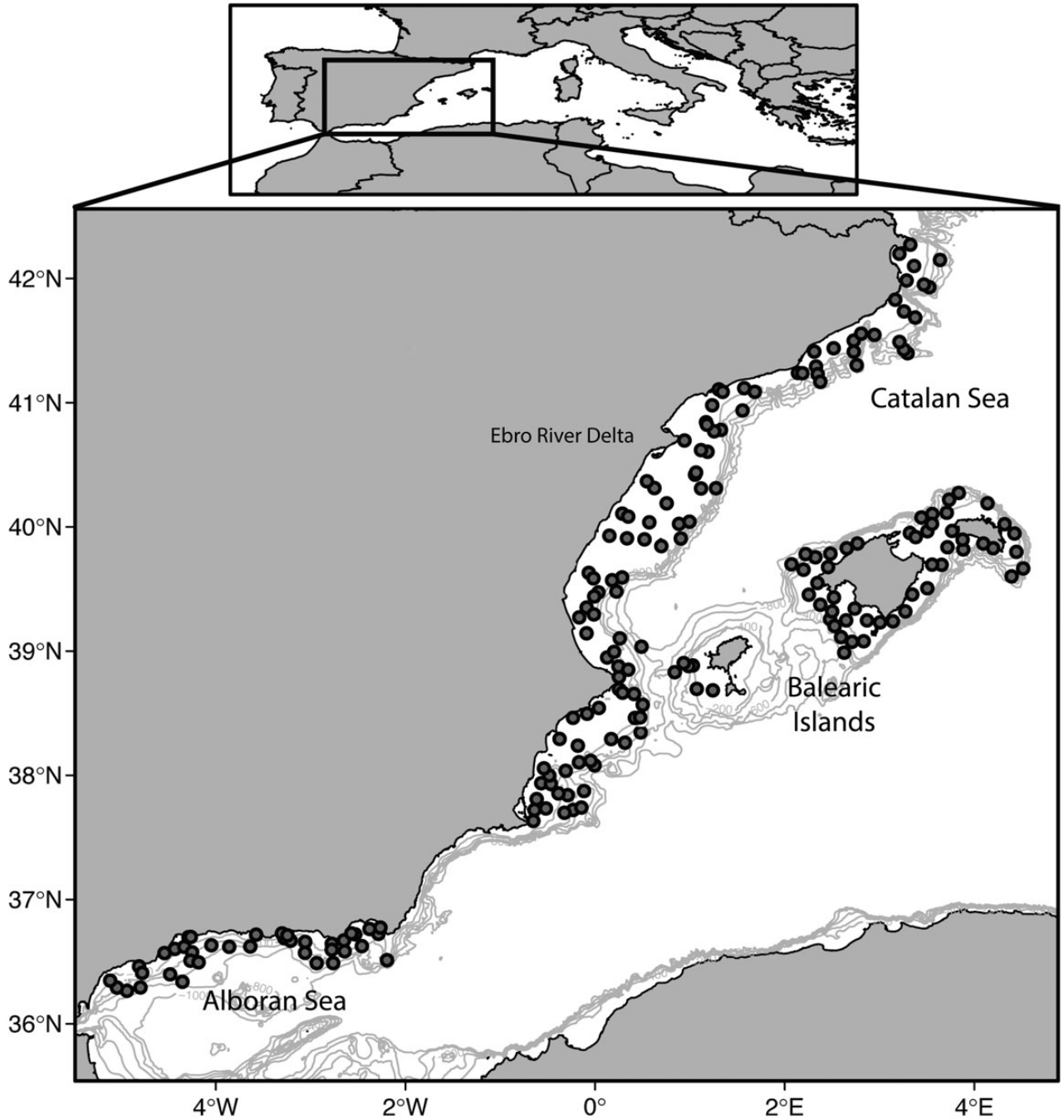

Figure 1. Sampling stations in the western Mediterranean Sea. Isobaths from 200 to 1000 m are shown.

2001). Due to the strong seasonality of the western Mediterranean Sea and the rapid increase in SST during spring and summer (Santoleri *et al.*, 1994), we applied generalized additive models (GAMs) to remove temporal trends in SST values associated with the differences in the dates of surveys. Residuals of SST were retained to be included as an explanatory variable in the model approach.

Data analysis

Overlap index

Spatial overlap between octopus and catshark was calculated as the natural logarithm of multiplied densities (x) of the two species at each sampling station (defined by latitude, ϕ and longitude, λ) and year (y), as following:

$$O_{(\phi,\lambda),y} = \log(x_{sp1,(\phi,\lambda),y} \cdot x_{sp2,(\phi,\lambda),y}).$$

Only stations where at least one of the species was present were included in the calculation of overlap. Before this calculation, species densities were standardized to make the overlap index dependent only on spatial variability, rather than interannual variability of population abundances. Standardization was performed

as follows:

$$\frac{x_{(\phi,\lambda),y} - \bar{x}_y}{\sigma_y^2} + \min(x_y),$$

where the density of each species at a station and year $x_{(\phi,\lambda),y}$ is demeaned and divided by standard deviation of density in the corresponding year. The minimum density value in the year y was then added to ensure (i) the overlap index were >0 (even if only one of the species were found) and (ii) the normal distribution of data.

In contrast to previous studies, the contribution of neighbour stations to density value at a given station were not taken into account (Ciannelli and Bailey, 2005; Hunsicker *et al.*, 2010), because the distances that the two species move from their dwelling areas (<20 km; Cobb *et al.*, 1995; Rodríguez-Cabello *et al.*, 2004, 2007; Boyle and Rodhouse, 2005) are shorter than the average distance between sampling stations.

Model formulation

GAMs were used to explore the influence of density-dependent effects (population size), trophic resources (prey densities), community indicators (total biomass and diversity), and environment (SST, Chl*a*) on species overlap. In heterogeneous systems, local conditions experienced by individuals across the geographic gradient can be very different from the mean averaged conditions in the entire region (Bacheler *et al.*, 2009; Bartolino *et al.*, 2011; Ciannelli *et al.*, 2012; Puerta *et al.*, 2015). Therefore, we applied a spatially explicit GAM where linear relationships between overlap index and the covariates are assumed, but these relationships are allowed to change smoothly in relation to the geographical position.

In the model formulation,

$$\begin{aligned} O_{(\phi,\lambda),y} = {} & s_1(\phi, \lambda) + s_2(\text{depth}_{(\phi,\lambda)}) + te(\phi, \lambda, \text{size}) + s_3(\phi, \lambda) \\ & \times \text{prey}_{(\phi,\lambda),y} + s_4(\phi, \lambda) \times \text{biomass}_{(\phi,\lambda),y} + s_5(\phi, \lambda) \\ & \times H_{(\phi,\lambda),y} + s_6(\phi, \lambda) \times SST_{(\phi,\lambda),y} + s_7(\phi, \lambda) \\ & \times \text{Chl}a_{(\phi,\lambda),y} \end{aligned}$$

geographic position (longitude ϕ, latitude λ) and depth were included as smoothing functions denoted by *s*. The spatially explicit terms were included for log-transformed prey densities (prey) and total biomass in the community (biomass), diversity index (H), residual SST, and Chl*a* concentrations. The variation in overlap (response) explained by the spatially explicit terms depends on the weighted sum of the same smoothing function evaluated at different covariate values. Additionally, the effects of population size (size) were tested independently for the two species. To do that, we used the formulation above in two different models, including octopus or catshark annual densities in the size term in each case. This allows evaluating density-dependent effects at different population sizes and testing the contribution of each species to overlap patterns, since large differences in the population abundances between species were observed in the preliminary analysis. A tensor product smoother (*te*) was included for the size term. Tensor products are more appropriate for interactions fitted over covariates with different units (combining different smoothers, a two-dimensional thin plate regression for ϕ, λ, and univariate cubic regression spline for size). This formulation assumes gradual changes in the overlap distribution related to variations in the population size. To reduce overfitting, the knots for univariate and two-dimensional smoothers were restricted to 4 and 20, respectively.

Starting from the full model above, a backward stepwise approach was performed by removing one term at a time. Full and reduced models were compared using Akaike information criterion (AIC) as a measure of goodness of fit and genuine cross validation (gCV) as a measure of the complete out-of-sample predicted mean squared error. The latter criterion determines which model was optimal for predictions. The best model was selected by minimizing both AIC and gCV criterions. Standard model diagnostics and residuals checking were performed for homogeneity of variance, the absence of temporal autocorrelation and violation of normality assumptions. Observations and model residuals were also checked for the lack of spatial correlation applying directional variograms and spatial plots to evaluate the best model. Additionally, the coefficients of regression (slopes) between the overlap index and each of the spatially explicit covariates were extracted from the best model. These coefficients (significant slopes based on 95% confidence interval) display the strength of the effect of a given covariate in the overlap at each geographical position. All calculations and models were coded in R software (version 3.1.2.), using the *vegan* and *mgcv* libraries.

Results

Spatial patterns in biotic and environmental factors

Spatial variability of the biotic and environmental factors in the study area is shown in Figure 2. Prey densities are patchily distributed, with higher abundances in the northern area of the mainland (Catalan Sea) and the Balearic Islands. These areas also presented higher community diversity values, especially in the islands. Total community biomass was larger in the southern area (Alboran Sea) and the islands. Chl*a* concentrations remained very low across the entire region, except in the Alboran Sea close to the Strait of Gibraltar. Finally, a north-south gradient of increasing temperatures is observed from residual SST.

Spatial patterns in overlap

A total of 1297 samples taken during 2001–2012 were included in the analysis (108 ± 14 trawls per year). Densities of catshark were much higher (250–800 individuals km^{-2}) than those of octopus (60–170 individuals km^{-2}). Spatial distribution of species densities and overlap index is shown in Figure 3. The distribution of high-density areas in octopus followed the deep continental shelf from the Catalan Sea down to the Balearic Islands, where intermediate densities were found (Figure 3a). Very low densities were detected in the Alboran Sea. In contrast, the catshark distribution showed high-density values across the entire study region, except the inshore waters in the central coast of the mainland under the influence of Ebro river run-off (Figure 3b). Areas of high species overlap mainly covered the Catalan Sea and the Balearic Islands (Figure 3c), and appeared to coincide with the distribution of *S. canicula*.

Model selection

Two model formulations were tested. They only differed in the inclusion of octopus or catshark population size, but the model outcomes and effects of covariates were the same. In both cases, all predictor covariates were retained except Chl*a*, which did not present significant effects on the overlap index (Table 1). The density-dependent effects of population size greatly improved the model fits. However, inclusion of octopus population size resulted in a better fit in terms of AIC, gCV, and deviance explained

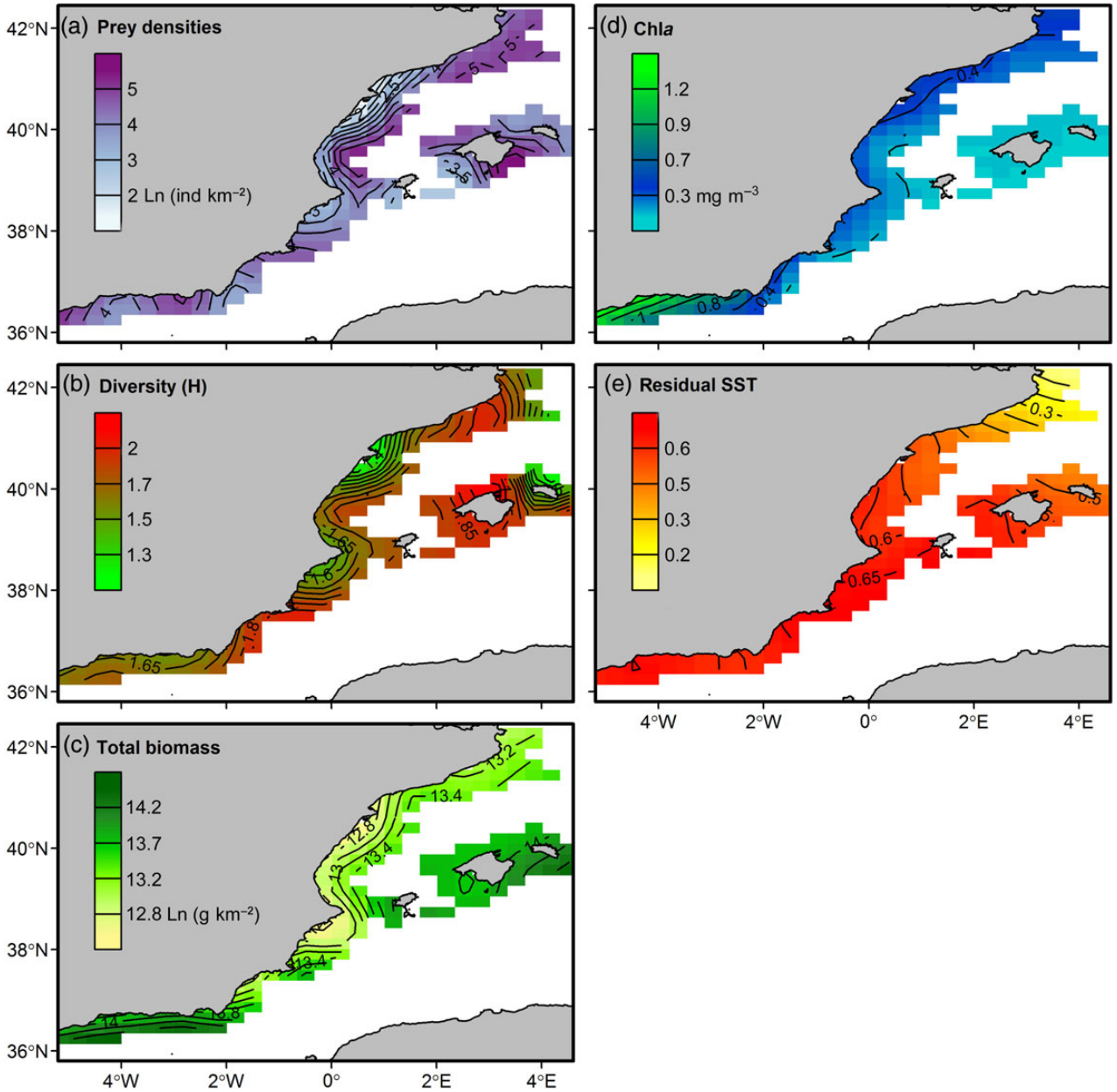

Figure 2. Spatial variability across the study area of the resources (prey densities), community indicators (Shannon – Wiener diversity index, H; total biomass) and environmental (chlorophyll *a* concentration, Chl*a*; residual SST) factors. This figure is available in black and white in print and in colour at *ICES Journal of Marine Science* online.

(61.8%). Therefore, the best model selected included the spatially explicit effects of prey densities, total biomass, diversity, and residual SST, along with density-dependent effect of the octopus population size and a mean bathymetric and geographic effect. Directional variograms (90 and 135 directions) of overlap index data showed a noticeable spatial autocorrelation. However, the model residuals did not showed any dependence pattern (Supplementary Figure S1). Since spatial correlation structure disappeared from the model, it should not influence the estimates and uncertainty.

Density-dependent effect of population size

Increases in the annual population size of octopus resulted in gradual changes in the overlap with catshark (Figure 4). Two spatial patterns were detected in relation to the variation in the overlap distribution. First, the overlap increased in the regions where high overlap values were previously detected, the Balearic Islands and the Catalan Sea. The Alboran Sea and the central coast of the mainland stayed uniform with low overlap values regardless of population size. Second, considering only the high overlap areas, overlap values increased from the boundaries to the centre of overlap area as the population size increased.

Spatially explicit effects

Significant slopes were found between the overlap index and all covariates included as spatially explicit terms in the model, showing contrasting local effects across the study area (Figure 5). Positive effects of prey densities were observed in the Catalan Sea and the islands, where the maximum overlap

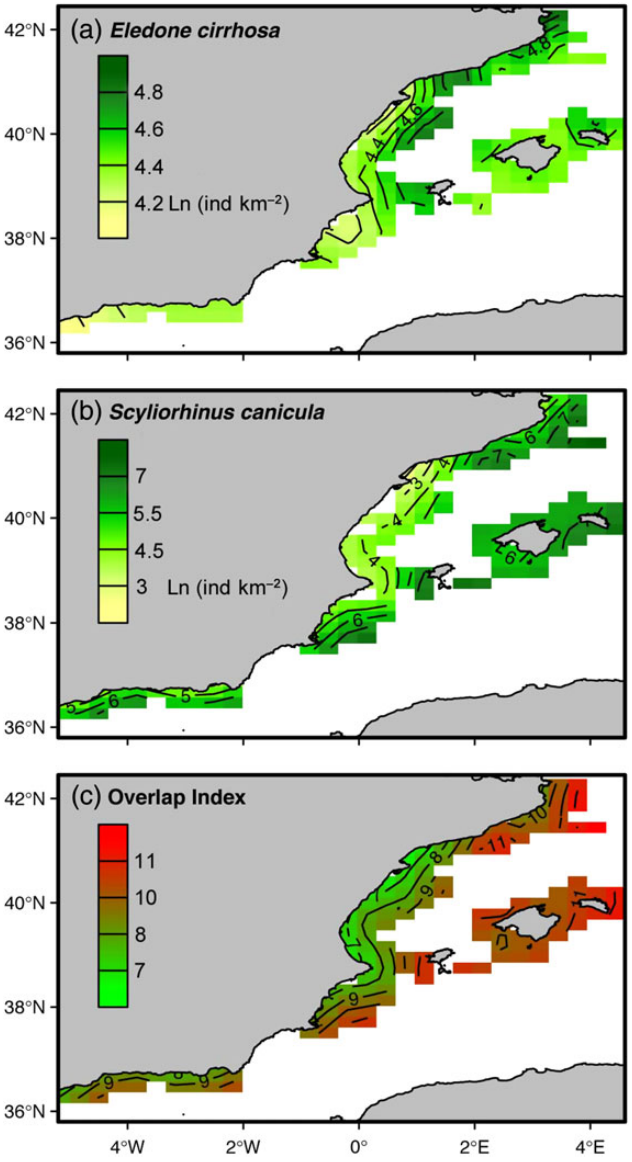

Figure 3. Spatial distribution of log-transformed densities of octopus (*Eledone cirrhosa*) and catshark (*Scyliorhinus canicula*) and the overlap index estimated for the two species. This figure is available in black and white in print and in colour at *ICES Journal of Marine Science* online.

between the species was observed. In contrast, the positive effects of total biomass in the community were generalized across the entire region. However, the strength of this effect was higher in the areas with maximum overlap. A different pattern was observed for the effects of the community diversity. Positive effects were present in the islands and continuing southwards throughout the mainland coast, following approximately the boundary of the overlap distribution. Additionally, negative effects of diversity were detected in the most southwestern region, close to the Strait of Gibraltar. Finally, both negative and positive effects were also observed related to residual SST. In the Catalan Sea, the overlap was negatively influenced by temperature, while the southern boundary of the overlap distribution and part of the Alboran Sea presented positive effects. The colder and warmer SST records characterized, respectively, these two regions.

Discussion

The spatial patterns of the octopus *Eledone cirrhosa* and the catshark *Scyliorhinus canicula* revealed that the overlap of these two species increased as their shared prey densities (benthic crustaceans) increased. Competition between the species could be expected as resource limitation might occur at small spatial and temporal scales in the western Mediterranean Sea. Oligotrophy, pronounced seasonality in productivity (Estrada, 1996; Bosc *et al.*, 2004; D'Ortenzio and Ribera d'Alcalà, 2009) and degradation of habitat conditions, community, and species interactions by fishing pressure (Coll *et al.*, 2006, 2012; Corrales *et al.*, 2015) can all lead to food limitations. Our model approach allows considering spatial patterns in a relative broad geographic area, while the species overlap and its drivers are evaluated at local scales where imprints of competitive interactions can be still discernible (Araújo and Rozenfeld, 2014). However, deducing processes from spatial patterns are still a challenge in ecological research and inferences should be taken with caution. The results showed that spatial and diet overlap does not necessarily imply competition and a constraint in the species-specific distributions. This is in accordance with the theoretical framework of species interactions which indicates that species overlap at broad scales are only evident when actually there is no negative relationship between those species (Gotelli *et al.*, 2010; Araújo and Rozenfeld, 2014). As we hypothesized, different ecological mechanisms allow for successful coexistence of species with the same resource requirements (Hofer *et al.*, 2004). Density-dependent, environmental, trophic, and community factors play a role in the coexistence between the octopus and the catshark across the study area.

Overlap was not spatially homogeneous, since the overlap index depends on the species abundance and distribution. Catshark showed much higher densities than octopus across the study area. Additionally, the spatial pattern in the overlap was similar to the catshark distribution. However, variability in octopus population size better described variations in overlap patterns. The differences in the species life history strategies may explain those patterns. Catshark is a long-lived species (k-strategy), which usually presents densities close to carrying capacity and successive coexisting generations. The long lifespan and the demographic buffering support more steady populations over time, and higher success in fluctuating environments (Reznick *et al.*, 2002 and references therein). Opposite traits (r-strategy) define the cephalopod life cycles. The short lifespan with no overlap among generations, make populations very sensitive to changing conditions (Pierce *et al.*, 2008), especially at local scales (Puerta *et al.*, 2014b). They display high fluctuations as a consequence.

High overlap values (i.e. high densities of the two species) were detected in the northern mainland (Catalan Sea) and the Balearic Islands, indicating a low or lack of competition in these areas. In contrast, the low overlap areas corresponded to low densities of catshark and octopus and were not affected by species population size. Catshark was only absent in the central coast of the mainland, where low biomass and diversity were also observed. These patterns in the community indicators agree with the high fishing pressure observed nearby the Ebro river mouth (Coll *et al.*, 2012; Navarro *et al.*, 2015, 2016). Due to the long-living strategy, elasmobranchs are very sensitive to long-term disturbances such as fishing pressure since populations present low resilience and recovery (Guijarro *et al.*, 2012; Barausse *et al.*, 2014; Navarro *et al.*, 2015, 2016; Quetglas *et al.*, 2016). In accordance with previous research (Cartes *et al.*, 2013; Navarro *et al.*, 2015, 2016), these results point the high fishing pressure of this area as responsible for the decline of elasmobranch

Table 1. Comparison of full and reduced GAMs of overlap index.

Model	AIC	gCV	Dev (%)
$O_{(\phi,\lambda)} = s_1(\phi,\lambda) + s_2(depth_{(\phi,\lambda)}) + te(\phi,\lambda,size.S) + s_3(\phi,\lambda)^*prey_{(\phi,\lambda),y} + s_4(\phi,\lambda)^*biomass_{(\phi,\lambda),y} + s_5(\phi,\lambda)^*H_{(\phi,\lambda),y} + s_6(\phi,\lambda)^*SST_{(\phi,\lambda),y} + s_7(\phi,\lambda)^*Chla_{(\phi,\lambda),y}$	4720.57	2.43	60.70
$O_{(\phi,\lambda)} = s_1(\phi,\lambda) + s_2(depth_{(\phi,\lambda)}) + te(\phi,\lambda,size.S) + s_3(\phi,\lambda)^*prey_{(\phi,\lambda),y} + s_4(\phi,\lambda)^*biomass_{(\phi,\lambda),y} + s_5(\phi,\lambda)^*H_{(\phi,\lambda),y} + s_6(\phi,\lambda)^*SST_{y(\phi,\lambda),y}$	4717.79	2.41	60.50
$O_{(\phi,\lambda)} = s_1(\phi,\lambda) + s_2(depth_{(\phi,\lambda)}) + te(\phi,\lambda,size.S) + s_3(\phi,\lambda)^*prey_{(\phi,\lambda),y} + s_4(\phi,\lambda)^*biomass_{(\phi,\lambda),y} + s_5(\phi,\lambda)^*H_{(\phi,\lambda),y}$	4719.72	2.39	60.40
$O_{(\phi,\lambda)} = s_1(\phi,\lambda) + s_2(depth_{(\phi,\lambda)}) + te(\phi,\lambda,size.E) + s_3(\phi,\lambda)^*prey_{(\phi,\lambda),y} + s_4(\phi,\lambda)^*biomass_{(\phi,\lambda),y} + s_5(\phi,\lambda)^*H_{(\phi,\lambda),y} + s_6(\phi,\lambda)^*SST_{(\phi,\lambda),y} + s_7(\phi,\lambda)^*Chla_{(\phi,\lambda),y}$	4704.83	2.43	61.80
$O_{(\phi,\lambda)} = s_1(\phi,\lambda) + s_2(depth_{(\phi,\lambda)}) + te(\phi,\lambda,size.E) + s_3(\phi,\lambda)^*prey_{(\phi,\lambda),y} + s_4(\phi,\lambda)^*biomass_{(\phi,\lambda),y} + s_5(\phi,\lambda)^*H_{(\phi,\lambda),y} + s_6(\phi,\lambda)^*SST_{(\phi,\lambda),y}$	**4700.87**	**2.38**	**61.80**
$O_{(\phi,\lambda)} = s_1(\phi,\lambda) + s_2(depth_{(\phi,\lambda)}) + te(\phi,\lambda,size.E) + s_4(\phi,\lambda)^*biomass_{(\phi,\lambda),y} + s_5(\phi,\lambda)^*H_{(\phi,\lambda),y} + s_6(\phi,\lambda)^*SST_{(\phi,\lambda),y}$	4708.82	2.40	61.20

Full model of overlap index ($O_{(\phi,\lambda)}$) includes longitude (ϕ), latitude(λ), depth, *E. cirrhosa* (size.E) or *S. canicula* (size.S) population size, prey densities (prey), total biomass in the community (biomass), diversity (H), sea surface temperature (SST) and chlorophyll concentration (Chla) as covariates. Dev, deviance explained; AIC, Akaike Information Criterion; gCV, genuine Cross Validation. Best model is in bold.

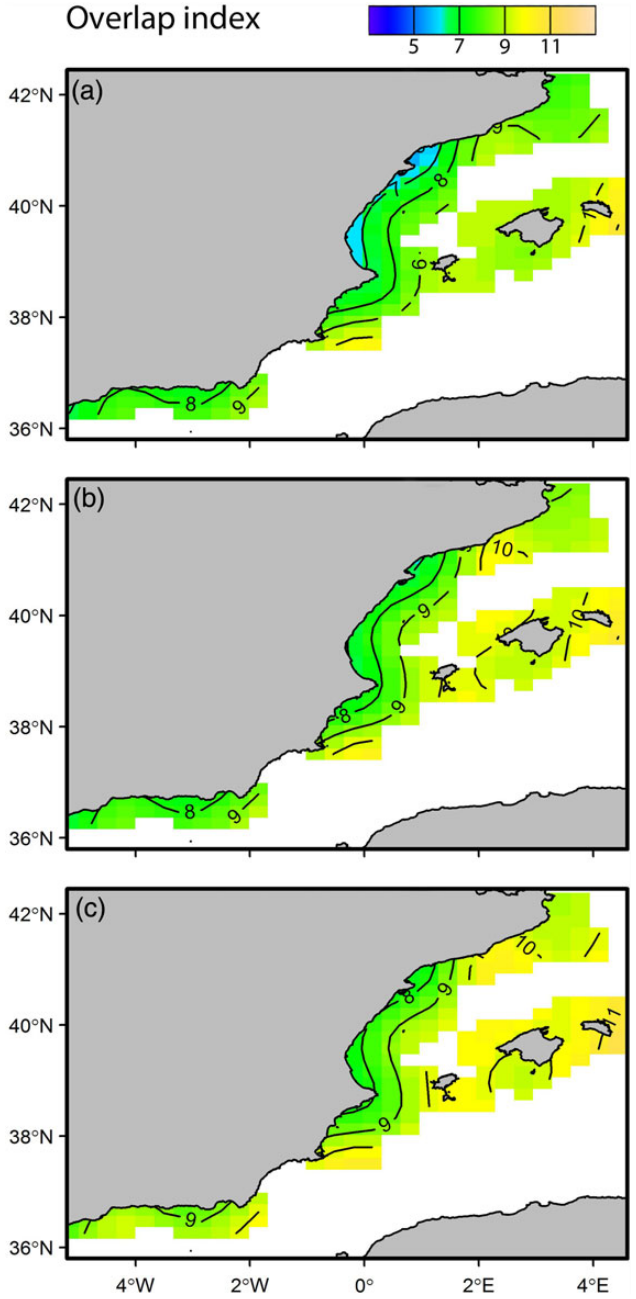

Figure 4. Changes in the spatial patterns of overlap index between octopus and catshark, with increases in the octopus population size. (a) Population size = 3000 ind km^2. (b) Population size = 9000 ind km^2. (c) Population size = 20 000 ind km^2. This figure is available in black and white in print and in colour at *ICES Journal of Marine Science* online.

populations, along with changes in salinity that can lessen habitat suitability. In contrast, the fast-living strategy makes cephalopod populations highly resilient and therefore, their spatial distribution is mainly forced by the short-term environmental variability, being no affected by fishing impact (Caddy and Rodhouse, 1998; Coll *et al.*, 2013; Navarro *et al.*, 2015; Quetglas *et al.*, 2016). The high hydro-dynamism and varying conditions in the southern area (Alboran Sea) may make this area less suitable to cephalopods (Puerta *et al.*, 2015). High densities in prey and catshark and low in octopus found in the Alboran Sea could also reflect a prior

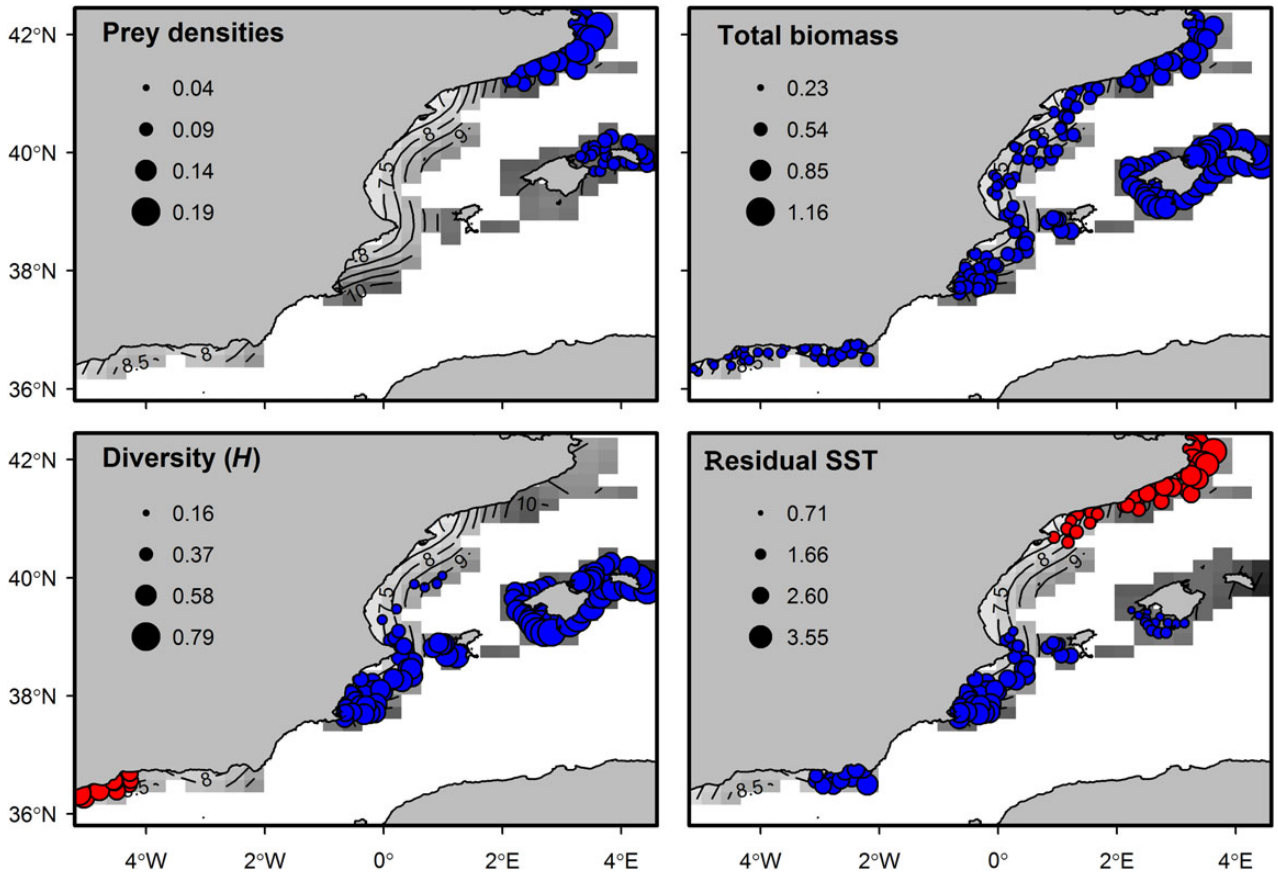

Figure 5. Spatially explicit effects of resources (prey densities), community indicators (Shannon – Wiener diversity index, H; total biomass), and environmental (residual SST) factors on the overlap index. Only significant positive (blue) and negative (red) effects (regression slopes based on 95% confidence interval) are shown. Patterns of spatial overlap are presented (grey contour), with high and low values of overlap indicated by dark and light grey shading, respectively. This figure is available in black and white in print and in colour at *ICES Journal of Marine Science* online.

competitive exclusion process in this area. However, the effects of other factors not considered in this study, e.g. substrate, predation, or local seasonality in octopus populations (Vargas-Yáñez *et al.*, 2009; Puerta *et al.*, 2014b) cannot be discarded.

According to the species range hypothesis, populations living at distributional boundaries are more influenced by environmental changes because habitat conditions are less suitable there than in the core distribution area (Rosenzweig, 1991; Brunel and Boucher, 2006). In a similar way, species overlap was more sensitive to population size effects in the boundaries of high overlap areas, i.e. Catalan Sea and Balearic Islands, where prey densities were lower compared with the core. As predator population sizes increased, their spatial overlap first increased in the boundaries, which might reflect a strategy to reduce competition and diversify diets (see below). In contrast, under high-population densities, the species overlap extended to the central area, where higher prey densities were found. In accordance with these results, positive effects of prey were observed in the high overlap areas. These results reinforced our hypothesis of shared resources as a mechanism for spatial overlap, where coexistence is allowed by other ecological processes. Despite the considerable fishing pressure reported in the Catalan Sea (Moranta *et al.*, 2008; Quetglas *et al.*, 2012; Navarro *et al.*, 2015, 2016), intermediate and high values of biomass and diversity, respectively, were observed in this area. The Catalan Sea is one of the most productive areas in the western Mediterranean due to the influence of the upwelling and nutrient-rich waters from the Gulf of Lions (Estrada, 1996; D'Ortenzio and Ribera d'Alcalà, 2009) that can supply enough resources to maintain prey and competitor populations at relatively high densities.

Very high diversity was observed around the Balearic Islands, where the high overlap was more related to this factor than to prey densities. High species diversity is associated with complex, diverse, and "healthy" seascapes in structure and functioning (Thrush *et al.*, 2006; Foley *et al.*, 2010 and references therein). This pattern is in agreement with the lower fishing pressure and better state of conservation observed in the islands compared with the mainland areas (Moranta *et al.*, 2008; Quetglas *et al.*, 2012; Navarro *et al.*, 2015, 2016). These systems provide more opportunities to exploit different resources, thus favouring species coexistence (Bonin *et al.*, 2009; Geange and Stier, 2010). Opportunistic species with wide range of prey items, such as octopus and catshark, may show slightly different feeding habits to avoid competition in high resource and complex ecosystems. For instance, in addition to benthic crustaceans, the two species also consume polychaetes, molluscs, or small fishes (Valls *et al.*, 2011; Puerta *et al.*, 2015). These results are in agreement with the regional effect observed for total biomass in the community, which showed a general increment in overlap when resources (specific prey items and others) are higher.

In the western Mediterranean, trophic pathways are the most plausible link between surface conditions, such as SST, and benthic

communities (Cartes *et al.*, 2009; Fanelli *et al.*, 2013). Residual SST showed contrasting spatial effects on overlap along the temperature-geographic gradient. Similar SST spatial effects were also detected in the distribution of the two species (Supplementary Figure S2), suggesting a common response to SST in the benthic community. This response is likely related to differences in the foodwebs and the energy transfer efficiency between northern and southern regions of the study area (Fanelli *et al.*, 2013). Benthic communities are mainly supported by surface primary production throughout vertical flux of organic matter (Turner, 2015 and references therein), which in turn depend on the type of phytoplankton community (Guidi *et al.*, 2009). In the western Mediterranean, phytoplankton composition change seasonally from a dominance of large cells during winter and spring blooms to a higher contribution of the pico-size fraction in summer (Agawin *et al.*, 1998, 2000; Arin *et al.*, 2005). Residuals of SST indicated that northern and southern areas were at different stages of the seasonal transition during spring (Figure 2). Therefore, opposite spatial effects of SST might reflect different mechanisms supplying resources from surface to deeper benthic communities via primary producers that lastly favour species overlap.

Lower values and negative spatial effects of SST observed in the Catalan Sea might be associated with the influence of colder and nutrient-richer waters from the Gulf of Lions over time (Miquel *et al.*, 2011; Heimbürger *et al.*, 2013; Estrada *et al.*, 2014) that trigger the spring bloom (Estrada, 1996; D'Ortenzio and Ribera d'Alcalà, 2009). In contrast, the southern areas are warmer and more oligotrophic, showing no blooms (D'Ortenzio and Ribera d'Alcalà, 2009). At the residual SST observed here, pico-phytoplankton community is expected to be already dominant (Agawin *et al.*, 1998, 2000; Partensky *et al.*, 1999; Arin *et al.*, 2005). Warmer temperatures increase productivity and turnover rates of pico-size cells (Agawin *et al.*, 1998, 2000), which might explain the positive effects of SST. Regardless of the mechanism, the rapid vertical fluxes (few days from subsurface production to seabed, Peterson *et al.*, 2005) might favour the octopus-catshark overlap. It is worth noting that during spring, a deep chlorophyll maximum is also observed under the thermocline (Estrada, 1996), which may also influence the benthic community.

The present study highlights the necessity of a deeper knowledge in species interactions combining small and large spatial scales. Distribution and interaction patterns between species arose from local variability in the seascapes across geographical ranges, where community and trophic features play an important role. However, some other factors should be considered in future research to improve the inference of competitive interactions from spatial patterns. For instance, information on fishing pressure could provide more accurate description of the spatial pattern in overlap. Additionally, the segregation by size described for the two species can also play a role in the octopus-catshark competitive interactions. The results described a spatial structuring not limited to population distributions and also observed for the species interactions (coexistence or exclusion). Areas with high resources in terms of specific prey items (Catalan Sea) or alternative supplies, such as niche opportunities and ecosystem functions, defined by community diversity (Balearic Islands) favoured species coexistence. Our study also suggests that pelagic seascapes (surface temperature and primary production) are not independent of the benthic realm, and the dynamic benthic-pelagic coupling needs to be taking into account in oligotrophic systems such as the Mediterranean Sea. Characterizing species interactions across space and time is pivotal to properly address community spatial dynamics and move towards ecosystem-based management (Sexton *et al.*, 2009; Foley *et al.*, 2010; Link and Auster, 2013) for sustainable fisheries and conservation planning.

Supplementary data

Supplementary material is available at the *ICESJMS* online version of the manuscript.

Acknowledgements

We are very grateful to all scientists and vessel crew that participated in the MEDITS surveys. This research is supported by the project "ECLIPSAME" (Synergistics effects of Climate and Fishing on the demersal ecosystems of the North Atlantic and western Mediterranean, CTM2012-37701) financed by the Spanish Ministry of Economy and Competitiveness. Surveys were co-funded by the Directorate-General for Maritime Affairs and Fisheries (DG-MARE) of the European Commission and the Spanish Institute of Oceanography (IEO). P.P. is supported by the funding of FPI grant BES-2010-030315 from the Spanish Ministry of Economy and Competitiveness. M.E.H.'s funding is provided by the Gordon and Betty Moore Foundation. M.H. was funded by MYFISH project (EU contract number 289257) and a post-doctoral contract from the regional government of the Balearic Islands, Dirección General d'Educació, Personal Docent, Universitats i Recerca, co-funded by the European Social Fund 2014-2020. L.C. acknowledges support from the National Science Foundation, grant number: 1140207.

References

Agawin, N. S. R., Duarte, C. M., and Agustí, S. 1998. Growth and abundance of *Synechococcus* sp. in a Mediterranean bay: seasonality and relationship with temperature. Marine Ecology Progress Series, 170: 45–53.

Agawin, N. S. R., Duarte, C. M., and Agustí, S. 2000. Nutrient and temperature control of the contribution of picoplankton to phytoplankton biomass and production. Limnology and Oceanography, 45: 591–600.

Albouy, C., Velez, L., Coll, M., Colloca, F., Le Loc'h, F., Mouillot, D., and Gravel, D. 2014. From projected species distribution to food-web structure under climate change. Global Change Biology, 20: 730–741.

André, J., Haddon, M., and Pecl, G. T. 2010. Modelling climate-change-induced nonlinear thresholds in cephalopod population dynamics. Global Change Biology, 16: 2866–2875.

Araújo, M. B., and Rozenfeld, A. 2014. The geographic scaling of biotic interactions. Ecography, 37: 406–415.

Arin, L., Estrada, M., Salat, J., and Cruzado, A. 2005. Spatio-temporal variability of size fractionated phytoplankton on the shelf adjacent to the Ebro river (NW Mediterranean). Continental Shelf Research, 25: 1081–1095.

Bacheler, N. M., Bailey, K. M., Ciannelli, L., Bartolino, V., and Chan, K-S. 2009. Density-dependent, landscape, and climate effects on spawning distribution of walleye pollock *Theragra chalcogramma*. Marine Ecology Progress Series, 391: 1–12.

Barausse, A., Correale, V., Curkovic, A., Finotto, L., Riginella, E., Visentin, E., and Mazzoldi, C. 2014. The role of fisheries and the environment in driving the decline of elasmobranchs in the northern Adriatic Sea. ICES Journal of Marine Science, 71: 236–240.

Bartolino, V., Ciannelli, L., Bacheler, N. M., and Chan, K-S. 2011. Ontogenetic and sex-specific differences in density-dependent habitat selection of a marine fish population. Ecology, 92: 189–200.

Belcari, P., Tserpes, G., González, M., Lefkaditou, E., Marceta, B., and Manfrin, G. P. 2002. Distribution and abundance of *Eledone cirrhosa* (Lamarck, 1798) and *E. moschata* (Lamarck, 1798) (Cephalopoda?: Octopoda) in the Mediterranean Sea. Scientia Marina, 66: 143–155.

Bertrand, J. A., Gil de Sola, L., Papaconstantinou, C., Relini, G., and Souplet, A. 2002. The general specifications of the MEDITS surveys. Scientia Marina, 66: 9–17.

Bonin, M. C., Srinivasan, M., Almany, G. R., and Jones, G. P. 2009. Interactive effects of interspecific competition and microhabitat on early post-settlement survival in a coral reef fish. Coral Reefs, 28: 265–274.

Bosc, E., Bricaud, A., and Antoine, D. 2004. Seasonal and interannual variability in algal biomass and primary production in the Mediterranean Sea, as derived from 4 years of SeaWiFS observations. Global Biogeochemical Cycles, 18: GB1005.

Boström-Einarsson, L. E., Bonin, M. C., Munday, P. L., and Jones, G. P. 2014. Habitat degradation modifies the strength of interspecific competition in coral dwelling damselfishes. Ecology, 95: 3056–3067.

Boyle, P., and Rodhouse, P. 2005. Cephalopods Ecology and Fisheries. Blackwell Science, London.

Boyle, P. R., Grisley, M. S., and Robertson, G. 1986. Crustacea in the diet of *Eledone cirrhosa* (Mollusca: Cephalopoda) determined by serological methods. Journal of the Marine Biological Association of the United Kingdom, 66: 867–879.

Brunel, T., and Boucher, J. 2006. Pattern of recruitmennt variability in the geographical range of the exploited northeast Atlantic fish species. Journal of Sea Research, 55: 156–168.

Butler, M. J., and Lear, J. A. 2009. Habitat-based intraguild predation by Caribbean reef octopus *Octopus briareus* on juvenile Caribbean spiny lobster *Panulirus argus*. Marine Ecology Progress Series, 386: 115–122.

Caddy, J. F., and Rodhouse, P. G. 1998. Cephalopod and groundfish landings: evidence for ecological change in global fisheries? Reviews in Fish Biology and Fisheries, 8: 431–444.

Cartes, J., Fanelli, E., Lloris, D., and Matallanas, J. 2013. Effect of environmental variations on shark and other megafauna assemblages in the deep Mediterranean Sea over the last 60 years. Climate Research, 55: 239–251.

Cartes, J. E., Maynou, F., Fanelli, E., Papiol, V., and Lloris, D. 2009. Long-term changes in the composition and diversity of deep-slope megabenthos and trophic webs off Catalonia (western Mediterranean): are trends related to climatic oscillations? Progress in Oceanography, 82: 32–46.

Ciannelli, L., and Bailey, K. M. 2005. Landscape dynamics and resulting species interactions: the cod-capelin system in the southeastern Bering Sea. Marine Ecology Progress Series, 291: 227–236.

Ciannelli, L., Bartolino, V., and Chan, K-S. 2012. Non-additive and non-stationary properties in the spatial distribution of a large marine fish population. Proceedings of the Royal Society B: Biological Sciences, 279: 3635–3642.

Ciannelli, L., Fauchald, P., Chan, K. S., Agostini, V. N., and Dingsør, G. E. 2008. Spatial fisheries ecology: recent progress and future prospects. Journal of Marine Systems, 71: 223–236.

Cobb, C. S., Williamson, R., and Pope, S. K. 1995. The responses to the epistellar photoreceptors to light and their effect on circadian rhythms in the lesser octopus, *Eledone cirrhosa*. Marine and Freshwater Behaviour and Physiology, 26: 59–69.

Coll, M., Navarro, J., Olson, R. J., and Christensen, V. 2013. Assessing the trophic position and ecological role of squids in marine ecosystems by means of food-web models. Deep Sea Research Part II: Topical Studies in Oceanography, 95: 21–36.

Coll, M., Palomera, I., Tudela, S., and Dowd, M. 2008. Food-web dynamics in the South Catalan Sea ecosystem (NW Mediterranean) for 1978–2003. Ecological Modelling, 217: 95–116.

Coll, M., Palomera, I., Tudela, S., and Sardà, F. 2006. Trophic flows, ecosystem structure and fishing impacts in the South Catalan Sea, Northwestern Mediterranean. Journal of Marine Systems, 59: 63–96.

Coll, M., Piroddi, C., Albouy, C., Ben Rais Lasram, F., Cheung, W. W. L., Christensen, V., Karpouzi, V. S., *et al.* 2012. The Mediterranean Sea under siege: spatial overlap between marine biodiversity, cumulative threats and marine reserves. Global Ecology and Biogeography, 21: 465–480.

Cormon, X., Loots, C., Vaz, S., Vermard, Y., and Marchal, P. 2014. Spatial interactions between saithe (*Pollachius virens*) and hake (*Merluccius merluccius*) in the North Sea. ICES Journal of Marine Science, 71: 1342–1355.

Corrales, X., Coll, M., Tecchio, S., Bellido, J. M., Fernández, Á. M., and Palomera, I. 2015. Ecosystem structure and fishing impacts in the northwestern Mediterranean Sea using a food web model within a comparative approach. Journal of Marine Systems, 148: 183–199.

Dambach, J., and Rödder, D. 2011. Applications and future challenges in marine species distribution modeling. Aquatic Conservation: Marine and Freshwater Ecosystems, 21: 92–100.

D'Ortenzio, F., and Ribera d'Alcalà, M. 2009. On the trophic regimes of the Mediterranean Sea?: a satellite analysis. Biogeosciences, 6: 139–148.

Ellis, J., Mancusi, C., Serena, F., Haka, F., Guallart, J., Ungaro, N., Coelho, R., *et al.* 2009. Scyliorhinus canicula. www.iucnredlist.org (last accessed 11 May 2015).

Estrada, M. 1996. Primary production in the northwestern Mediterranean. Scientia Marina, 60: 55–64.

Estrada, M., Latasa, M., Emelianov, M., Gutiérrez-Rodríguez, A., Fernández-Castro, B., Isern-Fontanet, J., Mouriño-Carballido, B., *et al.* 2014. Seasonal and mesoscale variability of primary production in the deep winter-mixing region of the NW Mediterranean. Deep Sea Research Part I: Oceanographic Research Papers, 94: 45–61.

Fanelli, E., Cartes, J. E., Papiol, V., and López-Pérez, C. 2013. Environmental drivers of megafaunal assemblage composition and biomass distribution over mainland and insular slopes of the Balearic Basin (Western Mediterranean). Deep Sea Research Part I: Oceanographic Research Papers, 78: 79–94.

Foley, M. M., Halpern, B. S., Micheli, F., Armsby, M. H., Caldwell, M. R., Crain, C. M., Prahler, E., *et al.* 2010. Guiding ecological principles for marine spatial planning. Marine Policy, 34: 955–966.

Gasalla, M. A., Rodrigues, A. R., and Postuma, F. A. 2010. The trophic role of the squid *Loligo plei* as a keystone species in the South Brazil Bight ecosystem. ICES Journal of Marine Science, 67: 1413–1424.

Geange, S. W., and Stier, A. C. 2010. Priority effects and habitat complexity affect the strength of competition. Oecologia, 163: 111–118.

Gotelli, N. J., Graves, G. R., and Rahbek, C. 2010. Macroecological signals of species interactions in the Danish avifauna. Proceedings of the National Academy of Sciences of the United States of America, 107: 5030–5035.

Gouraguine, A., Hidalgo, M., Moranta, J., Bailey, D. M., Ordines, F., Guijarro, B., Valls, M., *et al.* 2011. Elasmobranch spatial segregation in the western Mediterranean. Scientia Marina, 75: 653–664.

Guidi, L., Stemmann, L., Jackson, G. a., Ibanez, F., Claustre, H., Legendre, L., Picheral, M., *et al.* 2009. Effects of phytoplankton community on production, size, and export of large aggregates: a world-ocean analysis. Limnology and Oceanography, 54: 1951–1963.

Guijarro, B., Quetglas, A., Moranta, J., Ordines, F., Valls, M., González, N., and Massutí, E. 2012. Inter- and intra-annual trends and status indicators of nektobenthic elasmobranchs off the Balearic Islands (northwestern Mediterranean). Scientia Marina, 76: 87–96.

Heimbürger, L. E., Lavigne, H., Migon, C., D'Ortenzio, F., Estournel, C., Coppola, L., and Miquel, J. C. 2013. Temporal variability of vertical export flux at the DYFAMED time-series station (Northwestern Mediterranean Sea). Progress in Oceanography, 119: 59–67.

Hofer, U., Bersier, L. F., and Borcard, D. 2004. Relating niche and spatial overlap at the community level. Oikos, 106: 366–376.

Hunsicker, M., Ciannelli, L., Bailey, K., and Zador, S. 2010. Processes driving differences in major food web linkages of the Gulf of Alaska and eastern Bering Sea ecosystems. ICES CM 2010/S:06.

Johnson, A. F., Jenkins, S. R., Hiddink, J. G., and Hinz, H. 2013. Linking temperate demersal fish species to habitat: scales, patterns and future directions. Fish and Fisheries, 14: 256–280.

Kempf, A., Stelzenmüller, V., Akimova, A., and Floeter, J. 2013. Spatial assessment of predator-prey relationships in the North Sea: the influence of abiotic habitat properties on the spatial overlap between 0-group cod and grey gurnard. Fisheries Oceanography, 22: 174–192.

Kilpatrick, K. A., Podestá, G. P., and Evans, R. 2001. Overview of the NOAA/NASA advanced very high resolution radiometer Pathfinder algorithm for sea surface temperature and associated matchup database. Journal of Geophysical Research: Oceans, 106: 9179–9197.

Kordas, R. L., Harley, C. D. G., and O'Connor, M. I. 2011. Community ecology in a warming world: the influence of temperature on interspecific interactions in marine systems. Journal of Experimental Marine Biology and Ecology, 400: 218–226.

Link, J. S., and Auster, P. J. 2013. The challenges of evaluating competition among marine fishes: who cares, when does it matter, and what can one do about it? Bulletin of Marine Science, 89: 213–247.

Martinho, F., Sá, C., Falcão, J., Cabral, H. N., and Pardal, M. Â. 2012. Comparative feeding ecology of two elasmobranch species, *Squalus blainville* and *Scyliorhinus canicula*, off the coast of Portugal. Fishery Bulletin, 110: 71–84.

Miquel, J. C., Martín, J., Gasser, B., Rodriguez-y-Baena, A., Toubal, T., and Fowler, S. W. 2011. Dynamics of particle flux and carbon export in the northwestern Mediterranean Sea: a two decade time-series study at the DYFAMED site. Progress in Oceanography, 91: 461–481.

Moranta, J., Quetglas, A., Massutí, E., Guijarro, B., Hidalgo, M., and Diaz, P. 2008. Spatio-temporal variations in deep-sea demersal communities off the Balearic Islands (western Mediterranean). Journal of Marine Systems, 71: 346–366.

Navarro, J., Cardador, L., Fernández, Á. M., Bellido, J. M., and Coll, M. 2016. Differences in the relative roles of environment, prey availability and human activity in the spatial distribution of two marine mesopredators living in highly exploited ecosystems. Journal of Biogeography, 43: 440–450.

Navarro, J., Coll, M., Cardador, L., Fernández, Á. M., and Bellido, J. M. 2015. The relative roles of the environment, human activities and spatial factors in the spatial distribution of marine biodiversity in the Western Mediterranean Sea. Progress in Oceanography, 131: 126–137.

Orrock, J. L., and Watling, J. I. 2010. Local community size mediates ecological drift and competition in metacommunities. Proceedings of the Royal Society B: Biological Sciences, 277: 2185–2191.

Partensky, F., Blanchot, J., and Vaulot, D. 1999. Differential distribution and ecology of *Prochlorococcus* and *Synechococcus* in oceanic waters: a review. Bulletin de lInstitut Océanographique, 19: 457–475.

Pennino, M. G., Muñoz, F., Conesa, D., López-Quílez, A., and Bellido, J. M. 2013. Modeling sensitive elasmobranch habitats. Journal of Sea Research, 83: 209–218.

Peterson, M. L., Wakeham, S. G., Lee, C., Askea, M. A., and Miquel, J. C. 2005. Novel techniques for collection of sinking particles in the ocean and determining their settling rates. Limnology and Oceanography: Methods, 3: 520–532.

Pierce, G. J., Valavanis, V. D., Guerra, A., Jereb, P., Orsi-Relini, L., Bellido, J. M., Katara, I., *et al.* 2008. A review of cephalopod–environment interactions in European Seas. Hydrobiologia, 612: 49–70.

Puerta, P., Hidalgo, M., González, M., Esteban, A., and Quetglas, A. 2014a. Role of hydro-climatic and demographic processes on the spatio-temporal distribution of cephalopods in the Western Mediterranean. Marine Ecology Progress Series, 514: 105–118.

Puerta, P., Hunsicker, M. E., Quetglas, A., Álvarez-Berastegui, D., Esteban, A., González, M., and Hidalgo, M. 2015. Spatially explicit modeling reveals cephalopod distributions match contrasting trophic pathways in the western Mediterranean Sea. PLoS ONE, 10: e0133439.

Puerta, P., Quetglas, A., and Hidalgo, M. 2014b. Modelling seasonal variability of cephalopod abundances of three contrasting species from Western Mediterranean Sea. ICES CM 2014/P:02.

Quetglas, A., Guijarro, B., Ordines, F., and Massutí, E. 2012. Stock boundaries for fisheries assessment and management in the Mediterranean: the Balearic Islands as a case study. Scientia Marina, 76: 17–28.

Quetglas, A., Rueda, L., Alvarez-Berastegui, D., Guijarro, B., and Massutí, E. 2016. Contrasting responses to harvesting and environmental drivers of fast and slow life history species. PLoS ONE, 11: e0148770.

Reznick, D., Bryant, M. J., and Bashey, F. 2002. r- and K-selection revisited: the role of population regulation in life-history evolution. Ecology, 83: 1509–1520.

Rodhouse, P. G. K., Pierce, G. J., Nichols, O. C., Sauer, W. H. H., Arkhipkin, A. I., Laptikhovsky, V. V., Lipiński, M. R., *et al.* 2014. Environmental effects on cephalopod population dynamics: implications for management of fisheries. Advances in Marine Biology, 67: 99–233.

Rodríguez-Cabello, C., Sánchez, F., Fernández, A., and Olaso, I. 2004. Is the lesser spotted dogfish (*Scyliorhinus canicula*) population from the Cantabrian Sea a unique stock? Fisheries Research, 69: 57–71.

Rodríguez-Cabello, C., Sánchez, F., and Olaso, I. 2007. Distribution patterns and sexual segregations of *Scyliorhinus canicula* (L.) in the Cantabrian Sea. Journal of Fish Biology, 70: 1568–1586.

Rosenzweig, M. L. 1991. Habitat selection and population interactions?: the search for mechanism. The American Naturalist, 137: S5–S28.

Santoleri, R., Böhm, E., and Schiano, M. E. 1994. The sea surface temperature of the Western Mediterranean Sea: historical satellite thermal data. *In* Seasonal and Interannual Variability of the Western Mediterranean Sea, pp. 155–176. Ed. by P. E. La Viollette. American Geophysical Union, Washington, DC.

Sexton, J. P., McIntyre, P. J., Angert, A. L., and Rice, K. J. 2009. Evolution and ecology of species range limits. Annual Review of Ecology, Evolution, and Systematics, 40: 415–436.

Sims, D., Nash, J., and Morritt, D. 2001. Movements and activity of male and female dogfish in a tidal sea lough: alternative behavioural strategies and apparent sexual segregation. Marine Biology, 139: 1165–1175.

Staudinger, M. D., Juanes, F., Salmon, B., and Teffer, A. K. 2013. The distribution, diversity, and importance of cephalopods in top predator diets from offshore habitats of the Northwest Atlantic Ocean. Deep Sea Research Part II: Topical Studies in Oceanography, 95: 182–192.

Stewart, J. S., Hazen, E. L., Bograd, S. J., Byrnes, J. E. K., Foley, D. G., Gilly, W. F., Robison, B. H., *et al.* 2014. Combined climate- and prey-mediated range expansion of Humboldt squid (*Dosidicus gigas*), a large marine predator in the California Current System. Global Change Biology, 20: 1832–1843.

Thrush, S. F., Gray, J. S., Hewitt, J. E., and Ugland, K. I. 2006. Predicting the effects of habitat homogenization on marine biodiversity. Ecological Applications, 16: 1636–1642.

Turner, J. T. 2015. Zooplankton fecal pellets, marine snow, phytodetritus and the ocean's biological pump. Progress in Oceanography, 130: 205–248.

Valls, M., Quetglas, A., Ordines, F., and Moranta, J. 2011. Feeding ecology of demersal elasmobranchs from the shelf and slope off the Balearic Sea (western Mediterranean). Scientia Marina, 75: 633–639.

Vargas-Yáñez, M., Moya, F., García-Martínez, M., Rey, J., González, M., and Zunino, P. 2009. Relationships between *Octopus vulgaris* landings and environmental factors in the northern Alboran Sea (Southwestern Mediterranean). Fisheries Research, 99: 159–167.

Walton, C. C., Pichel, W. G., Sapper, J. F., and May, D. A. 1998. The development and operational application of nonlinear algorithms for the measurement of sea surface temperatures with the NOAA polar-orbiting environmental satellites. Journal of Geophysical Research: Oceans, 103: 27999–28012.

Worm, B., and Lotze, H. K. 2009. Changes in marine biodiversity as an indicator of climate change. *In* Climate Change: Observed Impacts on Planet Earth, pp. 263–279. Ed. by T. M. Letcher. Elsevier BV, Oxford. 492 pp.

Handling editor: Francis Juanes

ICES Journal of Marine Science

ICES Journal of Marine Science (2016), 73(7), 1912–1924. doi:10.1093/icesjms/fsv166

Contribution to the Themed Section: '*Seascape Ecology*'

Original Article

Using habitat association models to predict Alewife and Blueback Herring marine distributions and overlap with Atlantic Herring and Atlantic Mackerel: can incidental catches be reduced?

Sara M. Turner[1]*, John P. Manderson[2], David E. Richardson[1], John J. Hoey[1], and Jonathan A. Hare[1]

[1]*NOAA Northeast Fisheries Science Center, Narragansett, RI 02882, USA*
[2]*NOAA Northeast Fisheries Science Center, Highlands, NJ 07732, USA*

**Corresponding author: tel: +1 401 782 3260; fax: +1 401 782 3292; e-mail: sara.turner@noaa.gov; smturner483@gmail.com*

Turner, S. M., Manderson, J. P., Richardson, D. E., Hoey, J. J., and Hare, J. A. Using habitat association models to predict Alewife and Blueback Herring marine distributions and overlap with Atlantic Herring and Atlantic Mackerel: can incidental catches be reduced? – ICES Journal of Marine Science, 73: 1912–1924.

Received 1 June 2015; revised 27 August 2015; accepted 30 August 2015.

Concern over the impacts of incidental catches of Alewife, *Alosa pseudoharengus* and Blueback Herring, *A. aestivalis* (collectively managed as 'river herring') in the commercial Atlantic Herring (*Clupea harengus*) and Atlantic Mackerel (*Scomber scombrus*) fisheries has resulted in the recent implementation of river herring incidental catch limits. These incidental catches are highly variable in frequency and magnitude, and the environmental conditions associated with these catches are poorly understood. We used generalized additive models (GAMs) to describe habitat associations of Alewife, Blueback Herring, Atlantic Herring, and Atlantic Mackerel. Bottom temperature, bottom depth, bottom salinity, solar azimuth and elevation, and region of the Northeast U.S. continental shelf were all significant in the habitat models; GAMs explained 25.2, 16.9, 18.9, and 20.6% of the deviance observed for the presence/absence of Alewife, Blueback Herring, Atlantic Herring, and Atlantic Mackerel. A subset of the data was omitted from the model and the probability of presence was compared with observations; 66–77% of observations were correctly predicted. The individual probabilities of presence were used to quantify and evaluate the accuracy of modelled overlap of Alewife and Blueback Herring with Atlantic Herring (68–72% correct predictions) and Alewife and Blueback Herring with Atlantic Mackerel (57–69% correct predictions). Our findings indicate that environmental gradients influence the distributions and overlap of Alewife, Blueback Herring, Atlantic Herring, and Atlantic Mackerel, and with further testing and refinement these models could be developed into a tool to aid industry in reducing incidental catches of river herring.

Keywords: distribution models, generalized additive models, habitat associations, incidental catch avoidance.

Introduction

Population sizes of many North American diadromous species have declined dramatically since European settlement. These declines are largely the result of a combination of freshwater habitat alterations and reductions, as well as unsustainable harvest rates (Limburg and Waldman, 2009). Many directed fisheries for diadromous fish in the eastern United States have been closed, and a substantial amount of effort has been made to protect and restore freshwater habitats with varied levels of success. Many questions still remain regarding the role of marine mortality sources, with strong concerns about the impact of incidental catches in commercial fisheries (Limburg and Waldman, 2009). Fishery observer coverage has provided some insight into the general trends of seasonality and gear types associated with incidental catches of anadromous (freshwater spawning) species in the Northeast U.S. continental shelf. Observer data have also highlighted the high variability surrounding incidental catch events, introducing more questions regarding the drivers of species' overlap and incidental catches (Cieri *et al.*, 2008; Cournane *et al.*, 2013; Bethoney *et al.*, 2014).

For a range of marine species, distributions have been linked to environmental variables and habitat features—these relationships are likely a function of physiological requirements, food availability,

and predation (Jensen *et al.*, 2005; Ciannelli *et al.*, 2008; Hare *et al.*, 2012; Kitchens and Rooker, 2014). Marine and anadromous clupeid distributions have been consistently linked with environmental and seasonal variables. A suite of habitat features have been correlated with marine-phase anadromous Alewife, *Alosa pseudoharengus*, and Blueback Herring, *A. aestivalis* spatial and temporal distributions including dynamic seascape features such as bottom temperature and salinity, depth, and these associations may change over daily to seasonal time scales (Neves, 1981; Bethoney *et al.*, 2014; Lynch *et al.*, 2015). Similar associations with depth, temperature, and season have been observed for closely related anadromous American shad (*A. sapidissima*) in both the Atlantic and Pacific oceans (Dadswell *et al.*, 1987; Pearcy and Fisher, 2011). Atlantic Herring (*Clupea harengus*) habitat associations in the Northeast and Northwest Atlantic Ocean have been associated with temperature, depth, and salinity (Sinclair and Iles, 1985; Maravelias *et al.*, 2000; Maravelias, 2001). Similarly, Atlantic Mackerel (*Scomber scombrus*) distributions have been related to temperature, depth, and salinity (Walsh *et al.*, 1995; Overholtz *et al.*, 2011; Radlinski *et al.*, 2013).

Intraspecies population mixing of anadromous fish is common throughout their migrations, except spawning periods. This mixing facilitates dispersal among populations, allowing for natural recolonization of extirpated habitats and the rebuilding of depleted populations (Schtickzelle and Quinn, 2007; McDowall, 2008). Population mixing rates are difficult to estimate because population mixing during spawning homogenizes genotypes (Waples and Naish, 2009). Interspecies mixing, or temporary distribution overlap, is relatively common as well, and likely related to overlap of environmental associations and variability in environmental conditions through space and time (Cournane *et al.*, 2013; Bethoney *et al.*, 2014; Ianelli and Stram, 2015). When spatial and temporal overlap involves a commercially harvested species, US managers have the challenge of minimizing incidental catch (landed non-target catches) and bycatch (non-target catches discarded at sea), while maximizing the economic value of the fishery (Magnuson-Stevens Reauthorization Act 2006, 16 U.S.C. §1801). Bycatch/incidental catch reduction plans are becoming common features of management plans. Unfortunately, bycatch reduction plans are not always as effective as anticipated due to the difficulty associated with predicting when and where overlaps in distribution will occur (Cox *et al.*, 2007; Bethoney *et al.*, 2014; Ianelli and Stram, 2015).

The population and species' level impacts of incidental catches of Alewife and Blueback Herring in the Atlantic Herring and Atlantic Mackerel fisheries have become of increasing concern. The problem is exacerbated by the similar appearance of Alewife and Blueback Herring; the two species are difficult to distinguish without close inspection, thus in regional fisheries management, they are combined as "river herring", despite ecological differences. The high degree of spatial and interannual variability in incidental catches of "river herring" in conjunction with poor understanding of Alewife and Blueback Herring population sizes make the effects of incidental catch difficult to quantify (Cieri *et al.*, 2008; ASMFC 2012; Cournane *et al.*, 2013; Bethoney *et al.*, 2014). The spatio-temporal variability in species' overlap implies that migrations are driven by other ecological components of the seascape, especially abiotic factors related to physiological requirements and biotic interactions. Here, we postulate that habitat models can be used to explain and predict Alewife, Blueback Herring, Atlantic Herring, and Atlantic Mackerel marine distributions and overlap. Further, habitat models can potentially be used as a tool for reducing the incidental catch of Alewife and Blueback Herring in the Atlantic Herring and Atlantic Mackerel fisheries. The main goals of this study are (i) to identify seascape gradients related to each species' distribution to accurately model habitat associations and (ii) to evaluate the predictive capability of the habitat models by omitting a subset of the data and predicting species distributions and overlap for these observations. We used environmental data and species' observations collected as part of a long-term fishery-independent sampling programme to develop and test habitat models.

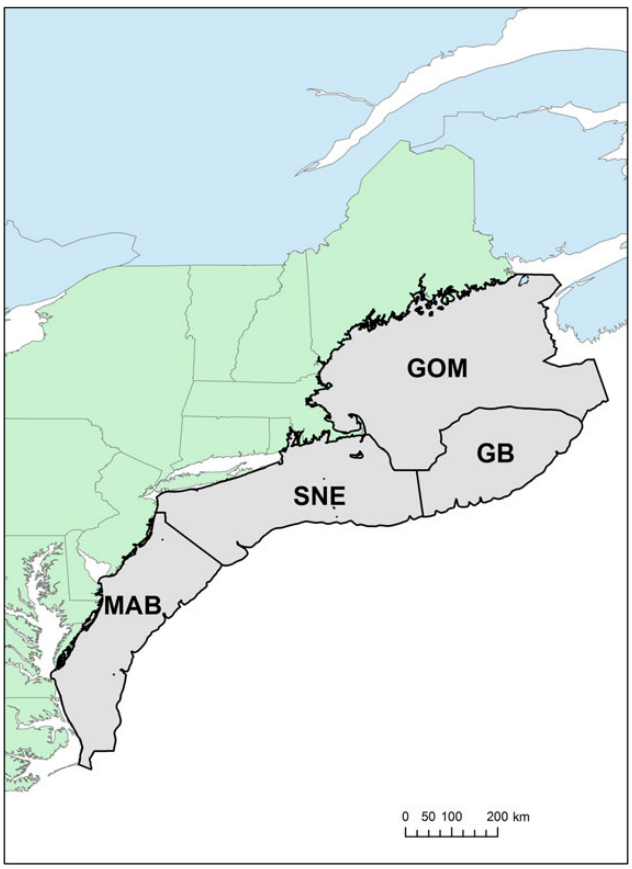

Figure 1. Map of the Northeast Fisheries Science Centre bottom trawl survey range in the Northwest Atlantic Ocean with regions labelled; GOM, Gulf of Maine; GB, Georges Banks; SNE, Southern New England; MAB, Mid-Atlantic Bight.

Methods

Study area

Alewife and Blueback Herring spawn and develop in freshwater and estuarine habitats throughout eastern North America (Florida, United States to Newfoundland, Canada) but the majority of their life cycle is spent in the ocean (Fay *et al.*, 1983). Alewife and Blueback Herring ocean migrations encompass a large portion of the Northwest Atlantic, including coastal estuaries and open shelf waters to depths near 200 m throughout the majority of the year. Atlantic Herring in the Northwest Atlantic Ocean occur from North Carolina, USA to Greenland (Kelly and Moring, 1986). The distribution of Atlantic Mackerel extends from Cape Lookout, North Carolina, United States to Newfoundland/Labrador (Sette, 1950). Here, we use data collected by the NOAA Northeast

Fisheries Science Center (NEFSC) bottom trawl survey which consistently samples federal waters from North Carolina, United States to the United States/Canadian border (Figure 1). While the bottom trawl survey was initially designed to sample demersal species, pelagic fish are regularly caught during the surveys, and data from bottom trawl surveys are currently the only fishery-independent data used in the Atlantic Herring and Atlantic Mackerel stock assessments (NEFSC, 2006, 2012). Further, the commercial Atlantic Herring fishery in Southern New England (SNE) uses bottom trawls, and this fleet often incidentally catches Alewife and Blueback Herring (Bethoney *et al.*, 2014).

Data collection

The NEFSC bottom trawl survey has been conducted two or more times each year from 1968 to present. The date, time, spatial coordinates (latitude and longitude), and number of catch and weight of catch by species are recorded at each trawl station. A stratified random sampling design is used to determine survey stations. Briefly, the survey used a standardized Yankee 36 bottom trawl through 2008 when the survey transitioned to a new vessel (Politis *et al.*, 2014). The new vessel (NOAA Ship *Henry B. Bigelow*) uses a standardized 3-bridle, 4-seam bottom trawl rigged with a rockhopper sweep with 20 min tow durations (on-bottom) at a speed of 3.0 knots; a more detailed explanation of sampling protocols can be found in Politis *et al.* (2014). The area swept of each trawl tow is ~24 000 m^2 and the median nearest neighbour distance between samples is 12 km. The extent of the survey is 224, 562 km^2. On average each seasonal survey takes ~53 days to complete.

Conductivity, temperature, and depth (CTD) sampling is conducted at every survey station, within 5 m of the bottom, within 3 h of the trawl sampling start, and within 3 nautical miles of the midpoint of the trawl path (Politis *et al.*, 2014).

Data from spring (March—early May) 1991–2013 and winter (February) 1993–2007 surveys were used to develop models of marine habitat association for Alewife, Blueback Herring, Atlantic Herring, and Atlantic Mackerel. The years were chosen because consistent environmental data collection with a CTD began in 1991 in the spring survey and 1993 in winter survey. Further, the winter survey was ended in 2007. The seasons were limited to February—early May because the dominant environmental drivers and potential habitats vary seasonally (Mann, 1993), and this is when the majority of mixed catches occur (see Supplementary Table S1 for the spatial, temporal, and environmental variable ranges observed). As different portions of migration circuits likely are driven by distinct environmental cues, the objective here is to model habitat associations and distribution overlap during a few month periods.

Model formulation and evaluation

Previous studies have found, temperature, salinity, and depth are related to Alewife and Blueback Herring occurrence, and all these variables were tested for model inclusion (Neves, 1981; Bethoney *et al.*, 2014; Lynch *et al.*, 2015). Solar azimuth and elevation, representing the position of the sun for a specific location and time, were derived from the date, time, and spatial coordinates ("maptools" package v. 0.8–36 in R) of stations and evaluated statistically. Solar position was included in models because diel vertical feeding migrations likely affect catchability (Neves, 1981; Kelly and Moring, 1986; Studholme *et al.*, 1999). Region of the study area was tested as a factor variable because distributions of all four species vary seasonally and thus the probability of observing fish in some regions will be higher in a given season.

Generalized additive models (GAMs; Hastie and Tibshirani, 1990) were used ("mgcv" package v. 1.8–6 for R software; Wood, 2006) to develop the presence/absence models for marine—phase Alewife, Blueback Herring, Atlantic Herring, and Atlantic Mackerel using a binomial link function. Smoothing functions were used for each environmental variable (temperature, salinity, and depth) and a tensor product smooth was used to model interactions between solar azimuth and elevation (Hastie and Tibshirani, 1990; Wood, 2006). Region was included as a factor variable with four levels—Gulf of Maine (GOM), Georges Banks (GB), SNE, and the Mid-Atlantic Bight (MAB) (Figure 1). Only observations with all variables were included in models. Backwards stepwise selection was used to determine all significant variables for inclusion (Hastie and Tibshirani, 1990). Models were run separately for each species:

$$\begin{aligned}\text{Presence/absence}_{\text{species } x} \sim\ & s(\text{bottom temperature}) \\ & + s(\text{bottom depth}) + s(\text{bottom salinity}) \\ & + te(\text{solar azimuth},\ \text{solar elevation}) \\ & + \text{Region}.\end{aligned}$$

Initially, separate models were evaluated for winter (February) and spring (March—early May) and inshore and offshore separately (results not included) to evaluate if migratory cues differed in time and space. The smooth functions were similar across spatial and seasonal datasets, so all data were pooled for each species. Month was included as a factor variable to further evaluate temporal effects, but was not significant in any of the models (results not reported). Similarly, in 2009 a new survey vessel was introduced, which has altered catch rates for many species (Miller *et al.*, 2010), so models were run including and excluding vessel as a factor variable. Vessel was significant, so models including and excluding data collected by the new vessel were evaluated. Differences in the explained deviance between the two models were minimal for all species, and because including data from the new vessel did not substantially change model results (estimated degrees of freedom, variable significance, and deviance explained), data from both vessels were included. The vessel effect would likely be more substantial if the response variables were abundance rather than presence/absence (Miller *et al.* 2010). The basis dimensions for smoothing functions were set based on the percentage of the deviance explained, the Akaike's information criterion (AIC), and negative log likelihood, and were held constant across all models. Spatial autocorrelation in model residuals was evaluated for all season/year combinations using Moran's I, and while spatial autocorrelation was significant in some combinations, the results were not consistent across years. Also, 108 of 112 Moran's I statistics were <0.4 (maximum was 0.56). Given this, we determined that use of a complex spatial mixed model was unwarranted.

Models were evaluated via the split-sample approach by omitting the most recent winter (2007) and spring (2013) observation sets. Receiver operator curves (ROCs) were constructed ("SDMTools" package v. 1.1–221 in R) to evaluate the ability of the model to predict species' presence/absence, with the area under the curve (AUC) indicating model fit (a value of one indicates perfect model fit; 0.5 suggests model results are equivalent to chance) (Murtaugh, 1996). Confusion matrices were used to quantify the

percentages of correct presence/absence predictions, as well as the false-negative and false-positive predictions (Murtaugh, 1996). The threshold for model-predicted presence/absence set to the optimum probability threshold where the sensitivity (the percentage of correct positives) equalled the specificity (the percentage of correct negatives) for each species (Lobo *et al.*, 2008). Habitat overlap was considered as trawl stations where both species were captured (Alewife with Atlantic Herring, Blueback Herring with Atlantic Herring, Alewife with Atlantic Mackerel, and Blueback Herring with Atlantic Mackerel). Model-predicted overlap probability was quantified as the product of two individual species occurrence probabilities; while more complex methods likely exist, we chose to (at least for preliminary model evaluations) use this simple approach. Overlap was quantified for all locations, regardless of individual species probabilities so that any potential biases (e.g. spatial or temporal) in overlap predictions could be identified. Overlap predictions were also evaluated via ROCs and confusion matrices, also using the optimum probability threshold as the presence/absence threshold (Lobo *et al.*, 2008).

Results

Model development

To establish which variables should be included in the predictive models, all variables were initially included and variable significance (based on *p*-values) was evaluated and compared across all species' models (Table 1; Supplementary Table S3). The model that consistently (for all four species) explained the highest percentage of deviance and had the lowest AIC and/or minimized the negative log likelihood included smoothing functions of bottom temperature, bottom salinity, and bottom depth; a tensor product smooth of solar azimuth and solar elevation; and region as a factor variable. All variables were significant in all models ($p < 0.01$). The number of basis dimensions for each variable (which constrains the complexity of the response curves) was set the same for each species' model, with temperature and salinity each set at $k = 6$, depth set to $k = 8$, and the tensor product of solar elevation and azimuth set at $k = 20$.

The final models, with the basis dimensions set (see above), explained 25.2, 16.9, 18.9, and 20.6% of the observed deviance in Alewife, Blueback Herring, Atlantic Herring, and Atlantic Mackerel presence/absence (Table 1). The bottom temperature curves were significant from 5 to 8.5°C for Alewife, 3 to 7.5°C for Blueback Herring, 5 to 9°C for Atlantic Herring, and 5 to 9.5°C for Atlantic Mackerel (Supplementary Table S2 and Figures S2–S5). The bottom depth curve for Alewife was significant from 115 to 240 m (influenced by occurrence in the GOM, which is deeper than other areas on the shelf), Blueback Herring were associated with depths <60 m, the Atlantic Herring curve was significant from 35 to 90 m, and the Atlantic Mackerel depth curve was significant from 35 to 110 m (Supplementary Table S2 and Figures S2–S5). The bottom salinity curve was significant <33 for Alewife and <34 for Blueback Herring, the Atlantic Herring bottom salinity curve was significant from 29 to 33.5, and Atlantic Mackerel were associated with salinities between 33 and 34 (Supplementary Table S2 and Figures S2–S5). Temperature, depth, and salinity associations were generally consistent with those described in previous studies (Supplementary Table S2). The effect of the interaction between solar elevation and solar azimuth was similar for Alewife and Blueback Herring, while the interactive effects on Atlantic Herring and Atlantic Mackerel were distinct (Supplementary Figures S2–S5). Differences in solar azimuth and elevation interactions suggest differences in species' vertical distributions, and therefore catches, related to the time of day (likely resulting from diel vertical migrations). The most significant regions (listed from most to least significant) were GOM and SNE for Alewife; GOM, MAB, and SNE for Blueback Herring; SNE, GOM, and MAB for Atlantic Herring; SNE, GOM, and MAB for Atlantic Mackerel (Supplementary Figures S2–S10).

Table 1. Summary of GAMs including smooth functions of bottom temperature, bottom salinity, and bottom depth, a tensor smooth function of the solar azimuth and elevation (proxies for location-based time of day), and region as a factor variable.

Species	% Stations present	Residual deviance	% Deviance explained
Alewife	35.5	6287.79	25.20
Blueback Herring	16.4	4793.95	16.93
Atlantic Herring	48.0	7254.74	18.92
Atlantic Mackerel	20.7	5234.03	20.60

The response variable was species' presence/absence; data are from the Northeast Fisheries Science Center bottom trawl survey from 1991 to 2013 and included 6462 stations.

Model evaluation

For initial model testing, data from spring 2013 and winter 2007 NEFSC bottom trawl surveys were omitted from the models and the probabilities of observing fish at those locations were predicted and compared with the actual observations. For all species and seasons, the model-predicted probability of presence was significantly greater where the species was observed vs. where it was not (one-tailed Mann–Whitney *U* test, $p < 0.004$; Figure 2). The AUC (a measure of test accuracy) was >0.8 for all species except Atlantic Mackerel (Alewife = 0.83 (CI: 0.79–0.86); Blueback Herring = 0.83 (CI: 0.79–0.87); Atlantic Herring = 0.83 (CI: 0.80–0.87); Atlantic Mackerel = 0.69 (CI: 0.64–0.75); Figure 2). The percentages of correct predictions, using the optimum probability threshold to define model-predicted presence/absence, ranged from 66 to 77%, the percentage of false positives from 23 to 31%, and false negatives from 25 to 34% (Table 2).

The accuracy of modelled species overlap was evaluated by taking the product of the two individual species' probability of presence and comparing the overlap probabilities with overlap observations (trawl stations where the both species were caught). The model-predicted probability of overlap between Alewife and Atlantic Herring, Blueback Herring and Atlantic Herring, Alewife and Atlantic Mackerel, and Blueback Herring and Atlantic Mackerel was significantly higher for trawl stations where overlap did occur than where it did not occur (one-tailed Mann–Whitney *U* test, $p < 0.0001$; Figure 3). The AUC was 0.82 (CI: 0.78–0.86) for Alewife and Atlantic Herring overlap, 0.80 (CI: 0.76–0.84) for Blueback Herring and Atlantic Herring overlap, 0.73 (CI: 0.68–0.78) for Alewife and Atlantic Mackerel overlap, and 0.73 (CI: 0.67–0.78) for Blueback Herring and Atlantic Mackerel overlap (Figure 3). Confusion matrices were used to further evaluate the overlap models, with the presence/absence thresholds set at the optimum probability threshold. Alewife and Atlantic Herring overlap was correctly predicted for ~72% of observations while Blueback Herring and Atlantic Herring overlap was correctly

predicted for 72% of co-occurrences and 68% of observations where the species' did not co-occur (Table 3). Correct predictions for Alewife and Blueback Herring overlap with Atlantic Mackerel were lower. Predictions for Alewife/Atlantic Mackerel overlap were correct for 66% of co-occurrences and 69% of observations where the two did not co-occur and correct predictions for Blueback Herring/Atlantic Mackerel overlap were 57% for co-occurrences and 68% of observations where the two did not co-occur (Table 3).

Temperature associations were relatively similar for all four species (Supplementary Table S2). The effect of temperature was greater for Atlantic Herring and Atlantic Mackerel (indicated by the height of the response curves and the associated partial deviance) and Blueback Herring were associated with somewhat lower temperatures when compared with the other species (Supplementary Figures S2–S5 and Table S3). Alewife were associated with deeper habitats than Blueback Herring, and Atlantic Herring and Atlantic Mackerel depth associations were between the two, overlapping with Blueback Herring that occurred in deeper water and approaching depths of Alewife (Supplementary Figures S2–S5). Alewife and Blueback Herring showed stronger associations with lower salinity habitats, but the upper extent of their salinity associations overlapped with the salinity associations of Atlantic Herring and

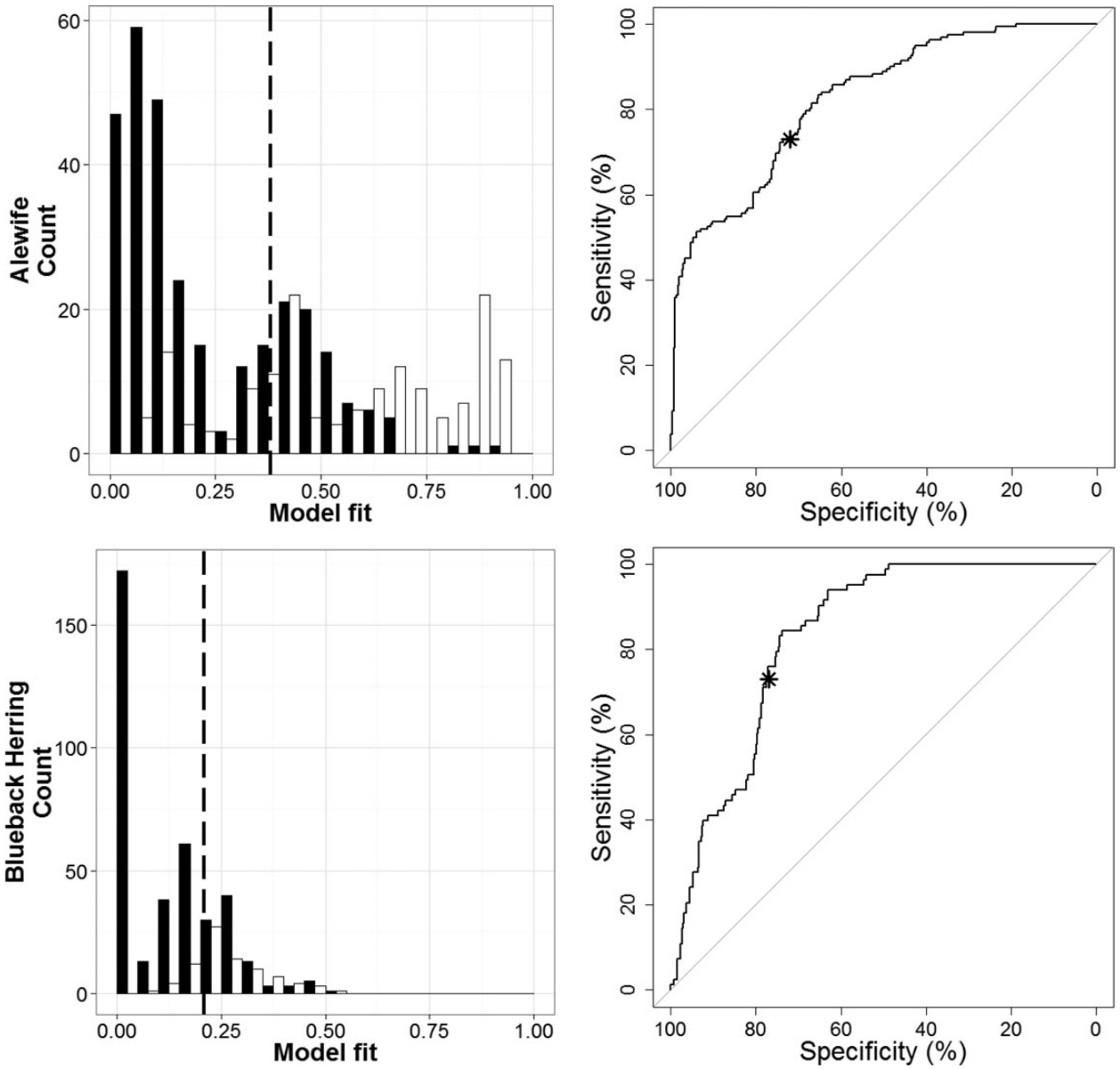

Figure 2. Histograms (left column) showing the predicted model fits from GAMs (including bottom temperature, depth, bottom salinity, solar azimuth, solar elevation, and region) of species presence/absence; data from Spring 2013 and Winter 2007 were omitted from model development and the model-predicted probability of fish presence was compared with observations. Solid bars indicate data for locations where fish were not observed and hollow bars are for locations where fish were observed; dashed lines represent the optimum probability threshold (where sensitivity equals specificity). The right column is the corresponding ROC evaluating the model predictions; asterisks indicate the point where the model specificity is equal to the sensitivity. All data were from the Northeast Fisheries Science Centre bottom trawl survey.

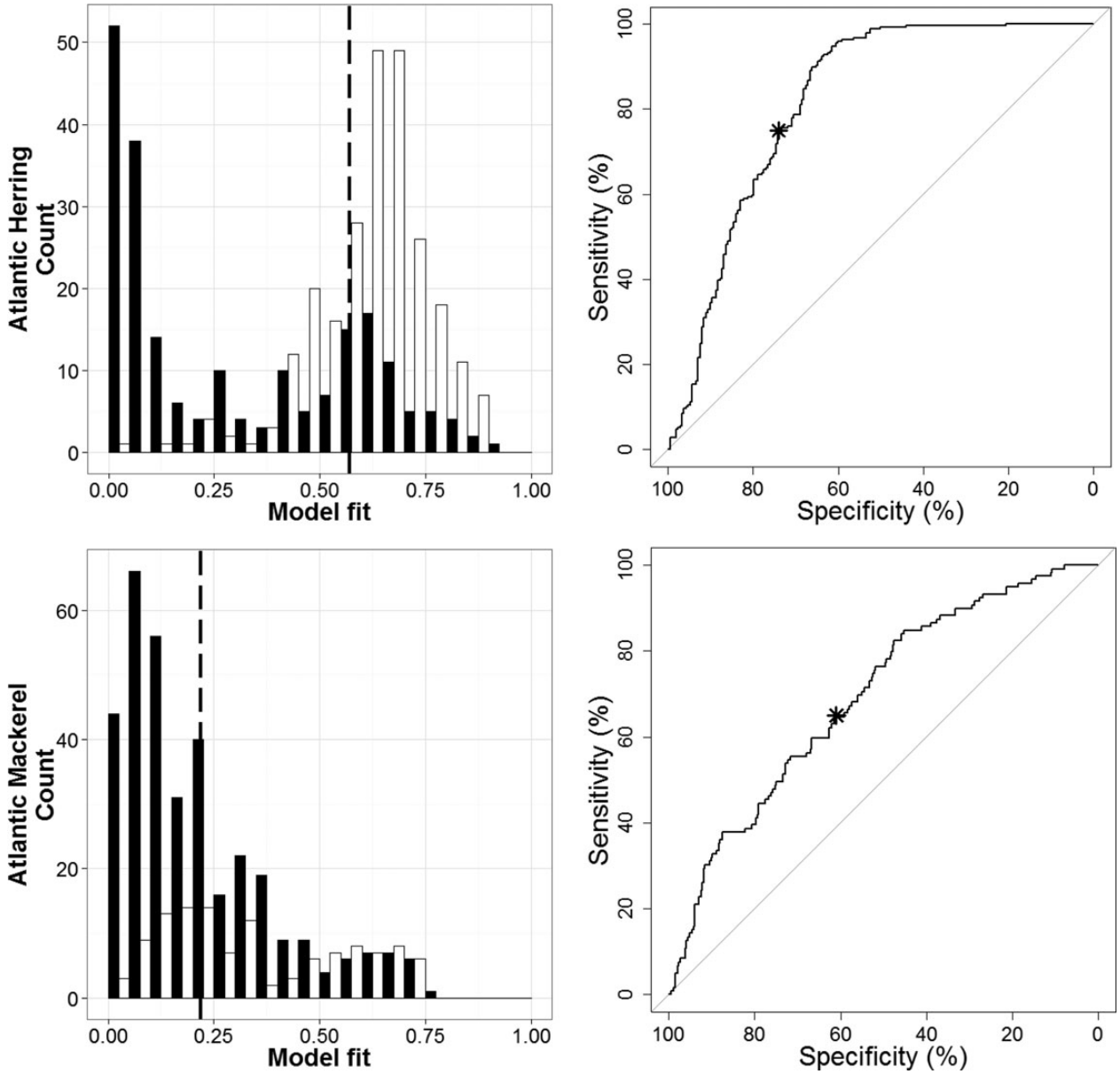

Figure 2. Continued.

Table 2. Results from confusion matrices of GAM model evaluation by omitting and predicting the probability of species' presence/absence for the spring 2013 and winter 2007 NEFSC bottom trawl survey.

	Alewife	Blueback Herring	Atlantic Herring	Atlantic Mackerel
Correct positives (%)	26	13	40	9
False negatives (%)	9	5	13	5
Correct negatives (%)	47	63	34	60
False positives (%)	18	19	12	27

Models were evaluated by setting the threshold for the probability of presence/absence at the optimum probability threshold (where sensitivity equals specificity; Alewife = 0.38, Blueback Herring = 0.21, Atlantic Herring = 0.57, Atlantic Mackerel = 0.22).

Atlantic Mackerel (Supplementary Figures S2–S5). The effect of the interaction between solar azimuth and elevation differed among Alewife, Blueback Herring, Atlantic Herring, and Atlantic Mackerel, but portions of the plots are similar (Supplementary Figures S2–S5). Observed and modelled overlap between Alewife and Atlantic Herring mainly occurred within GOM and SNE; observed and modelled Blueback Herring and Atlantic Herring overlap occurred in GOM, SNE, and MAB (Figure 4). Observed and modelled overlap of both Alewife and Blueback Herring with Atlantic Mackerel were distributed similarly to overlap with Atlantic Herring, although overlap with Atlantic Mackerel was less frequent (Figure 4).

Discussion

A substantial body of research indicates that species' distributions and migrations are associated with environmental gradients in space and time (Jensen *et al.*, 2005; Ciannelli *et al.*, 2008; Kitchens and Rooker, 2014). The most influential variables likely differ among species, ecosystems, and seasons. Here, we were able to

explain 16–25% of the observed deviance in the presence/absence of four small pelagic fish species in the Northeast U.S. continental shelf Ecosystem, based on environmental, spatial, and temporal gradients. When a subset of the data was omitted for model testing, models correctly predicted presence/absence for 66–77% of the observations when the optimum probability threshold was used for model evaluation. Alewife and Blueback Herring overlap with Atlantic Herring and Atlantic Mackerel was predicted at rates similar to the individual model predictions, suggesting that using the product of individual model fits is accurate, at least over the large spatial and temporal scales of this study.

GAM model development and evaluation

The percentages of the deviance explained by the models are comparable with the results of habitat modelling for a wide range of mobile, aquatic species, with similar environmental drivers (9–50%: Jensen *et al.*, 2005; 18%: Hare *et al.*, 2012; 11–48%: Kitchens and Rooker, 2014; 8–40%: Lynch *et al.*, 2015). Jensen *et al.* (2005) modelled habitat distribution of female blue crabs (*Callinectes sapidus*) in the

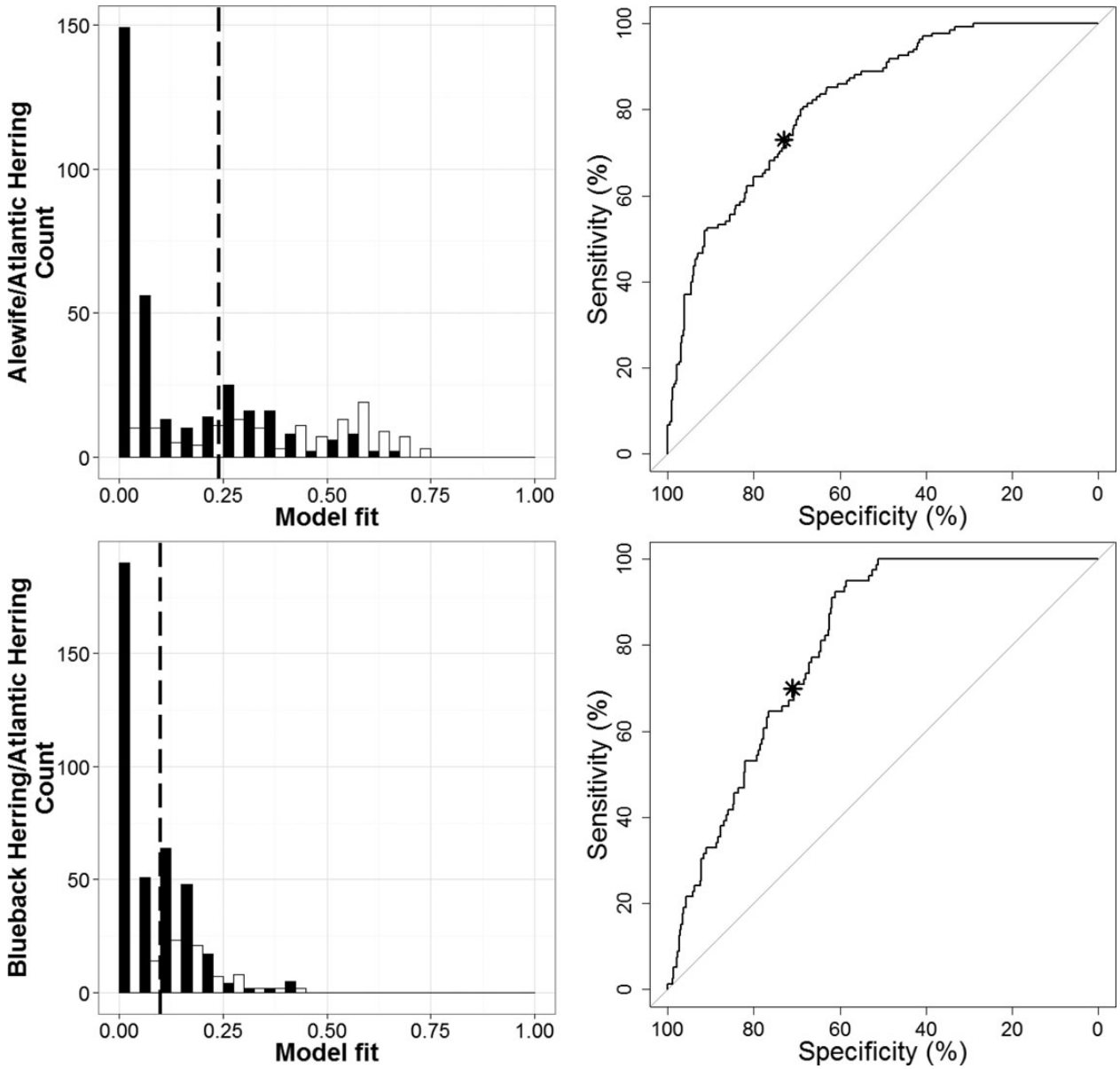

Figure 3. Histograms showing the predicted species' overlap [defined as the product of individual species' model fits from GAMs (including bottom temperature, depth, bottom salinity, solar azimuth, solar elevation, and region)]; data from Spring 2013 and Winter 2007 were omitted from model development and the model-predicted species' overlap was compared with observations. Solid bars indicate data for locations where overlap between the species' was observed and hollow bars are for locations where overlap was not observed; dashed lines represent the optimum probability threshold (where sensitivity equals specificity). The right column is the corresponding ROC evaluating the model predictions; asterisks indicate the point where the model specificity is equal to the sensitivity. All data were from the Northeast Fisheries Science Centre bottom trawl survey.

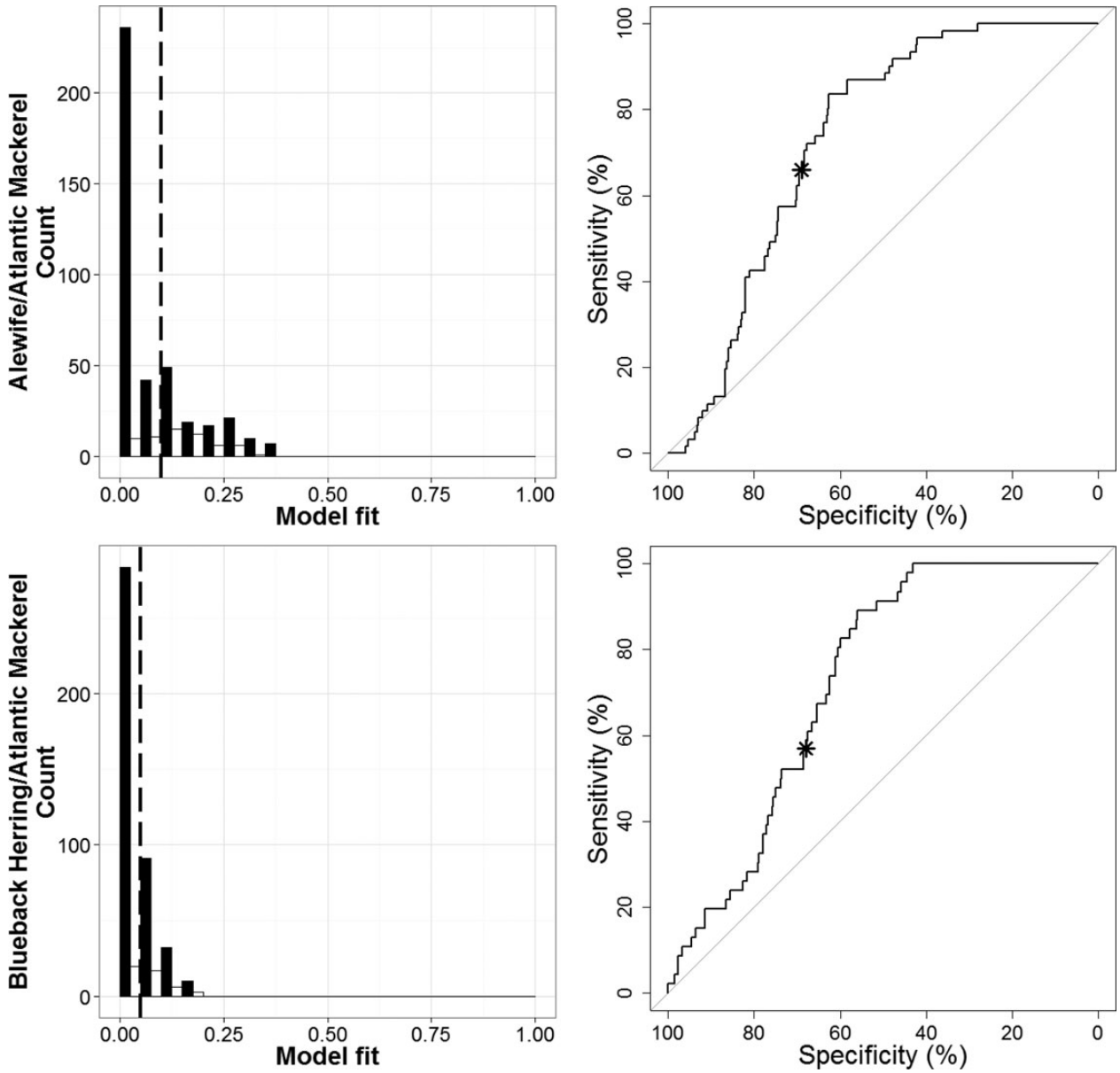

Figure 3. Continued.

Chesapeake Bay and found that temperature, salinity, and bottom depth were the most important environmental drivers of distributions. The historical and current distributions of Cusk (*Brosme brosme*) and Alewife and Blueback Herring were modelled as a function of corresponding temperature regimes (Hare *et al.*, 2012; Lynch *et al.*, 2015). These models were then used to predict distributions for some potential future temperature scenarios. Similarly, we found that Alewife, Blueback Herring, Atlantic Herring, and Atlantic Mackerel distributions were related to temperature, salinity, and depth. The unexplained deviance could result from species not occupying all potential habitats, as a result of reduced abundances, or from niche dimensions uncaptured by the models, such as localized conditions (e.g. vertical mixing) or biological interactions (e.g. prey abundance/distribution, predation).

The peaks in the response curves for our habitat models are consistent with habitat preferences reported in previous studies (Alewife and Blueback Herring: Neves, 1981; Atlantic Herring: Maravelias, 1999; Atlantic Mackerel: Studholme *et al.*, 1999; Atlantic Herring: Maravelias *et al.*, 2000; Atlantic Mackerel: Overholtz *et al.*, 2011; Alewife and Blueback Herring: Bethoney *et al.*, 2014; Alewife and Blueback Herring: Lynch *et al.*, 2015). The previous Alewife and Blueback Herring studies used the same data source (NEFSC bottom trawl survey) as our study, but had different objectives and used other statistical methods. Lynch *et al.* (2015) also used GAMs to explain Alewife and Blueback Herring distributions, but only included temperature as the aim of that study was to understand how distributions will likely change as ocean temperatures increase in the future. We included more habitat variables, with the final project objective of developing models that can accurately predict current distributions and species' overlap. Blueback Herring were observed in trawl catches substantially less than the other species, but this

Table 3. Results from confusion matrices of species' overlap predicted via GAM model evaluation by omitting and predicting the probability of presence/absence for each species' for the spring 2013 and winter 2007 NEFSC bottom trawl survey.

	Alewife/Atlantic Herring	Blueback Herring/Atlantic Herring	Alewife/Atlantic Mackerel	Blueback Herring/Atlantic Mackerel
Correct positives (%)	21	12	9	6
False negatives (%)	8	5	5	4
Correct negatives (%)	52	59	60	61
False positives (%)	19	24	27	29

Models were evaluated by setting the threshold for the probability of species' co-occurrence at the optimum probability threshold (where sensitivity equals specificity; Alewife/Atlantic Herring overlap = 0.24; Blueback Herring/Atlantic Herring overlap = 0.11; Alewife/Atlantic Mackerel overlap = 0.10; Blueback Herring/Atlantic Mackerel overlap = 0.05).

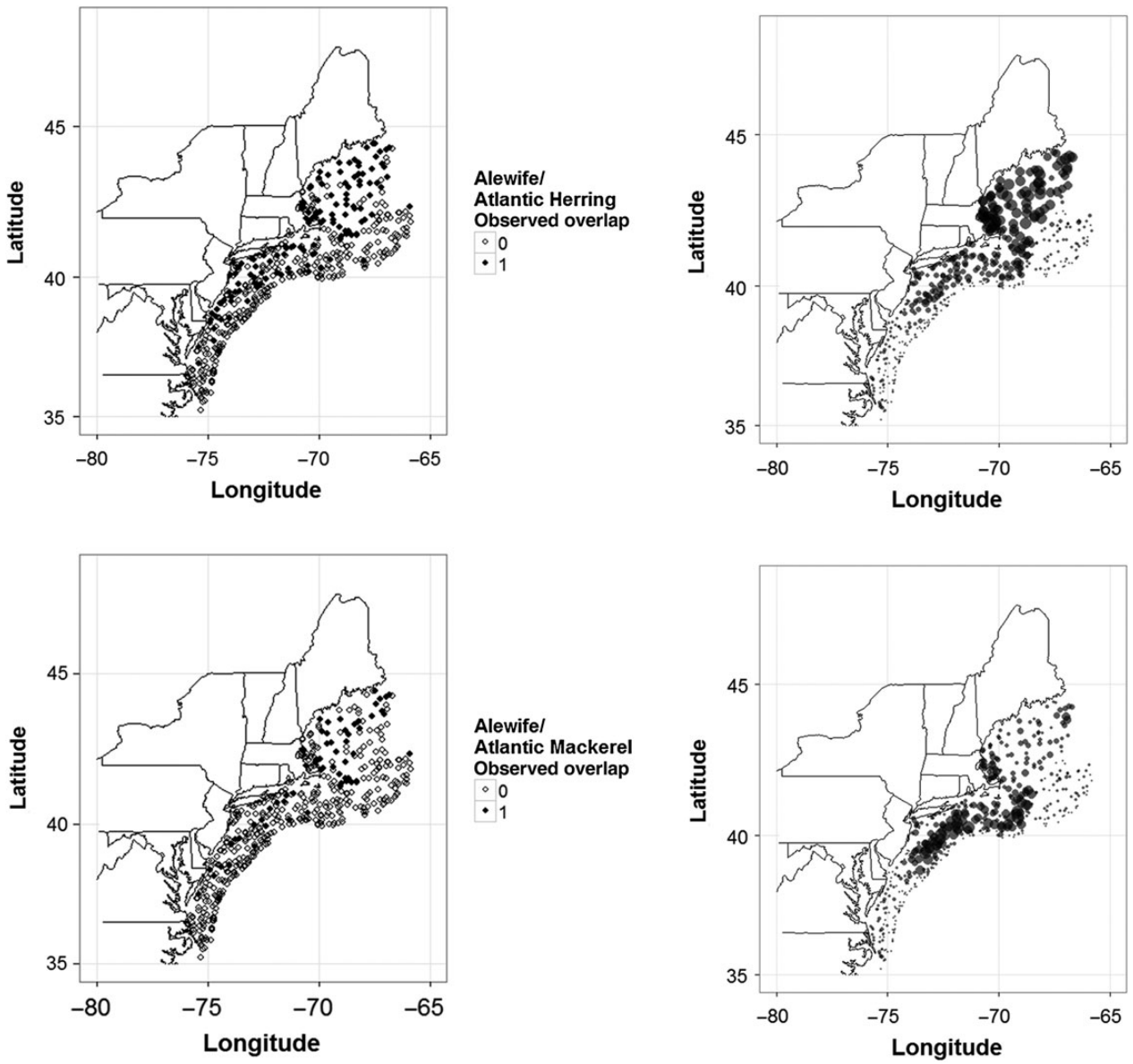

Figure 4. Maps showing the observed species overlap (left column); open circles indicate survey stations (from winter 2007 and spring 2013) where overlap was not observed, and filled circles indicate stations where overlap was observed. In the right column, are maps showing the GAM predicted probability of overlap; symbol size increases with probability. All data were from the Northeast Fisheries Science Centre bottom trawl survey.

is likely because Blueback Herring are typically associated with more shallow, in-shore habitats (Neves, 1981; Bonzek *et al.*, 2012; Bethoney *et al.*, 2014). Despite the lower number of stations at which Blueback Herring were observed, the rates of model accuracy were similar to those observed for Alewife which were observed at ~17% more stations, supporting the use of GAMs

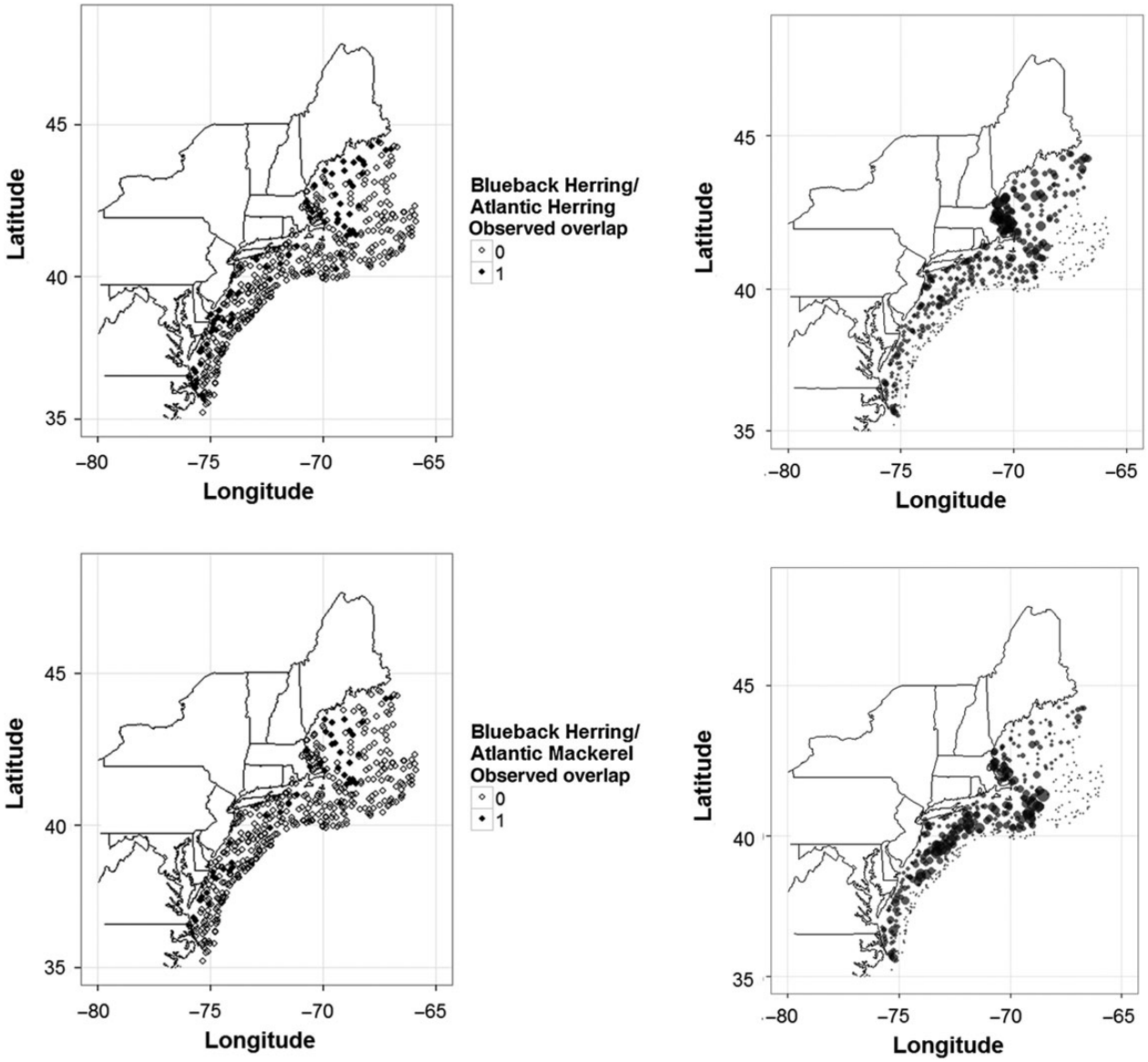

Figure 4. Continued.

as opposed to other models (e.g. zero-inflated negative binomial models).

In the Northeast Atlantic Ocean, Atlantic Herring habitat models were developed for prespawning distributions (June–July). While the observed depth associations of Atlantic Herring were similar to the present study, the temperature associations were higher (Maravelias *et al.*, 2000; Maravelias 2001). Associations with warmer waters would be expected given these studies were conducted during summer (i.e. temperature distributions were higher). Maravelias (2001) found differences in habitat associations between prespawning populations east and west of the Shetland Islands which was partially a function of the distinct environmental conditions in the two ecosystems. Across-shelf catch distributions of Atlantic Mackerel were consistently correlated with sea surface temperature variations for all size classes, but alongshelf distributions were only correlated with temperature for the largest size class (Radlinski *et al.*, 2013). Size-based differences in migrations (i.e. related to spawning behaviours) could be lowering the accuracy of model predictions, as Atlantic Mackerel spawn during the spring. Atlantic Herring spawn in late summer and early fall, and Alewife and Blueback Herring spawn in freshwaters, thus spawning (i.e. sized-based migration differences) would likely not affect the model accuracy for these species. The lower prediction accuracy of the Atlantic Mackerel model may also be related to the wide vertical distributions of Atlantic Mackerel observed in previous studies, as well as the lower percentage of observations especially relative to Atlantic Herring (Walsh *et al.*, 1995; Studholme *et al.*, 1999).

The results of our model evaluations provided further support that the habitat models have predictive capabilities, at least over similar spatial scales, seasons, and gear types. The optimum probability thresholds (where specificity equals sensitivity) used for model evaluation also resulted in roughly 25% incorrect predictions for observations where fish were (i.e. false negatives) and were not (i.e. false positives) observed. Some false predictions are expected, given the models are fitting the mean habitat associations; thus, by setting a cutoff value for the model fit, the tails of the distributions will be above/below

this point. False negatives are of greater concern here, suggesting that habitat should not be occupied when it is, and could result from missing niche dimensions in the habitat models or from fish being caught while migrating through or feeding in less favourable habitats. False positives could simply be the result of suitable habitat that is not currently occupied (potentially related to reduced population sizes). As the goal is to avoid Alewife and Blueback Herring catches in Atlantic Herring and Atlantic Mackerel fisheries, false negatives would increase the incidence of these events, while false positives would result in not fishing in areas where incidental catches will not occur despite modelled probabilities.

In the Northeast Atlantic, Atlantic Herring distribution and abundance were also related to zooplankton abundance, bottom structure (hardness and roughness), and thermocline depth (Maravelias, 1999, 2001; Maravelias *et al.*, 2000). These factors along with others could affect distributions in the Northwest Atlantic for all the study species. We chose to limit our models to environmental variables that have previously been shown (in different regions or contexts, such as predicting distribution changes related to climate change) to have a relationship with distributions of all four species and can be reliably forecasted (Neves, 1981; Maravelias, 1999, 2001; Maravelias *et al.*, 2000; Chen *et al.*, 2006; Overholtz *et al.*, 2011; Bethoney *et al.*, 2014; Lynch *et al.*, 2015).

Habitat overlap can be related to species' physiological requirements and habitat availability, or influenced by distributions of species' prey or predators. Given the amount of species' overlap modelled here, it is unlikely that competitive exclusion occurs among these species within the study area at the large-scales represented by the data analysed here. In addition to similarities among species' habitat associations, species overlap is likely influenced, to some degree, by similarities among migration routes. Based on the habitat models presented here and the similarities in their diets and predators (Fay *et al.*, 1983; Kelly and Moring, 1986; Studholme *et al.*, 1999; Langøy *et al.*, 2012), it appears that species' distributions would respond similarly to changes in local prey or predator densities; thus, changes in overlap likely infer overlapping physical habitat preferences.

Evaluating the accuracy with which the models can predict where two species overlap showed that multiplying the probabilities from individual species' models is an accurate method for predicting where species will co-occur. This is an important step towards developing an incidental catch avoidance tool. If observed overlap primarily occurred where one species model had a high rate of false-negative predictions, co-occurrence would be under-predicted by overlap models. Conversely, if model-predicted overlap predominantly occurred where the individual models had high rates of false positives, overlap models would predict overlap at higher rates than observed. The models predicted Alewife and Blueback Herring overlap with Atlantic Herring more accurately than for overlap with Atlantic Mackerel. This is partially related to the lower prediction accuracy for Atlantic Mackerel compared with the other individual species' models. Relatively few previous studies have compared habitat associations for different species, for different populations utilizing discrete habitats, or have modelled and evaluated species' overlap (Maravelias 2001; Langøy *et al.*, 2012).

Potential utility to commercial fisheries

Commercial fisheries directly and indirectly affect other parts of the target species' ecosystem. Strategies to mitigate these impacts are becoming increasingly common in fishery management plans, especially regulations aiming to minimize mortality of non-target species. Many of these measures involve some form of spatial and/or temporal closures to fisheries, which have varying degrees of success that can at least partially be attributed to variability in environmental conditions (Hall and Mainprize, 2005; Cieri *et al.*, 2008; Bethoney *et al.*, 2014; Ianelli and Stram, 2015). Programmes facilitating communication of bycatch/incidental catches within fleets are being used by some commercial sectors. "Fleet communication networks" are the result of management policies that penalize bycatch by triggering closures when caps of non-target species are reached or incentivize bycatch reductions (Gilman *et al.*, 2006; Bethoney *et al.*, 2013; Stram and Ianelli, 2015).

Understanding the spatial and temporal relationships between the environment, species' distributions, and distribution overlap at spatial scales relevant to the species' overall marine ranges will provide insight into how dynamic environmental conditions influence parts of migration circuits. Further, by addressing these issues at spatial and temporal scales relevant to fisheries, ecological models can help fishers optimize their operations. Habitat modelling has the potential to improve fisheries management by increasing economic potential and minimizing ecological damages from commercial fisheries. Fleet communication programmes allow quick responses in fishing behaviour to minimize incidental catches, but we propose to take this concept a step further. If coupled oceanographic forecast models and habitat association models can accurately predict overlap between target and non-target species, this will allow commercial fisheries to further reduce non-target harvests. While this approach is, in theory, relatively straightforward, we anticipate complications may arise from the relatively small spatial scales at which industry fish (compared with the scale of the survey used for model development). Complications may also be associated with variables that cannot be quantified, such as fisher knowledge and technology (i.e. acoustics). These issues will be addressed by refining models via commercial catch data and collaboration with industry for their input and to conduct fishery-dependent sampling. The work presented here provides an important starting point for the development of species overlap/mixing forecast tools to further decrease ecosystem impacts of commercial fisheries.

Supplementary data

Supplementary material is available at the *ICESJMS* online version of the manuscript.

Acknowledgements

This work was funded by the NOAA Greater Atlantic Regional Fisheries Office. Data for model development and testing were collected by the NEFSC Ecosystems Surveys Branch. Acknowledgment of the above individuals does not imply their endorsement of this work; the authors have sole responsibility for the content of this contribution. The views expressed herein are those of the authors and do not necessarily reflect the views of NOAA or any of its sub-agencies. Thanks to three anonymous reviewers for their comments on previous drafts.

References

ASMFC (Atlantic States Marine Fisheries Commission). 2012. River herring benchmark stock assessment volume 1. Stock Assessment Report No. 12–02 of the Atlantic States Marine Fisheries Commission, Washington, DC.

Bethoney, N. D., Schondelmeier, B. P., Stokesbury, K. D. E., and Hoffman, W. S. 2013. Developing a fine scale system to address river herring (*Alosa pseudoharengus*, *A. aestivalis*) and American shad (*A. sapidissima*) bycatch in the U.S. Northwest Atlantic midwater trawl fishery. Fisheries Research, 141: 79–87.

Bethoney, N. D., Stokesbury, K. D. E., and Cadrin, S. X. 2014. Environmental links to alosine at-sea distribution and bycatch in the Northwest Atlantic midwater trawl fishery. ICES Journal of Marine Science, 71: 1246–1255.

Bethoney, N. D., Stokesbury, K. D. E., Schondelmeier, B. P., Hoffman, W. S., and Armstrong, M. P. 2014. Characterization of river herring bycatch in the Northwest Atlantic midwater trawl fisheries. North American Journal of Fisheries Management, 34: 828–838.

Bonzek, C. F., Gartland, J., Gauthier, D. J., and Latour, R. J. 2012. Data collection and analysis in support of single and multispecies stock assessments in the Mid-Atlantic: Northeast Area Monitoring and Assessment Program Near Shore Trawl Survey (NEAMAP). Award Number: NA12NMF4540017. Annual Data Report to the National Oceanographic and Atmospheric Administration, National Marine Fisheries Service—Northeast Fisheries Science Center and the Mid-Atlantic Fishery Management Council. Virginia Institute of Marine Science, Gloucester Point, VA. 280 pp.

Chen, C., Cowles, G., and Beardsley, R. C. 2006. An unstructured grid, finite volume coastal ocean model: FVCOM User Manual, 2nd edn. SMAST/UMASSD Technical Report-06–0602. 315 pp.

Ciannelli, L., Fauchald, P., Chan, K. S., Agostini, V. N., and Dingsør, G. E. 2008. Spatial fisheries ecology: recent progress and future prospects. Journal of Marine Systems, 71: 223–236.

Cieri, M., Nelson, G., and Armstrong, M. A. 2008. Estimates of river herring bycatch in the directed Atlantic herring fishery. Report prepared for the Atlantic States Marine Fisheries Commission, Washington, DC. September 23, 2008.

Cournane, J. M., Kritzer, J. P., and Correia, S. J. 2013. Spatial and temporal patterns of anadromous alosine bycatch in the US Atlantic herring fishery. Fisheries Research, 141: 88–94.

Cox, T. M., Lewiston, R. L., Żydelis, R., Crowder, L. B., Safina, C., and Read, A. J. 2007. Comparing effectiveness of experimental and implemented bycatch reduction measures: the ideal and the real. Conservation Biology, 21: 1155–1164.

Dadswell, M. J., Melvin, G. D., Williams, P. J., and Themelis, D. E. 1987. Influences of origin, life history, and chance on the Atlantic coast migration of American shad. American Fisheries Society Symposium, 1: 313–330.

Fay, C. W., Neves, R. J., and Pardue, G. B. 1983. Species profiles: life histories and environmental requirements of coastal fishes and invertebrates (Mid-Atlantic) – Alewife/ Blueback Herring. U.S. Fish and Wildlife Service, Division of Biological Services, FWS/ OBS-82111.9. U.S. Army Corps of Engineers, TR EL-82–4. 25 pp.

Gilman, E. L., Dalzell, P., and Martin, S. 2006. Fleet communication to abate fisheries bycatch. Marine Policy, 30: 360–366.

Hall, S. J., and Mainprize, B. M. 2005. Managing by-catch and discards: how much progress are we making and how can we do better? Fish and Fisheries, 6: 134–155.

Hare, J. A., Manderson, J. P., Nye, J. A., Alexander, M. A., Auster, P. J., Borggaard, D. L., Capotondi, A. M., *et al.* 2012. Cusk (*Brosme brosme*) and climate change: assessing the threat to a candidate marine fish species under the US Endangered Species Act. ICES Journal of Marine Science, 69: 1753–1768.

Hastie, T., and Tibshirani, R. 1990. Generalized Additive Models. Chapman & Hall, London, UK.

Ianelli, J. N., and Stram, D. L. 2015. Estimating impacts of the Pollock fishery bycatch on western Alaska Chinook salmon. ICES Journal of Marine Science, 72: 1159–1172.

Jensen, O. P., Seppelt, R., Miller, T. J., and Bauer, L. J. 2005. Winter distribution of blue crab *Callinectes sapidus* in Chesapeake Bay: application and cross-validation of a two-stage generalized additive model. Marine Ecology Progress Series, 299: 239–255.

Kelly, K. H., and Moring, J. R. 1986. Species profiles: life histories and environmental requirements of coastal fishes and invertebrates (North Atlantic)—Atlantic herring. U.S. Fish and Wildlife Service Biological Report 82(11.38). U.S. Army Corps of Engineers, TR EL-82–4. 22 pp.

Kitchens, L. L., and Rooker, J. R. 2014. Habitat associations of dolphinfish larvae in the Gulf of Mexico. Fisheries Oceanography, 23: 460–471.

Langøy, H., Nøttestand, L., Skaret, G., Broms, C., and Fernö, A. 2012. Overlap in distribution and diets of Atlantic mackerel (*Scomber scombrus*), Norwegian spring-spawning herring (*Clupea harengus*) and blue whiting (*Micromesistius poutassou*) in the Norwegian Sea during late summer. Marine Biology Research, 8: 442–460.

Limburg, K. E., and Waldman, J. R. 2009. Dramatic declines in North Atlantic diadromous fishes. Bioscience, 59: 955–965.

Lobo, J. M., Jiménez-Valverde, A., and Real, R. 2008. AUC: a misleading measure of the performance of predictive distribution models. Global Ecology and Biogeography, 17: 145–151.

Lynch, P. D., Nye, J. A., Hare, J. A., Stock, C. A., Alexander, M. A., Scott, J. D., Curti, K. L., *et al.* 2015. Projected ocean warming creates a conservation challenge for river herring populations. ICES Journal of Marine Science, 72: 374–387.

Mann, K. H. 1993. Physical oceanography, food chains, and fish stocks: a review. ICES Journal of Marine Science, 50: 105–119.

Maravelias, C. D. 1999. Habitat selection and clustering of a pelagic fish: effects of topography and bathymetry on species dynamics. Canadian Journal of Fisheries and Aquatic Sciences, 56: 437–450.

Maravelias, C. D. 2001. Habitat associations of Atlantic herring in the Shetland area: influence of spatial scale and geographic segmentation. Fisheries Oceanography, 10: 259–267.

Maravelias, C. D., Reid, D. G., and Swartzman, G. 2000. Modelling spatio-temporal effects of environment on Atlantic herring, *Clupea harengus*. Environmental Biology of Fishes, 58: 157–172.

McDowall, R. M. 2008. Diadromy, history, and ecology: a question of scale. Hydrobiologia, 602: 5–14.

Miller, T. J., Das, C., Politis, P. S., Miller, A. S., Lucey, S. M., Legault, S. M., Brown, R. W., *et al.* 2010. Estimation of Albatross IV to Henry B. Bigelow calibration factors. Northeast Fisheries Science Center Reference Document 10–05. 233 pp.

Murtaugh, P. A. 1996. The statistical evaluation of ecological indicators. Ecological Applications, 6: 132–139.

Neves, R. J. 1981. Offshore distribution of alewife, *Alosa pseudoharengus*, and blueback herring, *Alosa aestivalis*, along the Atlantic coast. Fishery Bulletin, 79: 473–485.

Northeast Fisheries Science Center (NEFSC). 2006. 42th Northeast Regional Stock Assessment Workshop (42th SAW) Assessment Summary Report. U.S. Department of Commerce, Northeast Fisheries Science Center Ref Doc. 06–01. 61 pp.

Northeast Fisheries Science Center (NEFSC). 2012. 54th Northeast Regional Stock Assessment Workshop (54th SAW) Assessment Summary Report. U.S. Department of Commerce, Northeast Fisheries Science Center Ref Doc. 12–14. 40 pp.

Overholtz, W. J., Hare, J. A., and Keith, C. M. 2011. Impacts of interannual environmental forcing and climate change on the distribution of Atlantic Mackerel on the U.S. northeast continental shelf. Marine and Coastal Fisheries: Dynamics, Management, and Ecosystem Science, 3: 219–232.

Pearcy, W. G., and Fisher, J. P. 2011. Ocean distribution of the American shad (*Alosa sapidissima*) along the Pacific coast of North America. Fisheries Bulletin, 109: 440–453.

Politis, P. J., Galbraith, J. K., Kostovick, P., and Brown, R. W. 2014. Northeast Fisheries Science Center bottom trawl survey protocols for the NOAA Ship Henry B. Bigelow. U.S. Department of Commerce, Northeast Fisheries Science Center Ref Doc. 14–06. 138 pp.

Radlinski, M. K., Sundermeyer, M. A., Bisagni, J. J., and Cadrin, S. X. 2013. Spatial and temporal distribution of Atlantic mackerel (*Scomber*

scombrus) along the northeast coast of the United States, 1985–1999. ICES Journal of Marine Science, 70: 1151–1161.

Schtickzelle, N., and Quinn, T. P. 2007. A metapopulation perspective for salmon and other anadromous fish. Fish and Fisheries, 8: 297–314.

Sette, O. E. 1950. Biology of the Atlantic mackerel (*Scomber scombrus*) of North America, part II: migrations and habits. U.S. Fish and Wildlife Service Fishery Bulletin, 51: 251–358.

Sinclair, M., and Iles, T. D. 1985. Atlantic herring (*Clupea harengus*) distributions in the Gulf of Maine – Scotian Shelf area in relation to oceanographic features. Canadian Journal of Fisheries and Aquatic Sciences, 42: 880–887.

Stram, D. L., and Ianelli, J. N. 2015. Evaluating the efficacy of salmon bycatch measures using fishery-dependent data. ICES Journal of Marine Science, 72: 1173–1180.

Studholme, A. L., Packer, D. B., Berrien, P. L., Johnson, D. L., Zetlin, C. A., and Morse, W. W. 1999. Essential fish habitat source document: Atlantic mackerel, *Scomber scombrus*, life history and habitat characteristics. NOAA Tech Memo NMFS NE 141. 35 pp.

Walsh, M., Reid, D. G., and Turrell, W. R. 1995. Understanding mackerel migration off Scotland: tracking with echosounders and commercial data, and including environmental correlates and behavior. ICES Journal of Marine Science, 52: 925–939.

Waples, R. S., and Naish, K. A. 2009. Genetic and evolutionary considerations in fishery management: research needs for the future. *In* The Future of Fisheries Science in North America, pp. 427–451. Edited by R. J. Beamish, and B. J. Rothschild. Springer, Dordrecht.

Wood, S. N. 2006. Generalized Additive Models: An Introduction with R. CRC Press, Boca Raton, FL.

Handling editor: Manuel Hidalgo

ICES Journal of Marine Science

ICES Journal of Marine Science (2016), 73(7), 1925–1934. doi:10.1093/icesjms/fsv240

Contribution to the Themed Section: '*Seascape Ecology*'

Original Article

Identifying environmental factors associated with the genetic structure of the New Zealand scallop: linking seascape genetics and ecophysiological tolerance

Catarina N. S. Silva[1,2]* and Jonathan P. A. Gardner[1]

[1]*School of Biological Sciences, Victoria University of Wellington, PO Box 600, Wellington 6140, New Zealand*
[2]*Department of Biosciences, University of Helsinki, PO Box 65, Helsinki, Finland*

**Corresponding author: tel: +358 2941 57735; fax: +358 2941 57694; e-mail: catarina.silva@helsinki.fi*

Silva, C. N. S., and Gardner, J. P. A. Identifying environmental factors associated with the genetic structure of the New Zealand scallop: linking seascape genetics and ecophysiological tolerance. – ICES Journal of Marine Science, 73: 1925–1934.

Received 4 June 2015; revised 11 November 2015; accepted 18 November 2015.

Understanding the processes responsible for shaping the spatial genetic patterns of species is critical for predicting evolutionary dynamics and defining significant evolutionary and/or management units. Here, we investigated the potential role of environmental factors in shaping the genetic structure of the endemic New Zealand scallop *Pecten novaezelandiae* using a seascape genetics approach. For this, we assayed genetic variation at 12 microsatellite markers in 952 individuals collected from 14 sites throughout New Zealand, and used data for 9 site-specific environmental variables (3 geospatial and 6 environmental variables). Our results indicate that a combination of environmental factors may be contributing to the observed patterns of genetic differentiation, but in particular, freshwater discharge and suspended particulate matter concentration were identified as being important. Environmental variation in these parameters may be acting as a barrier to gene flow. In terms of their ecophysiology, scallops are not particularly tolerant of high concentrations of either freshwater input or suspended sediment, making the identification of an association between these environmental variables and genetic variation particularly relevant across the full distributional range of this species. Although geographic distance between populations was also an important variable explaining the genetic variation among populations, it appears that levels of genetic differentiation are not a simple function of interpopulation distance. This study has identified previously unknown environmental factors that may be acting on the genetic structure of the New Zealand scallop and highlights the utility of seascape genetic studies to better understand the processes shaping the genetic structure of organisms.

Keywords: barriers to gene flow, environmental variability, freshwater input, New Zealand, *Pecten novaezelandiae*, scallop, seascape genetics, suspended sediment.

Introduction

Population genetic studies of marine species can be challenging because it can be hard to identify clear geographic patterns and barriers to gene flow. It is recognized that the interactions between organisms and their environment play a crucial role in shaping spatial genetic structure. For example, genetic differentiation between pairs of populations may increase with environmental differences independent of the geographic distance among populations, but as a result of the interactions between organisms and their environment (Wang and Bradburd, 2014). Seascape genetics is a multidisciplinary approach that brings together genetic data with environmental data to assess how marine environmental features may contribute to the genetic structure of organisms (Liggins *et al.*, 2013). Complementing traditional population genetics techniques with environmental information can increase the explanatory power of population genetic studies to help elucidate the role of environmental features in shaping patterns of genetic structure (Wei *et al.*, 2013).

Seascape genetics studies typically use neutral genetic markers to understand associations between environmental factors and neutral genetic variation (Wei *et al.*, 2013). In this case, since there is no selection, genetic variability depends on neutral population processes such as gene flow, genetic drift, and mutation (Liggins *et al.*, 2013). Therefore, if a particular environmental factor explains the genetic

variation of a species, this environmental feature might be preventing gene flow among populations. However, tests for selection generally have low power (Slatkin, 1994, 1996), it is unclear how many studies that used genetic markers assumed to be neutral have been influenced by selection (Yang and Nielsen, 2008) and it is debatable whether any locus is ever absolutely neutral (Liggins *et al.*, 2013). Nonetheless, coding genes under selection can obscure the processes of genetic drift and migration among populations, and putatively neutral markers such as microsatellites are ideal for inferring demographic processes such as isolation or migration and changes in population size (Riginos and Liggins, 2013).

Organisms with a pelagic larval stage are particularly influenced by environmental variability, and their dispersal and successful recruitment are highly dependent on the prevailing environmental conditions. The use of multidisciplinary tools to investigate these processes is particularly important for marine taxa, increasing the power that describes the drivers of genetic patterns in species that often exhibit a relatively weak genetic signal (Selkoe *et al.*, 2008; Heath *et al.*, 2014). Our understanding of how environmental factors affect the maintenance of genetic structure and species evolution is still very limited. Multidisciplinary studies that integrate genetics with other tools to understand which and how environmental factors influence genetic patterns are scarce, but the field is now developing rapidly (see Gaggiotti *et al.*, 2009; Selkoe *et al.*, 2010; Wei *et al.*, 2013; Bert *et al.*, 2014 for recent examples).

Extending from subtropical to subantarctic waters, the New Zealand marine environment is complex and its different habitats are characterized by a wide range of environmental factors (Shears *et al.*, 2008). The endemic scallop *Pecten novaezelandiae*, a subtidal, soft substrate dwelling bivalve, is an ideal species to investigate the correlation between genetic and environmental variability because it is distributed throughout New Zealand's North, South, Stewart, and Chatham Islands (Shumway and Parsons, 2006), all of which encompass a wide range of environmental variation. A limited number of seascape genetic studies have been conducted in New Zealand on intertidal and shallow subtidal species, and all have identified sea surface temperature as a major environmental variable that is associated with species-specific genetic variation (Wei *et al.*, 2013; Constable, 2014; Hannan, 2014). This study aims to identify environmental variables that contribute to the population genetic structure of the New Zealand scallop *P. novaezelandiae* and therefore brings us one step closer to understanding the factors that shape genetic structure of marine coastal populations.

Material and methods

Genetic data collection

Multilocus microsatellite genetic data were obtained for 952 individuals of *P. novaezelandiae* collected from 14 sites around New Zealand between 2012 and 2014 (Figure 1). Sampling was dependent on the hotspots of distribution of the species. Scallops were collected from 15 locations using scuba diving from depths between 7 and 15 m and dredging from depths between 15 and 50 m. The number of individuals per location varied between 10 and 115 (Table 1). After collection, samples of the adductor muscle were preserved in 80% ethanol and frozen (−20°C) for later processing.

Total DNA was extracted from scallop adductor muscle using the Geneaid Genomic DNA Kit, following the manufacturer's

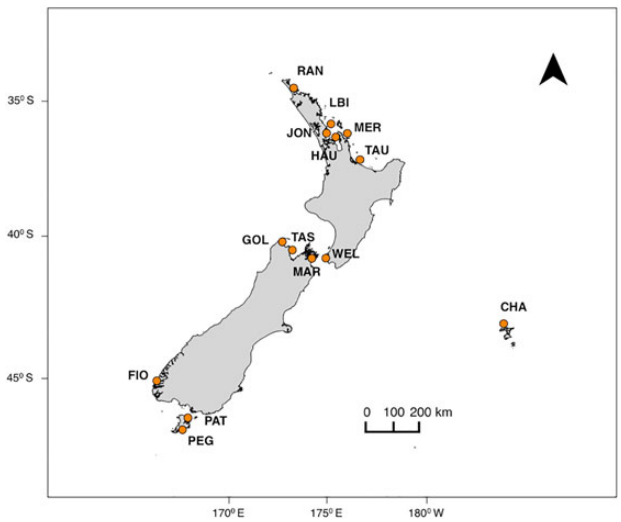

Figure 1. Map of sampling sites of *P. novaezelandiae* collected from New Zealand. Locations abbreviations as per Table 1.

Table 1. Summary of samples of *P. novaezelandiae* with collecting location descriptions, sample sizes (*N*), mean depth (m), dates, and geospatial coordinates.

Code	Location description	*n*	Depth (m)	Date collected	Latitude	Longitude
RAN	Rangaunu Bay	98	42	3 November 2012	−34° 49′ 2.8″	+173° 18′ 6.45″
LBI	Little Barrier Is	95	15	1 May 2012	−36° 13′ 51.0″	+175° 4′ 17.40″
JON	Jones Bay	40	10	15 November 2012	−36° 22′ 53.6″	+174° 48′ 59.48″
HAU	Hauraki Gulf	99	43	28 November 2012	−36° 34′ 9.60″	+175° 14′ 6.57″
MER	Mercury Is	69	15	1 May 2012	−36° 41′ 3.60″	+175° 43′ 33.60″
TAU	Tauranga	99	22	3 May 2012	−37° 40′ 14.4″	+176° 24′ 10.80″
WEL	Wellington Harbour	115	10	3 February 2012 31 May 2013	−41° 18′ 05.0″	+174° 48′ 35.0″
MAR	Marlborough Sounds	50	15	11 December 2012	−41° 11′ 54.8″	+174° 07′ 09.2″
TAS	Tasman Bay	48	22	13 May 2014	−41° 04′ 27.0″	+173° 05′ 48.0″
GOL	Golden Bay	48	20	14 May 2014	−40° 36′ 27.6″	+172° 46′ 40.8″
FIO	Fiordland	35	9	1 October 2012	−45° 35′ 7.51″	+166° 44′ 4.34″
PEG	Stewart Is, Port Pegasus	10	10	11 May 2012	−47° 10′ 6.53″	+167° 42′ 0.97″
PAT	Stewart Is, Paterson Inlet	48	7	4 April 2014	−46° 55′ 58.0″	+168° 04′ 15.0″
CHA	Chatham Is	98	50	11 March 2013	−43° 42′ 32.40″	−176° 23′ 38.40″
Total		952				

instructions. A NanoDrop™ ND-1000 (Thermo Scientific) was used to quantify DNA concentrations and the A260/A280 ratios. Individuals were genotyped at 12 polymorphic microsatellite loci (Silva and Gardner, 2014). Microsatellite loci were PCR-amplified in reactions of 15 μl containing 70 ng of DNA template, 0.5 units μl^{-1} *Taq* DNA polymerase, 67 mM Tris–HCl pH 8.8, 16 mM $(NH_4)SO_4$, 2 mM $MgCl_2$, 0.2 mM dNTPs, 0.3 μM of Forward and Reverse primers, and ddH_2O to volume. Primers were fluorescently labelled (FAM, NED, PET, and VIC) and primer pairs were PCR multiplexed using the conditions described in Silva and Gardner (2014). PCR products were visualized with an automated sequencer (ABI PRISM 3730 DNA Sequencer, Applied Biosystems) with the GeneScan-500 (LIZ) internal size standard. The software GeneMarker V2.2.0 (SoftGenetics) was used to analyse electropherograms for allele scoring and the AutoBin program (Guichoux *et al.*, 2011) was used to bin alleles with manual checking.

Genotyping artefacts were assessed using the software MicroChecker v.2.2.0.3 (Van Oosterhout *et al.*, 2004). Analysis of departure from Hardy–Weinberg equilibrium (HWE) and linkage disequilibrium (LD) were performed using the software GenePop on the web using the Markov chain method and Fisher's exact test (Rousset, 2008). False discovery rate (FDR) control (Verhoeven *et al.*, 2005) was applied to *p*-values in all statistical analyses that included multiple comparisons. An outlier analysis was performed using the software Lositan (Antao *et al.*, 2008), which identified outlier loci that have excessively high or low F_{ST} values compared with neutral expectations, considering the relationship between F_{ST} and H_E (expected heterozygosity) in an island model. Fifty thousand simulations were run with a confidence interval (CI) of 0.95 under the infinite alleles model (IAM) for a sample size of 50. The average neutral F_{ST} was used and the "force mean F_{ST}" option was selected to increase the reliability of mean F_{ST}.

The software HP-Rare (Kalinowski, 2005) was used to quantify genetic diversity as allelic richness (A_R) and private allelic richness (PA_R) with a rarefaction sample size of 24 individuals and a minimum sample size of 16 genes due to missing data. GenAlEx 6.5 (Peakall and Smouse, 2012) was used to quantify the number of private alleles per locations (Pa), observed (H_O) and expected (H_E) heterozygosity, and the fixation index (F_{IS}).

Genetic differentiation among populations was assessed using two different approaches. Pairwise F_{ST} values were calculated using the software GenePop on the web (Rousset, 2008). This F_{ST} value, formally known as theta (θ), was adapted by Weir and Cockerham (1984) for use with multi-allelic loci. An exact *G*-test (Goudet *et al.*, 1996) was also calculated in GenePop (Markov-chain parameters: 10 000 dememorization steps, 1000 batches, and 10 000 iterations per batch) for each population pair using the *G* log-likelihood ratio. Modified pairwise statistics (F'_{ST}) were calculated using the software GenoDive 2.0b25 (Meirmans and Van Tienderen, 2004). The F'_{ST} index is a modified version of F_{ST} designed specifically for highly variable multi-allelic markers such as microsatellites (Meirmans, 2006; Meirmans and Hedrick, 2011). It is a standardized measure based on a maximum possible value, given the observed amount of within-population diversity. Following Meirmans and Hedrick (2011), we employ F_{ST} and F'_{ST}. Allele frequencies were obtained using the software GenAlEx 6.5 (Peakall and Smouse, 2012).

A principal coordinate analysis (PCoA) was performed in GenAlEx 6.5 (Peakall and Smouse, 2012) to examine the variation among populations using co-dominant genetic distance. A Mantel test was also performed in GenAlEx 6.5 (Peakall and Smouse, 2012) using F_{ST} values and the shortest coastal distances between locations for the 13 locations in the mainland New Zealand.

Environmental and geospatial data collection

Although there is still a paucity of marine environmental data for seascape genetic analyses, there has been a recent increase in the number of local and global datasets that are available for such work. To investigate the influence of environmental factors on the genetic variation of *P. novaezelandiae*, different environmental datasets were used in this study. The New Zealand Marine Environmental Classification (MEC) system is an ecosystem-based spatial framework developed for marine management applications and is composed of a number of data layers with information on the New Zealand marine physical environment (Snelder *et al.*, 2005). The benthic-optimized marine environment classification (BOMEC) scheme was specifically developed to assess the impacts of bottom trawling on benthic organisms in New Zealand (Boyer *et al.*, 2005; Pinkerton and Richardson, 2005). Additional data layers covering a global scale now exist, some of which address gaps in the New Zealand-specific data. In addition, satellite-derived data are now widely available as free downloads from a number of websites. For example, the MODIS instrument (Moderate Resolution Imaging Spectroradiometer) from NASA (National Aeronautics and Space Administration), operating on Aqua spacecraft, views the entire surface of the Earth and acquires data every 1–2 d. The Ocean Color Data Processing System (OCDPS) produces and distributes the ocean colour data (Thomas and Franz, 2005). In combination, these sorts of environmental datasets now provide new and unparalleled opportunity to investigate associations between genetic and environmental variation.

Three geospatial variables were obtained from Google Maps for each site: (i) latitude (Lat), (ii) longitude (Lon), and (iii) index of geographic distance (Geo_dist) calculated as the sum of all shortest possible coastal distances (km) between all pairs of populations [a low value indicates a population's proximity to all other populations, whereas a high value indicates its isolation, e.g. Wei *et al.* (2013)]. Thirteen site-specific environmental variables were obtained from the MEC scheme (New Zealand Ministry for the Environment, 2005): depth (m), annual mean solar radiation (Rad_mean; Wm^{-2}), winter solar radiation (Rad_wint; Wm^{-2}), winter sea surface temperature (SSTwint; °C), annual amplitude of sea surface temperature (SSTanamp; °C), spatial gradient annual mean sea surface temperature (SSTgrad; °C km^{-1}), summertime sea surface temperature anomaly (SSTanom; °C), mean orbital velocity or the orbital velocity at the bed for the mean significant wave height calculated from a 20-year wave hindcast (Orb_v_mean; m s^{-1}), extreme orbital velocity or the orbital velocity at the bed for the 95th percentile significant wave height calculated from a 20-year wave hindcast (Orb_v_95; m s^{-1}), tidal current (Tidal; m s^{-1}), sediment type (Sed; categorical variable), seabed rate of change of slope (Bed_prof; 0.01 m^{-1}), freshwater fraction, or the proportion of freshwater based on river inputs (FW; proportion). These data are from the exclusive economic zone (EEZ) with a spatial resolution of 1 km and are drawn from multiple years between 1983 and 2000. The environmental variables salinity (Sal; psu; Boyer *et al.*, 2005), suspended particulate matter (SPM; arbitrary units), and dissolved organic matter (DOM; arbitrary units; Pinkerton and Richardson, 2005) were obtained from the BOMEC scheme (Leathwick *et al.* 2012). The open source Geographic Information System software QGIS 2.4 (QGIS Development Team, 2014) was used to obtain site-specific data from both MEC and BOMEC schemes for each of the 14 locations. The variables chlorophyll

a (Chl_a; mg chl *a* m^{-3}) and total suspended sediment (TSS; g m^{-3}) were obtained from the ocean colour satellite data MODIS project for multiple years between 2002 and 2014 (NASA, 2014). Chlorophyll *a* and total suspended sediment data were not available for the populations MAR, FIO, PEG, and CHA, which highlights that the marine environmental data available for seascape genetic studies are still limited (Supplementary Tables S1 and S2).

The software package Statistica 12.0 was used to test for independence of the environmental variables. A Pearson correlation test and a principal component analysis (PCA) were performed and a subset of environmental variables that were correlated at the 0.05 level was removed from further analysis.

The use of different analytical methods can increase confidence that the environmental variables are truly associated with the genetic variation. Therefore, to test the null hypothesis that none of the geospatial or environmental variables explains significant genetic variation in *P. novaezelandiae* in terms of F_{ST} values, F'_{ST} values, and allelic frequencies, three statistical methodologies were employed: (i) a generalized linear model (GLM), which is a multiple regression analysis between a dependent variable (mean value of F_{ST} or F'_{ST} across all loci) and a number of environmental variables (Wei *et al.*, 2013), (ii) a biological environmental stepwise analysis (BEST) that tests for the relationship between resemblance matrices of dependent and predictor variables (Wei *et al.*, 2013), and (iii) a distance-based linear model (DISTLM) routine in PERMANOVA+ (Anderson *et al.*, 2008) that tests for associations between genetic and environmental variation while controlling for geospatial data.

GLM analyses

The GLM was calculated using the software Statistica 12.0 (the GLZ routine). The Akaike information criterion (AIC) was used to rank the models (best fit model with the lowest AIC score) at the significance level of $p < 0.05$. A test of all effects was performed using the Wald statistic to determine the significance of the regression coefficient. The analyses were run for 14 locations using all variables and then repeated using only geospatial or only environmental variables to determine their relative importance in explaining genetic variation, following Wei *et al.* (2013). The contribution of each variable to the model was assessed using the type III likelihood ratio test that reports the log-likelihoods for the model that includes a particular effect and all effects that precede it. The incremental χ^2 statistic provides a test of the change in the log-likelihood that is attributable to each individual effect.

BEST analyses

The BEST routine was implemented in PRIMER v.6 (Clarke and Gorley, 2006) to examine the association between allele frequencies and environmental/geospatial variables, following Wei *et al.* (2013). First, the analyses were run for all variables and then repeated using only geospatial or only environmental variables to determine their relative importance in explaining genetic variation at 14 locations. A Bray–Curtis resemblance matrix was employed for the allele frequencies and a Euclidean distance resemblance matrix was employed for the environmental/geospatial variables. To test for correlation between the two matrices, the BIOENV subroutine of the BEST routine was implemented in PRIMER v.6 (Clarke and Gorley, 2006) using the Spearman correlation coefficient method (r_s) to test all combinations of factors. Models were considered significant at $p < 0.05$ after 1000 permutations. In addition, the association between allele frequencies and environmental/geospatial variables was also investigated for each locus for all 14 locations using the BEST routine to test for locus-specific responses.

DISTLM analyses

To test for spatial autocorrelation in the dataset, that is, to test for associations between genetic and environmental variation while controlling for geospatial data, we used the distance-based linear models (DISTLM) routine in PERMANOVA+ (Anderson *et al.*, 2008). This test is a permutational equivalent to partial redundancy analysis (Legendre and Anderson, 1999). DISTLM was used to perform an ordination of fitted values from a given model and is constrained to find linear combinations of predictor variables (environmental data) that explain the greatest variation in the data cloud (population-specific allele frequencies). Permutation of residuals is carried out under a reduced (or partial) model and because this is a permutational test, there are no assumptions about data normality (Anderson *et al.*, 2008). The distance-based Redundancy Analysis (dbRDA) routine was employed to visualize the fitted model in multidimensional space. Data were examined in PRIMER and PERMANOVA+ as draftsman plots of the variables (environmental data) for skewness and for extreme outliers. Preliminary testing revealed that neither data transformation [square root, fourth root, $\log(x + 1)$] nor resemblance index (Bray–Curtis, Euclidian) had a profound effect on the genetic dataset, so raw population-specific allele frequency data and the Bray–Curtis similarity index were employed to generate the resemblance matrix for the genetic dataset. In the DISTLM model, the three geospatial variables (Lat, Lon, Geo_dist) were entered first with the six environmental variables being entered thereafter (sequential tests). Once variation in the genetic dataset had been accounted for by the geospatial variables the test quantifies the contribution of the environmental variables to explaining variation in the genetic dataset. A total of 9999 permutations were employed and we used R^2 as a test of model fit to examine the contribution of all variables to the model. Subsequently, as a model building exploratory exercise, we used the DISTLM procedure to identify the contribution of individual variables (geospatial and environmental) to explaining variation in the genetic dataset. We employed the forward stepwise model building approach, starting from a null model containing no predictor variables. Forward selection adds predictor variables that result in the greatest improvement of the selection criterion (R^2).

Results

Micro-Checker identified putative null alleles at the loci *Pnova_02*, *Pnova_05*, *Pnova_10*, *Pnova_24*, *Pnova_27*, and *Pnova_33* due to homozygote excess in each case. No pattern of null allele frequency as a function of population or locus was identified. No long allele dropout was detected. After FDR correction for multiple tests, *Pnova_24* was identified as being significantly out of HWE at nine locations. No evidence of significant LD was detected between locus pairs. *Pnova_24* and *Pnova_31* had the most missing data at 21.3 and 19.1%, respectively, and the other ten loci had an average of 2.7 ± 2.4% of missing data.

Pnova_27 and *Pnova_28* were identified as candidates for balancing selection under the stepwise mutation model and *Pnova_27*, *Pnova_28*, and *Pnova_33* under the IAM. However, this is possibly an artefact because these are highly polymorphic loci. *Pnova_01, Pnova_02, Pnova_04*, *Pnova_05, Pnova_09*, *Pnova_10*, and *Pnova_32* were identified as neutral markers under the infinite allele and stepwise mutation models. *Pnova_24* and *Pnova_31* were identified as F_{ST} outliers and candidates for positive selection under the

Table 2. Pairwise F_{ST} values for *P. novaezelandiae* using ten loci are below the diagonal(significant F_{ST} values are in bold after FDR testing) and F'_{ST} values are above the diagonal.

Code	RAN	LBI	JON	HAU	MER	TAU	WEL	MAR	TAS	GOL	FIO	PEG	PAT	CHA
RAN	–	−0.008	−0.009	−0.007	0.002	0.003	0.001	−0.002	0.000	0.002	0.045	−0.003	0.057	0.012
LBI	−0.002	–	−0.002	−0.001	0.006	0.000	0.004	0.008	−0.009	−0.005	0.047	0.014	0.063	0.014
JON	−0.001	0.001	–	−0.004	0.000	0.001	0.00	0.003	−0.006	0.005	0.045	−0.021	0.063	0.017
HAU	−0.001	0.001	0.001	–	−0.002	0.003	0.000	−0.001	0.003	−0.003	0.034	−0.032	0.058	0.014
MER	0.002	0.003	0.002	0.000	–	−0.002	0.016	0.021	0.014	0.016	0.042	0.012	0.082	0.030
TAU	0.002	0.001	0.002	0.002	0.000	–	0.015	0.022	0.006	0.011	0.043	0.002	0.069	0.021
WEL	0.001	0.002	0.001	0.001	0.006	**0.007**	–	−0.001	−0.003	−0.007	0.037	0.001	0.048	0.019
MAR	0.001	0.004	0.002	0.002	**0.008**	**0.009**	0.001	–	−0.005	−0.002	0.027	−0.015	0.052	0.023
TAS	0.001	−0.001	0.000	**0.003**	**0.006**	0.003	0.000	0.001	–	−0.014	0.031	0.002	0.051	0.023
GOL	0.003	0.000	0.005	0.001	0.007	0.006	−0.001	0.003	−0.002		0.020	0.014	0.059	0.020
FIO	**0.017**	**0.018**	**0.018**	**0.014**	**0.016**	**0.017**	**0.015**	**0.012**	**0.013**	**0.010**		0.023	0.044	0.050
PEG	0.005	0.011	0.004	−0.003	0.009	0.008	0.007	0.004	**0.008**	0.015	**0.015**		−0.014	−0.004
PAT	**0.020**	**0.022**	**0.023**	**0.021**	**0.027**	**0.024**	**0.017**	**0.019**	**0.018**	**0.022**	**0.016**	0.000		0.053
CHA	**0.005**	**0.005**	**0.007**	**0.005**	**0.011**	**0.008**	**0.007**	**0.008**	**0.008**	**0.008**	**0.018**	0.002	**0.018**	

Location abbreviations as per Table 1. Negative F_{ST} and F'_{ST} values were converted to zero for the subsequent analyses.

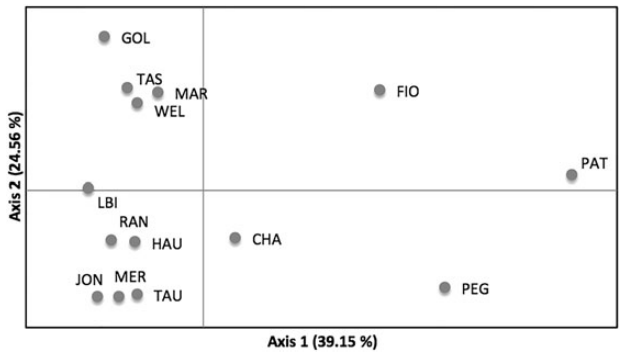

Figure 2. PCoA for *P. novaezelandiae* using pairwise genetic distance based on ten microsatellite loci. Locations abbreviations as per Table 1.

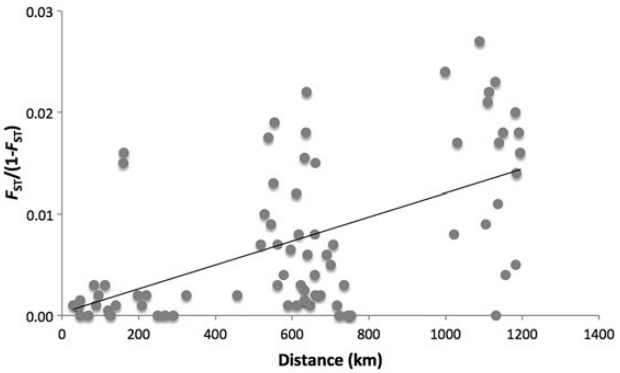

Figure 3. Scatterplot of Mantel test for 13 locations in the mainland New Zealand using F_{ST} values ($R^2 = 0.324$, $p < 0.01$).

infinite allele and stepwise mutation models. *Pnova_24* and *Pnova_31* were therefore excluded from the following analyses due to a combination of factors (i.e. missing data and F_{ST} outliers).

Genetic structure

Allelic richness ranged from 4.91 at FIO to 5.89 at RAN and private allelic richness ranged from 0.08 at FIO to 0.25 at RAN. In total, there were 27 private alleles across all populations; RAN had the highest number (8). Overall, values of H_O were lower than H_E except locations at Stewart Island. F_{IS} ranged from −0.090 at PEG to 0.146 at HAU and from −0.066 at *Pnova*_04 to 0.198 at *Pnova*_ 33 (Supplementary Tables S3 and S4). Pairwise F_{ST} values for all comparisons ranged from 0 to 0.027, while F'_{ST} values ranged from 0 to 0.082 (Table 2). The mean F_{ST} values ranged from 0.004 at HAU to 0.019 at PAT and the mean F'_{ST} values ranged from −0.001 at PEG to 0.052 at PAT (Table 2).

Genetic structure was apparent from the PCoA, in which axis 1 explained 39.15% of the variation and axis 2 explained 24.56%. Analysis grouped the northern North Island populations (RAN, LBI, JON, HAU, MER, TAU) separately from the central New Zealand populations (WEL, MAR, TAS, GOL). Fiordland (FIO), Stewart Island (PEG, PAT), and Chatham Islands (CHA) were plotted separately from all other locations (Figure 2). Mantel testing revealed a weak but significant isolation by distance signal ($R^2 = 0.324$, $p < 0.01$; Figure 3).

Correlation of variables

Pearson's correlation analyses and PCA showed that the environmental variables FW, DOM, and SPM were independent of all other variables. The variables Rad_mean, Rad_wint, SSTwint, SSTanamp, Sed, Sal, Chl_a, and TSS were correlated with latitude, while the variables Depth and Sed were correlated with longitude (Figure 4). Therefore, the three geospatial variables and the following six independent environmental variables were used for seascape analyses: spatial gradient annual mean sea surface temperature (SSTgrad; °C km^{-1}), mean orbital velocity (Orb_v_mean; m s^{-1}), tidal current (Tidal; m s^{-1}), freshwater fraction (FW; proportion), DOM (arbitrary units), and SPM (arbitrary units).

Generalized linear models

GLMs showed that the top ten best fitting models were all significant at $p < 0.01$ when testing variation in both F_{ST} and F'_{ST} values against variation in all nine geospatial and environmental variables. All the variables were included in the models; however, only the variables Lon, Geo_dist, Tidal, FW, and SPM were significant at $p < 0.05$ for the test of all effects (Table 3, Supplementary Table S5). The AIC values for the top ten models were not very different, suggesting that any of the models may be appropriate. However, for F_{ST}, the four variables SPM, FW, Tidal, and Geo_dist occurred in all ten models and Lon occurred in eight models, indicating that these

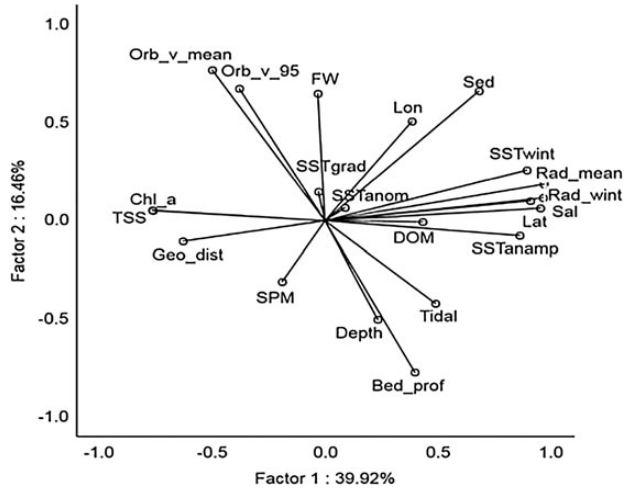

Figure 4. PCA of both the geospatial and environmental variables.

Table 3. Summary of results of the significant best fitting models of GLM analyses, BEST analyses, and DISTLM analyses testing for the contribution of all variables, geospatial and environmental variables to explain variation in F_{ST}, F'_{ST}, and allele frequencies for *P. novaezelandiae* at 14 locations.

Test	Significant variables at $p < 0.05$ (χ^2 value; p-value)[a]
GLM	
F_{ST}, all variables	Geo_dist (8.242; 0.004), Tidal (4.751; 0.029), FW (12.385; <0.001), SPM (53.115; <0.001)
F'_{ST}, all variables	Lon (8.932; 0.003), Tidal (3.604; 0.05), FW (7.336; 0.007), SPM (9.714; 0.002)
F_{ST}, geospatial	
F'_{ST}, geospatial	
F_{ST}, environmental	Tidal (3.530; 0.060), FW (4.352; 0.037), DOM (7.810; 0.006), SPM (23.829; <0.001)
F'_{ST}, environmental	SPM (8.492; 0.004)
BEST	
Allele frequencies, all variables	Lat, Tidal, FW, DOM, SPM
Allele frequencies, geospatial	Lat, Geo_dist
Allele frequencies, environmental	
DISTLM	
Allele frequencies, all variables	Lat, SPM

[a]Maximum likelihood test of individual effects—incremental χ^2 statistic and associated significance level (p-value).

five variables are likely to explain most variation in F_{ST}. For F'_{ST}, the four variables SPM, FW, Lon, and DOM occurred in all ten models (although DOM was not significant in the test of overall effects) and Tidal occurred in eight of the top ten models (Supplementary Table S5). Tests of the contribution of the five significant individual variables to the models for F_{ST} and F'_{ST} revealed that SPM explained most variation and that Tidal explained least variation in F_{ST} and F'_{ST} (Table 3).

When GLMs were run for only the three geospatial variables, the top six best fitting models were significant at $p < 0.01$ when testing variation in F_{ST} values, and included all the geospatial variables. When testing variation in F'_{ST} values against variation in geospatial variables, the top two best fitting models were significant at $p < 0.05$ and included only the variables Lat and Geo_dist (Table 3, Supplementary Table S6). For both F_{ST} and F'_{ST} analyses, the AIC values for the top ten models were not very different, suggesting that any of the models may be appropriate. Tests of all effects and ML tests of individual effects were all non-significant (Table 3, Supplementary Table S6), suggesting that no single geospatial variable alone contributes to explaining variation in F_{ST} or F'_{ST}.

GLMs for the six environmental variables revealed that the top ten best fitting models were all significant at $p < 0.01$ when testing variation in F_{ST} values against variation in environmental variables. All the environmental variables were included in the models, but only Tidal, FW, DOM, and SPM were significant at $p < 0.05$ for the test of all effects. The AIC values for the top ten models were not very different, suggesting that any of the models may be appropriate. However, SPM and DOM occurred in all ten models, FW occurred in eight models, and Tidal and Orb_v_mean occurred in six models, although Orb_v_mean was not significant in the test for all effects. The ML test of individual effects identified SPM as contributing most and Tidal as contributing least to the model of significant terms (Table 3). When testing variation in F'_{ST} values against variation in environmental variables, the top ten best fitting models were also all significant at $p < 0.01$. The AIC values for the top ten models were not very different, suggesting that any of the models may be appropriate. All the environmental variables were included in the models, but only SPM was significant at $p < 0.05$ for the test of all effects (Table 3, Supplementary Table S7). The ML test identified SPM ($p = 0.004$) and also DOM ($p = 0.048$) as contributing most to the model (Table 3).

BEST analyses

BEST analyses based on data from all 14 locations and 9 geospatial and environmental variables showed that the top two best fitting models were significant at $p < 0.05$ and both included the variables Lat, Tidal, FW, DOM, and SPM ($r_s = 0.588$). The remaining top eight best fitting models had similar Spearman's ρ values (0.587 and 0.586) and the variables Lat and SPM were included in all models (Table 3, Supplementary Table S8).

When only the three geospatial variables were analysed, BEST analyses showed that the two best fitting models were significant at $p < 0.01$ with $r_s = 0.560$ and included the variables Lat and Geo_dist. The remaining five best fitting models had very similar Spearman's ρ values, ranging from 0.559 to 0.499, and included all the geospatial variables (Table 3, Supplementary Table S9). When only the six environmental variables were analysed, BEST analyses showed that the ten best fitting models were not significant and had low Spearman's ρ values ranging from 0.327 to 0.234. The variable SPM was included in all the models and the variable FW was included in the eight best fitting models (Table 3, Supplementary Table S10).

BEST analyses of locus-specific data showed that Spearman's ρ values ranged from 0.265 for *Pnova*_33 ($p > 0.05$) to 0.572 for *Pnova*_04 ($p < 0.05$). Within the context of the limited statistical power of correlation analysis, these results suggest that genetic variation at some loci (such as *Pnova*_04, *Pnova*_09, and *Pnova*_10) may be more affected by environmental variation than genetic variation at other loci. The variable Lat occurred ten times in the top ten models for seven loci, the variable Lon occurred ten times for two

Table 4. Results of the BEST analyses testing for the contribution of 9 geospatial and environmental variables to explain variation in allele frequencies for each locus for *P. novaezelandiae* for all 14 locations.

Locus	r_s	*p*-value	Lat	Lon	Geo_ dist	SST grad	Orb_v_mean	Tidal	FW	DOM	SPM
*Pnova*_01	0.421	0.149						✓	✓	✓	✓
*Pnova*_02	0.536	0.087	✓					✓		✓	✓
*Pnova*_04	0.572	**0.030**	✓	✓					✓		✓
*Pnova*_05	0.320	0.417						✓	✓	✓	
*Pnova*_09	0.532	**0.003**	✓	✓					✓	✓	✓
*Pnova*_10	0.497	**0.034**	✓							✓	
*Pnova*_27	0.484	0.056	✓			✓		✓	✓	✓	✓
*Pnova*_28	0.365	0.322	✓								
*Pnova*_32	0.445	0.180	✓					✓			✓
*Pnova*_33	0.265	0.443				✓			✓	✓	
*Pnova*_01	–	–	0	0	0	5	0	4	8	6	10
*Pnova*_02	–	–	10	0	0	4	0	7	3	5	10
*Pnova*_04	–	–	**10**	**10**	**0**	**5**	**0**	**6**	**8**	**6**	**10**
*Pnova*_05	–	–	0	0	0	4	0	8	6	5	0
*Pnova*_09	–	–	**10**	**10**	**0**	**5**	**0**	**4**	**8**	**4**	**10**
*Pnova*_10	–	–	**10**	**0**	**0**	**5**	**0**	**2**	**6**	**6**	**0**
*Pnova*_27	–	–	10	0	0	5	0	4	8	6	10
*Pnova*_28	–	–	10	0	0	5	0	4	2	6	0
*Pnova*_32	–	–	10	0	0	5	0	6	2	4	10
*Pnova*_33	–	–	1	4	4	4	4	3	6	4	0

Top part of the table represents the best fitting model for each locus; the checkmarks (✓) indicate which variables were included in the model. Bottom part of the table indicates the number of times that each variable was included in the top ten best fitting models. Significant values are in bold.

loci, and SPM occurred ten times in the top ten models for six loci (Table 4).

DISTLM analyses

Draftsman plots revealed that all pairwise correlation coefficients were <0.525 and that only the variable Lon was right skewed. All variables were therefore retained in the DISTLM analysis. The overall fit for the model (R^2) was 0.812. Sequential testing revealed that of the three geospatial variables, only Lat was statistically significant ($p = 0.001$). Of the six environmental variables entered into the model after the geospatial variables, only SPM was significant ($p = 0.024$). The three geospatial variables explained 40.0% of the variation in the genetic dataset and the six environmental variables explained a further 41.1%. Model building using the forward stepwise approach revealed that Lat was the explanatory variable with greatest influence ($p < 0.05$), followed by Orb_v_mean, Geo_dist, SPM, and Lon (all $p < 0.10$). Significance (p) values for the remaining environmental variables were all $p > 0.210$, suggesting that inclusion of these variables (i.e. FW, DOM, SSTgrad, Tidal) does not increase substantially the explanatory power of the model (Table 3; Supplementary Table S11).

Discussion

A low but significant level of population genetic structure has been reported for *P. novaezelandiae* throughout its distributional range in New Zealand (Silva and Gardner, 2015). In the present study, a weak but statistically significant isolation by distance signal was detected and different combinations of environmental variables were correlated with the genetic variation. In general, the main variables driving the genetic structure were SPM and freshwater fraction (FW). Longitude was associated with genetic variation in terms of F'_{ST} values, but was not identified as being an important explanatory variable in the BEST analysis. Because sampling was based on the species' distribution and was not continuous along the coast, samples were obtained from three longitudinal groups: a western group with values ranging from $+166^\circ$ (FIO) to $+168^\circ$ (PAT), a central group ranging from $+172^\circ$ (GOL) to $+176^\circ$ (TAU), and to the east, the Chatham Islands at -176°. The inclusion of geospatial variables such as longitude, latitude, and even an index such as Geo_dist in seascape genetics analyses can be informative, but can also be misleading. All three variables are indirect estimates of geographic distance (km) among populations and when tested against indices such as F_{ST} and F'_{ST} (which are estimates of genetic distance among populations), such testing can be similar to the isolation by distance model. However, the three geospatial variables can be independent of each other (e.g. six sites that are equally spaced along in a line of latitude, such that all have the same latitudinal value, all have different longitudinal values, and three pairs of sites have similar Geo_dist values) and as such, seascape analyses may identify different geospatial variables as being able to explain genetic variation. The inclusion of latitude in seascape genetics models is not unexpected because latitude is a surrogate for many important environmental variables. However, the inclusion of longitude is harder to explain. In the present study, there is no obvious reason for the role that longitude may play in explaining scallop genetic variation, but we speculate that longitude may be a surrogate for genetic connectivity because beyond the confines of shallow water coastal systems, most of the oceanic current flow in this region is west to east. Thus, longitude may reflect gene flow at large spatial scales (100s to 1000s of km) in open water systems around New Zealand. The inclusion of other environmental variables (as discussed below) may better reflect small-scale coastal connectivity among populations. Ultimately, in a seascape genetics context, a species' population genetic variability will be a function of both small-scale (coastal) and large-scale (oceanic) processes that promote or retard genetic connectivity.

For most of the models, proportion of freshwater discharge was correlated with genetic variation in *P. novaezelandiae*. Given the physiological stress associated with salinity-induced osmotic changes that often occur over very short time-scales (minutes to hours) in

coastal systems, it is not surprising that environmental salinity variation may be an important explanation for genetic variation, either directly or indirectly as a barrier to gene flow between populations (e.g. Jørgensen *et al.*, 2005; McLeod and Wing, 2008; Hannan, 2014). Because most scallop species live in fully saline waters, not in waters characterized by fluctuating salinity, it is assumed that they are not tolerant of salinity variation. There have, however, been few studies addressing the salinity tolerance of scallop species, and in particular of the larval (dispersal) stage. *Argopecten gibbus* and *Aequipecten opercularis* do not survive well at reduced salinities (Shumway and Parsons, 2006) and *Argopecten purpuratus* is a stenohaline species occurring in bays along the Chilean coast where salinity fluctuations are generally small (34.5–35.2 psu; Uribe *et al.*, 2003). Although the present study does not test for causation, our results suggest that freshwater input might be an important factor limiting larval dispersal and thereby restricting gene flow between populations of *P. novaezelandiae*.

There was strong evidence supporting the correlation of genetic variation with levels of SPM and some of the models also showed correlation with DOM. Given that coastal areas are generally influenced by SPM and DOM, often from the same source (D'Sa *et al.*, 2007), these results are not surprising. Further, these results are in agreement with knowledge of the biology of bivalve species. Ecophysiological responses of many species are plastic, such that food ingestion rates may be regulated by changes in clearance rate, and prolonged exposure to SPM may affect both growth rate and survival (e.g. Bricelj and Malouf, 1984; Szostek *et al.*, 2013). Alternatively, for genetic markers such as microsatellites that are presumptively neutral, local changes in coastal oceanographic properties such as the concentrations of SPM and DOM (e.g. from riparian input) may act as a (partial) barrier to gene flow and thereby restrict larval movement between neighbouring regions or may reflect the mosaic nature of suitable habitat patchiness (e.g. Selkoe *et al.*, 2008). As such, differences in genetic variation may accumulate between two geographically close regions. Such barriers to gene flow may not be permanent, but may be semi-permeable as a consequence of seasonal variability in the nature of the barrier (e.g. Apte and Gardner, 2002; Veale and Lavery, 2011).

Tidal current as an environmental factor explained scallop genetic structure in some models. Strong tidal current flow may negatively affect scallop populations by scouring of the substratum or by preventing the successful settlement of juveniles, whereas weak tidal current flow may be associated with increased levels of sedimentation that may lead to gill clogging and impairment of physiological performance by scallops (Shumway and Parsons, 2006). As such, tidal current flow may not be entirely independent of site-specific SPM concentrations and may be an important environmental variable that both promotes gene flow (connectivity) between sites and indirectly provides habitat that is most suitable for scallops

GLM analyses revealed that genetic variation was correlated with the index of geographic distance (geo_dist) between locations. These results are in agreement with the weak but statistically significant isolation by distance signal detected, suggesting that the distance between locations is an important variable explaining genetic variation. The pattern of isolation by distance, where all populations are connected by continuous migration but gene flow is higher between nearby populations, has been shown for other bivalves (e.g. St-Onge *et al.*, 2013). However, for *P. novaezelandiae*, it appears that the level of genetic differentiation is not a simple function of the geographic distance between populations. For example, it is not evident that the distance between the Chatham Islands and the mainland acts as an important barrier to larval dispersal because there is clear evidence of high levels of connectivity between these remote islands and the NZ mainland that is ~850 km to the west (Silva and Gardner, 2015). Other environmental factors such as the subtropical convergence might be facilitating gene flow and thus minimizing the impact of geographic distance between the Chatham Islands and mainland New Zealand.

Sea surface temperature has been identified as one important explanatory factor for the observed genetic variation in other intertidal and very shallow subtidal (<5 m depth) coastal species (Wei *et al.*, 2013; Constable, 2014; Hannan, 2014). For New Zealand, which is defined by a latitudinal gradient in temperature, an association between sea surface temperature and species-specific genetic variation may not be surprising. However, there was no strong evidence that temperature is an important factor explaining scallop genetic variation, suggesting that it may be an environmental variable of lesser importance, possibly because of the slightly deeper subtidal habitat preferences expressed by scallops which provide some degree of thermal buffering against a pronounced seasonal temperature signal.

Conclusions

Our results show that a combination of environmental and geospatial variables is significantly associated with the population genetic structure of *P. novaezelandiae* across its full distributional range. There was strong evidence that levels of SPM and freshwater input are factors that may contribute to population genetic structure of *P. novaezelandiae*. Significantly, among a suite of nine different variables, these two (SPM and freshwater input) are tied to known ecophysiological tolerances of scallops. While these findings indicate that environmental forces may be influencing the genetic variation of New Zealand scallops, the mechanism(s) by which this happens is unknown and will require further detailed study. In particular, the role of localized environmental variation acting as a barrier to gene flow between populations that may be only a few kilometres apart vs. the role of large-scale environmental variation such as sea surface temperature variation over 1000s of kilometres requires further attention, given that both may operate at the same time, but at very different spatial scales.

As for most seascape genetic studies to date, the current study is not able to test for causation. Other techniques such as direct observation of dispersal and reproduction or functional genomics would be required to evaluate the link between genetic variation and a particular spatial or environmental factor (Liggins *et al.*, 2013). While more environmental and genetic data have become available for seascape genetic analyses, studies of this sort are still scarce and patchy, with the result that interpretation of results may be limited. Nevertheless, seascape genetics is a valuable tool to increase understanding of genetic structure, particularly for marine species exhibiting a weak genetic signal. By identifying previously unknown environmental factors that can be driving genetic variation, the emerging field of seascape genetics provides essential clues for further research.

Supplementary data

Supplementary material is available at the *ICESJMS* online version of the manuscript.

Acknowledgements

We thank J.R. Williams, D. McNaughtan, S. Geange, D. Freeman, B. Twist, and R. Forrest for sample collection and M. Pinkerton for generating the variables from the ocean colour satellite data MODIS

project. Financial support for this research was provided by the New Zealand Ministry of Primary Industries (ZBD2009-10) to JPAG and a Victoria University of Wellington Doctoral Scholarship to CNSS.

References

Anderson, M. J., Gorley, R. N., and Clarke, K. R. 2008. PERMANOVA+ for PRIMER: Guide to Software and Statistical Methods. PRIMER-E Ltd, Plymouth, UK.

Antao, T., Lopes, A., Lopes, R. J., Beja-Pereira, A., and Luikart, G. 2008. LOSITAN: a workbench to detect molecular adaptation based on a Fst-outlier method. BMC Bioinformatics, 9: 323.

Apte, S., and Gardner, J. P. A. 2002. Population genetic subdivision in the New Zealand greenshell mussel (*Perna canaliculus*) inferred from single-strand conformation polymorphism analysis of mitochondrial DNA. Molecular Ecology, 11: 1617–1628.

Bert, T. M., Arnold, W. S., Wilbur, A. E., Seyoum, S., McMillen-Jackson, A. L., Stephenson, S. P., Weisberg, R. H., *et al.* 2014. Florida Gulf Bay Scallop (*Argopecten Irradians Concentricus*) population genetic structure: form, variation, and influential factors. Journal of Shellfish Research, 33: 99–136.

Boyer, T., Levitus, S., Garcia, H., Locarnini, R., Stephens, C., and Antonov, J. 2005. Objective analyses of annual, seasonal, and monthly temperature and salinity for the world on a 1/4° grid. International Journal of Climatology, 25: 931–945.

Bricelj, V. M., and Malouf, R. E. 1984. Influence of algal and suspended sediment concentrations on the feeding physiology of the hard clam *Mercenaria mercenaria*. Marine Biology, 165: 155–165.

Clarke, K. R., and Gorley, R. N. 2006. PRIMER v6: User Manual/Tutorial. PRIMER-E, Plymouth.

Constable, H. B. 2014. Population structure, temporal stability and seascape genetics of two endemic New Zealand Pleuronectiformes, *Rhombosolea plebeia* (sand flounder) and *R. leporina* (yellowbelly flounder). PhD thesis. Victoria University of Wellington. 169 pp.

D'Sa, E. J., Miller, R. L., and McKee, B. A. 2007. Suspended particulate matter dynamics in coastal waters from ocean color: application to the northern Gulf of Mexico. Geophysical Research Letters, 34: 1–6.

Gaggiotti, O. E., Bekkevold, D., Jørgensen, H. B. H., Foll, M., Carvalho, G. R., Andre, C., and Ruzzante, D. E. 2009. Disentangling the effects of evolutionary, demographic, and environmental factors influencing genetic structure of natural populations: Atlantic herring as a case study. Evolution, 63: 2939–2951.

Goudet, J., Raymond, M., de Meeüs, T., and Rousset, F. 1996. Testing differentiation in diploid populations. Genetics, 144: 1933–1940.

Guichoux, E., Lagache, L., Wagner, S., Chaumeil, P., Léger, P., Lepais, O., Lepoittevin, C., *et al.* 2011. Current trends in microsatellite genotyping. Molecular Ecology Resources, 11: 591–611.

Hannan, D. A. 2014. Population genetics and connectivity in *Paphies subtriangulata* and *Paphies australis* (Bivalvia: Mesodesmatidae). PhD thesis. Victoria University of Wellington. 231 pp.

Heath, M. R., Culling, M. A., Crozier, W. W., Fox, C. J., Gurney, W. S. C., Hutchinson, W. F., Nielsen, E. E., *et al.* 2014. Combination of genetics and spatial modelling highlights the sensitivity of cod (*Gadus morhua*) population diversity in the North Sea to distributions of fishing. ICES Journal of Marine Science, 71: 794–807.

Jørgensen, H. B. H., Hansen, M. M., Bekkevold, D., Ruzzante, D. E., and Loeschcke, V. 2005. Marine landscapes and population genetic structure of herring (*Clupea harengus* L.) in the Baltic Sea. Molecular Ecology, 14: 3219–3234.

Kalinowski, S. T. 2005. Hp-Rare 1.0: a computer program for performing rarefaction on measures of allelic richness. Molecular Ecology Notes, 5: 187–189.

Leathwick, J. R., Rowden, A., Nodder, S., Gorman, R., Bardsley, S., Pinkerton, M. H., Baird, S. J., *et al.* 2012. A benthic-optimised marine environment classification (BOMEC) for New Zealand waters. New Zealand Aquatic Environment and Biodiversity Report, 88. 54 pp.

Legendre, P., and Anderson, M. J. 1999. Distance-based redundancy analysis: testing multispecies responses in multifactorial ecological experiments. Ecological Monographs, 69: 1–24.

Liggins, L., Treml, E. A., and Riginos, C. 2013. Taking the plunge: an introduction to undertaking seascape genetic studies and using biophysical models. Geography Compass, 7: 173–196.

McLeod, R. J., and Wing, S. R. 2008. Influence of an altered salinity regime on the population structure of two infaunal bivalve species. Estuarine, Coastal and Shelf Science, 78: 529–540.

Meirmans, P. G. 2006. Using the Amova framework to estimate a standardized genetic differentiation measure. Evolution, 60: 2399–2402.

Meirmans, P. G., and Hedrick, P. W. 2011. Assessing population structure: F(ST) and related measures. Molecular Ecology Resources, 11: 5–18.

Meirmans, P. G., and Van Tienderen, P. H. 2004. Genotype and genodive: two programs for the analysis of genetic diversity of asexual organisms. Molecular Ecology Notes, 4: 792–794.

NASA. 2014. Ocean colour satellite data used courtesy of NASA Goddard Space Flight Center (MODIS project). Products generated by Matt Pinkerton, NIWA, Wellington.

New Zealand Ministry for the Environment. 2005. The New Zealand Marine Environment Classification. Wellington. 80 pp.

Peakall, R., and Smouse, P. E. 2012. GenAlEx 6.5: genetic analysis in Excel. Population genetic software for teaching and research-an update. Bioinformatics, 28: 2537–2539.

Pinkerton, M. H., and Richardson, K. R. 2005. Case 2 climatology of New Zealand: final report. NIWA Client Report WLG2005-49. 16 pp.

QGIS Development Team. 2014. QGIS Geographic Information System. Open Source Geospatial Foundation Project. http://qgis.osgeo.org.

Riginos, C., and Liggins, L. 2013. Seascape genetics: populations, individuals, and genes marooned and adrift. Geography Compass, 7: 197–216.

Rousset, F. 2008. genepop'007: a complete re-implementation of the genepop software for Windows and Linux. Molecular Ecology Resources, 8: 103–106.

Selkoe, K. A., Henzler, C. M., and Gaines, S. D. 2008. Seascape genetics and the spatial ecology of marine populations. Fish and Fisheries, 9: 363–377.

Selkoe, K. A., Watson, J. R., White, C., Horin, T. B., Iacchei, M., Mitarai, S., Siegel, D. A., *et al.* 2010. Taking the chaos out of genetic patchiness: seascape genetics reveals ecological and oceanographic drivers of genetic patterns in three temperate reef species. Molecular Ecology, 19: 3708–3726.

Shears, N. T., Smith, F., Babcock, R. C., Duffy, C. A. J., and Villouta, E. 2008. Evaluation of biogeographic classification schemes for conservation planning: application to New Zealand's coastal marine environment. Conservation Biology, 22: 467–481.

Shumway, S. E., and Parsons, G. J. 2006. Scallops: Biology, Ecology and Aquaculture. Elsevier B.V., Amsterdam, The Netherlands. 1460 pp.

Silva, C. N. S., and Gardner, J. P. A. 2014. Development and characterisation of 12 microsatellite markers for the New Zealand endemic scallop *Pecten novaezelandiae*. Conservation Genetics Resources, 6: 327–328.

Silva, C. N. S., and Gardner, J. P. A. 2015. Emerging patterns of genetic variation in the New Zealand endemic scallop *Pecten novaezelandiae*. Molecular Ecology, 24: 5379–5393.

Slatkin, M. 1994. An exact test for neutrality based on the Ewens sampling distribution. Genetical Research, 64: 71–74.

Slatkin, M. 1996. A correction to the exact test based on the Ewens sampling distribution. Genetical Research, 68: 259–260.

Snelder, T., Leathwick, J., Day, K., Weatherhead, M., Fenwick, G., Francis, M., Gorman, R., *et al.* 2005. The New Zealand Marine Environment Classification. Wellington, NewZealand. 80 pp.

St-Onge, P., Sévigny, J.-M., Strasser, C., and Tremblay, R. 2013. Strong population differentiation of softshell clams (*Mya arenaria*) sampled across seven biogeographic marine ecoregions: possible selection and isolation by distance. Marine Biology, 160: 1065–1081.

Szostek, C. L., Davies, A. J., and Hinz, H. 2013. Effects of elevated levels of suspended particulate matter and burial on juvenile king scallops *Pecten maximus*. Marine Ecology Progress Series, 474: 155–165.

Thomas, D., and Franz, B. 2005. Overview of MODIS Aqua Data Processing and Distribution. National Aeronautics and Space Administration (NASA). http://oceancolor.gsfc.nasa.gov/DOCS/MODISA_processing.html.

Uribe, E., Blanco, J. L., and Yamashiro, C. 2003. Effect of salinity on the distribution of *Argopecten purpuratus* on the SW Pacific coast. Book of Abstracts, 14th International Pectinid Workshop, St Petersburg, Florida, USA, 23–29 April 2003, pp. 125–126.

Van Oosterhout, C., Hutchinson, W. F., Wills, D. P. M., and Shipley, P. 2004. Micro-Checker: software for identifying and correcting genotyping errors in microsatellite data. Molecular Ecology Notes, 4: 535–538.

Veale, A. J., and Lavery, S. D. 2011. Phylogeography of the snakeskin chiton *Sypharochiton pelliserpentis* (Mollusca: Polyplacophora) around New Zealand: are seasonal near-shore upwelling events a dynamic barrier to gene flow? Biological Journal of the Linnean Society, 104: 552–563.

Verhoeven, K. J. F., Simonsen, K. L., and Mcintyre, L. M. 2005. Implementing false discovery rate control: increasing your power. OIKOS, 3: 643–647.

Wang, I. J., and Bradburd, G. S. 2014. Isolation by environment. Molecular Ecology, 23: 5649–5662.

Wei, K., Wood, A. R., and Gardner, J. P. A. 2013. Seascape genetics of the New Zealand greenshell mussel: sea surface temperature explains macrogeographic scale genetic variation. Marine Ecology Progress Series, 477: 107–121.

Weir, B. S., and Cockerham, C. C. 1984. Estimating F-statistics for the analysis of population structure. Evolution, 38: 1358–1370.

Yang, Z., and Nielsen, R. 2008. Mutation-selection models of codon substitution and their use to estimate selective strengths on codon usage. Molecular Biology and Evolution, 25: 568–579.

Handling editor: Lorenz Hauser

ICES Journal of Marine Science

ICES Journal of Marine Science (2016), 73(7), 1935–1945. doi:10.1093/icesjms/fsv158

Contribution to the Themed Section: '*Seascape Ecology*'

Original Article

Modelling the effect of demographic traits and connectivity on the genetic structuration of marine metapopulations of sedentary benthic invertebrates

Mariana Padrón* and Katell Guizien

Sorbonne Universités, UPMC Univ Paris 06, CNRS, Laboratoire d'Ecogéochimie des Environnements Benthiques (LECOB), Observatoire Océanologique, 66650 Banyuls sur Mer, France

**Corresponding author: tel: +33 468887394; e-mail: mpadron@obs-banyuls.fr*

Padrón, M., and Guizien, K. Modelling the effect of demographic traits and connectivity on the genetic structuration of marine metapopulations of sedentary benthic invertebrates. – ICES Journal of Marine Science, 73: 1935–1945.

Received 4 May 2015; revised 11 August 2015; accepted 16 August 2015.

Accounting for connectivity is essential in marine spatial planning and the proper design and management of marine protected areas, given that their effectiveness depends on the patterns of dispersal and colonization between protected and non-protected areas. The genetic structure of populations is commonly used to infer connectivity among distant populations. Here, we explore how population genetic structure is affected by pre- and settlement limitations with a spatially explicit coupled metapopulation-gene flow model that simulates the effect of demographic fluctuations on the allele frequencies of a set of populations. We show that in closed populations, regardless of population growth rate, the maintenance of genetic diversity at saturating initial population density increases with species life expectancy as a result of density-dependent recruitment control. Correlatively, at low initial population density, the time at which a population begins to lose its genetic diversity is driven larval and post-settlement mortality (comprised in the recruitment success parameter)—the larger the recruitment success, the stronger the genetic drift. Different spatial structures of connectivity established for soft bottom benthic invertebrates in the Gulf of Lions (NW Mediterranean, France) lead to very different results in the spatial patterns of genetic structuration of the metapopulation, with high genetic drift in sites where the local retention rate was larger than 2%. The effect of recruitment failure and the loss of key source populations on heterozygosity confirm that transient demographic fluctuations help maintain genetic diversity in a metapopulation. This study highlights the role of intraspecific settlement limitations due to lack of space when the effective number of breeders approaches saturating capacity, causing a strong reduction in effective reproduction. The present model allows to: (i) disentangle the relative contribution of local demography and environmental connectivity in shaping seascape genetics, and (ii) perform *in silico* evaluations of different scenarios for marine spatial planning.

Keywords: connectivity, Gulf of Lions, metapopulation, seascape genetics, sedentary benthic invertebrates, spatially explicit model.

Introduction

Connectivity strongly impacts the dynamics and persistence of marine populations because it influences key processes, from short-term demography to long-term evolution, including resistance to disturbances and environmental changes. Therefore, understanding the development and maintenance of connectivity patterns is essential in marine spatial planning and the proper design and management of marine protected areas (MPAs; Palumbi, 2004; Botsford *et al.*, 2009). However, the quantitative study of connectivity and the identification of connectivity bottlenecks that could compromise the ability for populations to recover after disturbances are current scientific challenges (Pineda, 2000; Burgess *et al.*, 2014).

For sedentary marine benthic species, understanding connectivity translates into understanding larval dispersal, given that it is during the pelagic larval stage that the exchange of individuals and genes among populations takes place (Pineda *et al.*, 2007; Cowen and Sponaugle, 2009). Hence, to analyse the patterns of connectivity among populations and study, in more detail, the

mechanisms that shape and maintain connectivity patterns through time, the dispersal of organisms should be taken into account (Hastings and Botsford, 2006; Aiken and Navarrete, 2011).

Different approaches have been undertaken to try to quantify dispersal and connectivity in marine ecosystems. Population genetics has been one of the most frequently used tools to provide direct and indirect measures of connectivity in several marine species (Hellberg *et al.,* 2002; Saenz-Agudelo *et al.,* 2009; Lowe and Allendorf, 2010). The dispersal potential of the larvae produced by sedentary benthic species has been expected to be correlated with gene flow and was even used as a predictor of population genetic structure (Siegel *et al.,* 2003), although some studies showed that larval dispersal (modelled) and gene flow (observed) do not necessarily match (Foster *et al.*, 2012).

Using estimates of pelagic larval duration (PLD) as a proxy to measure realized dispersal distance, several studies showed that the correlation between PLD and genetic isolation by distance was consistent with the expectation that migration was the key factor driving the genetic structuration of marine populations (Hellberg, 1996; Gilg and Hilbish, 2003). However, recent dataset reviews (Riginos *et al.,* 2011; Selkoe and Toonen, 2011; Faurby and Barber, 2012) have now shown that the relationship between PLD and genetic structuration might be weaker than previously thought.

The influence of several processes (e.g. larval behaviour, availability of suitable habitat, and biotic interactions) can cause the patterns of population connectivity to be different from what would be expected from flow integration along PLD alone (Pineda, 2000; Guizien *et al.,* 2006; Butler *et al.*, 2011). Among these processes, settlement or recruitment regulation of dispersal alters gene flow (Pineda *et al.,* 2007), in addition to the local demography. This temporal and spatial variability in the strength of gene and demographic flow due to bottlenecks during larval settlement and recruitment implies that there is a set of interacting processes operating across various scales, which introduces complexity into the system. Therefore, inferring connectivity by only one disciplinary approach (either genetic or biophysic) does not provide the necessary information to properly describe population persistence in a network of MPAs (Hastings and Harrison, 1994; Marko and Hart, 2011).

It is therefore necessary, to efficiently inform conservation management decisions, to use tools that integrate biophysical models with information regarding local demographic traits driving genetic linkages that result from larval exchange among populations (Werner *et al.,* 2007; Cowen and Sponaugle, 2009). However, detecting the genetic signatures caused by the transient dynamics of demographic changes remains a challenge (Alcala *et al.,* 2013).

Although genetic models incorporating larval dispersal and demographic parameters have recently been developed to quantify connectivity among marine populations (Galindo *et al.,* 2006; Kool, 2009; Munroe *et al.,* 2012), they have some limitations when attempting to understand connectivity patterns among non-equilibrium populations. The model Galindo *et al.* (2006) developed, for example, does not take into account demographic variability, as population sizes were kept constant over time. The approach Kool (2009) developed, although allowing changes in population size, does not account for overlapping generations but, more important, being an individual-based model, population sizes were limited to ten individuals. Recently, Munroe *et al.* (2012) presented a modelling case study for Eastern oysters in Delaware Bay (USA) in which they relaxed population size limitations and assigned each population its own demographic dynamics.

In an attempt to generalize Munroe *et al.*'s (2012) approach, we present a spatially explicit coupled demographic gene flow model that assesses the effect of demography variability on allele frequencies in a marine metapopulation of sedentary benthic species with population densities being limited by space. The seascape model was used to examine how: (i) demographic traits influence the development of genetic structure in closed populations over time, (ii) different patterns of connectivity affect the loss or maintenance of genetic diversity in a metapopulation, (iii) fluctuations in local population density help maintain genetic diversity over time, and (iv) local population demographic stability impacts genetic diversity to provide relevant information for conservation decisions in the Gulf of Lions, France.

Methods

A seascape genetic model for benthic invertebrates with a pelagic larval phase

To simulate the transient demographic effect on local allele frequencies arising from environmental variability modulating connectivity through time, a seascape genetic model was developed. The seascape model relies on the forcing of a spatially explicit dynamical model of allele probability by a spatially explicit metapopulation model (Guizien *et al.,* 2014, adapted from Hastings and Botsford, 2006; Figure 1). The combination of these models allows us to project the development of a population genetic structure through time, resulting from demography dynamics driven by local survival and larval transfer on a regional scale.

The spatially explicit metapopulation model simulates the population density $N_i(t)$ at each site i at any time t resulting from the balance of adult survival and input of new recruits resulting from reproduction of adults present in the previous time-step. Therefore, N_i represents the adult census size per unit surface, and it is equal to the effective number of breeders per unit surface for the next reproductive event (as defined by Waples *et al.*, 2013). It must be emphasized that such formulation implicitly hypothesized that age at first reproduction and the time lapse between reproductive events are both equal to the model time-step, ensuring that the effective number of breeders does not vary with population age structure. Larval transfer rate among sites is estimated from a set of realistic connectivity matrices obtained using the larval dispersal model (Guizien *et al.,* 2012), and recruitment success (interspecific competition or predation) is limited by saturating population density [intraspecific competition; Equations (1) and (2); Guizien *et al.,* 2014].

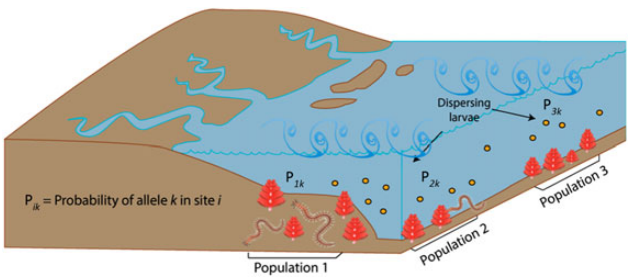

Figure 1. Schematic representation of seascape genetic model. The frequency of each allele *k* is calculated at any given time in every site *i*, as a result of mixing between the surviving individuals with allele *k* in site *i* and to the input of new recruits with allele *k*, coming from any other site.

$$N_i(t+1) = \min(G(t)N_i(t), N_{\max}), \quad (1)$$

where $N_i(t+1)$ is the vector of spatial density of individuals at each site at time $t+1$ (ind. m^{-2}); $N_i(t)$ the vector of spatial density of individuals at each site at time t (ind. m^{-2}); $N_{\max}$ the saturating population density based on space limitation (ind. m^{-2}); with the transfer matrix $G(t)$ defined by:

$$G_{ji}(t) = a_i C_{ji}(t) b_j + s_{jj}\delta_{ji}, \quad (2)$$

where a_i is the propagule production rate at site i (larvae per adult); $C_{ji}(t)$ the propagule transfer rate from site i to site j multiplied by the ratio of surface of site i to surface of site j (no units); b_j the recruitment success at site j (adults per larva); s_{jj} the adult survivorship rate at site j (no units); δ_{ji}, Kronecker symbol (1 when $i = j$, 0 otherwise).

Maximum population growth rate (P_i) of a closed population in site i is then defined by:

$$P_i = a_i b_i + s_{ii}. \quad (3)$$

The time it takes for a population at any initial density N_o to reach its saturating density, $N_{\max}$, from any given initial density was estimated as:

$$T = \frac{\ln(N_{\max}/N_o)}{\ln(P_i)}. \quad (4)$$

In the seascape genetics model, the frequency of each allele k is calculated at any given time in every site i, as a result of mixing between the surviving individuals with allele k in site i and the input of new recruits with allele k, coming from any other site [Equation (5)]. Given the large number of larvae produced by each adult and the high recruitment success (i.e. larval and juveniles survival) values assigned (10%) compared with estimated regional retention rates (3%), genetic drift due to larval and juveniles mortality is neglected and, thus, a proportional and uniform loss was applied to the larval pool with allele k produced at each site embedded in the recruitment success parameter. The effect of genetic drift is therefore simulated by the random sampling of the alleles lost during two different periods in the life cycle: larval dispersal and settlement. Simplifying assumptions were that: (i) mating takes place randomly every year among diploid organisms, (ii) allele frequencies are identical among sexes, (iii) generations are discrete but overlapping, (iv) populations are not age-structured, (v) given the relatively short period considered in the simulations (100 years), mutation is assumed to be negligible compared with genetic drift and migration, and thus set to zero, and (vi) selection can be neglected.

During larval dispersal, the pool of larvae with allele k produced by each site, remaining in the region (accounting for regional retention rate), is randomly sampled before being redistributed among the destination sites according to the connectivity matrix [Equations (6) and (7)]. The number of larvae with allele k that will survive dispersal is computed by sorting out the rank of the allele carried by the surviving larvae. During settlement, saturating density limits the number of arriving larvae that can actually settle at each site; therefore, a random subset of alleles carried by the pool of larvae arriving at each site actually settle.

$$p_{ik(t+1)} = \frac{(s_{ii}N_{i(t)}\, p_{ik(t)}) + b_j \sum_j \left((C_{ij}/\sum_l C_{lj}(S_l/S_j))n'_{jk}{}^{i}\right)}{N_{i(t+1)}}, \quad (5)$$

where n'_{jk} is a random number between 0 and n_{jk}, with the constraint that $\sum_k n'_{jk}{}^{i} = n'_j i$

$$n'^{i}_{j} = A_j a_j \left(\sum_l C_{lj}\frac{S_l}{S_j}\right), \quad (6)$$

$$n_{jk} = p_{jk} A_j a_j, \quad (7)$$

where $p_{ik}(t+1)$ is the frequency of allele k at site i at time $t+1$ (no units); $p_{ik}(t)$ the frequency of allele k at site i at time t (no units); $p_{jk}(t)$ the frequency of allele k at site j at time t (no units); S_i the surface area of site i (m^2); A_j the density of individuals in site j (ind. m^{-2}); $n'_{jk}{}^{i}$ the number of larvae produced per unit surface in site j having allele k that remain in the region and will survive until sexual maturity in site i; n'^{i}_{j} the number of larvae produced per unit surface in site j that remain in the region and survive until sexual maturity in site i; n_{jk} the number of larvae with allele k produced in site j per unit surface.

Test cases

The simulations were designed to evaluate the changes in allele frequencies due to variations in species demographic parameters and connectivity structure. Although this modelling approach applies to any sedentary species with a reproductive dispersive stage, to test the sensitivity of the model, we focused on marine benthic species with four different life expectancies (2, 5, 10, and 20 years) that reproduce each year. The values of recruitment success were varied to test the effect of maximum population growth in the maintenance of genetic diversity over time. Recruitment success was also the same in all populations (10%), although it was limited by saturating spatial density, which was set to $N_{\max} = 6250$ ind. m^{-2} per population.

Six groups of simulations were performed (Table 1). All simulations were run for 100 iterations, one iteration being the time lapse between two reproductive events. The initial genetic structure was described by ten different alleles present simultaneously in every site. To examine the variability due to specific initial conditions of genetic structure, simulations were repeated at least 100 times with different and random initial conditions of allele frequencies each time.

The first group consisted of simulations of a closed population (no larval inputs) in which life expectancy was raised from 2 to 20 years. Groups 2, 3A, 3B, 4A, and 4B, consisted of simulations of a metapopulation of a species with a life expectancy of 10 years, distributed among 32 sites along the Gulf of Lions (northwestern Mediterranean; Supplementary Figure S1), in which spatial structure was driven by connectivity only. These groups of simulations correspond to the test case of dominating species of the soft-bottom benthic communities in the Gulf of Lions (polychaetes). The continuous sandy-bottom habitat of these polychaetes, which is delimited by the 10 and the 30 m isobaths, was described by sites of approximately the same width (~20 km) contiguously distributed along the coast. Based on these criteria, the areas of the 32 sites ranged from 6.2 to 121 km^2. Survival and fecundity rates were the same among populations within the metapopulation and were kept constant over time in all the simulations.

Larval transfer between the 32 sites was computed from Lagrangian larval dispersal simulations based on regional hydrodynamic simulations performed with the coastal circulation model SYMPHONIE (Marsaleix *et al.*, 2008). Larval dispersal was simulated by releasing larvae at the average site depth (20 m).

Table 1. Settings of six simulation groups.

	Group 1	Group 2	Group 3A	Group 3B	Group 4A	Group 4B
Connectivity	NO	D	S	S	S	S
Initial population density (ind. m^{-2})	50, 1000, N_{max}	50	50	50	50	50
Fecundity	1000	2000	2000	2000	2000	2000
Life expectancy	2, 5, 10, and 20 years	5 years	10 years	10 years	10 years	10 years
Number of simulations	100	100	500	500	500	500
Disturbance	NO	NO	NO	Recruitment failure	Habitat loss (source sites)	Habitat loss (betweenness)

Connectivity, when present, was set either deterministically (D) using the same matrix every year (either 1 of the 20 variants) or stochastically (S) picking a different matrix among the 20 variants every year. Disturbance scenarios were only applied to the groups with stochastic connectivity.

Connectivity matrices containing larval transfer probabilities were produced for 20 sets of 10-day long spawning periods in 2004 and 2006 with an average PLD of 4 weeks (Guizien *et al.*, 2014). A total of 20 different connectivity matrices were used for this analysis.

Simulations of Group 2 were performed to evaluate the effect of the distinct connectivity structure on heterozygosity. In this case, connectivity was set deterministically using the same connectivity matrix every year (either 1 of the 20 variants) and, thus, simulations were run 100 times.

Groups 3A, 3B, 4A, and 4B were performed to test the effect of recruitment (3A and 3B) and habitat loss (4A and 4B) on metapopulation size and the maintenance of heterozygosity within a metapopulation over time. Metapopulation size was represented as average regional coverage, defined as the ratio between regional average population density and saturating density. Connectivity was set stochastically using a different connectivity matrix among the 20 variants every year and, thus, simulations were run 500 times to reach the convergence of the mean when combining stochasticity in connectivity and initial condition. Group 3A simulated gene flow among all populations, and recruitment success was constant every year. Group 3B explored a scenario where recruitment failure (no recruitment) occurred every 3 years. Group 4A simulated the loss of four populations (sites 17–20). These populations were identified as being essential for the regional persistence of species at minimum recruitment success in metapopulation modelling, comparing the vulnerability to habitat loss of four ports in the Gulf of Lions (Guizien *et al.*, 2014). Nonetheless, it must be emphasized to mention that for the present simulations, the values of minimum recruitment success and fecundity were set to ensure long-term persistence of the metapopulation after removing those four sites, unlike in Guizien *et al.* (2014). Group 4B evaluated a scenario where only one population (site 21) was lost from the metapopulation. This site was characterized by consistently showing the highest values of betweenness in the metapopulation when applying graph theory analysis to connectivity matrices (Costa, pers. comm.).

Metrics and statistics

Heterozygosity and allelic richness are two measures of genetic diversity commonly used in the population genetics literature, and in the present study, both were used. Heterozygosity (He_i), was estimated taking into account all individuals at each site i over time [Equation (8)].

$$He_i(t) = 1 - \sum_{k=1}^{n} (p_{ik}(t))^2, \tag{8}$$

where $p_{ik}(t)$ is the frequency of the kth allele of n alleles in site i at time t [no units].

However, heterozygosity and allelic richness describe the state of genetic diversity of a population at a particular time and not its dynamics. To measure the speed at which genetic diversity varied as a function of demographic parameters (regulating genetic drift) and connectivity structure, new metrics describing the initial and average slope of the evolution of genetic diversity over time are introduced: (i) allele drifting time (T_d), which is the moment at which allelic diversity starts decreasing, meaning the time when the first allele is lost from the population or the metapopulation. (ii) Allele fixation time (T_f), which is the time lapse between the first loss of an allele (T_d) and the fixation of any allele (Supplementary Figure S2).

These metrics were defined on allelic richness rather than heterozygosity to avoid ambiguity in defining genetic diversity reference points and given the known sensitivity of allelic richness to the loss of rare alleles (Allendorf, 1986).

Results

Do differences in demographic parameters affect genetic diversity in closed populations?

Figure 2a and b displays the loss of genetic diversity in closed populations at saturating initial density as a function of the ratio between mortality (being complementary to unity of survival) and recruitment success. This ratio, having the dimensions of larvae/adult/year, depicts the origin of recruitment regulation (*sensu* by Hixon *et al.*, 2002) and informs on the relative contribution of intrinsic vs. extrinsic drivers: high values indicate recruitment regulation due to low recruitment success driven by interspecific competition or predation, while low ratio values indicate recruitment regulation due to space limitation at a high population density (intraspecific competition). It should be stressed here that, in closed populations, low recruitment success depicts not only limitation in larval and juveniles survival, but it also includes limitation in the proportion of settlers by local retention rate. Therefore, the acceleration of the loss of genetic diversity (measured as T_d) shown when recruitment success increases in these simulations is also expected when local retention rate increases.

Figure 2a shows that the number of reproductive events after which the population begins to lose its genetic diversity (T_d/Re) increases with the ratio between mortality and recruitment success. This demonstrates a reduction in genetic drift when recruitment success decreases for any given life expectancy. However, genetic drift is inhibited at high levels of recruitment success, as depicted by low and almost constant T_d/Re for the lowest values of the ratio between mortality and recruitment success. Such minimum T_d/Re is of the order of magnitude of the number of reproductive events in a life expectancy. For a recruitment frequency of 0.18, short-lived species (2 years) could start loosing their genetic diversity after 3 years, while it would take around 14 years for a

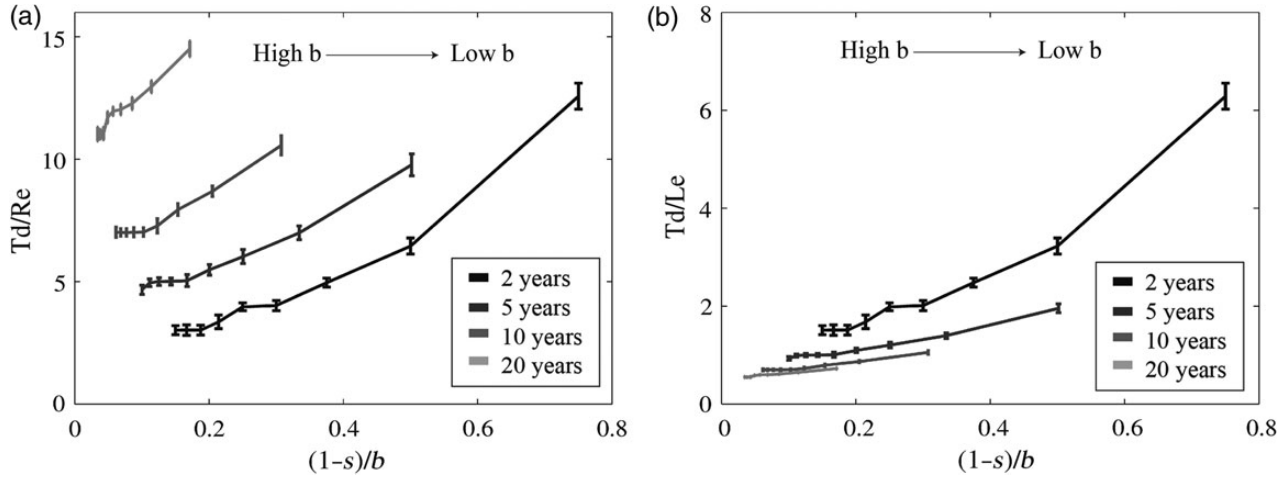

Figure 2. Effect of different life expectancies on the loss of genetic diversity, measure as allele drifting time (T_d), for an isolated population at initial saturating capacity (6250 ind. m^{-2}). Adimentionalizing allele drifting time by the number of reproductive events (T_d/Re) (a) represents the differences in the number of generations it takes for a species with different life expectancies to start loosing its genetic diversity as a function of the ratio between mortality and recruitment success. In contrast, adimentionalizing allele drifting time by the life expectancy (T_d/Le) of a species (b) provides a different vision corresponding to population turnover.

long-lived species (20 years). This reflects the effect of genetic drift inhibition by the reduction in reproductive events due to the lack of space caused by the presence of adults as life expectancy increases.

Similarly, the maintenance of genetic diversity, measured by the number of reproductive events before allele fixation (T_f/Re), in closed populations at saturating initial density increases with life expectancy, regardless of whether the population growth rate is low (<2.5) or high (>2.5; Figure 3). This confirms that genetic drift is limited by population inertia due to recruitment inhibition as a result of space limitation, as neither fecundity nor recruitment success affects the relationship.

However, when dealing with overlapping generations, it must be taken into account that the reduction in genetic drift by space limitation during the first population turnover decreases with species longevity. This is exhibited by the different hierarchies between life expectancy curves when representing the time at which the population starts to lose its genetic diversity in terms of population turnover (adimensionalizing T_d by the life expectancy of the species; Figure 2b). Species with short life expectancies begin to experience a reduction in their genetic diversity after a more population turnovers than do long-lived species, as fewer reproductive events occur during a short life expectancy compared with during a long one. This result confirms that genetic drift can be controlled by effective reproduction (which may be limited by long life expectancy or recruitment success intensity) and its frequency along the species lifespan in a context of finite population size.

Different initial population densities also affect the time at which a population starts loosing genetic diversity (Figure 4a)—for any value of the ratio between mortality and recruitment success, the lower the initial density of the population, the slower the loss of genetic diversity. This result points out that genetic drift is slower when considerable space is available for recruitment compared with at saturating density where space availability is regulated by mortality. Quantifying space availability by the time, it will take a population to reach saturating density (6250 ind. m^{-2}) shows that it would take twice as long for a population with an initial density of 50 ind. m^{-2} compared with a population with an initial density of 1000 ind. m^{-2} (Figure 4b). Allele drifting time increases linearly with the time necessary to reach saturating density.

The population growth rate triggers the effect of initial population density when it comes to the maintenance of genetic diversity, measured as T_f (Figure 3). While in fast-growing populations, the maintenance of genetic diversity is not sensitive to initial density, in slow-growing populations, the maintenance of genetic diversity lasts longer and is more variable when the initial population size is small (50 ind. m^{-2}) compared with when it is at saturating density. Such sensitivity to initial population size is amplified at small life expectancies.

Overall, in closed populations, genetic drift is the quickest when the population is at saturating density with high recruitment success, slowing down at low recruitment success or when population size is lower than saturating density. This result demonstrates the importance of transient demography in regulating the speed of genetic drift.

Do different patterns of connectivity affect the maintenance of genetic diversity in a metapopulation?

Simulated heterozygosity patterns among populations forming a metapopulation varied according to each connectivity matrix. The two most contrasting spatial patterns with low heterozygosity values either in the west (A) or in the east (B) of the Gulf of Lions are shown in Figure 5. A plausible explanation is the different spatial patterns of local retention (defined as the proportion of larvae produced locally that remain in the same spatial unit) vs. import (estimated as the proportion of all larvae produced among all sites that settled within the focal site). For connectivity matrix 1, the ratio between local retention and import was higher in the west than in the east (0.074 and 0.027, respectively). On the contrary, for connectivity matrix 2, the values of the same ratio were higher in the east compared with the west (0.069 and 0.0085, respectively). However, simulations demonstrated that the relationship between T_d and import do not exhibit any trend with no linear correlation ($R^2 = 0.011$; $p < 0.01$; Supplementary Figure S3). Similarly, T_d was not linearly correlated with local retention rate values obtained

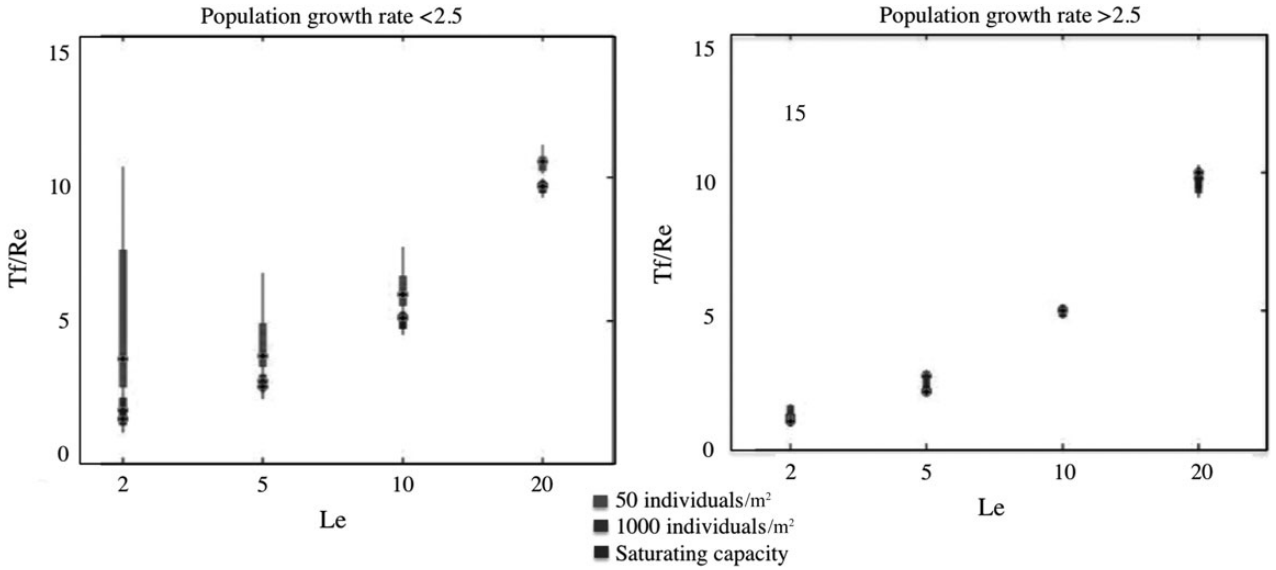

Figure 3. Effect of population growth rate over allele fixation time (T_f) for three different initial conditions of population abundance (50, 1000, and 6250 ind. m^{-2}) as a function of species life expectancy (Le) in a closed population.

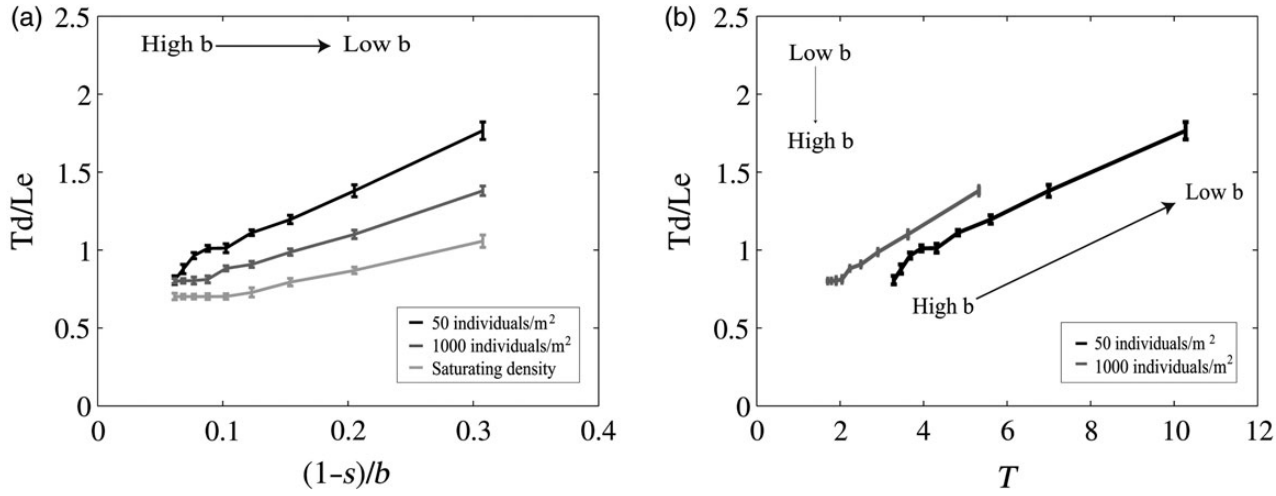

Figure 4. Effect of different initial population abundances (50, 1000, and 6250 ind. m^{-2}) on the loss of genetic diversity, measured as allele drifting time (T_d), as a function of (a) the ratio between mortality and recruitment success [$(1-s)/b$], and (b) the time to reach saturating capacity (T). T_d is adimensionalized by the life expectancy (T_d/Le) of a species that lives 10 years, thus representing the number of population turnovers to start loosing genetic diversity in an isolated population.

from the analysis of the 20 connectivity matrices ($R^2 = 0.031; p > 0.05$). However, T_d was delimited by a piecewise function enabling the discrimination between two groups (Figure 6)—populations with low levels of local retention (<2%) that show high variability in the time they begin to loose their genetic diversity (T_d/Le ranging from 0.2 to 50) and populations with high local retention (>2%) where genetic drift is much quicker and less variable (T_d/Le ranging from 0.2 to 12). This indicates that the speed of genetic drift is regulated locally only at a high local retention rate (larger than 2%) while, for local retention rates lower than 2%, the strength of genetic drift depends on the regional structure of connectivity. According to the direction of the transfer and the genetic characterization of the contributing populations, genetic drift will then be accelerated or slowed down in the focal population.

How does local population stability affect heterozygosity in a metapopulation?

When looking into the variation of the average heterozygosity in the metapopulation through time for a species with a life expectancy of 10 years, it becomes clear that changes in population density have a major effect on the loss of genetic diversity in a metapopulation (Figure 7). The rate at which a metapopulation reaches a stable regional coverage influences its possibility to maintain genetic diversity over time, even in the presence of migration.

Overall, we observe that as soon as regional coverage reaches 80%, heterozygosity values decrease rapidly and genetic diversity is lost. Scenario A shows how, with constant recruitment success, the effect of migration among populations homogenizes allele frequencies over time and leads to the fixation of the same allele in

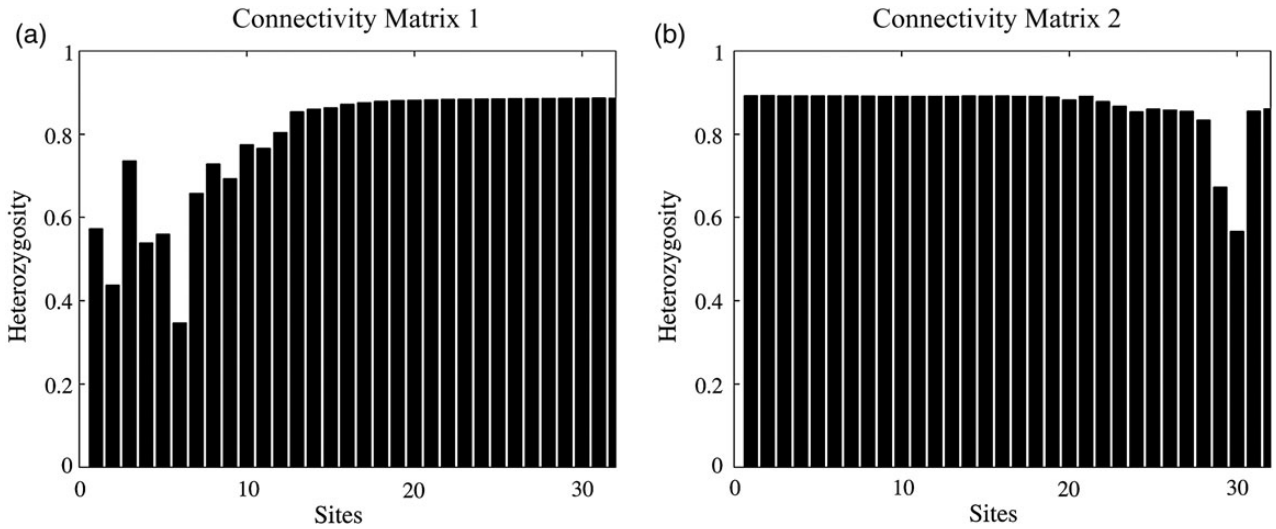

Figure 5. Spatial pattern of genetic diversity caused by distinct connectivity structures. Variability of heterozygosity for 32 sites forming a metapopulation for a species with a life expectancy of 5 years.

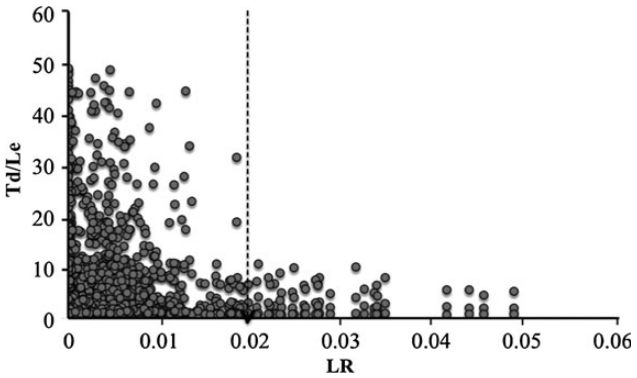

Figure 6. Relationship between local retention (LR; defined as the proportion of larvae produced in one population that remain in the same population) and the number of population turnovers to start loosing genetic diversity (T_d/Le), in a metapopulation over time. Values correspond to 20 connectivity matrices, and species with three different life expectancies (2, 5, and 20 years). Dashed arrow indicates the threshold at which the effect of LR on T_d/Le begins to decrease.

all populations over a relatively short period. Most interestingly, in scenario B, we find that high variability in metapopulation regional coverage due to recurrent failures in recruitment actually helps maintain genetic diversity over time. Stochastic connectivity leading to demographical fluctuations in populations enables the maintenance of genetic diversity.

On the other hand, scenario C exemplifies how, in the Gulf of Lions, removing populations (sites 17–20) responsible for bringing demographic persistence to the metapopulation at minimum recruitment success divides it into an eastern and western group, causing a slightly faster decrease in genetic diversity in the latter group than in the former. However, scenario D shows how the loss of only one site, identified as essential for maintaining the integrity of the connectivity graph, indeed disrupts the genetic connectivity of the metapopulation by augmenting the differentiation between the eastern and western groups in terms of the loss of heterozygosity, with drifting starting earlier in the eastern part. In scenarios C and B, recruitment success was set to ensure that the loss of sites within the metapopulation would still allow for species persistence. It should be noticed that in both scenarios, a similar constant metapopulation size was maintained, even if not at saturating density. The effect of migration in this case will also lead to the loss of genetic diversity in the metapopulation over time, although at a slower rate.

Discussion

The present study highlights that genetic drift increases considerably with settlement limitations by lack of space when the effective number of breeders approaches saturating capacity, causing a strong reduction in effective reproduction.

Early authors had extensively shown how changes in genetic diversity are related to effective population size (Wright, 1931; Kimura, 1955). Nonetheless, it has been demonstrated theoretically that some life cycle processes, like overlapping generations (Jorde and Ryman, 1995), and demographic parameters can also affect the amount of temporal allele frequency change and should be taken into account (Ryman, 1997). Our results highlight the role of life cycle processes, other than age at first reproduction (Lee *et al.*, 2011), in reducing effective reproduction in populations with large number of breeders and increasing the effect of genetic drift on a short evolutionary time-scale. In closed populations with saturating density, actual recruitment regulates the speed of genetic drift, demonstrating the relevance of transient demography in shaping the genetic structuration of marine species. In open populations, genetic drift is slowed down as a result of larval exchange. The effect of recruitment failure and the loss of key source populations on heterozygosity confirm that transient demographic fluctuations, when remaining above the risk of regional extirpation and actually avoiding reaching saturating density, help maintain genetic diversity over time.

Recently, several meta-analyses and empirical studies evaluating the relationship between PLD and population genetic differentiation across different marine species indicated a weak correlation

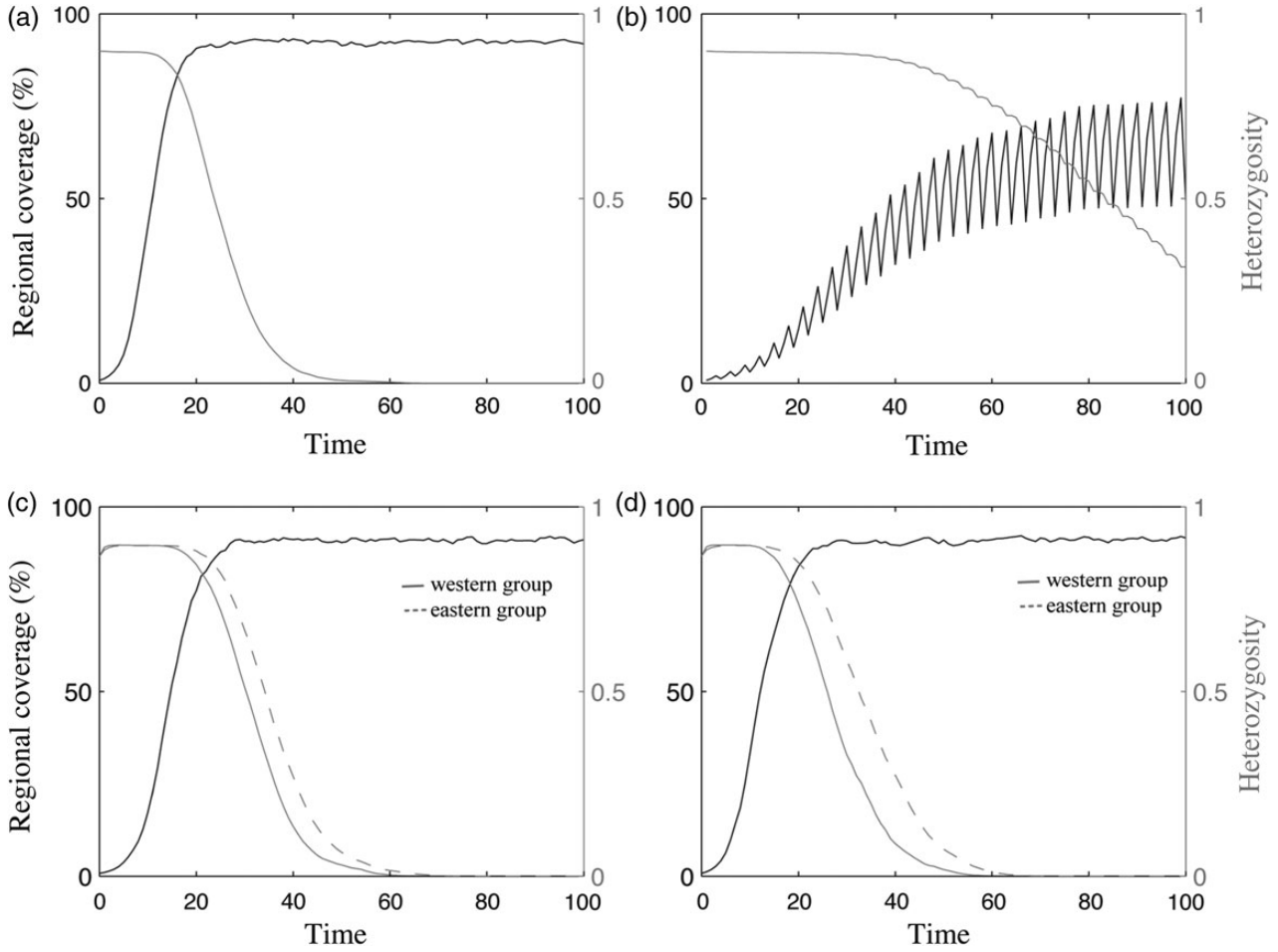

Figure 7. Effect of fluctuations in local population stability on heterozygosity over time. Scenarios: (a) Simulates gene flow among all of the populations forming a metapopulation with constant recruitment success every year. (b) Simulates recruitment failure (no recruitment) every 3 years. (c) Simulates the loss of four source sites (sites 17–20) in the metapopulation, while keeping recruitment success constant every year. (d) Simulates the loss of one key population (site 21) for maintaining genetic connectivity in the metapopulation.

between the two (Selkoe and Toonen, 2011; Faurby and Barber, 2012). In some cases, the high uncertainty in the estimates of larval dispersal and measures of population differentiation were suggested as the main causes for the unexpected results, while other studies suggested that differential mortalities and levels of abundance among populations were more relevant (Munroe *et al.*, 2012). The results from our simulations support these findings, while further demonstrating that considering other demographic parameters (such as life expectancy and population growth rate) and the inclusion of transient dynamics caused by recruitment failure, would help explain better the variability of genetic connectivity in a metapopulation.

Dawson *et al.* (2014) found that differences in fecundity, population size, and PLD could account for the differences in population genetic structure between eight co-distributed rocky intertidal invertebrate species in the eastern North Pacific. They found that population size was positively related to population genetic structure and they attributed the variability among species to differences in recruitment and demography. Furthermore, they highlighted that the differences in migration potential found between theoretical and empirical data could be attributed to the role of genetic drift and natural selection. Here, we corroborate their hypotheses by demonstrating how the strength of genetic drift is influenced by recruitment success, local retention, and fluctuations in population density due to habitat fragmentation and recruitment.

The present study exhibits an acceleration of genetic drift when the number of reproductive adults increases in a population. Although counterintuitive, such acceleration depicts the strong decrease in effective reproduction when recruitment is reduced by lack of space. However, relating genetic drift acceleration explicitly to a strong reduction in effective adult population size was not possible in the present case, given that the filter controlling effective reproduction applies to the fate of the larvae and not on the adults contributing to reproduction. Yet, we demonstrate that a long life expectancy and low recruitment success regulate the temporal variation of allele frequencies and reduce the loss of genetic diversity over time. This provides an alternative explanation to empirical evidence of strong genetic structure in long-lived species, when recruitment success is likely limited by space availability (Costantini *et al.*, 2007).

Population regulation occurs when at least one demographic rate is density-dependent (Hixon *et al.*, 2002). Clear evidence of genetic drift acceleration due to recruitment regulation is observed in our simulations for closed populations at the saturating initial density.

Furthermore, the evaluation of the ratio between mortality and recruitment success allowed for disentangling the relative contribution of intrinsic (intraspecific competition) vs. extrinsic drivers (interspecific competition or predation).

In open systems, it was already suggested that the amount of local retention could have a strong influence on the relative importance of demographic vs. connectivity parameters in the dynamics of metapopulations (Figueira, 2009). Our results confirm those findings and indicate that local retention rate values larger than 2% diminish the influence of the connectivity structure over genetic drift, as genetic drift accelerates in those populations close to saturating density. This is particularly relevant for the spatial planning of MPAs. Whether an MPA is created for the conservation of biodiversity or for fishery management, its main purpose is to maintain the persistence of its populations. For marine metapopulations, local retention is considered the currency of persistence: the higher the local retention, the closer the population is to its saturating capacity (Burgess *et al.*, 2014). Nonetheless, it must be emphasized that, as Figueira (2009) suggested, under the same flow structure, differences in PLD among species could cause distinct patterns of local retention for different species in the same place, making biodiversity conservation efforts even more difficult. In any case, the loss of genetic variability through genetic drift at a high local retention rate can diminish future adaptability to a changing environment, which might be detrimental to local conservation efforts, strongly advocating for a network of MPAs formed by sites with lower local retention rate.

The maintenance of genetic diversity in the metapopulation over at least 100 years for regular recruitment failure, creating regional demographic fluctuations, was not unexpected. These results, incorporating realistic spatially explicit connectivity matrices, extend previous theoretical studies that found that demographic instability and fluctuations in migration produce major changes in the evolution of genetic variation and population differentiation (Whitlock, 1992). Given that disturbances can cause variations in key demographic and biological processes, disturbance history may be one of the major drivers shaping the patterns of genetic diversity in many natural populations (Banks *et al.*, 2013). The pattern of genetic diversity maintenance over time observed in our simulations has been reported in an empirical study on natural populations of frogs, where no losses of genetic diversity after a disturbance were found when survival was high or when recovering populations recruited many individuals from multiple sources (Spear *et al.*, 2012). In addition, Larson *et al.* (1984) suggested, based on a survey of 22 species of salamanders, that historical influences are much more important in describing genetic variation patterns than is recent migration. Exhibiting that recruitment limitation by lack of space can be a strong filter to gene flow, even when larval dispersal connects populations, the present study provides an explanation for the discrepancy between modelled and observed connectivity between coral populations in the Caribbean (Foster *et al.*, 2012).

Although demographic disturbances leading to population bottlenecks have also been shown to induce strong genetic drift, in the present study, demographic disturbances around saturating capacity can reversely reduce the effect of genetic drift. The present study, thus, highlights that demographic disturbances can have contrasting effects on genetic drift whether they affect populations with small or large size compared with their saturating capacity: (i) decelerating genetic drift when population census size is close to saturating capacity (release of recruitment limitation), or (ii) accelerating genetic drift when population census size is low compared with saturating capacity (reduction in the effective number of breeders).

Previous studies in the Gulf of Lions identified the spatial structuration of population vulnerability to habitat loss driven by hydrodynamical connectivity. Four sites essential for species regional persistence at minimum recruitment success were identified from metapopulation modelling around the port of Sète (sites 17–20, Guizien *et al.*, 2014). However, analysis of the same connectivity graph used in the metapopulation model depicted those four sites as high bridging centrality, spanning across the two subclusters of the region. Another site (site 21) was instead identified for maintaining network integrity, as depicted by the highest betweeness (Costa *et al.*, pers. comm.). Here, we show that both the loss of four essential populations and the loss of the highest betweenness site divide the metapopulation into two genetically distinct subpopulations (eastern and western). Nevertheless, the loss of only site 21 leads to a higher level of genetic differentiation in the metapopulation. This result suggests that the highest betweeness of hydrodynamical connectivity graph could be interpreted for relaying gene flow and maintaining genetic connectivity, similar to how Rozenfeld *et al.* (2008) interpreted the highest betweenness of genetic distance. This example encourages further investigation of the potential of graph analysis of hydrodynamical connectivity matrices to identify sites important for conservation of genetic diversity.

By pinpointing the differential effect of demographic parameters and flow connectivity on population persistence and genetic diversity, the present study opens a question for management: to protect species persistence and genetic diversity, should we be seeking a compromise between preserving populations that are low in terms of diversity but are also demographically stable vs. highly diverse but unstable populations? The present model, by combining demography and gene flow in realistic conditions, allows to answer this question by (i) disentangling the relative contribution of local demography and environmental connectivity in shaping seascape genetics, and (ii) performing *in silico* evaluations of different scenarios for marine spatial planning.

Supplementary data

Supplementary material is available at the *ICESJMS* online version of the manuscript.

Acknowledgements

This work was (co-)funded through a MARES Grant. MARES is a Joint Doctorate programme selected under Erasmus Mundus coordinated by Ghent University (FPA 2011-0016). Check www.mares-eu.org for extra information. This work was also partly funded by the French National Program LITEAU IV of the Ministère de l'Ecologie et de l'Environnement Durable under project RocConnect—Connectivité des habitats rocheux fragmentés du Golfe du Lion (PI, K. Guizien, Project Number 12-MUTS-LITEAU-1-CDS-013). We would like to thank Proof-reading-service.com for English edition and corrections of the manuscript, and Dr Lorenzo Bramanti for an early critical review of the manuscript.

References

Aiken, C., and Navarrete, S. 2011. Environmental fluctuations and asymmetrical dispersal: generalized stability theory for studying metapopulation persistence and marine protected areas. Marine Ecology Progress Series, 428: 77–88.

Alcala, N., Streit, D., Goudet, J., and Vuilleumier, S. 2013. Peak and persistent excess of genetic diversity following an abrupt migration increase. Genetics, 193: 953–971.

Allendorf, F. 1986. Genetic drift and the loss of alleles versus heterozygosity. Zoo Biology, 5: 181–190.

Banks, S. C., Cary, G. J., Smith, A. L., Davies, I. D., Driscoll, D. A., Gill, A. M., Lindenmayer, D. B., *et al.* 2013. How does ecological disturbance influence genetic diversity? Trends in Ecology and Evolution, 28: 670–679.

Botsford, L., White, J., Coffroth, M., Paris, C., Planes, S., Shearer, T., Thorrold, S., *et al.* 2009. Connectivity and resilience of coral reef metapopulations in marine protected areas: matching empirical efforts to predictive needs. Coral Reefs, 28: 327–337.

Burgess, S., Nickols, K., Griesemer, C., Barnett, L., Dedrick, A., Satterthwaite, E., Yamane, L., *et al.* 2014. Beyond connectivity: how empirical methods can quantify population persistence to improve marine protected-area design. Ecological Applications, 24: 257–270.

Butler, M. J., Paris, C. B., Goldstein, J. S., Matsuda, H., and Cowen, R. K. 2011. Behaviour constrains the dispersal of long-lived spiny lobster larvae. Marine Ecology Progress Series, 422: 223–237.

Costantini, F., Fauvelot, C., and Abbiati, M. 2007. Genetic structuring of the temperate gorgonian coral (*Corallium rubrum*) across the western Mediterranean Sea revealed by microsatellites and nuclear sequences. Molecular Ecology, 16: 5168–5182.

Cowen, R., and Sponaugle, S. 2009. Larval dispersal and marine population connectivity. Annual Review of Marine Science, 1: 443–466.

Dawson, M., Hays, C., Grosberg, R., and Raimondi, P. 2014. Dispersal potential and population genetic structure in the marine intertidal of the eastern North Pacific. Ecological Monographs, 84: 435–456.

Faurby, S., and Barber, P. 2012. Theoretical limits to the correlation between pelagic larval duration and population genetic structure. Molecular Ecology, 21: 3419–3432.

Figueira, W. 2009. Connectivity or demography: defining sources and sinks in coral reef fish metapopulations. Ecological Modelling, 220: 1126–1137.

Foster, N. L., Paris, C. B., Kool, J. T., Baums, I. B., Stevens, J. R., Sanchez, J. A., Bastidas, C., *et al.* 2012. Connectivity of Caribbean coral populations: complementary insights from empirical and modelled gene flow. Molecular Ecology, 21: 1143–1157.

Galindo, H., Olson, D., and Palumbi, S. 2006. Seascape genetics: a coupled oceanographic-genetic model predicts population structure of Caribbean corals. Current Biology, 16: 1622–1626.

Gilg, M., and Hilbish, T. 2003. The geography of marine larval dispersal-coupling genetics with fine-scale physical oceanography. Ecology, 84: 1–11.

Guizien, K., Belharet, M., Marsaleix, P., and Guarini, J. M. 2012. Using larval dispersal simulations for marine protected area design: application to the Gulf of Lions (northwest Mediterranean). Limnology and Oceanography, 57: 1099–1112.

Guizien, K., Belharet, M., Moritz, C., and Guarini, J. M. 2014. Vulnerability of marine benthic metapopulations: implications of spatially structured connectivity for conservation practice in the Gulf of Lions (NW Mediterranean Sea). Diversity and Distributions, 20: 1–11.

Guizien, K., Brochier, T., Duchêne, J. C., Koh, B. S., and Marsaleix, P. 2006. Dispersal of *Owenia fusiformis* larvae by wind-driven currents: turbulence, swimming behaviour and mortality in a three-dimensional stochastic model. Marine Ecology Progress Series, 311: 47–66.

Hastings, A., and Botsford, L. 2006. Persistence of spatial populations depends on returning home. Proceedings of the National Academy of Sciences of the United States of America, 103: 6067–6072.

Hastings, A., and Harrison, S. 1994. Metapopulation dynamics and genetics. Annual Review of Ecology, Evolution, and Systematics, 25: 167–188.

Hellberg, M. 1996. Dependence of gene flow on geographic distance in two solitary corals with different larval dispersal capabilities. Evolution, 50: 1167–1175.

Hellberg, M., Burton, R., Neigel, J., and Palumbi, S. 2002. Genetic assessment of connectivity among marine populations. Bulletin of Marine Science, 70: 273–290.

Hixon, M., Pacala, S., and Sandin, S. 2002. Population regulation: historical context and contemporary challenges of open vs. closed systems. Ecology, 83: 1490–1508.

Jorde, P., and Ryman, N. 1995. Temporal allele frequency change and estimation of effective size in populations with overlapping generations. Genetics, 139: 1077–1090.

Kimura, M. 1955. Random genetic drift in multi-allelic locus. Evolution, 9: 419–435.

Kool, J. 2009. An object-oriented, individual-based approach for simulating the dynamics of genes in subdivided populations. Ecological Informatics, 4: 136–146.

Larson, A., Wake, D., and Yanev, K. 1984. Measuring gene flow among populations having high levels of genetic fragmentation. Genetics, 106: 293–308.

Lee, A., Engen, S., and Saether, B. 2011. The influence of persistent individual differences and age at maturity on effective population size. Proceedings of the Royal Society B: Biological Sciences, 278: 3303–3312.

Lowe, W., and Allendorf, F. 2010. What can genetics tell us about population connectivity? Molecular Ecology, 19: 3038–3051.

Marko, P., and Hart, M. 2011. The complex analytical landscape of gene flow inference. Trends in Ecology and Evolution, 26: 448–456.

Marsaleix, P., Auclair, F., Floor, J., Herrmann, M., Estournel, C., Pairaud, I., and Ulses, C. 2008. Energy conservation issues in sigma-coordinate free-surface ocean models. Ocean Modelling, 20: 61–89.

Munroe, D., Klinck, J., Hofman, E., and Powell, E. 2012. The role of larval dispersal in metapopulation gene flow: local population dynamics matter. Journal of Marine Research, 70: 2441–4677.

Palumbi, S. 2004. Marine reserves and ocean neighborhoods: the spatial scale of marine populations and their management. Annual Review of Environment and Resources, 29: 31–68.

Pineda, J. 2000. Linking larval settlement to larval transport: assumptions, potentials and pitfalls. Oceanography of the Eastern Pacific, I: 84–105.

Pineda, J., Hare, J., and Sponaugle, S. 2007. Larval transport and dispersal in the coastal ocean and consequences for population connectivity. Oceanography, 20: 22–39.

Riginos, C., Douglas, K., Jin, Y., Shanahan, D., and Treml, E. 2011. Effects of geography and life history traits on genetic differentiation in benthic marine fishes. Ecography, 34: 566–575.

Rozenfeld, A., Arnaud-Haond, S., Hernández-García, E., Eguíluz, V., Serrão, E., and Duarte, C. 2008. Network analysis identifies weak and strong links in a metapopulation system. Proceedings of the National Academy of Sciences of the United States of America, 105: 18824–18829.

Ryman, N. 1997. Minimizing adverse effects of fish culture: understanding the genetics of populations with overlapping generations. ICES Journal of Marine Science, 54: 1149–1159.

Saenz-Agudelo, P., Jones, G., Thorrold, S., and Planes, S. 2009. Estimating connectivity in marine populations: an empirical evaluation of assignment tests and parentage analysis under different gene flow scenarios. Molecular Ecology, 18: 1765–1776.

Selkoe, K., and Toonen, R. 2011. Marine connectivity: a new look at pelagic larval duration and genetic metrics of dispersal. Marine Ecology Progress Series, 436: 291–305.

Siegel, D., Kinlan, B., Gaylord, B., and Gaines, S. 2003. Lagrangian descriptions of marine larval dispersion. Marine Ecology Progress Series, 260: 83–96.

Spear, S., Crisafulli, C., and Storfer, A. 2012. Genetic structure among coastal tailed frog populations at Mount St. Helens is moderated

by post-disturbance management. Ecological Applications, 22: 856–869.

Waples, R., Luikart, G., Faulkner, J., and Tallmon, D. 2013. Simple life-history traits explain key effective population size ratios across diverse taxa. Proceedings of the Royal Society B: Biological Sciences, 280: 20131339.

Werner, F., Cowen, R., and Paris, C. 2007. Coupled biological and physical models. Oceanography, 20: 1–16.

Whitlock, M. 1992. Temporal fluctuations in demographic parameters and the genetic variance among populations. Evolution, 46: 608–615.

Wright, S. 1931. Evolution in Mendelian populations. Genetics, 16: 97–159.

Handling editor: Manuel Hidalgo